Directed evolution of Chinese Hamster Ovary cells

Katie Louise Syddall

A thesis submitted for the degree of

Doctor of Philosophy

Department of Chemical and Biological Engineering

The University of Sheffield

February 2016

Lonza

The University Of Sheffield.

BBSRC bioscience for the future

Declaration

I, Katie Louise Syddall, declare that I am the sole author of this thesis and that the research presented within is a result of my own efforts. Where this is not the case, this has been clearly stated. I confirm that this work has not been submitted for any other degrees.

Acknowledgments

My sincere thanks go to Professor David James for his guidance and supervision throughout the duration of this project. I would also like to thank my industrial supervisor Dr. Robert Young for all his contributions and advice, and also to Dr. Tom Payne for all the support during my time in Cambridge. Much gratitude extends to the BBSRC and Lonza Biologics for funding my studies. Thanks also go to all post-docs and academic staff members that have provided valuable insights and recommendations throughout. Thank you to Dave Wengraf for all the times he fixed lab equipment that always seemed to break at the worst possible moments!

Thanks go to all the members of the DCJ laboratory, both past and present. Each one of you has undoubtedly at some point shared your knowledge and wisdom to point me in the right direction (even if it was just towards the pub). Specific mentions must go to following: both Darren Geoghegan and Joe Cartwright for being there from day one and through each milestone and tribulation that followed, but most importantly thanks for becoming more a friend than a coworker; Jo Longster for being my Lonza buddy, fellow cat lover and for the many words of wisdom over a cup of tea; Joseph Longworth for being my favorite lab matron and BBQ host; Claire Bryant for being the most daft yet most brilliant person at the same time; Yash Patel for your injection of industrial efficiency to the last year of my research; also to Devika Kalsi, Danielle Fairbrass, Charlotte Bjork, Ben Thompson, Olivia Mozley, Neil Johnson, Gregory Fowler, Josselin Noirel and all the members of D72 (too numerous to mention!) for all the laughs along the way. Thanks to great friends outside of Sheffield or the University, namely Emma Fisher, Amy Harvey (and the rest of the Highfields clan), Shaun Renton and Victoria Madsen, for all the good times spent talking about anything other than my work!

To my partner Stephen Jaffé, I thank you for your endless love and support, and for letting me get a cat. Thanks for also being patient through the times when I got mad at you instead of science! In all sincerity, I would have not made it to this point without you. To said cat: your company and happy (if sometimes crooked) little face made thesis writing more bearable, you also had the knack of jumping on my lap at just the right moment, sparing me from those daily breakdowns – thank you Owen.

Finally, I would like to deeply thank all my family, near and far, for their infinite love and kind encouragement: To Dad, for keeping my feet on the ground and putting things in perspective, reminding me of the bigger picture when I lost sight of it. Thanks for helping me find joy in the little things (a Maazi). Your philosophies are inspiring. To Mum, for your ever-ready words of support, always looking on

the bright side, and somehow always knowing exactly when to offer me that glass of wine. You're a brick. Both of you have always had faith in me that I haven't always shared. I thank you for always welcoming me home (or to the caravan!) with open arms when I've needed the escape. To my brother Daniel, for your kindness and calmness in response to everything, and also for never really asking me about my PhD, even though I know you would understand every detail of it! Also to Archie for always being a dude. To Copper, Milo, Bandit, Pebble and Harry: you brought so much joy over many years and are sorely missed.

Without any of the individuals mentioned above, I would not have survived the last four years, and for that I am eternally grateful.

Abstract

Chinese Hamster Ovary (CHO) cells are the industrial standard and production vehicle of choice for recombinant therapeutic protein manufacture. This is largely due to their capacity to be suspension adapted to warrant a high cell density and scale-up in large bioreactors and also their ability to execute post-translational modifications such as glycosylation (Tescione *et al.* 2015). Their prevalence has lead to constant commercial competition to improve and develop new CHO cell lines that are better able to produce therapeutic products, either in terms of their cell specific productivity, their growth rate or of the quality and efficacy of the final drug product. A popular method of improving cell specific productivity is to shift dense cell cultures, proliferating at their optimum temperature (~37°C) to hypothermic conditions (~32°C), arresting cell cycle progression. This strategy has been correlated positively on numerous occasions with multi-fold increases in cell specific production rates (Kumar *et al.* 2008; Tan *et al.* 2008; Masterton *et al.* 2010). However, it is realised that if this effect could be simulated without the hindrance of cell cycle arrest, then overall titre could be improved even further. A common attempt at resolving this as been to adapt stably producing CHO cells to hypothermia by long-term exposure to sub-optimal temperatures. However, examples so far have been limited in success, with cells becoming fragile (Sunley *et al.* 2008) or productivity levels decreasing over the course of adaptation (Yoon *et al.* 2006).

The work described in first research chapter of this thesis demonstrates an alternative approach in which a host (not stably producing) CHOK1SV cell line is adapted to hypothermia prior to stable transfection. Once adapted, it was observed that cell size is increased substantially compared to the parental phenotype. Not only this, but protein content and RNA content were shown to also increase proportionately whilst the number of sets of chromosomes (ploidy) remained normal, implying inherently improved transcription rates in the hypothermia-adapted cells.

Following this, in second research chapter, production functionality was assessed in the hypothermia-adapted cultures which showed an impressive ~100% increase in reporter protein (SEAP) production compared to the parental cultures. This high productivity was also mirrored using industrially relevant proteins, cB72.3 and Enbrel, where in both transient and stable production platforms the hypothermia-adapted cell line consistently outperforms the parental cell line. Supportive evidence is also presented that the evolution process, that was required to develop this cell line, has not affected the glycan processing capabilities.

In the final research chapter, mechanistic analyses were performed to understand the biology that may underpin the observed differences. There is strong supporting evidence, including low reactive oxygen species (ROS) and disparities in mitochondrial function, that the evolved cell line could be undergoing *adaptive non-shivering thermogenesis* to overcome the stress of hypothermia. Using Affymetrix® differential gene expression analysis, 974 significantly up-regulated transcripts were observed in the evolved cell line. Such transcripts concerned: adaptive thermogenesis, increase in cell membrane fluidity (a common response to cold-stress), large cell size, cell cycle progression and transcripts involved in the unfolded protein response that have been linked to high productivity. Additionally, amino acid transporter transcripts were differentially expressed, however, overall amino acid import and export flux remained similar between evolved and parental cell lines. That said, some amino acid-specific differences were observed, perhaps most interestingly in the increased uptake of proline in the evolved cell line. Uptake of proline has been shown in other model organisms to: act as a cryoprotectant and molecular chaperone to stabilise the structure of proteins in hypothermic conditions; play a key role in antioxidant systems by reducing ROS concentrations; influence membrane fluidity and also maintain osmotic balance (Kumar & Yadav 2009; Ishmayana *et al.* 2011; Hayat *et al.* 2012; Koštál *et al*. 2012; Liu *et al.* 2013).

Many potential gene-engineering targets have been identified as a result of the mechanistic analysis that could permit the development of new cell lines without the need for a long, directed evolution process. That said, however, the shear magnitude and breadth of change to the cell observed via this process demonstrates the power of directed evolution as a cell line development system.

Contents

List of figures:

4.17 N-glycans of recombinant proteins: A) cB72.3 and B) Enbrel, produced via either stably transfected pools of evolved or parental CHOK1SV cells, or evolved or parental CHOK1SV cells in a fed-batch transient lipofection platform.

5.1 Autofluorescence of unstained samples for A) parental cells and B) evolved cells, and Forward Scatter (FSC-A) and Side Scatter (SSC-A) information for C) CellROX® Oxidative Stress Deep Red Reagent treated parental cells and D) CellROX® Oxidative Stress Deep Red Reagent treated evolved cells.

5.2 Fluorescence of parental and evolved cell lines stained with CellROX® Oxidative Stress Deep Red Reagent.

5.3 Insights into cellular mitochondrial respiration, including oxygen consumption rate from: basal respiration; ATP Production; overcoming proton leak; maximal respiration; spare respiratory capacity and also non-mitochondrial respiration, can be revealed using a sequential combination of Oligomycin, FCCP and Antimycin A & Rotenone.

5.4 Optimisation titrations of A) Oligomycin, B) FCCP and C) Antimycin A & Rotenone for use in the XF24 Mitochondrial respiration assay system.

5.5 The OCR of parental and evolved cell lines over the time course of a complete XF24 mitochondrial assay.

5.6 Individual parameters (basal respiration (A), maximal respiration (B), ATP production (C), proton leak (D), non-mitochondrial respiration (F) and spare-respiratory capacity (E)) that can be inferred from measurements of oxygen consumption rates (OCR) from the Seahorse XF24 mitochondrial assay.

5.7 Example of an electropherogram produced by the Agilent 2100 Bioanalyzer.

5.8 Volcano plot representing significantly differentially expressed transcripts ($p \leq 0.01$, FDR corrected ANOVA).

5.9 The ranked distribution of fold changes according to whether they are up-regulated in the evolved cell line (+ve fold change) or the parental cell line (-ve fold change).

5.10 Transcript expression (Avg. fluorescence) ranges for both parental and evolved cell lines.

5.11 Functional grouping of significantly differentially expressed transcripts with a fold change of ≥ 2.

5.12 Expression of cytoskeletal–associated transcripts in the evolved cell line versus the parental cell line.

5.13 Expression of glycosylation–associated transcripts in the evolved cell line versus the parental cell line.

5.14 Expression of unfolded protein response (UPR)–associated transcripts in the evolved cell line versus the parental cell line.

5.15 Expression of endoplasmic reticulum (ER)–associated transcripts in the evolved cell line versus the parental cell line.

5.16 Expression of oxidative stress–associated transcripts in the evolved cell line versus the parental cell line.

5.17 Expression of mitochondria/ mitochondrial energy metabolism–associated transcripts in the evolved cell line versus the parental cell line.

5.18 Expression of cell cycle–associated transcripts in the evolved cell line versus the parental cell line.

5.19 Expression of transcripts associated with cellular responses to stress in the evolved cell line versus the parental cell line.

5.20 Expression of amino acid metabolism–associated transcripts in the evolved cell line versus the parental cell line.

5.21 Expression of housekeeping–associated transcripts in the evolved cell line versus the parental cell line.

5.22 Notched box plots showing the relative degree of change of sets of transcripts between the parental and the evolved cell line.

5.23 KEGG metabolism pathway.

5.24 KEGG pathways in cancer.

5.25 KEGG pathways in cell cycle.

5.26 KEGG protein processing in the endoplasmic reticulum.

5.27 Absolute amino acid concentrations in supernatant throughout fed batch culture of the parental (A) and evolved (B) cell lines.

5.28 Specific amino acid transport rates of the parental and evolved cell lines through early-exponential, mid-exponential and stationary phases of fed batch culture.

5.29 Summed specific amino acid import and export transport rates of the parental and evolved cell lines through early exponential, mid exponential and stationary phases of fed batch culture and also total transport throughout culture.

5.30 Summed directionless specific amino acid transport rates of the parental and evolved cell lines through early exponential, mid exponential and stationary phases of fed batch culture and also total transport throughout culture.

List of tables:

Abbreviations

ADCC	Antibody dependent cell-mediated cytotoxicity
ANOVA	Analysis of variance
APC	Anaphase promoting complex
ATP	Adenosine triphosphate
BCA	Bicinchoninic acid
BHK	Baby hamster kidney
BiP	Binding immunoglobulin protein
CD	Chemically defined
CDC	Complement dependent cytotoxicity
CDR	Complementary determining region
CHO	Chinese hamster ovary
CHOK1SV	Chinese hamster ovary K1 suspension variant
CIRP	Cold-inducible RNA binding protein
CMV	Cytomegalovirus
CO_2	Carbon dioxide
cRNA	Complementary RNA
d.d. H_2O	Double distilled H_2O
Da	Daltons
DHFR	Dihydrofolate reductase
DI H2O	Distilled H2O
DMSO	Dimethyl sulphoximine
DNA	Deoxyribonucleic acid
DSB	Double stranded break
ECAR	Extracellular acidification rate
ECM	Extracellular matrix
ELISA	Enzyme-linked immosorbent assay
EPO	Erythropoietin
ER	Endoplasmic reticulum
ETC	Electron transport chain
GMP	Good manufacturing practice
Fab	Fragment antigen binding
FACS	Fluorescence activated cell sorting
Fc	Fragment crystallisable
FCCP	Carbonyl cyanide-4-(trifluoromethoxy)phenylhydrazone
FDA	Food and drug administration (USA)
FDR	False discovery rate
FSH	Follicle-stimulating hormone
Fuc	Fucose
Fv	Fragment variable

Gal	Galactose
GFP	Green fluorescent protein
GN	Generation number
GS	Glutamine synthetase
GS	Glutamine synthetase knock-out
HAMA	Human anti-mouse antibody
HCP	Host cell protein
HEK	Human embryonic kidney
HPLC	High performance liquid chromatography
ID	Identity
IFN	Interferon
IMM	Inner mitochondrial matrix
IVCC	Integral viable cell concentration
IVCD	Integral viable cell density
KEGG	Kyoto Encyclopaedia of Genes and Genomes
LCFA	Long chain fatty acid
mAb	Monoclonal antibody
MACS	Magnetic activated cell sorting
Man	Mannose
MCB	Master cell bank
MFU	Median fluorescence unit
miRNA	Micro RNA
MMR	Mismatch repair
mRNA	Messenger ribonucleic acid
MSX	Methionine sulphoximine
MTX	Methotrexate
NHEJ	Non-homologous end joining
NS0	Murine myeloma
OCR	Oxygen consumption rate
PAGE	Polyacrylamide gel electrophoresis
PBS	Phosphate buffered saline
PDI	Protein disulphide isomerase
PFA	Paraformaldehyde
pH	Potential hydrogen
PI	Propridium iodide
pNPP	Paranitrophenyl phosphate
qP	Cell specific productivity
RFU	Relative fluorescence unit
RIN	RNA integrity number
RIPA	Radioimmunoprecipitation assay
RNA	Ribonucleic acid
ROS	Reactive oxygen species
rpm	Revolutions per minute
rRNA	Ribosomal ribonucleic acid

scFv	Single chain fragment variable
SD	Standard deviation
SDS	Sodium dodecyl sulphate
SEAP	Secreted alkaline phosphatase
siRNA	Small interfering RNA
TAC	Transcriptome analysis console
TBE	Tis/Borate/EDTA
TCA	Tricarboxylic acid cycle
TE	Tris/EDTA
THF	Tetrahydrofolate
TPA	Tissue plasminogen activator
Tris-HCL	Tris/Hydrocholric acid
TRL	Technology readiness level
tRNA	Transfer ribonucleic acid
UCP	Uncoupling protein
UPLC	Ultra performance liquid chromatography
UPR	Unfolded protein response
VCD	Viable cell density
VH	Variable heavy
VL	Variable light
WCB	Working cell bank

Chapter 1:

Introduction

This chapter introduces and discusses the literature that underpins the work described later in this thesis. Specifically, this section will review the history of the biopharmaceutical industry with a spotlight on recombinant therapeutic protein production, focusing on crucial milestones and highlighting examples of the advantages, disadvantages, obstacles and achievements that the industry has experienced to date. A more detailed examination on the use of mammalian cell culture, particularly Chinese Hamster Ovary (CHO) cells, for the production of large and complex products such as monoclonal antibodies (mAbs) will follow this. The future and predicted directions for the industry will also be considered alongside emerging technologies. To conclude this section, the biology and relevant literature associated with hypothermic cell culture and 'directed evolution' as a strategy for improving biopharmaceutical production will be discussed.

The Biopharmaceutical industry

1.1 A brief history of the biopharmaceutical industry

Most available medicines today can be categorised into four groups depending on their method of manufacture: Throughout history, the majority of medicinal substances are organic compounds of relatively low molecular weight created by direct chemical synthesis. Related to this is the category of those obtained by semi-

synthesis, where the initial substance is derived from a natural host but is subsequently modified by organic chemistry to become a biologically active pharmaceutical, for example semi-synthetic antibiotics. Thirdly, there is the group of drugs that are acquired by direct extraction from a natural biological source, for example, alkaloids. Finally and most recently there is the category of biopharmaceuticals that has shown dramatic growth since its establishment, with an average annual sales increase of about 20% (Walsh & Murphy 1999; Matasci *et al.* 2008). Biopharmaceuticals can be most simply defined as medical drugs produced using biotechnology. Specifically, biopharmaceuticals are non-native products manufactured by an engineered host organism or cell, as opposed to direct extraction or derivatives of inherent, natural compounds (Walsh 2010). The biopharmaceutical industry encompasses a range of product types, such as proteins and nucleic acids, constructed via a variety of methods in a vast assortment of different hosts or industrial *workhorses*.

The production of the first recombinant protein approved for therapeutic use occurred in 1982 and was developed by a company called Genentech. The substance was biosynthetic human insulin, marketed as Humulin, which was produced in *Escherichia coli* using recently pioneered work on recombinant DNA technology (Johnson 1983). Recombinant DNA technology fundamentally involves molecular cloning to bring together genetic material from two or more sources to create a genetic sequence of nucleic acids that would not otherwise be found in nature (Gualandi-Signorini & Giorgi 2001). As Humulin has a relatively simple polypeptide structure, not requiring any complex post translational modifications such as glycosylation (the addition of carbohydrate moieties to specific amino acid residues of the protein), the production capabilities of *E. coli* made it an ample host choice for this therapeutic. However, many drugs demand more complex processing capacities from the host and in such cases mammalian cells are considered appropriate workhorses due to their ability to perform such tasks (Hu 2012). In 1986, the emergence of mammalian cell culture as the biopharmaceutical industry's main host of choice was triggered. This was due to the approval of recombinant tissue plasminogen activator (TPA), a therapeutic protein used to

treat acute myocardial infraction and embolic or thrombotic stroke, which was produced in Chinese Hamster Ovary cells, again by Genentech (Goldhaber *et al.* 1986; Walsh 2010). Mammalian cells have inherent capacity for correct folding, assembly and post-translational modifications of proteins that are to be fit for therapeutic purposes in humans (Hu 2012).

Although the first therapeutic recombinant protein was approved in 1982, the first monoclonal antibody (mAb) (now the most predominant type of biopharmaceuticals) was produced years before in 1975 by hybridoma technology (Köhler & Milstein 1975). In short, this technology comprises of exposing (immunising) a mammal, e.g. a mouse, to the antigen that an antibody is to be generated against, B cells are then isolated from the mammal's spleen and these are then fused with immortalised myeloma (cancer) cells and after a period of selection, culture and screening, the antibodies produced by the fused cells are harvested (Nelson *et al.* 2000). However, the first therapeutic mAb produced by hybridoma technology was not ready to be released on the market until 1986 and still then such products harnessed immunogenic side effects, such as the HAMA (human anti-mouse antibody) response in which the human body would create a new set of antibodies against the hybridoma, with patients suffering symptoms from mild rashes to life-threatening renal failure (Tjandra *et al.* 1990). Not only this, but the efficacy of the mAbs was poor which is commonly attributed to reduced synergy of the antibody with the patient's immune system (Waldmann 2003). In 1984, recombinant DNA technology was employed to produce *chimeric* antibodies, comprised of a human constant region (Fc) and mouse antigen binding domains: the heavy and light chain variable regions (VH and VL) (Morrison *et al.* 1984). Chimeric antibodies are around two-thirds human, however, despite eliciting the desired immune responses equivalent to those of a human antibody, they also stimulated undesired immunogenic reactions (Waldmann 2003). A couple of years later in 1986, *humanised* anitbodies were developed which were 90% human. These are distinct from chimerised antibodies as the protein sequence of a humanised antibody is identical to that of a human except for the complementary determining regions (CDR), which are mouse derived (Jones *et al.*

1986; Riechmann *et al.* 1988). In 1990, phage display technology was implemented into antibody discovery processes. In phage display, recombinant proteins, such as single-chain Fv (scFv) or Fab' molecules are displayed on the surface of a filamentous bacteriophage. This is achieved by fusing sequences encoding the protein to be displayed with genes encoding the pIII or pVIII coat proteins. Screening a large combinatorial phage library of heavy and light chain variable regions for binding to a particular antigen (in Fab' or scFv format) allows identification of phage displaying scFv or Fab'-specific for the antigen (McCafferty *et al.* 1990; Carmen & Jermutus 2002). These phage can be purified and the variable region sequenced cloned. At this stage the variable regions can be engineered into a full mAb if desired.

By 2002, phage display had provided approximately 30% of all human antibodies in clinical development (Kretzschmar & Rüdent 2002). By 2005 there were also over 30 different drugs in clinical testing which contained variable regions encoded by human sequences from *transgenic animals*. Animals that are transgenic contain a gene or set of genes that have been transferred from a different organism or species. Antibodies produced in this way, in addition to phage display technologies, are considered fully human, with none of the immune responses associated with, for example, chimeric antibodies, and therefore such products had better success in the clinic (Lonberg 2005).

Over time, a variety of host cell systems have emerged that can be employed for the production of different recombinant proteins; these include mammalian cells, yeast (particularly *Saccharomyces cerevisiae*), bacteria (particularly *E. coli*), hybridomas, transgenic animals, insect cells and even plants. Figure 1.1 shows the proportion of use of different hosts in 2009 (Ferrer-Miralles *et al.* 2009).

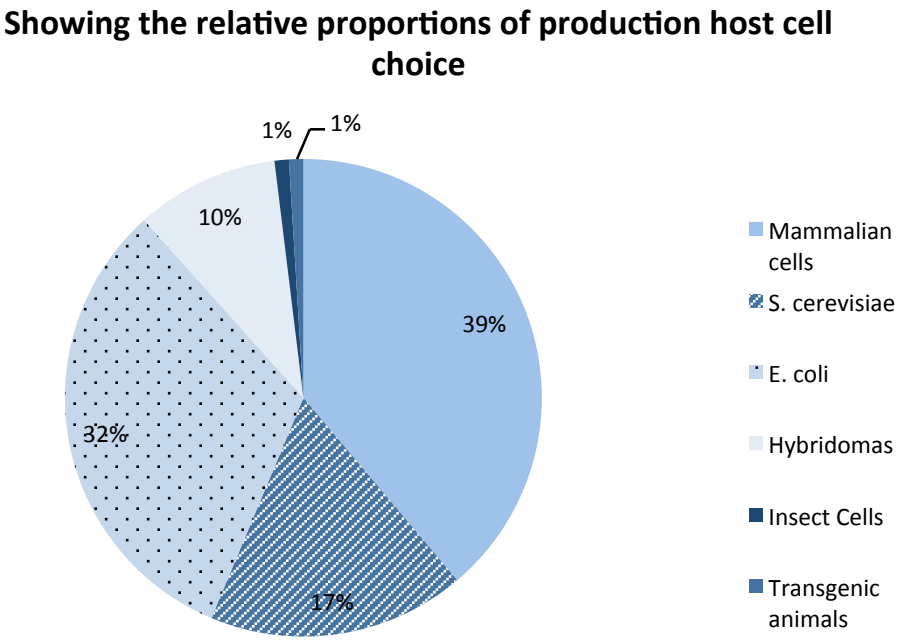

Figure 1.1 The percentage usage of different host cell systems for production of recombinant proteins approved by 2009 for biopharmaceutical purposes. It can be seen that mammalian cells constitute the largest percentage of all host cell systems.

Today, mammalian cell culture is the preferred choice for production of monoclonal antibodies (and other recombinant therapeutic proteins) due to their inherent cellular machinery that allows for better protein production, including crucial post-translational modifications such as glycosylation (addition of carbohydrate molecules) which promotes proper protein folding and stability. Glycosylation also has dramatic impact on the function and solubility of recombinant proteins (Bork *et al.* 2009; Hu 2012).

The next section will focus on the process of producing recombinant proteins in mammalian cells, particularly within CHO cell lines, with a brief justification and history of this popular host choice.

1.2 Mammalian cell culture and the predominance of CHO

An array of cell lines are available for therapeutic protein expression, including Chinese Hamster Ovary (CHO) cells, Baby Hamster Kidney (BHK) cells, murine lymphoid (NS0 and 5P2/0) cells, Human Embryonic Kidney (HEK) cells and cells derived from the human retina known as PER-C6 cells (Jones *et al.* 2003; Hu 2012). Most of these cell lines are suspension adapted to warrant a high cell density and effective protein production through efficient mass transfer and scale-up in large bioreactors (Tescione *et al.* 2015). Partly as a result of CHO's long history of use - since the start of production of the licensed biopharmaceutical tissue plasminogen activator in the 1980's - CHO cells have become the dominant choice for commercial mAb production (Kelley 2009). Since then, much knowledge and expertise has accumulated surrounding CHO cells, ensuring they have remained, and are predicted to persist as, the industry's premier workhorse with around 70% of all therapeutic recombinant proteins being a product manufactured in CHO cells (Jayapal *et al.* 2007). In recent years, of the top 10 selling biologic drugs, CHO cells accounted for US$39 billion in worldwide annual sales, while the other production cell lines accounted for only US$14 billion (Jayapal *et al.* 2007; Noh *et al.* 2013). A short account of the history of the Chinese hamster and its contribution to scientific research is given in box 1 below.

Box 1. The Chinese Hamster and its contribution to scientific research.

Chinese hamsters, *Cricetulus griseus*, belong to a family of rodents native to Mongolian and northern Chinese deserts. They were first used as a laboratory specimen for typing *pneumococci* in 1919. By the early 1920's they became valuable tools for research into epidemiology due to often being carriers of a parasite known as *Leishmania* that causes black fever. As a consequence of this, when they were smuggled into the United States, those responsible (Dr. R. Watson and Dr. C. H. Hu) were later accused of war crimes resulting in the imprisonment of Dr. C. H. Hu (Yerganian 1985). In the mid-20th century, efforts at domestication of the Chinese hamster led to a large degree of inbreeding and

consequently the development of hereditary diseases. Because of this, an interest in hamster genetics was provoked which led to the discovery of the low chromosome number that Chinese hamsters' possess (2n=22). Low chromosome number made these animals useful models in tissue culture studies and radiation *cytogenetics* (a branch of genetics concerned with the structure and function of the cell, particularly the chromosomes). In 1957, Dr Theodor T. Puck of the University of Colorado first isolated an ovary from a female Chinese hamster and successfully established cells in culture plates (Tjio & Puck 1958). The resilience of these cells and their ease of *in vitro* cultivation became obvious very quickly and karyotype heterogeneity between cell populations became a key area of interest and a model system for chromosome abnormality studies. CHO cells later became an in important contribution to biomedical and cell biology research (Jayapal *et al.* 2007). The transition from laboratory model to industrial bioreactors was brought about by early work involving mutagenesis of these cells and isolation of certain *auxotrophs* (a mutant individual that has a nutritional requirement not shared by the parent, e.g. losing the ability to synthesise particular compounds required for growth) (Puck & Kao 1967). Specifically, such auxotrophic mutants showed unique requirements for maintaining viability and growth over long time periods in culture. Certain cells had deficiencies in metabolic enzymes and one bioprocess-relevant example of this was the mutagenesis of CHO-K1 that produced DXB11 (or DUKX), a cell line with a deletion of one dihydrofolate reductase (DHFR) allele and an inactivating mutation in the second allele. This cell line has now become a standard expression system in many upstream processes requiring vector-mediated gene transfer into the cell (Urlaub & Chasin 1980; Jayapal *et al.* 2007) (see section 1.2.2 for more details). Being able to transfect, select, amplify and subsequently stably express biologically active proteins quickly become of great interest to many biopharmaceutical companies. There is a sense of irony that these hamsters, originally thought to be planned for use as agents of biological warfare have instead save thousands of lives from illnesses as serious as cancer every year (Jayapal *et al.* 2007).

1.2.1 Producing the therapeutic - Introduction

The first step in developing a producing cell line is the delivery of the recombinant DNA, via a plasmid expression vector or virally, into the host cell nucleus for chromosomal integration (although integration is not always necessary – see below). This process is called transfection and there are several protocols commonly used including lipofection, electroporation and polyethylenimine (PEI) mediated transfection. The term 'transduction' is preferred for virus-mediated DNA transfer (Hu 2012). Recombinant therapeutic proteins can be produced by two methods, stable gene expression and transient gene expression, which are both outlined below.

1.2.2 Stable gene expression

Typically, recombinant proteins that are produced on a large-scale for market supply are manufactured using stable gene expression, as this method is renowned for generating the best yields and also provides better product consistency due to the clonality of cell lines being used. When recombinant DNA is stably transfected into the host cell it means that it has integrated into the host chromosome and the transgene is subsequently replicated with host genomic DNA during all following cell divisions (at mitosis) (Hu 2012). The probability that the transgene integrates into the host chromosome is very low and even lower for integrating into loci where it will be sufficiently well expressed. Hence, after the host cells have been transfected, a selection and screening strategy is required to determine in which cells this has successfully occurred. Further rounds of screening along with a cloning step are usually required to identify the most suitable cell lines for a manufacturing process. Depending on the expression system being used, there may also be a requirement for a gene amplification strategy and including the aforementioned steps the complete process could all take several months (Porter *et al.* 2010; Lai *et al.* 2013).

The two most commonly used selection systems used in industry are the dihydrofolate reductase (DHFR)/ methotrexate (MTX) system and the glutamine synthetase (GS)/ methionine sulphoximine (MSX) system, both of which are outlined below (Butler 2007).

1.2.2.1 Dihydrofolate reductase (DHFR)/ methotrexate (MTX)

DHFR is a small monomeric enzyme that catalyses the conversion of a common vitamin, folic acid, into tetrahydrofolate (THF). THF is a cofactor carrier for one-carbon moieties required for multiple biosynthetic reactions including purine, thymidine and glycine synthesis. There are two DHFR deficient ($DHFR^-$) CHO cell mutants which were both isolated by Chasin and colleagues in the early 1980's that are currently used as host cell lines, DG44 (Urlaub & Chasin 1980; Urlaub *et al.* 1983; Urlaub *et al.* 1986) and DXB11 (Graf & Chasin 1982). Both of these cell lines are derivatives of a proline auxotroph established in the late 1960's by Dr Theodor T. Puck's group at the University of Colorado (Kao & Puck 1968). Cell lines can be obtained from $DHFR^-$ host cells by transfection with a DHFR gene and selection in medium lacking purine derivative (hypoxanthine), thymidine and glycine, as $DHFR^-$ cells are auxotrophic for these nutrients. Amplification of the cloned DNA can be achieved by subsequent culture in media containing a folic acid analogue, methotrexate (MTX) that blocks DHFR activity. Successive increases in the concentration of MTX are applied during each round of selection. This sequentially raises the selection pressure, requiring the transfected cell to increase expression of DHFR in order to stay viable, in which cells must survive further reduction in DHFR activity by increased MTX. Surviving cells, in theory, will have amplified the copy number of the DHFR loci and due to the genetic linkage between this and the transfected gene of interest, this process ensures that the transgene is too co-amplified, increasing the chances of isolating a high producing strain (Butler 2007; Jayapal *et al.* 2007; Lai *et al.* 2013). Due to the successive rounds of increasing inhibitor treatment, it is not unusual for the above process to take over six months before the producing cell line can enter the product production and evaluation stage (Jayapal *et al.* 2007).

1.2.2.2 Glutamine synthetase (GS)/ methionine sulphoximine (MSX)

Comparable to the DHFR system, this system works on the principle of a key metabolic pathway and a relevant inhibitor for amplification and again, like the DHFR system, the gene for glutamine synthetase and the gene for the recombinant protein product are co-transfected for integration into the host cell genome. Glutamine synthetase is the enzyme responsible for the biosynthesis of glutamine from glutamate and ammonia. In a mammalian cell, this reaction is the only pathway for glutamine formation. When glutamine is not present in growth medium, the GS system is essential for mammalian cell viability in culture (Butler 2007). Certain mammalian cell lines do not express sufficient glutamine synthetase to survive without supplemented glutamine. Mouse myeloma cells are an example of this and with such cell lines a transfected GS gene can function as a selectable marker by permitting growth in glutamine free media. CHO cell lines are different in the way that they inherently can express sufficient glutamine synthetase without glutamine supplementation in the growth media. Because of this, a glutamine synthetase inhibitor, methionine sulphoximine (MSX), is often used to inhibit endogenous glutamine synthetase activity so that only cells with additional glutamine synthetase activity can survive. Such transfectants should, in theory, also now be carriers of the gene of interest. The GS system, proprietary of Lonza Biologics, allows for rapid selection of high yielding cell lines, typically generating the lead cell line in less than 20 weeks (Butler 2007; Jayapal *et al.* 2007; Hu 2012). This system can be further enhanced by using a GS-knockout parental cell line which has had the endogenous GS gene specifically targeted, meaning the efficiency of CHO cell line generation is improved. Not only this, but culture productivity has been shown to increase two- to three-fold through the use of GS-knockout as parent cells (Fan *et al.* 2012; Le *et al.* 2015; Rajendra *et al.* 2015)).

The highest producing clones that are selected through the above processes will go on to be cultured and expanded to inoculate the bioreactor where the recombinant protein will be expressed, harvested and purified in the downstream process (Hu 2012).

1.2.3 Transient gene expression

Transient transfection has been used for many years in biological laboratories but only in the last two decades has it been scaled up for use in biopharmaceutical work. Transient gene expression is typically reputed for producing lower yields of recombinant product compared to stable gene expression as the genetic material is only transiently expressed. In this type of gene expression, all of the cells are transfected but the introduced DNA is not usually integrated in to the nuclear genome of the host cell and over time the introduced DNA will be diluted through mitosis or degraded. Transient transfection can be improved by transfecting cells with as many copies of the introduced DNA as is possible and also by transfecting a high proportion of the cell population (i.e. increasing transfection efficiency), this is because those cells that have not been transfected will still be viable and consequently use up nutrients and space in the culture media that would be more valuable if utilised by the productive cells. However, some transfection methods can be toxic to cells so the optimisation process often has to determine a balance between these factors (Geisse & Fux 2009; Hu 2012).

Transient transfection is often employed at the early stages of development, commonly to test the effect of the production process on the end characteristics of the recombinant product (Condreay *et al.* 1999; Butler 2007). This is because, compared to stable gene expression, the transient process is multiple-fold faster and conducted in a matter of weeks as opposed to many months. Performing product tests from stable cell lines would be costly in terms of consumables and labour, particularly if the product possessed undesirable characteristics at the end of it (Butler 2007; Le *et al.* 2015). Product characteristic tests are crucial in

biopharmaceutical production, for example, the glycosylation of a mAb determines the half-life and efficacy of that drug in the patient and glycosylation patterns can vary from cell line to cell line - the process is often considered to be as important as the product and the choice of cell line is paramount to process performance (Jenkins *et al.* 1996; Croset *et al.* 2012). Transient production also offers the opportunity for small amounts of new drugs to be manufactured for early stage clinical trials and also production on a small scale for prospective personal drugs or drugs for rare illnesses. However, the yields from transient gene expression are increasing as technology advances and protocols are optimised and there is expected growth in the use of transient gene expression for general therapeutic protein manufacture (Geisse & Fux 2009; Butler & Meneses-Acosta 2012; Rajendra *et al.* 2015).

1.3 Downstream processing – a brief summary

After cell line development, scale-up procedures and production of the recombinant protein in the bioreactor, the product is then harvested and must be purified into its final, safe, pure, active and marketable form. To follow FDA guidelines, every product has to conform to an eight-point model (Yu 2008):

1. Identity – *is the exact amino acid sequence known?*
2. Quality – *has the process provided a product comparable to other successful methods?*
3. Purity – *what other, undesired substances are present?*
4. Activity – *does the product provide the medicinal objective it was intended to?*
5. Heterogeneity – *are all the protein products consistent within that batch?*
6. Stability – *for how long is molecular stability of the product maintained?*
7. Process consistency – *are the cell line and following manufacturing methods reliable, reproducible and predictable?*
8. Safety – *are there any risks associated with the product and are these outweighed by the medical benefits?*

The obvious contaminants that need to be removed are the biomass (cell debris, host cell proteins which can damage the product, DNA etc.) and water. In addition to these, product variants (for example if the protein product has become truncated, aggregated or hydrophobic) must also be removed during downstream purification. Since mAbs are secreted into the cell culture medium, the removal of cells is usually achieved by centrifugation, however, this process does not completely remove all cell components and subsequently *depth filtration* steps are implemented. Depth filtration refers to the use of porous materials that are capable of capturing particulates throughout its matrix rather than just on its surface (Fiore *et al.* 1980; Shukla *et al.* 2007). In bioprocessing, such tools usually comprise of polypropylene or cellulose fibres with a filter aid and binder and are single use. The pore size usually ranges from 0.2 μm to 0.45 μm and removal of certain contaminants in this step has shown to prevent potential issues in the next step, such as problems with turbidity during elution of the capture Protein A chromatography column (Gagnon 1995). Protein A is an immunoglobulin-binding molecule making it a useful tool for the capture of mAbs. Fundamentally, Protein A is covalently fixed to beads that are packed into a column in which the cell culture supernatant can be directly loaded. After a wash step, only mAbs that have a high affinity for Protein A will be retained in the column and all other nonbinding proteins will flow through. The mAb product can then be eluted from the column using a low pH solution that disrupts the protein A–mAb complexes. This process is highly selective and can yield a product of over 99% purity (Gagnon 1995; Shukla *et al.* 2007). The FDA stipulates two orthogonal dedicated steps for viral reduction and the next purification stage is a low pH viral inactivation. Low pH treatment has been shown to fully inactivate retroviruses for a variety of products in the biopharmaceutical industry (FDA Q5A Guidance Document 1998). The addition of an acid solution, such as 0.5 M phosphoric acid, to the elution pool lowers the pH to below 3.8. Strong acids such as HCl are not usually used due to the risk of local protein denaturation where the product is added (Shukla *et al.* 2007).

Following this, the solution is then neutralised so the pH range allows the product exist more stably. Subsequent steps are known as 'polishing chromatographic steps' that are aimed at reducing high molecular weight aggregates, host cell protein impurities, DNA and leached Protein A that has persisted after the Protein A chromatography step. Viral filtration is often next employed in which the fluid is driven though viral filters with pore sizes in the nanometre range, with the aid of pressurised tanks. Following the above downstream purification processes, the product is then buffer exchanged in an ultrafiltration/ diafiltration system. The retentate from this step is then filtered to generate the bulk drug substance – this step is called absolute filtration. The product is then ready for 'fill and finish operations' which incorporate a range of processes depending on the product, including freeze-thawing, freeze drying/ lyophilisation and filling (dispensing the product into vials, syringes, etc.) (Patro *et al.* 2002; Shukla *et al.* 2007).

Downstream process, although not central to the work described later in this document, is an extremely important part of biopharmaceutical bioprocessing and in the case of monoclonal antibodies accounts for 80-90% of the total production costs. It is relevant to upstream processes in the way that modifications of upstream processes can have considerable knock-on effects downstream. For example, if viable cell density during expression can be increased, or cell specific productivity can be significantly improved, there will be a higher proportion of product in the culture supernatant and consequently less supernatant running through expensive downstream equipment, for example, chromatography columns, which would cut down materials costs. The purification process can also be affected by factors that may vary from culture to culture, for example the presence of antifoam or other cell line specific media additives (Doran 1995).

1.4 The current state and outlook of cell culture technology for biopharmaceutical production

The impact of advances in biopharmaceutical manufacturing, particularly using CHO cell lines, on the pharmaceutical industry as a whole is vast. Monoclonal antibodies in particular constitute the largest product category by far. For example, in 2003 there were 75 candidate mAbs in production and just three years later this number rose to 400 by which time the global annual sale of mAbs was US$20.6 billion (Coco-Martin & Harmsen 2008). By 2009, another three years later, mAb sales grew to US$38 billion out of the total US$99 billion biopharmaceutical market (Evers 2010; Walsh 2010). Most of this growth has been attributed to better production of cell lines and optimisation of cell culture strategies as opposed to simple but costly expansion of culture volumes and reactor sizes (Walsh 2010).

There are two key approaches of cell and metabolic engineering strategies that have greatly increased titre of product; 1) increasing cell specific productivity (qP) and 2) increasing the integral viable cell concentration/ density (IVCC/ IVCD) – the total amount of cellular biomass that can be maintained in a viable state in a bioreactor over the culture time period. These two approaches are exemplified by two significant pieces of research conducted by different groups. Firstly, the identification and subsequent delay or even elimination of programmed cell death has been important for increasing IVCD. Initial work on this focussed on Bcl-2/ Bcl-X(L), which are effectors of apoptosis well characterised by cancer studies. These genes were overexpressed in CHO cells and it was found that overall titre could be greatly increased without loss of product quality (Majid *et al.* 2007; Carlage *et al.* 2012). It was also demonstrated that Bcl-2 transfected cell lines became more robust in the sense that they became more resistant to changes in pH, hyperosmotic media and high concentrations of ammonia and lactate (Dorai *et al.* 2009). Although not historically as successful as attempts at increasing IVCD, research into increasing qP is still prevalent. There are two main bottlenecks surrounding qP, the rate of translation of mRNA to protein and the rate of folding

and assembly of the protein product. These rates can vary greatly, introducing time costs during production. Increases in qP have been demonstrated by the manipulation of certain molecular chaperones associated with the protein folding of an antibody. BiP (binding immunoglobulin protein) and PDI (protein disulphide isomerase) are examples of such chaperones that are used to make the antibody in the endoplasmic reticulum. In 2005, Borth *et al.* hypothesised that an increase in folding and assembly machinery would make the cellular production of a mAb quicker and consequently increase qP. They found that overexpression of PDI alone caused an increase in specific product secretion rate by 37% (Borth *et al.* 2005; Butler & Meneses-Ascosta 2012).

The expression level of the transgene can also be attributed to the vector design as well as the loci of integration of that vector and vast improvements have been made in this area (Le *et al.* 2015). For example, there has been much focus on the optimisation of the promoter region (the region that drives the expression of the transgene). Typically, promoters have been chosen because of their availability and most frequently this has included promoters derived from viruses, humans and mice. However, more recently, promoters from CHO cells have also gained attention including time-dynamic promoters that can, for example, drive expression of the transgene in concert with cell growth. Endogenous promoters such as these offer more predictable expression levels (Le *et al.* 2013). The construction of synthetic promoters has also been of interest as way of modulating gene expression levels (Brown *et al.* 2014). Synthetic promoters allow the regulatory motifs to be customised into different combinations offering precise control of recombinant transcriptional activity, whilst also being less species-restricted. It is thought that the use of synthetic promoters in the future could allow for more consistent and stable gene expression than using natural promoters (Le *et al.* 2015).

Epigenetics and genome editing strategies are increasingly being employed in cell line development; for example, gene silencing can be used to alter the nutritional requirements of the cell and consequently transgene expression (Seth *et al.* 2006;

Osterlehner *et al.* 2011). It is predicted that efforts in genome editing will likely be directed towards identifying transgene integration sites that can lead to long–term expression stability and high expression levels, as well as engineering the host cells characteristics (Le *et al.* 2015). As more and more genome sequences of host and producer cell lines become readily available (Xu *et al.* 2011; Brinkrolf *et al.* 2013; Lewis *et al.* 2013), there is a growing trend towards the use of genomic, transcriptomic and proteomic tools in the development of future cell lines, a topic which is discussed in more detail in box 2 (Le *et al.* 2015).

Box 2. "'Omics" and its contribution to advances in biopharmaceutical production

Since the publication of the full human genome sequence in 2003, a key milestone in genetic research, it has become ever easier, faster and cheaper to sequence macromolecules (DNA, RNA etc.). This has meant the information that can be derived from such data is no longer an unattainable notion to researchers in many fields (Kandpal *et al.* 2009). Subsequently, research focus has moved beyond the genome to the role of genes, including transcriptional regulation, biochemical functions of the gene products and how they influence metabolism. This has resulted in a collection of fields of research (such as transcriptomics, proteomics and metabolomics) that have collectively been coined 'omics, inspired by the original term, genomics. Through further bioinformatics analysis, useful information can be derived, for example, identifying potential gene targets and key pathways for engineering purposes (Yan *et al.* 2015). To put this in perspective, in the last half-decade, over 1000 peer-reviewed articles have been published involving 'omics technologies in combination with CHO cells alone – not accounting for other types of production hosts. Prior to this, less than 200 studies of this vein had been published in total, demonstrating the rapid growth of interest in this area (Lewis *et al.* 2016). The use of 'omics in the biopharmaceutical industry is vast, providing improvements in many areas of

the production process; several examples of this will be demonstrated here.

As has been previously discussed, cell lines in industry are commonly genetically modified to achieve more desirable, fit-for-purpose phenotypes. However, unwanted genetic modifications can also arise, including genetic duplications and chromosomal rearrangements, often due to environmental stresses such as media adaptation and other culture conditions. As a consequence of this, industrial cell lines show distinctive genomes and epigenetic profiles. However, comparison between recombinant cell lines has been found to be rather complex, and such cell lines tend to be preferentially compared to their parental, unmodified versions that serve as a reference. This information, coupled with reliable gene annotation, has been used to understand cell-line specific cellular responses to system perturbations as well as enabling high throughput methodologies such as microarray profiling (Becker *et al.* 2011; Rupp *et al.* 2014). Other work has examined transcripts that are differentially expressed through the course of batch culture, including lag, exponential and stationary phases. Over 1400 mRNAs were found to be differentially regulated over this time frame, alongside 100 micro (mi)RNAs whose primary role is to regulate mRNAs. This work gave valuable insights into understanding growth-phase dependant regulation of genes, highlighting that any actions in future experiments and production processes should consider timing as an important factor owing to the way gene regulation may effect, or be effected by, any system inputs and modifications (Bort *et al.* 2012).

Proteomics, too, has provided valuable information for biopharmaceutical production processes. For example, one research group has been able to characterise CHO cell host cell proteins (HCPs), which, as previously discussed, the removal of such proteins is an important step in downstream processing to ensure patient safety (Valente *et al.* 2014a). The same group has also quantified HCPs along a long-term cell culture process, enabling them to link the age of cells to specific HCP profiles (Valente *et al.* 2014b). In addition to this, as a separate study, this group have evaluated HCP-mAb interactions (Levy *et al.* 2014). More

sophisticated proteomic techniques have allowed the characterisation of glycosylation patterns to be linked to corresponding genomic modifications (North *et al.* 2010).

A common problem in research and development in the biopharmaceutical industry lies in the scale up from bench to manufacturing volumes - there is often disparity when trying to predict how a cell line will perform in large-scale bioreactors from laboratory scale experiments, even though culture media and parameters are kept the same (Lewis *et al.* 2016). Metabolite profiling is a branch of 'omics that has shed some light on this issue. For example, Aranibar *et al.* (2011) compared the intra and extracellular metabolite profiles of a recombinant CHO cell line grown at bench (7L) and industrial (5000L) scales. They demonstrated that at larger scales, the cell line showed a tendency to rely on glycolysis and found also that low viability at such scales was associated with reduced galactose consumption (Aranibar *et al.* 2011).

From the emergence of 'omics technologies in many areas of bioprocess development, alongside continual investment from large biopharmaceutical companies in to the improvement of sequencing platforms, it is evident that the way in which we learn about, manipulate and choose our host cell lines for protein production is changing. However, there is still much room for improvement in this area: although obtaining the data is becoming easier and cheaper, interpreting such information is the principal bottleneck, alongside the lack of sufficient computational tools. There is demand for an improved, standardised workflow for 'omics technologies and a framework for their integration (Lewis *et al.* 2016).

In upcoming years it is also expected that disposable, single use and reusable technologies will be increasingly adopted by GMP (good manufacturing practice) laboratories due to the associated economic benefits, for example, it has been estimated that a production facility designed with single-use systems can reduce

capital costs by approximately 40% (Shukla & Gottschalk 2013). Continuous bioprocessing is another example of an emerging application that could change the way many recombinant proteins are manufactured. Simply, this involves running a bioreactor at a fixed cell concentration and fixed volume for up to 90 days, during which time there is a constant flow of culture media allowing a constant harvest volume to be obtained (Langer & Rader 2014). Other great improvements in mammalian cell based biopharmaceutical production have been made, and continue to advance, in areas such as: media, feed and nutrients, process control to improve product quality, dissolved oxygen control and ammonia reduction (Zhu 2012; Le *et al.* 2015). One commonly employed yet relatively simple method of enhancing production is to introduce a phase-shift in temperature, which, due to its extensive relevance to the work in this thesis, is discussed separately in section 1.6.

As patents expire and research expands, alternative strategies to improve biopharmaceutical processes are constantly anticipated. A moderately novel approach to improving biopharmaceutical yields is that of directed evolution which has only been partially exemplified in the literature a handful of times. These examples are discussed in section 1.5, where the concepts and justifications of directed evolution for cell line improvement are reviewed in more detail.

1.5 Directed evolution as a strategy for cell line improvement

Introduction

This section will focus on directed evolution as a strategy for improving cell lines used in bioprocessing, particularly in CHO cells. For background purposes and in order to understand why certain methods are employed, the heterogenetic nature of CHO cells is described. Following this, evolution itself and the mechanisms by which it manifests will be explored whilst being put into context of a cell culture

environment. Finally, current examples of directed evolution in this industry are outlined along with the rationale of this project.

1.5.1 Heterogeneity and instability of CHO cells

Since their development as an immortal cell line in 1957, CHO cells have long been studied with regards to their chromosome structure, karyotyping and gene mapping. As is common for many transformed cell lines, CHO cell populations are functionally heterogeneous, meaning they are diverse in their functional phenotypes. This diversity derives from an inherent genetic instability that can modify chromosomal arrangement, transcriptional activity and gene copy number (Derouazi *et al.* 2006, Xu *et al.* 2011, Davies *et al.* 2013). Since their isolation, it can be estimated that CHO cells have undergone about 25000 generations/ division events. This, along with their inherent heterogeneity means their genome has undergone constant rearrangement that has allowed the evolution of new phenotypes that have permitted cells to adapt and proliferate in a range of synthetic environments (Hu 2012). This heterogeneity has been exploited by the biopharmaceutical industry to generate numerous functional cell lines that can be used against different selection marker systems (Jayapal *et al.* 2007), can be used in different growth medias and can reach high cell densities and maintain high viabilities over a long culture period (Prentice *et al.* 2007).

Although genetic heterogeneity is often used to an advantage in terms of generating new cell lines with useful metabolic traits, it is also undesirable because it is difficult to control, creating unpredictability in the performance and manufacture of recombinant protein product. An example of this was shown in the work by Kim *et al.* (1998) who found that a decrease in DHFR expression was due to loss of the recombinant gene, owing to the instability of the CHO cell line. Sub-populations of cells with a new phenotype, such as absent productivity, can arise in short time periods and, if a new phenotype confers a *selection advantage* (see section 1.5.2), parental phenotypes may be outcompeted and eventually completely disappear from the population.

Random, spontaneous mutations in genes controlling apoptosis and also DNA repair and replication are key drivers of genetic instability. Such events facilitate a high rate of genomic acquisitions, alterations and deletions (see section 1.5.2.1 on DNA mutation) (Lengauer *et al.* 1998). Although relatively few specific genetic instability studies have been performed using CHO cell lines specifically, a large amount of information can be derived from research using cancer cells as they too have inherent genetic instability. Findings made in this area can be extrapolated to CHO cells in order to understand how inherent genetic instability impacts the gain or loss of cell functions and phenotypes (O'Callaghan & James 2008; Negrini *et al.* 2010). Associations between the presence of genomic instability and mutations in genes that maintain a stable genome, for example DNA mismatch repair (MMR) genes, have been made. Without a fully functional mismatch repair system, damage to DNA or improper synthesis of DNA during replication cannot always be rectified. This is likened to the process of *carcinogenesis*, where a normal cell is genetically reprogrammed to undergo uncontrolled proliferation due to an initial mutation in a DNA repair gene, which then leads to a subsequent mutation in a proto-oncogene. Mutations in proto-oncogenes can cause that gene to become an oncogene, which in turn can lead to the inactivation of other tumour suppressor genes (O'Callaghan & James 2008).

This project aims to manipulate this genetic instability by directed evolution in order to generate CHO cells with enhanced biomanufacturing properties. Specifically, culturing regimes for rapid *in vitro* evolution are to be deciphered, which requires an understanding of key evolutionary processes that take place in a sub-culturing environment, namely; mutation events with respect to natural selection, adaptation and genetic drift. These mechanisms of evolution are described in section 1.5.2 below.

1.5.2 Evolution: Mutation, natural selection, adaptation and genetic drift

1.5.2.1 Mutation

Genetic mutations encompass a variety of changes in the nucleotide sequence of an organism genome. They are a result of DNA damage that has bypassed relevant repair processes. Errors such as these most often occur during DNA replication as part of cell division. Depending on the location and severity of a mutation, conformational changes in the protein encoded by that gene may be induced that can result in the appearance of a new phenotype in that organism. Alternatively, some mutations are silent, meaning no observable or discernable changes have resulted from the mutation, usually because the codon reads for the same amino acid (Alberts *et al.* 2002). Mutation types are discussed in more detail in box 3.

Box 3. Types of mutation

Genetic mutations can be categorised according to their cause. There are several causes including:

1) Spontaneous mutation by molecular decay – this includes molecular alterations such as nucleotide base changes from the repositioning of a hydrogen atom known as tautomerism (altering the hydrogen bonding in that base leading to incorrect base pairing during replication). Base hydrolysis is also included in this category, for example the deamination of cytosine to uracil (which can usually be corrected by DNA repair mechanisms) (Alberts *et al.* 2002; Lodish *et al.* 2008).
2) Mutagen induced mutations – these can be a consequence of exposure to certain chemical agents such as nitrous acid (which converts amine groups on adenine and cytosine to diazo groups, changing the hydrogen bonding which as previously mentioned leads to incorrect base pairing). Radiation is a non-chemical mutagen, for example, ultraviolet radiation

can cause two adjacent pyrimidine bases to become covalently joined as a dimer (Alberts *et al.* 2002; Lodish *et al.* 2008).

3) Naturally occurring DNA damage from error prone replication by-pass – this process occurs during DNA replication and is a form of DNA damage tolerance in which the cells DNA replication machinery is 'allowed' to replicate past the point of existing DNA damage (such as thymine dimers). This involves switching from the use of regular DNA polymerases to specialised *translesion* polymerases that often have active sites that facilitate the insertion of bases opposite the damaged nucleotide(s). This subset of polymerases are characterised by a high propensity to insert incorrect bases (have low fidelity) on intact DNA strands compared to regular polymerases, however, many are more efficient at inserting the correct bases opposite specific types of DNA damage. This mechanism, although intended to avoid more drastic DNA repair mechanisms or even cell death, does carry the risk of introducing point mutations (Alberts *et al.* 2002; Lodish *et al.* 2008).
4) Naturally occurring errors during DNA repair processes – common causes in this category are often due to double-strand breaks (DSBs). Although DSBs occur naturally at a relatively low frequency, their repair often carries a high chance of resulting mutations. The main repair pathway for DSBs is non-homologous end joining (NHEJ), a process which comprises of the realignment and re-joining (ligation) of the two ends by the addition of new nucleotides with no homologous template. When the overhanging ends of a DSB are compatible, NHEJ typically provides accurate repair. However, when overhangs are not compatible, nucleotides are often lost to allow ligation and this is where imprecise repair can occur, leading to mutations (Alberts *et al.* 2002; Lodish *et al.* 2008).

Of the types of mutation described in box 3, research has shown that the majority of natural spontaneous mutations arise due to error prone replication (DNA damage tolerance) and errors introduced during DNA damage repair. In mammalian cells, it has been estimated that naturally occurring DNA damage appears between 10000 to 100000 times per day (Ames *et al.* 1993). This DNA damage leads to mutations through the tolerance and incorrect repair attempts (as described in parts 3 and 4 of box 3 above). The types of mutations that occur will differ in their effect on gene structure, phenotypic function and organism fitness. Small-scale structural alterations to the gene can be categorised as follows:

Point mutations – the exchange of an individual nucleotide for another. It is more common for a purine to be replaced by a purine or a pyrimidine by a pyrimidine (transition) as opposed to purine replace by a pyrimidine or vice versa (transversion). As it takes three nucleotide bases to code for one amino acid, the replacement of one base may be classed as silent (where the replaced base codes for the same amino acid as the original base triplet), neutral (where the replaced base codes for a different, but chemically similar amino acid, resulting in no significant protein change), missense (where the replaced base codes for a different amino acid) or nonsense (where the replaced base codes for a stop codon) (Alberts *et al.* 2002). Mutagens or erroneous DNA replication processes commonly cause such mutations (Lodish *et al.* 2008).

Insertions – the addition of one or more extra nucleotides into the DNA. Insertions may result in a reading frame-shift, meaning the triplet grouping of the nucleotides into codons has changed from the point of mutation (See figure 1.2). Reading frame-shifts can be avoided if the number of extra nucleotides inserted is a multiple of 3. Insertions in the coding region of a gene can alter mRNA splicing, if a splicing site is abolished it can result in one or more introns persisting in the mature mRNA leading to abnormal proteins (Alberts *et al.* 2002).

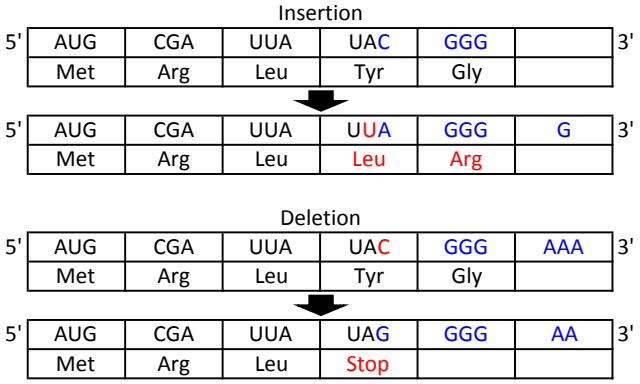

Figure 1.2 An insertion and deletion mutation, both resulting in a reading frame shift. The insertion has resulted in an amino acid substitution whereas the deletion has resulted in a stop codon.

In addition to the small-scale deletions described above, larger scale mutations in chromosomal structure also occur. These include:

- Deletions of chromosomal regions – resulting in the loss of the genes within the region(s)
- Amplifications (duplications) – resulting in multiple copies of that chromosomal region and the genes within.
- Rearrangement mutations that juxtapose pieces of DNA that were previously independent – this can occasionally result in functionally novel *fusion genes*. Such mutations include:
    - Chromosomal translocations – the exchange of chromosome parts from non-homologous chromosomes.
    - Chromosomal inversions – reversing the orientation of a region of the chromosome so it is essentially 'flipped' back on itself.
    - Interstitial deletions – intra-chromosome deletion removing a region of the chromosome leading to the joining of two previously distant genes.
- Loss of heterozygosity – the loss of one allele (in organisms that ordinarily have two different alleles). This typically occurs by deletion or recombination events (Lodish *et al.* 2008).

It is important to note that mutations in diploid organisms can be heterozygous or homozygous, meaning that the mutation is present in only one allele or both alleles, respectively. Mutations can also be classed according to their effect on phenotypic function and ultimately effect on *evolutionary fitness*, summarised below.

Effect on phenotypic function

- Gain of function mutations – these are the consequence of the new gene product (usually a protein with altered primary, secondary or tertiary structure) now having a new, novel phenotype that is functionally superior to the original gene product. Resulting phenotypes from these mutations are often dominant.
- Loss of function (amorphic) mutations – are the result of the new gene product having less of a function than the wild type. Sometimes, the new gene product can have no function whatsoever. Phenotypes arising from this type of mutation are often recessive.
- Lethal mutations – these are severe mutations that lead to the death of the organism carrying the mutation.
- Dominant negative (antimorphic) mutations – these mutations result in a gene product that is antagonistic to the wild type allele. They are often dominant and have been implicated in cancer and autosomal diseases, for example, Marfan syndrome where it is suggested that mutations of the defective glycoproteins from the fibrillin gene antagonises the gene product of the normal allele. However, it can be difficult to distinguish whether such phenotype changes are truly due to the presence of the abnormal allele or rather just the absence of the additional normal allele.
- Reversions or back mutation – these are secondary mutations that restores the original sequence after a primary mutation, hence restoring the original wild type phenotype (Maynard Smith 1998; Lodish *et al.* 2008).

Effect on *evolutionary fitness*

To understand these effects, it is important to clearly define what is meant by 'evolutionary fitness'. Evolutionary fitness is manifested by an individual's phenotype (observable traits), and it describes the ability to survive and reproduce due to such phenotypes in a given environment. Because the environment as well as underlying genetics influences the phenotype it is therefore possible for two individuals with the same genotype but subjected to differ environmental pressures to have different finesses. If two different alleles of a gene confer phenotypes of varying fitness, the frequencies of each allele will change from generation to generation, with the allele of higher fitness eventually becoming more common (Maynard Smith 1998; Michod 2000). This is the core principle of natural selection, one of the main processes of evolution (discussed in section 1.5.2.2). The different effects that mutations can have on fitness are described as the following:

- Neutral – these mutations have no overall harmful or beneficial effect on the organism, meaning no decrease or increase in the fitness of the organism.
- Advantageous – these mutations result in beneficial effects on the phenotype, increasing the organism's fitness.
- Deleterious – mutations of this type have a negative effect on the phenotype, decreasing fitness.

It is important to note that mutations may be only very slightly advantageous or deleterious, marginally effecting fitness. In such cases, natural selection processes occur more slowly for or against that phenotype (Barton *et al.* 2007).

1.5.2.2 Natural selection and adaptation

Natural selection is a non-random process by which particular phenotypes become more or less frequent in a given population. Phenotypic variation exists in all

populations (and as described earlier there is much heterogeneity in CHO cell populations), which occurs because of genomic changes from mutation events. Some phenotypes will convey greater fitness over others, and although the word 'selection' may imply the involvement of cognisant and active choice, natural selection is simply the result of those organisms of greater fitness having greater ability to reproduce and pass on that beneficial phenotype to its offspring, resulting in that phenotype being present in a larger proportion of the next generation (Darwin 1859; Fisher 1930). As this process is repeated from generation to generation, the population evolves until that phenotypic trait (and underlying alleles) is present in every individual or, until it no longer conveys a selection advantage (see figure 1.3 for schematic of the natural selection process). The former scenario is likely to occur if the population is undergoing *adaptation* to a particular environmental condition or challenge. Adaptation is another evolutionary process that is maintained by natural selection. When a population is exposed to adverse conditions, adaptation allows survival and elevated fitness where a non-adapted population would struggle or fail to survive (Mayr 1982).

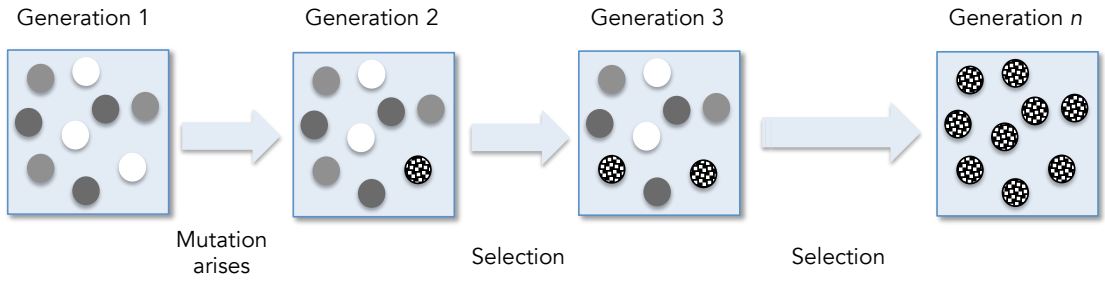

Figure 1.3 Schematic of the natural selection process. A beneficial mutation (dots) appears as generation 1 gives rise to generation 2. This mutation conveys a selection advantage that better enables that individual to survive and consequently pass on its genes (generation 3). Over time, a beneficial mutation will propagate through the population (so long as it remains selectively advantageous) until it becomes fixed (generation *n*).

Mutation, natural selection and adaptation are very important processes of evolution but are not the only processes. For the sake of completeness, all mechanisms of evolution are listed below, some of which are more relevant to this

project than others. Of the others listed below, genetic drift is the only mechanism that will be further discussed for interest of this project (see section 1.5.2.3).

Mechanisms/ processes of evolution (Campbell & Reece 2004):

1) Mutation (previously described)
2) Natural selection (previously described)
3) Adaptation (previously described)
4) Speciation – an evolutionary process in which, by one or a combination of other evolutionary processes (e.g. mutation and adaptation), the evolved population has become so genetically different to the original population that individuals from each would no longer be able to produce fertile offspring. As this project concerns the subculture of an immortal cell line *in vitro*, evolution by speciation is not further discussed.
5) Geneflow (gene migration) – this evolutionary process describes the transfer of alleles from one geographically distinct population to another, again not pertinent considering the *in vitro* nature of this project.
6) Genetic drift – In short, genetic drift is the change in frequency of an allele in a population due to random sampling. In a sub-culturing regime, as is routine practice in mammalian suspension adapted cell culture, random sampling occurs at every passage, making this evolutionary process very relevant to this project. Genetic drift is described in more detail below.

Evolution in standard *in vitro* conditions essentially occurs in a pattern as can be seen in figure 1.4 below. If selection pressures are added, natural selection and adaptation processes will also occur.

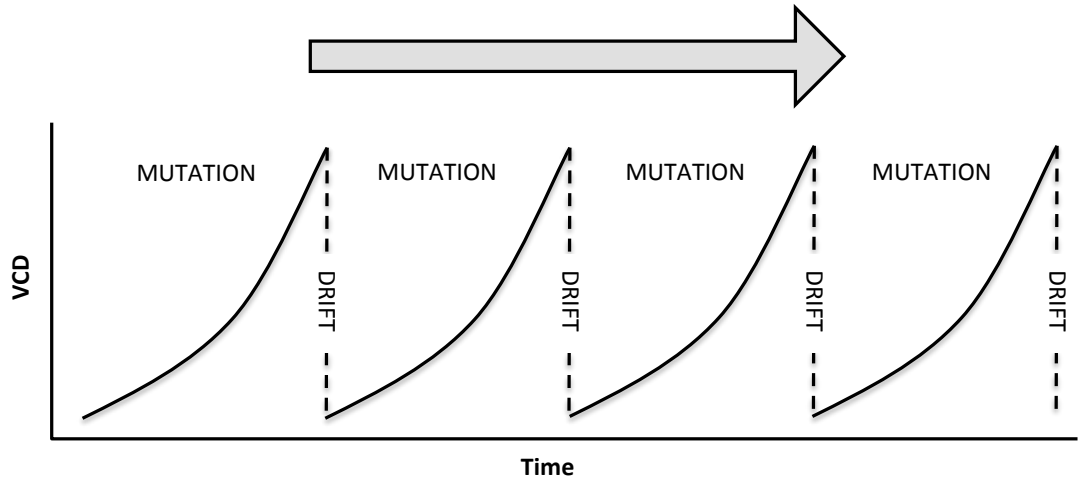

Figure 1.4 The evolution process *in vitro*. As cells grow, they undergo mitosis where DNA is replicated and cells divide (an opportunity in which mutation can occur). At passage, the population is subjected to genetic drift as it becomes diluted to seed the next passage. During cell culture, this cycle of mutation – drift continues for as long as they are sub-cultured.

1.5.2.3 Genetic drift

Genetic drift, or the change in frequency of gene variants in a population as a result of random sampling events, occurs because the alleles in one generation are only a 'sample' of the alleles from the parent (previous) generation (Masel 2011). Over time, genetic drift can cause certain alleles to completely be abolished or be *fixed* within a population. When an allele is fixed it simply means that every individual in that population possesses that allele. Fixation can happen due to natural selection of beneficial alleles or due to genetic drift in the case of neutral alleles (Futuyma 1998).

Genetic drift is not concerned with the fitness conveyed by particular alleles; rather, it is the role of pure chance that some alleles just happen to get passed on to the next generation while other alleles do not. With genetic drift, beneficial, neutral or disadvantageous alleles are no more or less likely to be subjected to such random events that can change allele frequency, for example, a certain area of a population gets killed off due to a natural disaster (Campbell & Reece 2004). When alleles of a gene do not differ with regard to fitness, it is said that *on average*

the number of carriers in one generation is proportional to the number of carriers in the next generation. However, this 'average' is never tallied as each generation populations will parent the next generation only once. Because of this, the frequency of alleles among the offspring generation often differs from the frequency in the parent generation. In this circumstance, the allele frequencies are said to have drifted (Futuyma 1998) (see figure 1.5 for schematic of this process). In an *in vitro* cell-culturing setting, extracting a sample for passage is an example of a random event that will create genetic drift.

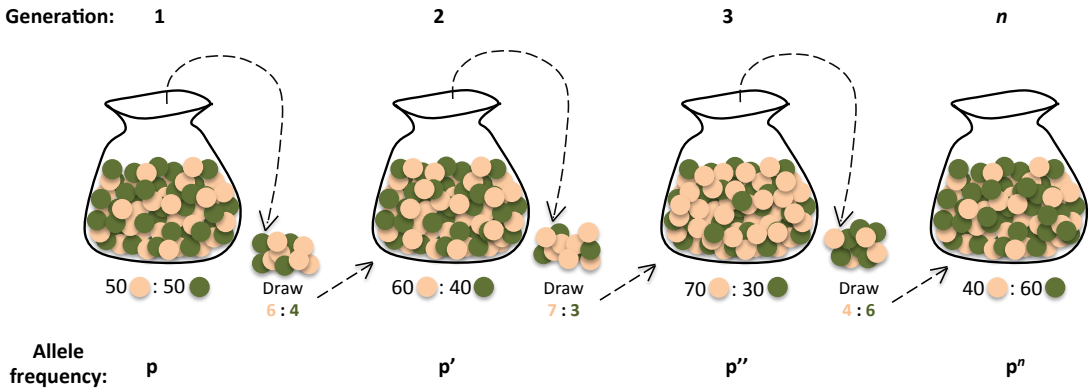

Figure 1.5 Schematic of genetic drift. Using the analogy of a bag (population) of two different coloured marbles, where each colour represents one allele with equal fitness to the other: Each generation is parented only once and often, due to random sampling, the allele frequency in the next generation (p') differs from that of the parent generation (p). The allele frequencies are now said to have drifted.

As opposed to the case with allele fitness, allele frequency, conversely, does effect genetic drift: when there are many copies of an allele in a given population that allele is less sensitive to the effect of genetic drift (as during sampling events there is greater chance of selecting that allele meaning it is more likely to persist in the next generation), whereas when there are few copies of an allele it is more sensitive to the effect of genetic drift (likely resulting in a change in frequency of that allele in the next generation) (Ewens 2004). Population size is also a factor that can vary the effect of genetic drift and the *time to fixation* of an allele in a population - smaller populations are more susceptible to drift and alleles reach fixation in shorter time periods. The projected number of generations until fixation

is proportional to population size, such that fixation is predicted to take longer in larger populations (Futuyma 1998).

During *in vitro* sub-culturing, the principal genes under evolutionary constraint, or evolutionary pressure for selection, are those that effect cellular growth rate. It has been shown by colleagues in house that, over time, fast growing cells (high μ) come to dominate the population (Davies *et al.* 2013). Many other genes not concerned with growth rate are neutral in an evolutionary context; the alleles of such will 'drift' in frequency from generation to generation. If other selection pressures are applied, which they will have been during the course of this project, formerly evolutionary neutral genes may now bear evolutionary advantages under such pressure and therefore be selected for. There is another, related source of allele frequency change not mentioned thus far and that is genetic draft, also known as genetic hitchhiking. Genetic draft is a process by which an allele may increase in frequency due to being proximal (linked loci) to genes that are under positive evolutionary selection pressure (Gillespie 2001).

As discussed, genetic drift can vary due to different population characteristics (population/ sample size, allele frequency) that can influence the rate at which alleles become fixed or abolished from a population. The very first part of this project will investigate the optimal degree of genetic drift to apply to *in vitro* cultures of CHO cells for rapid evolution. Genetic drift can in effect be controlled by changing the *dilution ratio* at passage, i.e. the sample size of the previous passage harvested for seeding the following passage. As an example, if a culture reaches a final VCD of 4 $x10^6$ cells/mL, harvesting to seed the subsequent passage at 0.2 $x10^6$ cells/mL would result in a smaller dilution ratio (0.05) than if one was to seed at 1 $x10^6$ cells/ mL (dilution ratio 0.25). Passaging of cultures is similar to the 'founder effect', which is defined as a loss of genetic variation that occurs when a new population is established by a very small number of individuals from a larger population. This effect occurs when a sample of 'founder' members are not genetically representative of the population from which they originated (Mayr 1942; Provine 2004). Small 'founder' populations, i.e. the seeding population of

cells *in vitro*, are very sensitive to genetic drift, hence why a smaller dilution ratio at passage would enhance genetic drift.

1.5.3 *In vitro* directed evolution

This project centralises round the aim that CHO cells with enhanced biomanufacturing properties can be attained through directed evolution. This type of engineering approach has so far not been ordinarily applied as a mammalian cell line development technique in industry, and whole mammalian cell directed evolution is seldom seen in bioprocessing literature (Hu 2012). Just as yeast and bacteria have often been adapted to tolerate production process by-products, such as ethanol during fermentation, mammalian cells too can be adapted for better performance in industrial processes, as will be discussed in this section.

In 1992, a population of leukaemia cells (HL-60) were purposely exposed to concentrations of lactate and ammonia in the toxic range. Surviving cells resistant to these major metabolic wastes were isolated and characterised for improved viability and growth in such conditions where it was found that the metabolic profile of adapted cells had changed – lactate and ammonia formation was inhibited in the presence of high lactate and ammonia in the medium, while alanine production and arginine consumption was enhanced (Schumpp & Schlaeger 1992). In addition to this, antibody-secreting hybridoma cells were also found to adapt to stepwise increases in ammonia concentrations over time, which showed that it could be possible to adjust cells to become more 'fit for purpose' to some of the key industrial stressors found in the high density cell culture environment common to recombinant protein production processes (Matsumura *et al.* 1991).

One example of more recent work related to this topic was performed by Prentice and colleagues who repeated rounds of bioreactor stressors to select for CHO cells adapted to a range of harsh conditions in a process they termed 'bioreactor

evolution'. This bioreactor evolution essentially comprised of subjecting a DG44 CHO host cell line along with a recombinant production cell line to bioreactor stressors, such as shear stress, hypoxia and nutrient deprivation, in an iterative manner whereby surviving cells were selected for another, harsher round of stress. As a result, the 'evolved' host cell line reached a 2-fold increase in maximum cell density and a 72% increase in IVCD. Furthermore, these host cells maintained the same transfection efficiency as the parent population and the recombinant cell line obtained a 36% increase in product titre with no adverse impacts on product quality (Prentice *et al.* 2007).

Another adaptation study concerning metabolic by-products was performed by Bort and colleagues whose aim was to adapt CHO-K1 cells to grow in glutamine-free media. Although glutamine is supplemented as an alternative energy source for rapidly growing cells that oxidise glucose inefficiently, the resulting by-product is highly concentrated ammonia that has a negative impact on protein product glycosylation. This group adapted CHO-K1 cells to progressively reduced glutamine concentrations (8 mM, 4 mM, 2 mM then 0 mM), each time resulting in decreased maximum cell density and viability. Surviving cells were harvested by FACS (Fluorescence Activated Cell Sorting) or MACS (Magnetic Activated Cell Separation) once viability dropped to 10% and were subsequently seeded at high densities to assist rapid evolution. The final population achieved higher viable cell density and viabilities than all ancestral populations. Again, similar to the findings of Schumpp & Schlaeger (1992) with their HL-60 cells, it was shown that a metabolic profile-shift had occurred, with evolved cells in this study compensating for the lack of glutamine by increasing consumption of aspartate and glutamate (Bort *et al.* 2010).

The above studies are examples of whole cell adaptations towards inherent or environmental stresses with a view to improving and maintaining the evolved population with a phenotype better suited to industrial bioprocess conditions. However, as mammalian cells are renowned for slow growth rates, relying on spontaneous mutation and subsequent adaptation may be perceived as too slow to

be of any practical use in industry. Alternatively, radiation and chemical methods of mutagenesis can be employed to generate greater phenotypic diversity and, in theory, generate the improved target phenotype more rapidly. However, mutagen-based applications in commercially relevant cell lines, as a tool for directed evolution, has not been as extensive as environmental adaptation approaches (Majors *et al.* 2009). This could be for a number of reasons including the fact that it is often the case that chemical mutagens are inherently harsh, frequently rendering the surviving cells sick, displaying short, finite growth characteristics upon expansion (Nicolaides *et al.* 2005). The use of radiation and chemicals as a method for mutagenesis in cell lines intended for biopharmaceutical production may also introduce more criteria that need to be met for FDA approval, potentially making the process lengthy, costly and difficult to achieve. An example of one concern would be the removal of all mutagenic agents in the final product, and these contaminants would be much more of a hazard than the ordinary contaminants found at present, such as host cell proteins (Majors *et al.* 2009).

There are also specific genetic methods of mutagenesis that could be employed in directed evolution strategies. For example, genomic instability, an inherent property of cancer cells and CHO cells causes such cell lines to be natural mutators. In 1998, a research group lead by Bert Vogelstein found that in some colorectal cancer cells, defects in the DNA mismatch repair (MMR) machinery introduces microsatellite instability resulting in a mutator phenotype in such cells (Nicolaides *et al.* 1998). The cause of the MMR defects and consequent mutator phenotype was found to be due to a truncation mutation in the human postmeiotic segregation (hPMS2) gene. The study proceeded to show that the introduction of a mutant hPMS2 gene inhibited MMR mechanisms and caused the subsequent mutation of an exogenous β-galactosidase gene in HEK 293 and normal hamster cells. The hPMS2 gene was termed ‘morphogene’ and when expressed in any cell line the MMR mechanisms can be reversibly inhibited, leading to mutations and changed cell phenotypes. This technique was applied to CHO cells and as well as leading to increased monoclonal antibody productivity, also resulted in the generation of cells producing antibodies with altered binding characteristics (higher affinity). In

addition to this, cells exhibiting these new phenotypes could be 'cured' to inhibit the morphogene, permitting an element of control on the degree of mutation created (Nicolaides *et al.* 1998; Grasso *et al.* 2004; Nicolaides *et al.* 2005; Majors *et al.* 2009).

Whether implementing environmental stressors, radiation or chemical mutagens or introducing mutation through genetic manipulation, each of these approaches to directed evolution have advantages and disadvantages. For example, relying on spontaneous mutation and adaptation to environmental stress can be an inherently slow process, while mutagens to speed the process up could introduce obstacles by way of approval by appropriate authoritative bodies and also intellectual property disputes once any licensed product, chemical substance or genetic engineering strategy is used in the development of a cell line.

1.6 Hypothermia and temperature shift as a method for enhanced titre and product quality

It is well practiced in industry to apply a bi-phasic temperature shift to cell cultures producing a protein product. Typically, a bi-phasic method will include an initial rapid cell proliferation stage achieved by optimal cell culture conditions (often 37°C) followed by a phase in which the cell culture is shifted to a lower temperature (usually in the range of 28-33°C) (Kumar et al. 2008). This section explains the biology behind this process and also the drawbacks of the method, followed by a discussion regarding how directed evolution can be implemented as a potential solution to such problems.

Although sounding detrimental to cellular health, hypothermic temperatures still maintain cell viability but arrest the cell cycle in G1-phase. Temperature reduction actually extends the culture viability period as a result of delayed onset of apoptosis. One study has identified the specific increase in expression of the preciously discussed anti-apoptotic gene, Bcl-2, in response to mild hypothermia (Slikker *et al.* 2001). Once apoptosis is initiated the manner of cell death is similar to what can be observed at optimum temperatures (Moore *et al.* 1997). Cell cycle arrest has been correlated positively with increased production due to approximately a 1.7 fold increase in cell specific production rates (qP). When you consider this with the fact that cells are viable for longer and therefore producing for longer at lower temperatures, the overall product titre one can yield often reaches reach several fold more than cultivation at standard temperatures, as IVCD has been improved as well as qP (Kaufmann *et al.* 1999; Becerra *et al.* 2012). Notably, yields from hypothermic perfusion culture using CHO cells producing follicle-stimulating hormone can be improved 13-fold compared to equivalent cultures at 37°C (Yoon *et al.* 2007).

Although cell cycle arrest in industrial bioprocesses can be achieved by chemical means, for example through the addition of sodium butyrate, a temperature shift is

more commonly applied (Damiani *et al.* 2013). This is most likely due to the lack of any additional cost to the process and the array of additional cell culture benefits that have been observed which are discussed over the following paragraphs.

Other phenomena that occur at low temperature include a reduction in glucose and oxygen uptake, reduction in waste (lactate and ammonia) accumulation, reduced proteolytic activity, improved shear stress resistance and also increased levels of mRNA coding for the recombinant protein (Chuppa *et al.* 1997). This latter observation has been attributed to increased mRNA stability at lower temperatures or enhanced levels of transcription (Yoon *et al.* 2004). There are also more than 20 proteins, including cold-inducible RNA binding protein (CIRP), that have been reported to become unregulated during a phase shift to lower temperatures. Out of these many proteins, it is CIRP that has been studied most extensively. This protein functions as an RNA chaperone, modulating transcription and translation and it has been shown that overexpression of CIRP can increase recombinant protein production (performed in CHO cells) and also arrests cell growth (Kumar *et al.* 2008; Tan *et al.* 2008). In addition to productivity enhancements, post-translational events have been shown to occur with higher accuracy and fidelity at 32°C that 37°C, resulting in a yield that is a higher proportion active protein (Masterton *et al.* 2010). Glycosylation is one such post-translational event that is modified through growth arrest, with sialilation in particular being modified which can improve the *in vivo* efficacy of the product (Nam *et al.* 2008).

The activities of certain beneficial enzymes are also increased under hypothermic conditions. For example, glutathione peroxidase (one of the more efficient antioxidants) levels were found to be significantly higher in CHO cells at lower temperatures, meaning CHO cells at lower temperatures should be more resistant to oxidative stress. This was demonstrated by exposing CHO cells at different temperatures (ranging from 37°C to 30°C) to 100 μM hydrogen peroxide (an oxidant) – it was found that significantly higher cell viability could be observed in the cells at the lowest temperature in the study (Slikker *et al.* 2001). This is an

area of interest to biopharmaceutical research as reactive oxygen species (ROS) tend to increase in late exponential/ early stationary phase of growth, causing oxidative stress which can lead to premature death of a host cell, potentially causing a reduction in product titre (Templeton *et al.* 2013; Young 2013).

Despite the large number of studies that show positive effects of mild hypothermia on specific productivity of recombinant proteins, no experimental approach has addressed the detrimental effect of lower temperatures on specific cell growth rate (Vergara *et al.* 2014): although a lot of the benefits of production under hypothermic conditions are attributed to the arrest in cell cycle progression, this phenomenon consequently negatively effects growth rate which in terms of titre can sometimes negate the positive effects of a temperature shift, such as enhanced qP (Sunley *et al.* 2008). In addition to this unwanted effect on growth rate, the magnitude of the desired effects of mild hypothermia can be different between cell lines and expression systems as well as being dependent on the recombinant protein product itself (Kaufmann *et al.* 1999, Becerra *et al.* 2012; Mason *et al.* 2014).

As an attempt at solving the problem of reduced growth rates under hypothermic conditions, some researchers have attempted to adapt CHO cells to low temperatures. The shared aim in these studies was to attain a cell type that possess the same desirable productivity attributes of a cell under hypothermic "shock" (temperature phase shift), yet retain growth rates as if they were growing at optimal temperatures (37°C). In 2006, Yoon and colleagues adapted recombinant CHO cells producing erythropoietin (EPO) and also CHO cells producing follicle-stimulating hormone (FSH) to growth at 32°C. They did this by repeated batch culture in spinner flasks, inoculating each successive flask with cells from the previous batch at seeding density of $2x10^5$ cell/mL. They found that cell specific growth rates gradually improved during this adaptation process, with the EPO producing cell line increasing by 73% and the FSH producing cell line by 20%. However, specific productivities decreased by 49% and 22% for the EPO and FSH producing cell lines, respectively. The group concluded that adaptation does not

appear to be applicable for enhancing production of recombinant proteins (Yoon *et al.* 2006).

A separate study by a different research group conducted work in which a recombinant CHO-K1 cell line producing interferon-β (β-IFN) was adapted to growth at 32°C. This was achieved by static culture in 75 cm^2 T-flasks that were continuously subcultured every 8 days for a total of around 300 days. They found that the adapted cell population achieved a growth rate 2-fold greater than non-adapted CHO-K1 cells at 32°C, whilst maintaining an elevated level of cell-specific β-IFN production. This meant that volumetric titre of β-IFN was enhanced by 70% which rose to 2-fold when a temperature shift strategy was employed in which the adapted cells were initially grown at 37°C to boost growth early on in culture. However, the merits of this study fell short when the low-temperature adapted cells were too fragile and died when scaled up to agitated cultures, which is a necessary requirement for a cell line that could be used in industry. The group attempted to resolve the problem by using *macroporous microcarriers* to support cell growth – these are essentially small cellulose beads in which the cells become embedded in an inner matrix, protecting them from the shear forces generated by agitation. However, this introduces additional costs, impracticalities and potential contamination risks upon traditional production platforms, which could be difficult for the industry to widely accept (Sunley *et al.* 2008).

Of the examples in the literature that attempt to evolve/ adapt CHO cells to hypothermic conditions for the aforementioned reasons, all perform their adaptation process on recombinant stably producing cell lines, rather than a CHO host cell line that has not yet been stably transfected with the gene of interest. A major component of this thesis explores this uncharted area of research, as is summarised in the following thesis overview.

1.7 Thesis overview

As outlined in the literature review, directed evolution strategies have the potential to deliver multiple and large-scale improvements to biopharmaceutical production. The work in this thesis continues investigating this concept, specifically focussing on the acceleration of evolution *in vitro* and the generation of a hypothermia adapted host cell line, as well as subsequent characterisation and analysis that could ultimately identify and assist future engineering targets.

The key aims of this project are as follows:

- Determine an optimised cell culture regime for rapid evolution that can be applied *in vitro* by manipulating basic parameters
- Use directed evolution to enable a CHOK1SV host cell line adapt to hypothermic conditions (32°C) and characterise phenotypic changes
- Assess the industrial ability of this host cell in terms of transfection (transient and stable) and productivity
- Retrospectively investigate the biology that underpins similarities and differences between the parental and evolved CHOK1SV host cell lines to infer potential future engineering targets

Outline of chapters:

The next chapter, chapter two, details the common materials and methods that were used throughout this thesis.

Chapter three firstly presents an optimised cell-culturing regime that can be applied for rapid evolution rates *in vitro*. Following this, the evolution of a hypothermia (32°C) adapted CHOK1SV host cell line is described. Cellular alterations that arose through this process are characterised, including: cell diameter, cell volume, biomass content, RNA content and ploidy. Comparative growth rate over time is also presented as well as further studies into the response

of the evolved cell line at extreme hypothermia (30°C) and native (37°C) temperatures.

Chapter four examines more thoroughly the performance of the evolved cell line in an industrial context, with an aim to assess the functional attributes that are often considered important in cell line development. This includes transient electroporation transfection productivity and efficiency, long-term transient lipofection performance in a fed-batch platform, and stable pool generation. Titre of stable pools producing either a well characterised "easy to express" mAb (cB72.3) or a "difficult to express" Fc-fusion protein (Enbrel) is assessed alongside the glycan profile of such proteins in order to infer whether evolution has altered product quality.

In chapter five, biological mechanisms underpinning the changes observed in the work detailed in the previous two chapters are explored. Much of this centralises around the hypothesis that the hypothermia-adapted cell line is producing heat by way of *adaptive thermogenesis* – an increase in inner mitochondrial membrane permeability that allows protons to return to the matrix, generating heat in the process. Seahorse XF technology is employed here, allowing information on the mitochondria, such as basal respiration, ATP production and maximal respiration, to be gathered. A general consequence of adaptive thermogenesis is a reduction in reactive oxygen species and therefore lower oxidative stress – this concept is also examined in the hypothermia-adapted cell line and presented here. Other mechanistic analysis documented in this chapter includes comparative amino acid flux through culture between the parental and evolved cell lines, in addition to differential gene expression analysis via the Affymetrix® CHO Gene ST Array system.

Chapter six is composed of the final discussion summary and conclusions of the research documented in the previous research chapters. Future areas of work that could follow on from this project are also highlighted here.

This page is intentionally left blank.

Chapter 2:

Materials and methods - *generic*

This chapter describes in detail the universal, frequently used materials and methods that were used to conduct work described in subsequent chapters of this thesis. Materials and methods in this chapter are those that were common to multiple chapters, all other methods are described within chapters, specific to the body of work presented therein.

2.1 Cell culture techniques

The only cell line used throughout this project was Lonza Biologics' CHOK1SV, a suspension adapted CHO (Lonza Biologics, Cambridge, UK). All routine culture of CHO cells was performed in a cell culture grade laboratory in which hairnets, shoe covers, gloves and a lab coat were worn at all times. Work conducted on CHO cell cultures was performed under a laminar flow cabinet that was cleaned with 70% ethanol wipes (and allowed to dry) before use. Anything entering the laminar flow cabinet was always sprayed with 70% Ethanol to prevent contamination of CHO cell cultures. Unless stated otherwise, the culture media used was CD CHO (Invitrogen, Paisley, UK) supplemented with either 4% 200 mM L-Glutamine (8.0 mM final concentration) (Fisher, Loughborough, UK), or, supplemented with 25 µM Methionine sulfoximine (MSX) (Sigma Aldrich, Dorset, UK), if culturing stably transfected cells.

When not being used for experimentation or routine culturing, cells were stored in 1.5 mL cryovials (Nunc, Thermo Scientific, Loughborough, UK), organised by

'master' or 'working' cell banks surrounded by liquid nitrogen at approximately -196°C. Cells which are preserved in this way must first be prepared using the following procedure:

2.1.1 Master/ working cell bank

A Master Cell Bank (MCB) and a Working Cell Bank (WCB) were initially created from an early passage parental CHOK1SV cell batch. This is important as it ensures all cell used in future work will have originated from the same starting population. Cells to be preserved in these banks must be harvested in mid-exponential phase of growth with viability above 95%. The viability, along with viable cell density (VCD), is attained by taking a 0.6 mL sample from the culture for viability analysis using a Vi-CELL XR cell viability analyser (Beckmann Coulter, High Wycombe, UK). The Vi-CELL XR uses the trypan blue exclusion method to distinguish living cells amongst those that have undergone apoptosis (cell membranes no longer intact). Now that the VCD has been established, and knowing that each cryovial should contain 1.5 mL of cells suspended in cryopreservation medium (total media for all vials = Vc) at a density of 1 $\times 10^7$ cells/ mL, one can work out the amount of cell suspension (Vsps) that needs to be extracted for the required number of cryovials:

$$Vsps = \frac{(1\times10^7\ cells)\times Vc}{X_i}$$

Equation 2.1

Where Vc = volume of cryopreservation medium (mL), X_i = VCD (cells/ mL) and 1 $\times 10^7$ = cell density to be added in each vial (cells/ mL).

The cryopreservation medium is made up to contain 86% CD CHO, 4% 200 mM L-Glutamine, and 10% DMSO (dimethyl sulphoxide) (Fisher, Loughborough, UK), this is then stored at 4°C until time of use (N.B. L-Glutamine is omitted if stably transfected cell lines are being cryopreserved). The predetermined volume of

culture (Vsps) is then centrifuged at 200 ×*g* for 5 minutes to pellet the cells out of the culture medium that is then removed. The pellet is then re-suspended in the cryopreservation media (Vc). The VCD and % viability is then checked again using the Vi-CELL XR. Aliquots of 1.5 mL of this suspension are dispensed into sterile cryovials, which are then transferred into the rate-controlled freezer (Mr. Frosty™ Thermo Scientific, Loughborough, UK), which ensures a slow rate of freezing when transferred to the -80°C freezer overnight. The next day the cryovials are transferred to liquid nitrogen cryostats for long-term storage.

2.1.2 Revival from cryopreservation

Unlike the slow, progressive cooling of cells for cryostorage, the thawing and revival of cells must be carried out quickly. Once removed from the cryostat, the cryovial is held in a small beaker of sterile filtered 37°C water in a 37°C water bath until the contents have defrosted. The liquid contents are then transferred to a sterile falcon (Fisher, Loughborough, UK) and re-suspended in 6 mL of 4°C CD CHO. This volume is then centrifuged at 200 ×*g* for 5 minutes to form a pellet of cells. The remaining media is removed and the pellet is re-suspended in 30 mL of pre-warmed (37°C) sterile media (CD CHO supplemented with 4% 200 mM L-Glutamine). Viability and VCD are determined using the Vi-CELL XR and the culture is incubated in a 125 mL Erlenmeyer flask (with vent cap, Fisher, Loughborough, UK) at 37°C, 140 rpm and 5% CO_2. The cells are then sub-cultured after 3 days to ensure any traces of DMSO are removed as soon as possible whilst ensuring the cells have reached exponential growth. Subsequently, cells can be sub-cultured (passaged) on a 4/3-day split regime.

2.2 Routine sub-culturing and cell growth characterisation

As mentioned, the cultured cells are maintained by sub-culturing (also commonly referred to as passaging) every three or four days, where cells are seeded in fresh media (usually 30 mL in volume) typically at a density of 0.2 ×10^6 cells/ mL. Over time, key growth characteristics can be derived from simple measurements such as viable cell density and time:

2.2.1 Cell specific growth rate, μ, in hours^{-1} or days^{-1} (commonly referred to simply as growth rate)

Using the Vi-CELL XR, cell density measurements from different time points in culture can be used in the following equation to determine a value for cell specific growth rate, μ, over the time course of one passage:

$$\mu = \frac{lnNx - lnN0}{tx - t0} = \frac{ln\left(\frac{Nx}{N0}\right)}{tx - t0}$$

Equation 2.2

Where:

Nx = Number of cells per mL at final time

*N*0 = Number of cells per mL at initial time

tx = final time

*t*0 = initial time

2.2.2 The cell doubling time, DT, (defined as the period of time required for a given population of cells to double in number) can consequently be calculated as follows:

$$DT = \frac{ln(2)}{\mu}$$

Equation 2.3

2.2.3 The generation number, GN, (defined as the number of times that a given cell population has doubled in number) can be calculated as follows:

$$N0 \times 2^{GN} = Nx$$

$$2^{GN} = \frac{Nx}{N0}$$

$$GN\ ln\ (2) = ln\frac{Nx}{N0}$$

$$GN = \frac{ln\frac{Nx}{N0}}{ln(2)}$$

$$GN = log_2\ \frac{Nx}{N0}$$

Equation 2.4

GN can also be defined as:

$$GN = \frac{lnNx - lnN0}{ln(2)} = \frac{\mu(tx - t0)}{ln(2)}$$

Equation 2.5

2.2.4 Integral Viable Cell Density

Another commonly calculated parameter is the integral viable cell density (IVCD) which is simply the area under the growth curve and it signifies the number of working 'cell hours' per unit volume of culture. The IVCD between two sampling times can be calculated as follows:

$$IVCD = \left(\frac{N_t + N_{t-1}}{2}\right) \times (t_1 - t_{t-1})$$

Equation 2.6

Where:

N_t = Number of cells per mL at later sample time

N_{t-1} = Number of cells per mL at previous sample time

t_t = time later sample taken

t_{t-1} = time previous sample taken

2.2.5 Number of total cell divisions, $D_{TOTALCELLS}$, (defined as the total number of cell divisions that have occurred over a given period of time in a given cell population) can be calculated as follows:

$$= Nx - N0$$

Equation 2.7

2.3 Cell fixing using paraformaldehyde (PFA)

The cells were usually washed prior to fixing, this was done by centrifuging at 200 ×*g* for 5 minutes, medium was removed and cells resuspended in 1X phosphate-buffered saline (PBS) (Sigma-Aldrich, Dorset, UK) to a concentration of 1 ×10^6 cells/ mL. The cells were then centrifuged again for 5 minutes at 200 ×*g* and the PBS supernatant removed. To fix cells, refrigerated paraformaldehyde (PFA) (approx. 4°C) was then added to the cells to reach a concentration of 1 ×10^7 cells/ mL. Cells in PFA were then incubated on ice for 15 minutes. After this, cells were centrifuged again at 200 ×*g* for 5 minutes, the PFA supernatant removed and the cells resuspended in PBS at a concentration of 1 ×10^6 cells/ mL

Chapter 3:

Optimising cell culture parameters for rapid evolution and attaining a hypothermia-adapted CHOK1SV cell line

This chapter addresses the first and second aims outlined at the end of chapter 1: Firstly, a cell culturing regime that delivers an enhanced rate of evolution is defined by manipulating and optimising basic parameters such as culture seeding density and dilution ratio at passage. Secondly, directed evolution is used to adapt a host CHOK1SV cell line to growth in hypothermic conditions. Initial characterisation of key phenotypic differences and similarities between the evolved cell line and control and parental cultures is presented in terms of growth rate, cell size, biomass content and RNA content in relation to chromosome number (ploidy). In addition to this, heritability of the new traits that the evolved cell line exhibits were tested for heritability through freeze-thaw cycles (cryopreservation) and stability over long-term culture, as these features are necessary for any industrial cell line.

3.1 Introduction

In chapter 1 the merits of directed evolution as a strategy for cell line development and improvement were reviewed and discussed. Notable approaches included the work of Prentice and colleagues (2007) for their "bioreactor evolution" which included iteratively subjecting host and recombinant (producing) CHO cells to

stressors that cells would typically be exposed to in the bioreactor, such as shear stress, hypoxia and nutrient deprivation. This resulted in an evolved host cell line that could reach a 72% increase in IVCD and an evolved producing cell line that gave a 36% increase in recombinant protein product titre (Prentice *et al.* 2007). Another method that intended to reduce the levels of glycosylation-impacting ammonia accumulating in culture was to adapt cells to growth in glutamine free media: ultimately this study resulted in cells of higher viability that had shifted their metabolic profile by increasing consumption of aspartate and glutamate to compensate for the lack of glutamine (Bort *et al.* 2010).

It is clear from the literature that directed evolution is a powerful tool for generating cell lines that possess unique or beneficial phenotypes, however, what is not mentioned in the literature is any attempts at how the evolution processes could be achieved more quickly. One of the main aims of this chapter is to outline an optimised cell culturing regime that facilitates more rapid evolution than would ordinarily be achieved under standard culturing conditions. This is achieved by manipulating the basic parameters at passage: seeding density and dilution ratio (i.e. the proportion of the previous culture that is discarded). As described in chapter 1, opportunities for evolutionarily beneficial mutations occur at cell division when DNA is replicated: errors made during DNA replication can lead to advantageous phenotypes arising in a population which will consequently be selected for via natural selection. In terms of a cell culture population, we can increase the chance of beneficial mutation arising in that population by increasing the population size i.e. increase the cell density at which we seed the subsequent flask at passage. However, increasing the seeding cell density reduces the time a culture can be sustained in exponential growth for (as nutrients become depleted faster) and it also affects the dilution ratio at passage as a larger proportion of the previous population is used to seed the next. As mentioned in chapter 1 (section 1.5.2.3), there is evidence that dilution ratio has an influence on evolution rate due to the effect it has on genetic drift (described as the change in frequency of gene variants in a population as a result of random sampling events). The optimum dilution ratio for mammalian cells has not been studied in this context, however

work on other asexual populations has suggested that a dilution ratio of 0.1 to 0.2 is most favourable to "minimise the chance that rare beneficial mutations are lost", although more severe dilutions have been used in the literature (Wahl *et al.* 2002). As mentioned, the opportunity for mutation (influenced by seeding density) and the degree of genetic drift (applied through dilution at passage) are interdependent in *in vitro* cell culture, as seeding density will alter the ultimate dilution ratio. The initial work described in this chapter describes an optimisation study to determine the optimum balance of these parameters in order to achieve a rapid evolution rate. Seeding density is varied which as stated results in varying dilution ratios, but to further inform the optimisation process, passage time (i.e. days of culture) is also altered to give further variations of seeding density and dilution ratios. The indicator for evolution rate in this study is taken as rate of change in growth rate ($\Delta\mu$), which is based upon in-house work by Davies and colleagues (2013) who identify the primary selection pressure in cell culture as proliferation rate and subsequently use the comparative evolution of proliferation rates to indirectly identify clonal variants that may differ in genomic mutation rate (Davies *et al.* 2013). In this study, a parental pool of non-clonal CHOK1SV cells are used to identify optimised sub-culturing parameters that permit rapid evolution of proliferation rate. Further details of how this is experimentally performed can be found in the methods section of this chapter.

The following work described in this chapter is concerned with the adaptation of a parental host CHOK1SV cell line to growth in hypothermic conditions. As discussed in the literature review, there can be multiple benefits of implementing a cold-shock culturing strategy for enhanced biopharmaceutical production. Typically this strategy will include a period of culture at optimum temperatures for rapid proliferation (~37°C), followed by a shift to a significantly lower temperature (usually in the range of 28-33°C) (Kumar *et al.* 2008). The latter phase has been associated with extended culture viability and delayed onset of apoptosis, reduction in toxic waste product accumulation and impressive, multiple-fold increases in product titre (Chuppa *et al.* 1997; Kaufmann *et al.* 1999; Slikker *et al.* 2001; Sunley *et al.* 2008; Becerra *et al.* 2012; Vergara *et al.* 2014). However, there

is also the pre-discussed burden of cell cycle arrest, a consequence of hypothermia that can sometimes negate the positive effects of a temperature shift: the ideal scenario would be a cell line that shares the production advantages of "cold-shocking" but also continues to proliferate at a normal rate (Sunley *et al.* 2008). In order to achieve this, attempts have been made to adapt recombinant, stably producing CHO cell lines to growth in hypothermic conditions. One example of this is demonstrated in the work by Yoon *et al*. (2006) which was described in chapter 1: to recap, this group took a follicle-stimulating hormone (FSH) producing cell line and a erythropoietin (EPO) producing cell line and repeatedly passaged cells in batch, shake-flask culture at 32°C. Over time, vast improvements in growth rate were noticed, however, productivities of both producing cell lines decreased significantly over the adaptation process (Yoon *et al.* 2006). Another similar example (that was also fully described in chapter 1) included the work of group who used a similar approach but iteratively sub-cultured their interferon-β producing cell line at 32°C in static T-flasks rather than agitated cultures. They found that both growth rate and productivity was significantly improved, however, when scaling their adapted cultures up to larger, agitated vessels they found that the cells were too fragile and soon died in these conditions. Although superficially successful, for this groups work to be used in an industrial setting, expensive and largely impractical solutions (such as microcarriers) would have to be incorporated (Sunley *et al.* 2008).

This chapter addresses the proposition of adapting a host (non-producing) CHOK1SV cell line as an alternative to adapting stable cell lines (that are already producing a specific recombinant protein), which, as has been discussed, has had a history of limited success. This work is also motivated by the lack of any attempt of this nature existing in the literature, providing an opportunity to conduct novel work that could serve at least as a proof of concept that could be taken forward and applied to industrial manufacture. Additionally, the concept of a hypothermia-adapted host cell line could possibly be more appealing to industry as it provides a flexible cell line that can subsequently be tailored for both transient and stable production of recombinant proteins of the companies' choice.

3.2 Materials and methods

This section describes the experimental design of culturing regimes that were used to optimise culture parameters for rapid *in vitro* evolution. It also details the materials and methods used in the generation and primary characterisation of an evolved, hypothermia-adapted CHOK1SV cell line. The reader is referred to chapter 2 for details on any other experimental techniques mentioned in this chapter.

3.2.1 Designing a set of culturing regimes to determine the optimum parameters for rapid evolution

As previously described, introducing a high seeding density increases the number of cell divisions per unit time per mL of culture medium (which increases the chance of mutation in that population). In addition to this, the degree of dilution at passage is also known to effect evolution by altering the probability that beneficial mutations are lost or kept in that population. This study aims to find out more about the effect these variables can have with respect to $\Delta\mu$ over time, ultimately defining an ideal seeding density/ dilution combination that provides rapid evolution. To do this, cultures with various seeding densities were harvested for passage in a staggered manner along their exponential growth phase: cells that are harvested later along the exponential phase require a larger degree of dilution to return to the original seeding density. Keeping the seeding densities fixed but varying the passage time will result in a range of combinations of 'number of cell divisions' and 'dilution ratio'. To support the readers understanding of this, a hypothetical example is explained in figure 3.1.

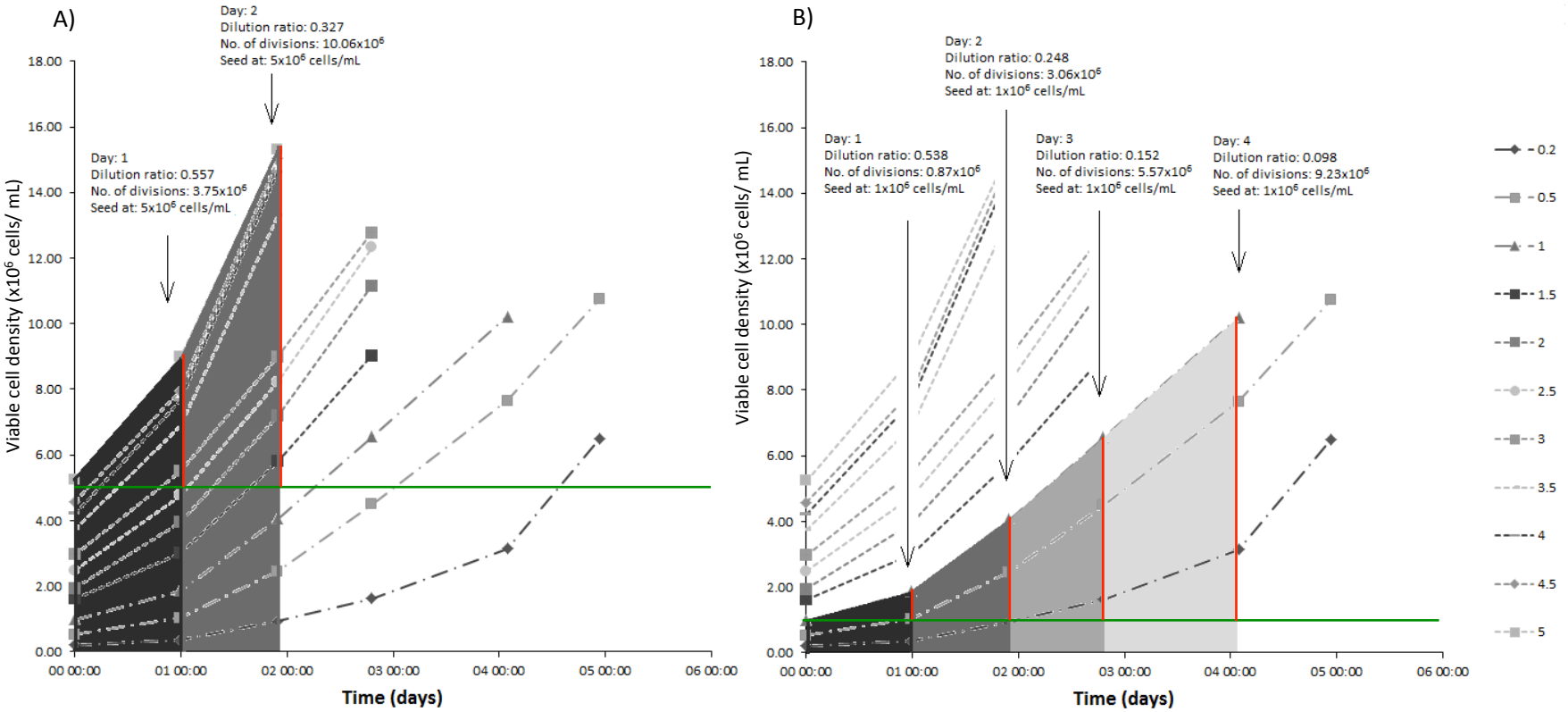

Figure 3.1 A staggered passaging regime schematic to show how different combinations of dilution ratio and number of cell divisions can be achieved. Growth curves in this figure are based on actual CHOK1SV growth curves and show the exponential component of growth for each seeding density. As can be seen and would be expected, higher seeding densities can sustain exponential growth for shorter time periods. Passaging later along the exponential phase requires a larger degree of dilution (smaller dilution ratio) (denoted by the red vertical lines) to return to the original seeding density at the following passage (horizontal green lines). Seeding at a high density provides a larger no. of cell divisions per unit time (shown in graph A here) compared to seeding at a lower density (graph B), however, dilution ratios are larger with a high seeding density passage plan and exponential is sustained for less time. Culturing cells at range of seeding densities with different lengths of passage time provides a range of combinations of no. of cell divisions and dilution ratios. These passaging regimes are continued over long-term culture and $\Delta\mu$ is monitored over time to inform which combination of parameters provides the most rapid change. Seeding density will be kept static, so slight changes in dilution ratio are expected from passage to passage due to natural variation in final cell density, and as changes in μ occur over time.

3.2.1.1 Number of cell divisions

For this study, it was valuable to determine the number of cell divisions that had occurred in a culture over a given amount of time as at each cell division, DNA is replicated introducing the chance of errors to be made and mutations to be incorporated into the genome. In order to determine the relationship between generation number (GN), number of cells in a population at GN, and number of cell divisions by this time, it is more simplistic to think in terms of a population that starts with just one cell (as shown in table 3.1):

Table 3.1 The relationship between increasing generation number, number of cells and number of cell divisions.

Parameter	Count					
Generation number (GN)	0	1	2	3	4	5
No. of cells at time (2^{GN})	1	2	4	8	16	32
No. of cell divisions by time ($2^{GN} - 1$)	0	1	3	7	15	31

As can be seen from table 3.1 above, the relationship between number of divisions (D) and generation number (GN) in a population starting with one cell can be defined by:

$$D = 2^{GN} - 1$$

Equation 3.1

Therefore, where the starting cell density is N0 cells/mL, the relationship between number of total cell divisions, ($D_{TOTAL\ CELLS}$), can be defined as:

$$D_{TOTAL\ CELLS} = (2^{GN} - 1) \times N0$$

GN has previously been defined in chapter 2 as $GN = log_2 \frac{Nx}{N0}$:

$$D_{TOTAL\ CELLS} = (2^{log_2 \frac{Nx}{N0}} - 1) \times N0$$

$$= \left(\frac{Nx}{N0} - 1\right) \times N0$$

$$= N0\left(\frac{Nx}{N0}\right) - N0$$

$$= Nx - N0$$

Equation 3.2

Therefore, to work out the number of divisions per mL in any culture is simply the final cell density (in cells/ mL) minus the initial cell density (in cells/ mL).

3.2.1.2 Dilution ratio

As has been mentioned, the dilution ratio at passage can affect the degree of genetic drift occurring in an *in vitro* sub-culturing system. It can be calculated simply by:

$$= \frac{N0'}{Nx}$$

Equation 3.3

Where *N*0' = Number of cells per mL at the start *of the following passage.*

3.2.1.3 Practical implementation of culturing regimes

125 mL Erlenmeyer flasks (with vent cap, Fisher, Loughborough, UK) containing 30 mL of CDCHO media supplemented with 6mM L-Gluatmine (both Invitrogen, Paisley, UK), were seeded at a density of 5 $\times 10^6$, 3 $\times 10^6$, or 1 $\times 10^6$ cells/ mL and passaged according to the following regimes:

- Seeding at 5 $\times 10^6$ cells/ mL to be passaged every 1 day
- Seeding at 5 $\times 10^6$ cells/ mL to be passaged every 2 days

- Seeding at 3 $\times 10^6$ cells/ mL to be passaged every 1 day
- Seeding at 3 $\times 10^6$ cells/ mL to be passaged every 2 days
- Seeding at 3 $\times 10^6$ cells/ mL to be passaged every 3 days
- Seeding at 1 $\times 10^6$ cells/ mL to be passaged every 1 day
- Seeding at 1 $\times 10^6$ cells/ mL to be passaged every 2 days
- Seeding at 1 $\times 10^6$ cells/ mL to be passaged every 3 days
- Seeding at 1 $\times 10^6$ cells/ mL to be passaged every 4 days

Each regime was performed in triplicate, giving a total of 27 cultures. In addition to this, 3 control cultures were set up that were passaged on a 3-4 day passage routine, seeding at 0.2 $\times 10^6$ cells/ mL each time (these parameters are standard in-house laboratory protocol). The regime was continued for approximately 6 weeks. Cultures seeded at 5 $\times 10^6$ cells/ mL are only passaged every 1 or 2 days as exponential phase is not sustained beyond day 2; cultures seeded at 3 $\times 10^6$ cells/ mL are only passaged every 1, 2 or 3 days as exponential phase is not sustained beyond day 3; and cultures seeded at 1 $\times 10^6$ cells/ mL are passaged every 1, 2, 3 or 4 days exponential phase is not sustained beyond day 4. 1 $\times 10^6$ cells/ mL was chosen as the lowest seeding to density to be used in this study as it was shown to be the highest seeding density that could sustain growth for 4 days (see figure 3.1). Also, it is not common laboratory practice to passage standard cultures at any larger time increments than 4 days as there is risk of entering stationary phase of growth (Makrides 2003; Hu 2012), so lower seeding densities (than control densities) and a longer passage period than 4 days were not chosen for this reason. The other two seeding densities, 5 $\times 10^6$ cells/ mL and 3 $\times 10^6$ cells/ mL, were also chosen as they were the largest seeding densities that could sustain exponential growth for 2 days and 3 days, respectively. The largest sustainable seeding densities were chosen as more cells are present in those cultures and therefore more total cell divisions are occurring per unit time, maximising the opportunity for mutations to occur.

3.2.2. Evolution of a hypothermia-adapted host CHOK1SV cell line and primary characterisation studies

3.2.2.1 Long term culturing of CHOK1SV parental (host) cells

The following methods were performed with the intention of attaining a cell line that can actively proliferate in hypothermic conditions at a similar rate to the same cells in optimum conditions (37°C). To adapt CHOK1SV cells to hypothermic growth, cultures were continuously sub-cultured in an incubator (Infors, Reigate, UK) set to 32°C, with all other parameters set to standard levels (5% CO_2, 140 rpm) for approximately 160 generations. For control purposes, cultures were also continuously sub-cultured at 37°C (5% CO_2, 140 rpm) for the same duration. In terms of replicates and cell source, one vial of CHOK1SV cells was received from Lonza Biologics cell banking department (Slough, UK). This vial was then expanded in house to create a working cell bank (in which 20 vials were created for potential future use). From this bank, 3 vials revived from cryostorage and after 3 passages in standard conditions, another bank was made of each of the three cultures (this was done for future comparison and reference purposes as these parental cultures mark the start of the evolution experiment). Following this, each of these cultures were used to seed two new cultures: from each pair, one culture was returned to standard conditions and one was subsequently incubated at 32°C. This created three lineages, referred to hereafter as A, B and C, each lineage comprising of a culture at 32°C and 37°C. Figure 3.2 shows set up this schematically. This process resulted in 6 cultures: 3 that had been cultured long-term at 32°C (A, B and C) and 3 that had been cultured long-term at 37°C (A, B and C). The three cultures at 37°C were control cultures, used to monitor the natural variation in parameters over long-term culture. At each passage during long-term culture, growth rate, cell size and cell viability were monitored for cultures at both 32°C and 37°C. Periodic cell banking was also performed over the course of the long-term culturing process for precautionary reasons (for example, in case a contamination occurred). All cell cultures were 30 mL in volume contained in 125 mL Erlenmeyer flasks.

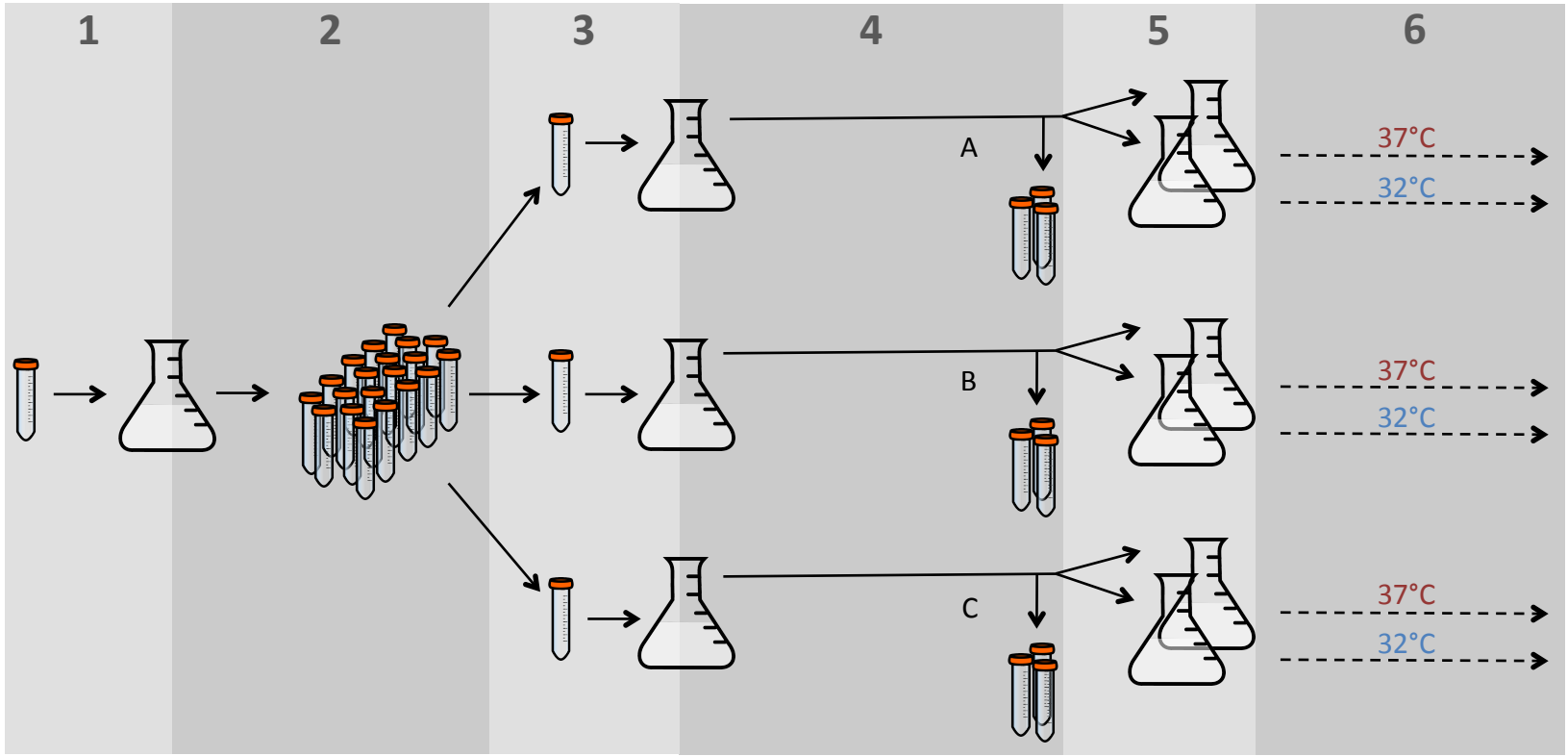

Figure 3.2 A Schematic to show the source and generation of cell cultures that were used in the adaptation of CHOK1SV cells to hypothermic conditions. Numbers 1 to 6 and the corresponding shaded blocks represent different steps in the process, which are described as follows: **1)** a single vial of CHOK1SV cells was received from Lonza Biologics cell banking department which was revived and seeded into 125mL Erlenmeyer flask (containing standard 6 mM glutamine supplemented CD CHO under standard conditions of 5%, CO_2 and 140 rpm, which is used in all flasks mentioned hereafter) and cultured at 37°C; **2)** after 3 passages, a large primary working cell bank was made; **3)** three vials from the working cell bank were then revived and seeded into Erlenmeyer flasks; **4)** each of the three cultures, termed A, B and C were passaged under standard conditions at 37°C for 3 passages before the final of each was used to create banks, which mark the beginning of the adaptation process. These banks are referred to as the parental cell lines and were created for future reference and comparison purposes; **5)** the final flask of A, B and C was also used to seed two cultures, providing a pair of flasks from A, B and C lineages; **6)** one flask from each pair was then cultured at 32°C and the other flask from the pair was cultured at 37°C (to serve as a control), and growth rate, cell size and cell viability were monitored at each passage that followed.

3.2.2.2 Further adaptation of evolved, 32°C-adapted CHOK1SV cells to more severe hypothermia (30°C) and returning evolved, 32°C-adapted CHOK1SV cells to standard conditions (37°C)

Once adapted to growth at 32°C, the hypothermia adapted cells from A, B and C lineages (figure 3.2) were used to also seed 3 new 125 mL Erlenmeyer flasks (containing 6 mM glutamine supplemented CD CHO under standard conditions of 5%, CO_2 and 140 rpm) that were then incubated at 30°C. In addition to this, un-evolved (parental) cells from lineages A, B and C (i.e. from the vials that were banked in step 4 of figure 3.2) were also cultured at 30°C for control/comparison purposes. Cultures were passaged for 6 weeks and growth rate, cell size and cell viability were monitored at each passage.

Additionally, hypothermia-adapted cells from A, B and C lineages (figure 3.2) were used to also seed another 3 new 125mL Erlenmeyer flasks (containing 6 mM glutamine supplemented CD CHO under standard conditions of 5%, CO_2 and 140 rpm) that were then returned to incubation at 37°C. These cultures were passaged for ~3 weeks and growth rate, cell size and cell viability were monitored at each passage.

3.2.2.3 Quantification of total cell protein

Total cell protein was quantified using a Pierce® BCA (bicinchoninic acid) Protein Assay Kit (Thermo Scientific, Loughborough, UK), according to the manufacturers protocol. This is summarised as follows: On day 3 post sub-culture, samples were harvested from batch Erlenmeyer cultures and cell density and viability were measured using the Vi-CELL XR cell viability analyser (Beckmann Coulter, High Wycombe, UK). Using the viable cell density just measured, triplicate aliquots of 5 $\times 10^6$ cells were taken from each culture. The cells were then pelleted by centrifuging at 200 $\times g$ for 5 minutes. The supernatant was removed and discarded and the cells were washed in cold PBS and pelleted again by centrifuging at 200 $\times g$ for 5 minutes. To lyse the cells, 1 mL of RIPA buffer (150mM NaCl, SDS 0.1% w/v, sodium deoxycholate 0.5% w/v, Triton X-100 1% v/v, in 0.05M Tris-HCl buffer at

pH 8) was added to each aliquot of 5 $\times 10^6$ cells and mixed by pipetting. The aliquots were then incubated on ice for 15 minutes. Following this, the aliquots were centrifuged at 2500 $\times g$ for 5 minutes to pellet cell debris. For each aliquot, triplicate transfers of 25 µL of supernatant was added to wells of a flat-bottomed 96 well plate (Sigma-Aldrich, Dorset, UK). The same was performed for the standards that were made up at the following concentrations of Bovine serum albumin (BSA): 2000, 1500, 1000, 750, 500, 250, 125 and 25 µg mL^{-1} as well as a blank (0 µg mL^{-1}). Once all samples and standards have been transferred to the 96 well plate, 200 µL of the working reagent (prepared by mixing BCA reagent A and BCA reagent B from the kit to the ratio of 50:1) is added to each well (giving individual total well volumes of 225 µL each), the plate is covered and then incubated at 37°C for 30 minutes. The plate is then cooled to room temperature (to ensure condensation does not skew readings) before measuring the absorbance at 562 nm on a plate reader. The average 562 nm absorbance measurement of the blank standard replicates is then subtracted from the 562 nm absorbance measurement of all the other sample replicates (unknown samples as well as standards). A standard curve is then generated using the blank-corrected measurements of the standards versus the corresponding concentrations (in µg mL^{-1}) to which the standards were prepared. The protein concentration of each sample can now be determined using this curve and protein content per cell can be calculated by dividing the total protein per sample by the number of cells that were used to generate the sample (5 $\times 10^6$ cells).

3.2.2.4 Quantification of total cell RNA content

On day 3 post sub-culture, samples of cell cultures were harvested from batch Erlenmeyer cultures in order to measure cell density and viability using the Vi-CELL XR cell viability analyser. Using the Vi-CELL viable cell density measurements, triplicate aliquots of 5 $\times 10^6$ cells were taken from each culture for RNA extraction and quantification. An RNeasy® Mini Kit (QIAGEN, Manchester, UK) was used to extract total RNA from cell samples. The cells were first disrupted (membranes lysed) using Buffer RLT and homogenised (reducing the viscosity of

the lysate by shearing high-molecular weight genomic DNA and other high-molecular weight components) by passing the lysate through a QIAshredder QIAGEN, Manchester, UK). The lysate then was centrifuged at maximum speed (13000 rpm) in a bench-top centrifuge and the supernatant carefully removed by pipetting. One volume of 70% ethanol was then added to this supernatant and thoroughly mixed by pipetting, this creates conditions that promote selective binding of RNA to the RNeasy spin column. This mixture is then applied to the RNeasy spin column (up to 700 µL at a time) placed in a 2 mL collection tube. This is the centrifuged for 15 seconds at 8000 ×*g* and the flow-through is discarded. Following this, 500 µL of Buffer RPE was added to the RNeasy spin column and centrifuged for 15 seconds at 8000 *g*, again, discarding the flow through. Another 500 µL of Buffer RPE was then added and the column centrifuged for 2 minutes at 8000 *g*. At this point, the RNeasy spin column is placed in a new 2 mL collection tube, 50 µL of RNase-free water is added directly to the spin column membrane and the column plus collection tube is centrifuged for 1 minute at 8000 ×*g* to elute the RNA.

The concentrations of the extracted RNA samples were assessed using a NanoDrop™ 2000 Spectrophotometer (Thermo Scientific, Loughborough, UK). The arm was then wiped clean with lint-free microscope lens tissue and samples were added and analysed in turn with the arm being cleaned in this way between each sample. Each sample was measured on the NanoDrop™ in triplicate.

3.2.2.5 Ploidy testing using flow cytometry

The number of sets of chromosomes (ploidy) that the evolved (32°C-adapted) cell line possessed was determined and compared to a culture from the primary cell bank (figure 3.2, step 2). In addition to this, the hypothermia adapted cells that were cultured long-term at more severe hypothermic conditions of 30°C were also analysed. This was done using FxCycle™ PI/RNase Staining Solution (Thermo Scientific, Loughborough, UK), which was detected using a BD LSRII Flow Cytometer (BD Biosciences, Oxford, UK). FxCycle™ PI/RNase Staining Solution contains propidium iodide (PI) that binds to DNA by intercalating between the

bases with minimal sequence preference. Propidium iodide also binds to RNA, hence the requirement of RNase so that only DNA is stained. The measurement of DNA in this way allows the study of cell populations in various phases of the cell cycle as well as ploidy detection. DNA content can be measured by fluorescent stains such as FxCycle™ PI/RNase Staining Solution as the emission signal is proportional to DNA mass. A frequency histogram can be produced which reveals the number of cells undergoing certain cell growth phases: G_0/G_1 (one paired set of chromosomes per cell), S (DNA synthesis – variable amounts of DNA between G_0/G_1 and G_2/M) and G_2/M (two sets of paired chromosomes per cell). Anything larger than the amount of DNA in G2/M indicates polyploidy.

Staining was performed as follows: On day 3 post sub-culture, cell viability and density was measured using the Vi-CELL XR. Using these measurements, 1×10^6 cells were harvested from day three of culture (3 days post sub-culture) and fixed according to the paraformaldehyde (PFA) fixing protocol (described in chapter 2). The cells were then washed with PBS to ensure all fixative was removed before staining, three washes were performed in total, centrifuging at 200 ×*g* for 5 minutes and removing the supernatant after each wash. After this, 0.5 mL of FxCycle™ PI/RNase Staining Solution stain is then added to each pellet and mixed well by pipetting. The samples are then incubated for 30 minutes at room temperature, protected from light. The samples are then analysed without washing, using 532 nm excitation and emission collected with a 585/42 bandpass filter. Histograms showing DNA content distribution were obtained for each sample.

3.3 Results

3.3.1 Optimisation of culturing regimes for rapid evolution of growth rate

Using only the parameters that can be manipulated during ordinary cell culture (routine passaging), parameters such as seeding density, length of culture and dilution ratio, differential degrees of change in growth rate can be achieved over a culture period of approximately six weeks. Control cultures (those passaged every 3-4 days and seeded at 0.2 $\times 10^6$ cells/ mL) showed very little change in growth rate over this time period. All cultures retained high viability throughout the study (>95%). The viable cell densities over time for each set of culturing regimes (described in section 3.2.1.3), plus controls, are shown in figures 3.3 to 3.7. The change in growth rate over time that was observed for each of the culturing regimes, plus controls, are shown in figures 3.8 to 3.12.

The calculation to determine the change in growth rate over time *for each culture* was as follows: [Mean of final three passage growth rates] – [Mean of first three passage growth rates].

When *average change in growth rate* for each regime is mentioned this refers to the averaged change in growth rate over time of all three culture repeats in a given passaging regime (summed and divided by three).

Table 3.2 and figure 3.13 summarise this data for clarity purposes.

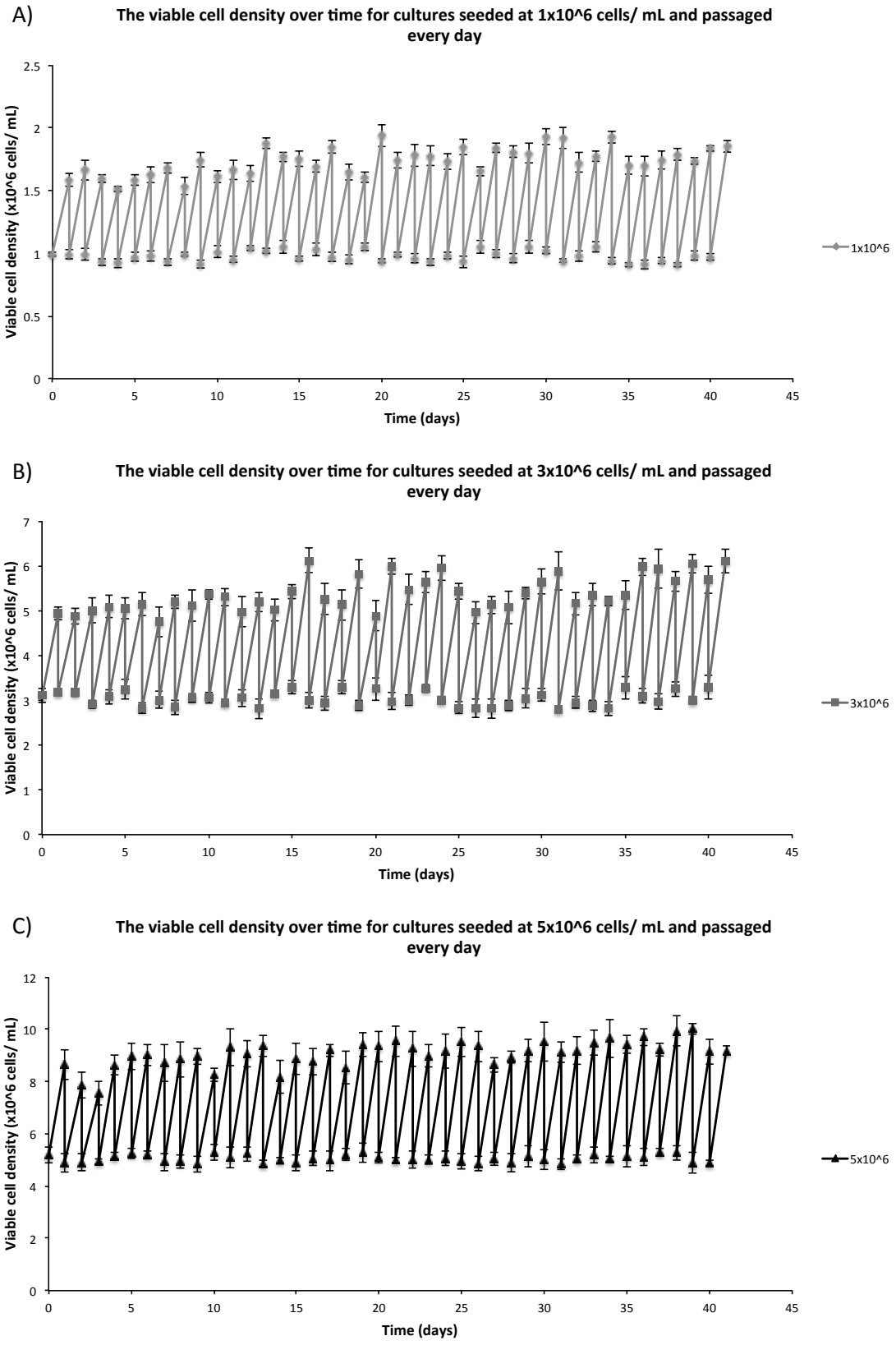

Figure 3.3 The viable cell density over time for cultures seeded at A) 1 ×10^6 cells/ mL, B) 3 ×10^6 cells/ mL and C) 5 ×10^6 cells/ mL, and passaged every day. Markers represent the actual seeding density recorded (~1, ~3, or ~5 ×10^6 cells/ mL) and the maximum viable cell density achieved 1 day later, when cultures were passaged again. Error bars, SD; N = 3.

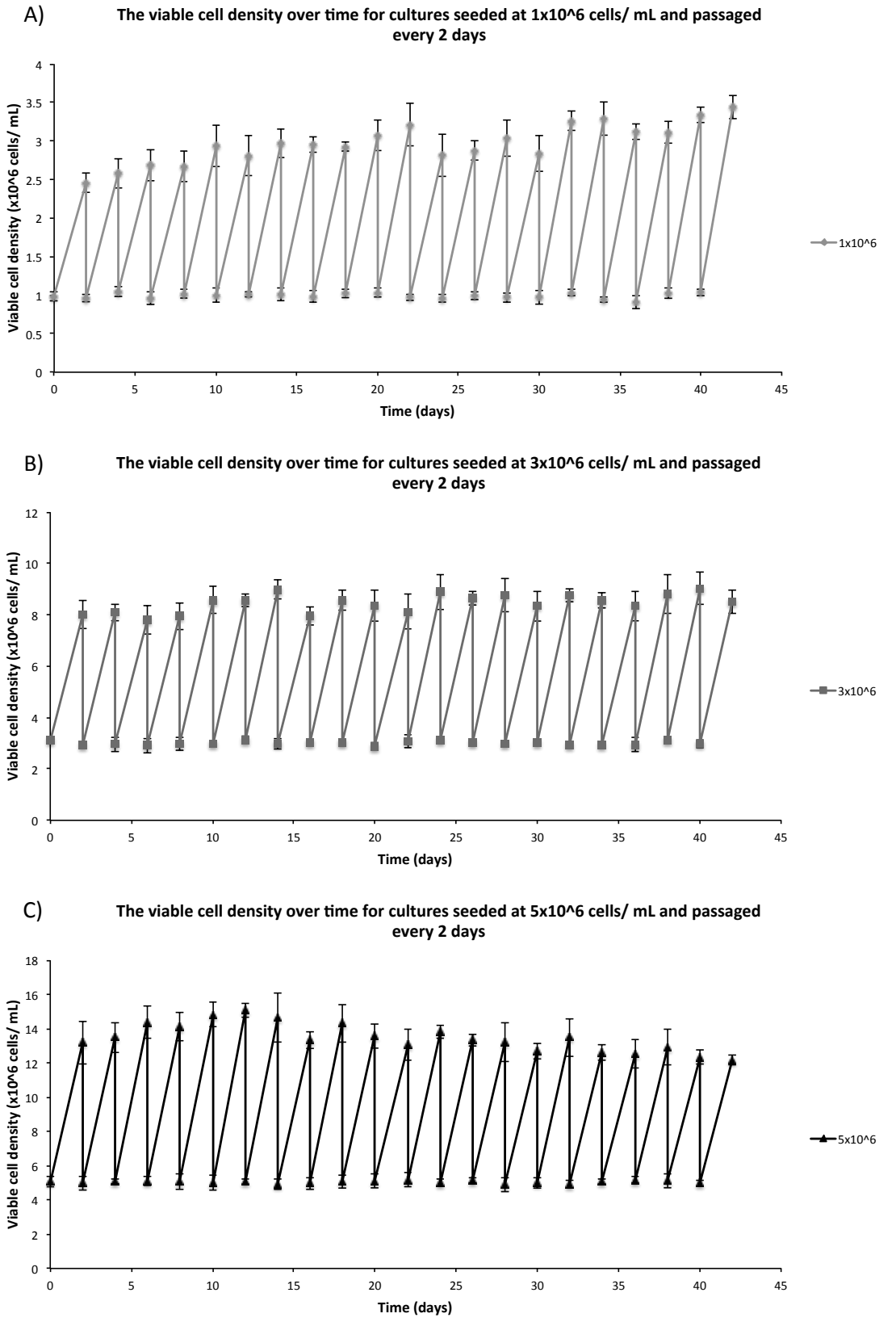

Figure 3.4 The viable cell density over time for cultures seeded at A) 1 ×10⁶ cells/ mL, B) 3 ×10⁶ cells/ mL and C) 5 ×10⁶ cells/ mL, and passaged every 2 days. Markers represent the actual seeding density recorded (~1, ~3, or ~5 ×10⁶ cells/ mL) and the maximum viable cell density achieved 2 days later, when cultures were passaged again. Error bars, SD; N = 3.

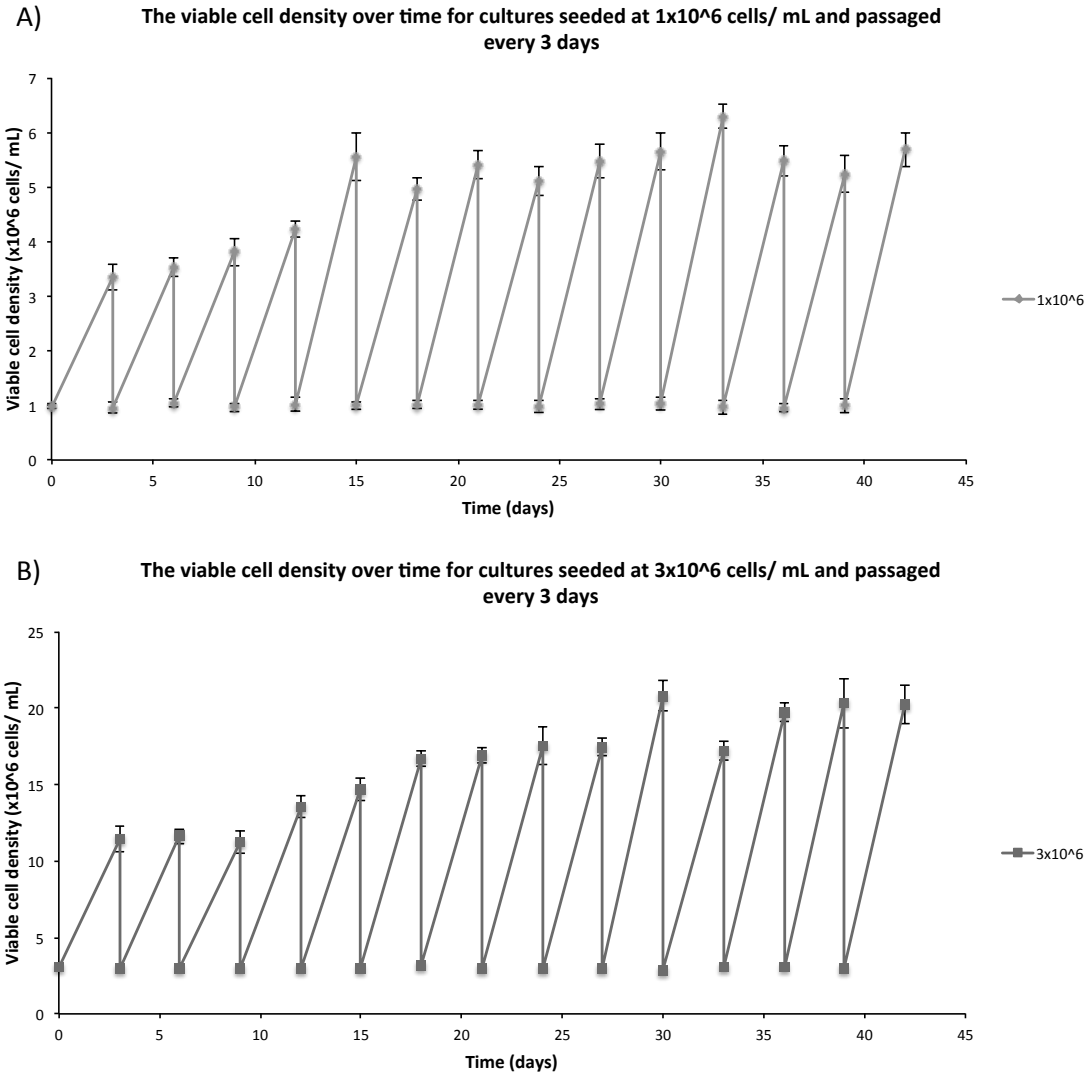

Figure 3.5 The viable cell density over time for cultures seeded at A) 1 ×10^6 cells/ mL and B) 3 ×10^6 cells/ mL, and passaged every 3 days. Markers represent the actual seeding density recorded (~1 or ~3 ×10^6 cells/ mL) and the maximum viable cell density achieved 3 days later, when cultures were passaged again. Error bars, SD; N = 3.

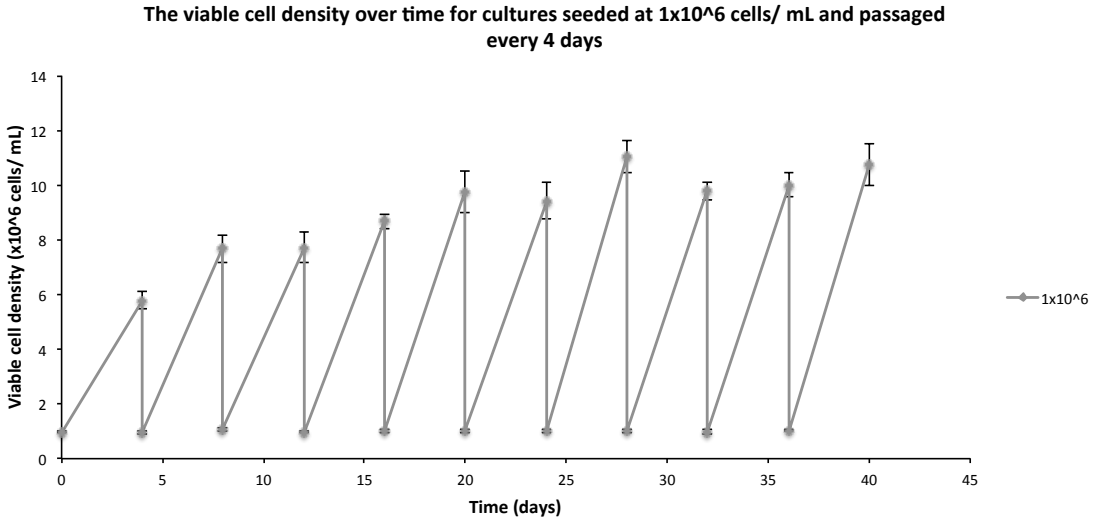

Figure 3.6 The viable cell density over time for cultures seeded at 1 ×10^6 cells/ mL and passaged every 4 days. Markers represent the actual seeding density recorded (~1 ×10^6 cells/ mL) and the maximum viable cell density achieved 4 days later, when cultures were passaged again. Error bars, SD; N = 3.

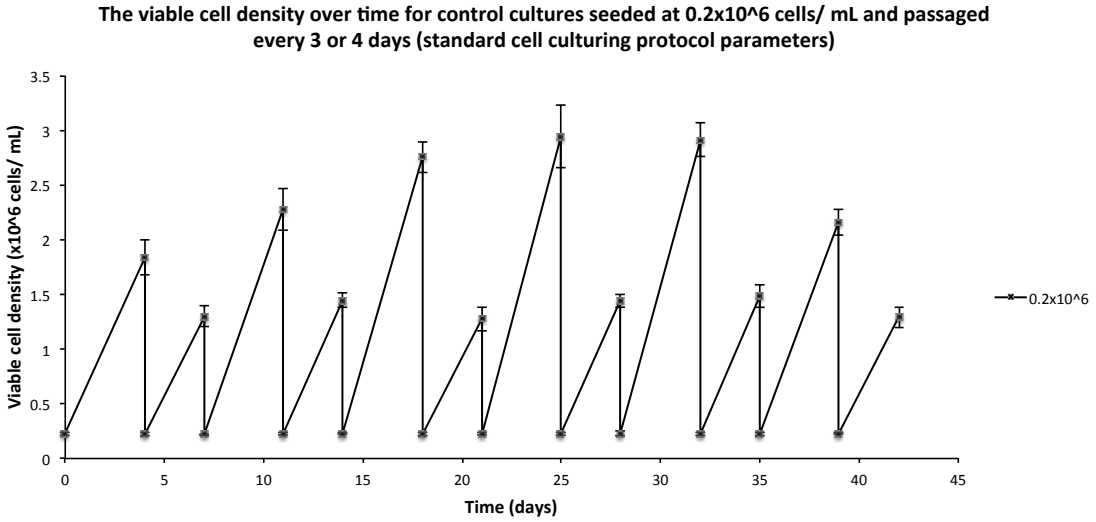

Figure 3.7 The viable cell density over time for control cultures seeded at 0.2 ×10^6 cells/ mL and passaged every 3 or 4 days. These parameters are used for standard cell culture and have been implemented for control purposes. Markers represent the actual seeding density recorded (~0.2 ×10^6 cells/ mL) and the maximum viable cell density achieved 3 or 4 days later, when cultures were passaged again. Error bars, SD; N = 3.

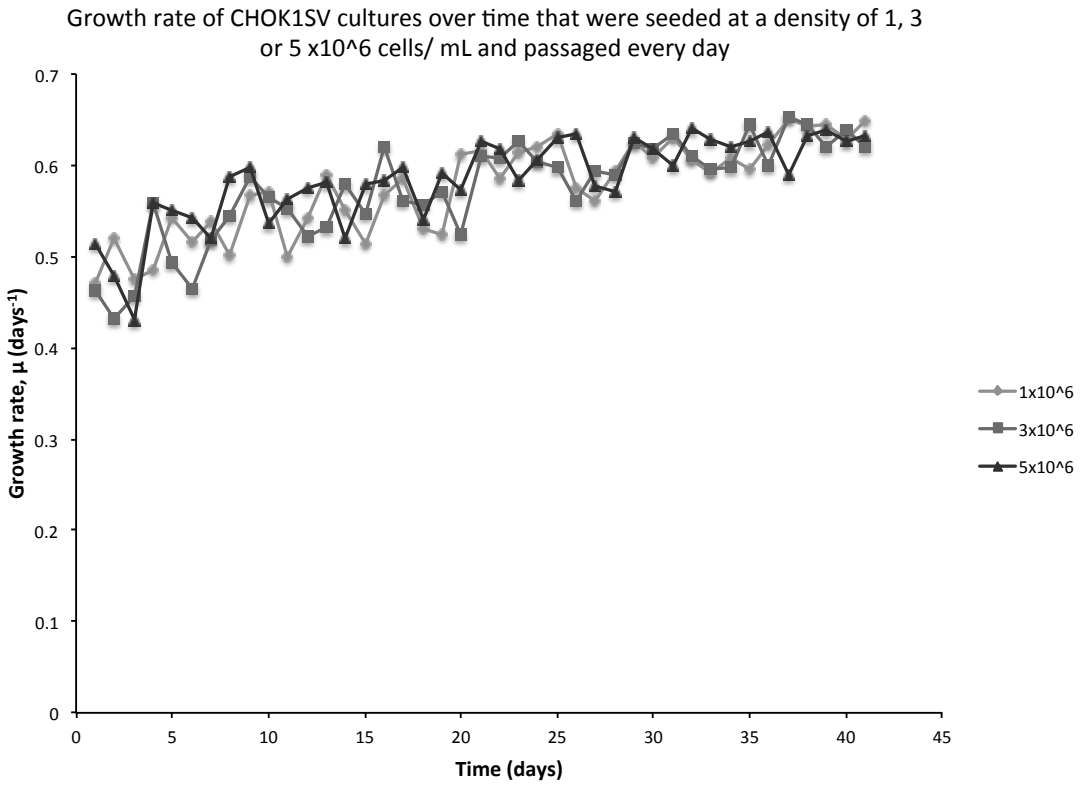

Figure 3.8 The growth rate, μ (days^{-1}), over time for cultures seeded at 1 ×10^6 cells/ mL, 3 ×10^6 cells/ mL and 5 ×10^6 cells/ mL and passaged every day. Markers represent the growth rate of cells during one passage and are the average of three cultures (error bars have been omitted for clarity purposes). The average change in growth rate per day from the start of the study to the end was 3.61 ×10^{-3} days^{-2} for cultures seeded at 1 ×10^6 cells/ mL, 4.19 ×10^{-3} days^{-2} for cultures seeded at 3 ×10^6 cells/ mL and 3.75 ×10^{-3} days^{-2} for cultures seeded at 5 ×10^6.

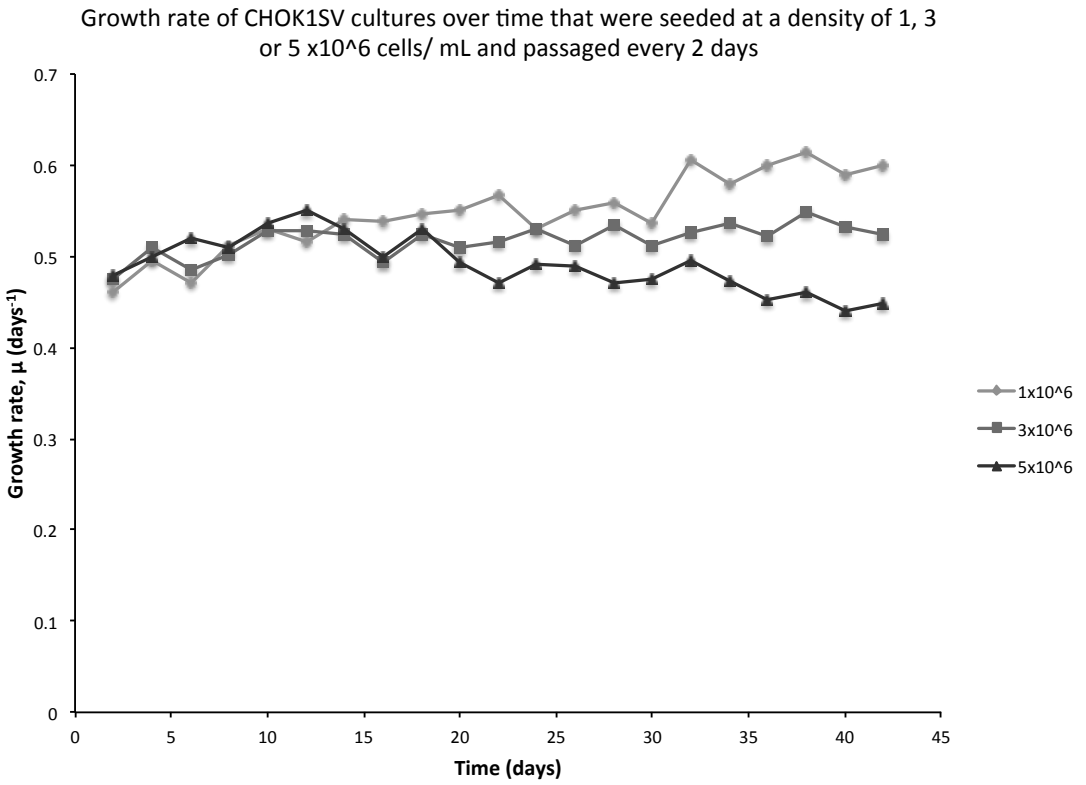

Figure 3.9 The growth rate, μ (days^{-1}), over time for cultures seeded at 1 ×10^6 cells/ mL, 3 ×10^6 cells/ mL and 5 ×10^6 cells/ mL and passaged every 2 days. Markers represent the growth rate of cells during one passage and are the average of three cultures (error bars have been omitted for clarity purposes). The average change in growth rate per day from the start of the study to the end was 3.00 ×10^{-3} days^{-2} for cultures seeded at 1 ×10^6 cells/ mL, 1.09 ×10^{-3} days^{-2} for cultures seeded at 3 ×10^6 cells/ mL and -1.19 ×10^{-3} days^{-2} for cultures seeded at 5 ×10^6.

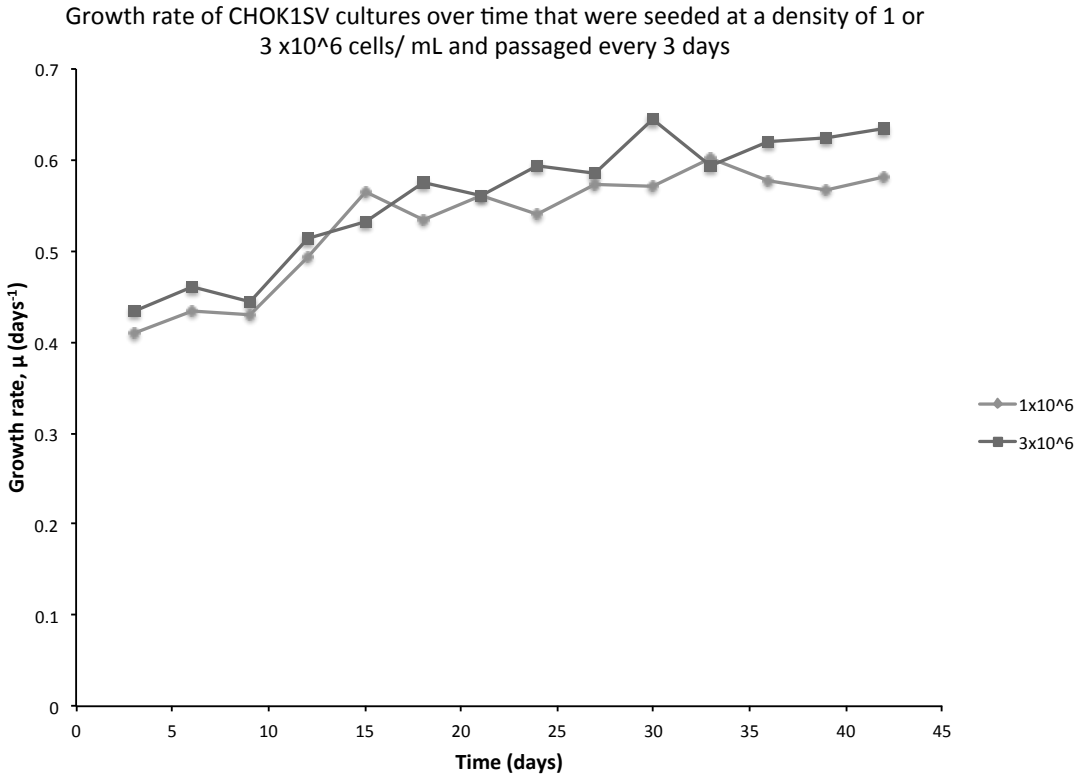

Figure 3.10 The growth rate, μ (days^{-1}), over time for cultures seeded at 1 ×10^6 cells/ mL and 3 ×10^6 cells/ mL and passaged every 3 days. Markers represent the growth rate of cells during one passage and are the average of three cultures (error bars have been omitted for clarity purposes). The average change in growth rate per day from the start of the study to the end was 3.56 ×10^{-3} days^{-2} for cultures seeded at 1 ×10^6 cells/ mL and 4.29 ×10^{-3} days^{-2} for cultures seeded at 3 ×10^6 cells/ mL.

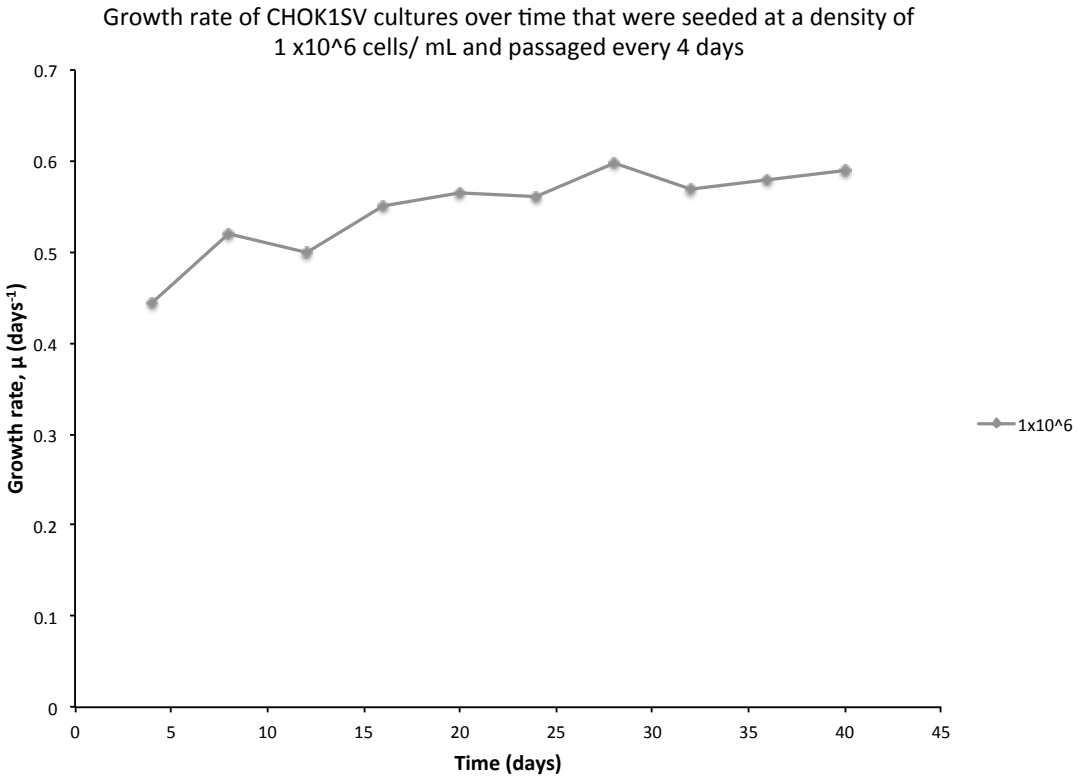

Figure 3.11 The growth rate, μ (days^{-1}), over time for cultures seeded at 1 ×10^6 cells/ mL and passaged every 4 days. Markers represent the growth rate of cells during one passage and are the average of three cultures (error bars have been omitted for clarity purposes). The average change in growth rate per day from the start of the study to the end was 2.27 ×10^{-3} days^{-2} for cultures seeded at 1 ×10^6 cells/ mL.

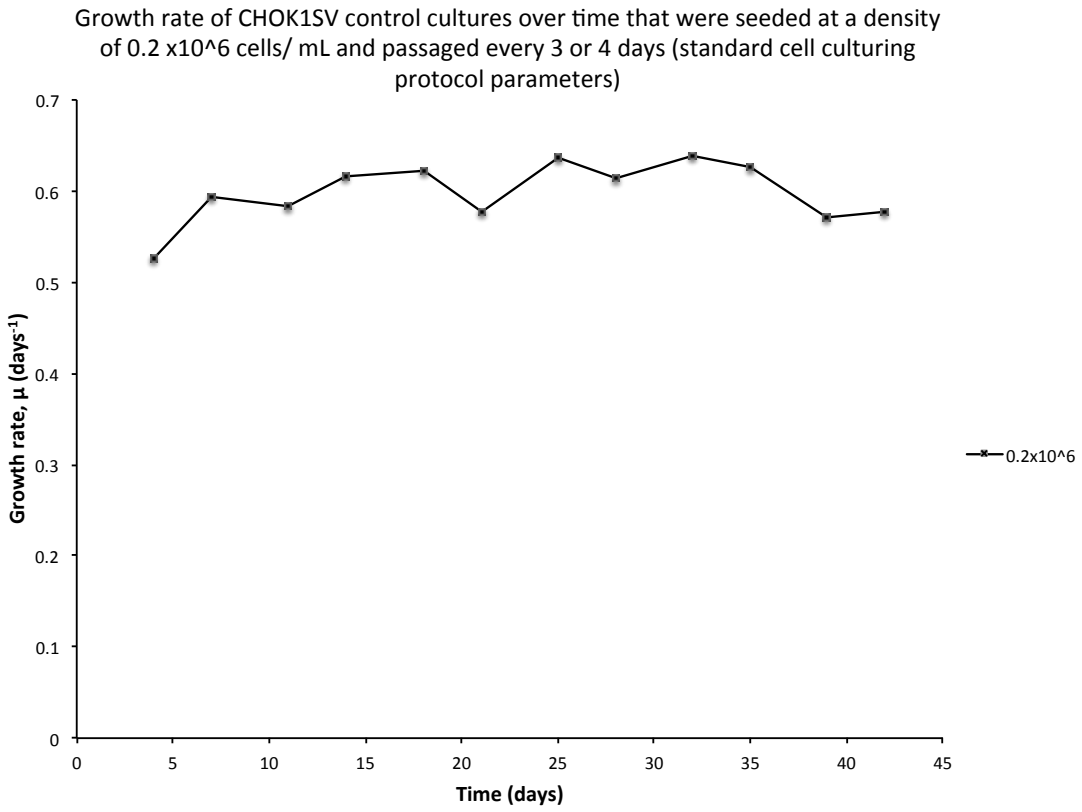

Figure 3.12 The growth rate, μ (days^{-1}), over time for cultures seeded at 1 ×10^{6} cells/ mL and passaged every 3 or 4 days. Markers represent the growth rate of cells during one passage and are the average of three cultures (error bars have been omitted for clarity purposes). The average change in growth rate per day from the start of the study to the end was 0.57 ×10^{-3} days^{-2} for cultures seeded at 0.2 ×10^{6} cells/ mL.

Table 3.2 A summary of data from the optimisation of cell culture passaging parameters for rapid evolution of growth rate. Altering seeding density and the frequency of passage will result in different dilution ratios at passage, as can be seen in the table. These parameters also affect the number of cell divisions per day and it can be seen that the *rate of change in growth rate* (i.e. the average change in growth rate *per day*) does also differ between different passaging regimes.

Passage frequency:	1 day			2 days			3 days		4 days	3-4 days
Seeding density (cells/ mL):	1×10^6	3×10^6	5×10^6	1×10^6	3×10^6	5×10^6	1×10^6	3×10^6	1×10^6	0.2×10^6
Total days cultured	42	42	42	42	42	42	42	42	40	42
Average change in growth rate (d^{-1})	152.0×10^{-3}	176.3×10^{-3}	157.7×10^{-3}	126.3×10^{-3}	46.0×10^{-3}	-50.3×10^{-3}	149.8×10^{-3}	180.0×10^{-3}	91.1×10^{-3}	23.9×10^{-3}
Average change in growth rate per day (d^{-2})	3.61×10^{-3}	4.19×10^{-3}	3.75×10^{-3}	3.00×10^{-3}	1.09×10^{-3}	-1.19×10^{-3}	3.56×10^{-3}	4.29×10^{-3}	2.27×10^{-3}	0.57×10^{-3}
Average no. cell divisions/day/mL ($\times 10^6\ d^{-1}\ mL^{-1}$)	0.761	2.356	4.020	0.990	2.729	4.221	1.330	4.463	2.016	0.486
Average dilution ratio at passage	0.562	0.562	0.556	0.334	0.355	0.374	0.200	0.183	0.110	0.117
Number of times passaged	42	42	42	21	21	21	14	14	10	12

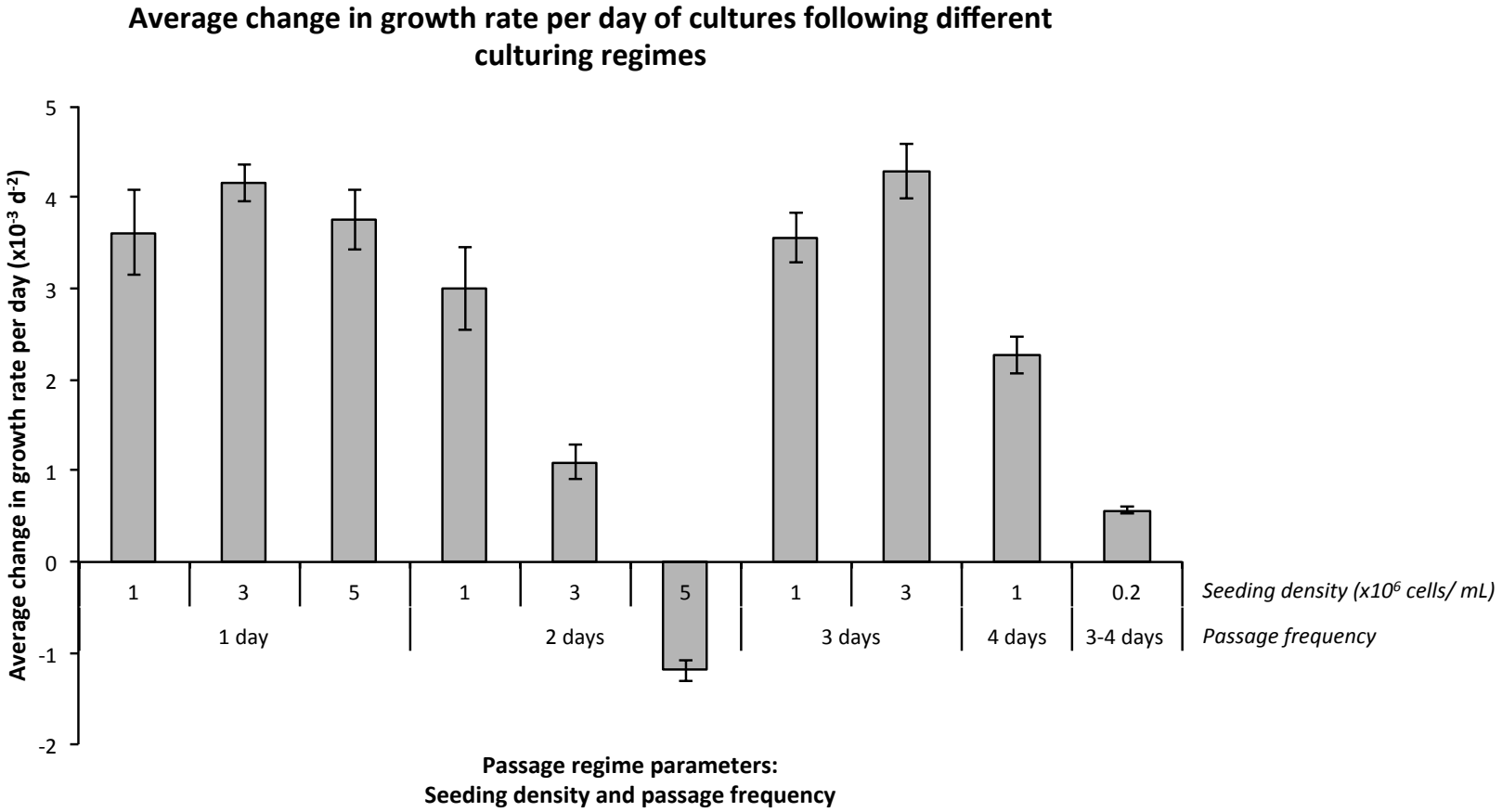

Figure 3.13 A summary of change in growth rate data from the optimisation of cell culture passaging parameters for rapid evolution of growth rate. It can be seen that the rate of change in growth rate (average change in growth rate per day) differs largely between different passaging regimes. Error bars, SD; N = 3.

As can be seen from figure 3.13 and table 3.2, there are clear differentials in the evolution of growth rate according to cell culture regime parameters: when passaging cultures every day, little difference in average change in growth rate per day is observed *between* cultures seeded at 1, 3 and 5 $\times 10^6$ cells/ mL (ranging between 3.61 $\times 10^{-3}$ days^{-2} and 4.19 $\times 10^{-3}$ days^{-2}), however the change in growth rate is positive i.e. cells in these cultures proliferate faster over the course of the study, and they do so at a much quicker rate than the control cultures, whose average change in growth rate per day was a relatively low 0.57 $\times 10^{-3}$ days^{-2}. It is also observed that these cultures have very large average dilution ratios ($\sim$0.56), meaning that under half of the cell population is removed at passage.

When passaging every 2 days, there are much larger differences observed in average change in growth rate per day between cultures seeded at 1, 3 and 5 $\times 10^6$ cells/ mL: seeding at 1 $\times 10^6$ cells/ mL results in a positive change but not as large as when passaging every day (3.00 $\times 10^{-3}$ days^{-2}); seeding at 3 $\times 10^6$ cells/ mL still results in a positive change but at a considerably smaller rate (1.09 $\times 10^{-3}$ days^{-2}) and seeding at 5 $\times 10^6$ cells/ mL actually results in a negative change (-1.19 $\times 10^{-3}$ days^{-2}), meaning the rate of proliferation of the cells in these cultures actually decreased over the time course of this study. The dilution ratio of these cultures was similar again, with average ratios of 0.33 to 0.37, meaning that approximately two thirds of the cell population is removed at passage.

When passaging every 3 days, we see large average changes in growth rate per day, with those cultures seeded at 1 $\times 10^6$ cells/ mL showing an average of 3.56 $\times 10^{-3}$ days^{-2} and those seeded at 3 $\times 10^6$ cells/ mL showing an average of 4.46 $\times 10^{-3}$ days^{-2}, which is the largest average rate of change observed in this study. As has been previously mentioned, there were no cultures seeded at 5 $\times 10^6$ cells/ mL and passaged every 3 days, as exponential phase can not be sustained for this long a time period at this seeding density. Average dilution ratios following these regimes were 0.18 to 0.20, meaning that approximately 80% of the cell population is removed at passage.

When passaging every 4 days, a moderate average change in growth rate per day (2.27×10^{-3} days^{-2}) is observed in those cultures seeded at 1×10^6 cells/ mL, which show an average dilution ratio of 0.11, meaning that approximately 90% of the cell population is removed at passage. There were no cultures seeded at 3×10^6 cells/ mL or 5×10^6 cells/ mL and passaged every 4 days, for reasons previously stated.

As mentioned, the control cultures which were seeded at 0.2×10^6 cells/ mL and passaged every 3 or 4 days showed very little change in growth rate over the course of this study (compared to the other culture regimes), and the average dilution ratio was ~0.11.

One-way ANOVA with Tukey's multiple comparisons test was performed on above data for statistical significant differences, see appendix I.

3.3.2 Evolution of a hypothermia adapted host CHOK1SV cell line

3.3.2.1 Long term culturing of CHOK1SV parental (host) cells

Using a long-term culturing approach, three cultures of CHOK1SV host cells were subjected to hypothermic conditions (32°C) and eventually adapted to these conditions, returning to normal growth rates that would be expected in optimum conditions (37°C). These three cultures were termed 32A, 32B and 32C and each of the three cultures had control counterparts that were cultured long-term at 37°C, named correspondingly: 37A, 37B and 37C.

Figures 3.14 and 3.15 show the change in cell size (cell diameter) and growth rate of these cultures with increasing generation number. Generation number is used here as it provides a reference to how many times the cell population has divided (doubling time of the cell was initially extremely slow when cells were first subjected to hypothermic conditions). Figure 3.16 shows the growth rate of the hypothermia-cultivated CHOK1SV cultures (that are now adapted to growth at 32°C) when they are returned back to standard conditions (37°C). Both the hypothermia adapted cultures (32A, 32B and 32C) and their standard-condition control counterparts (37A, 37B and 37C) were subsequently cultured at 30°C to

determine whether the cultures could survive and be adapted to an even harsher hypothermic environment. The results of this study are shown in figures 3.17 and 3.18.

A)

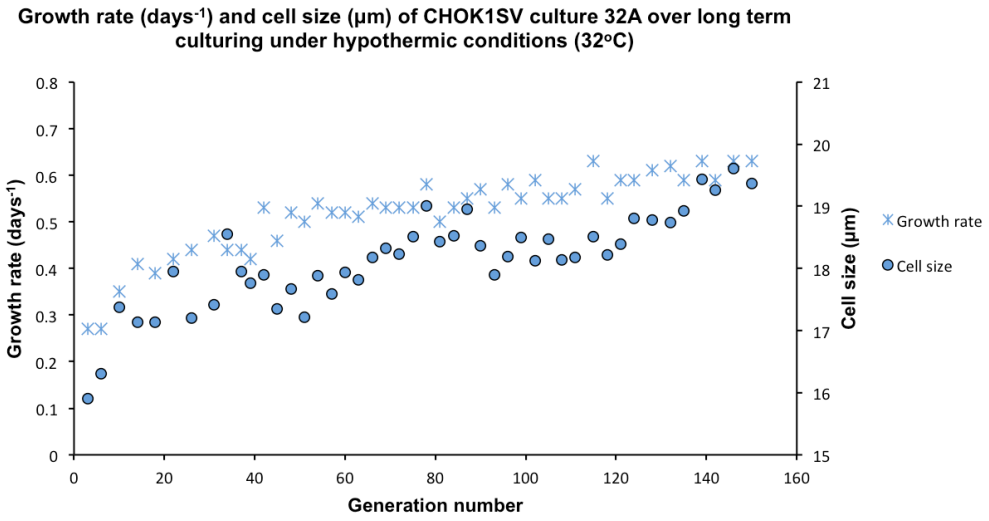

B)

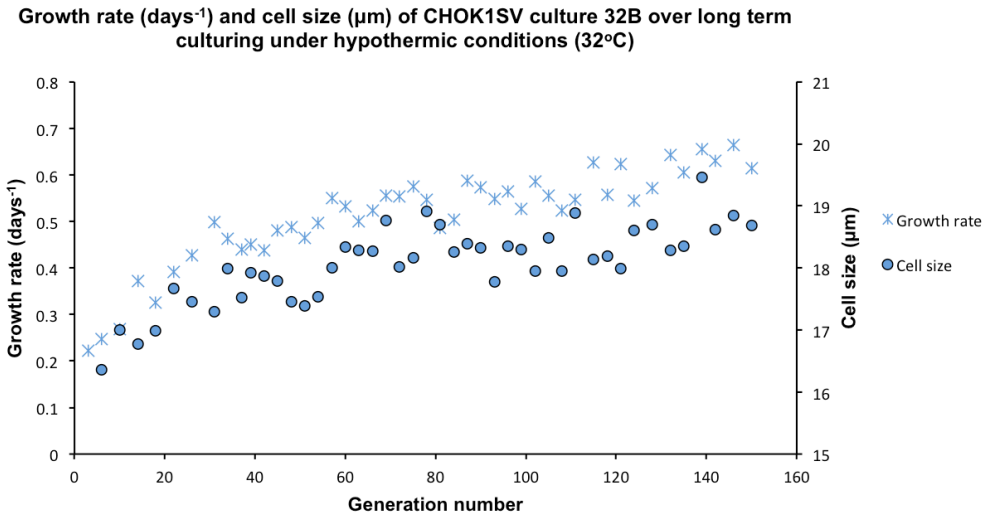

C)

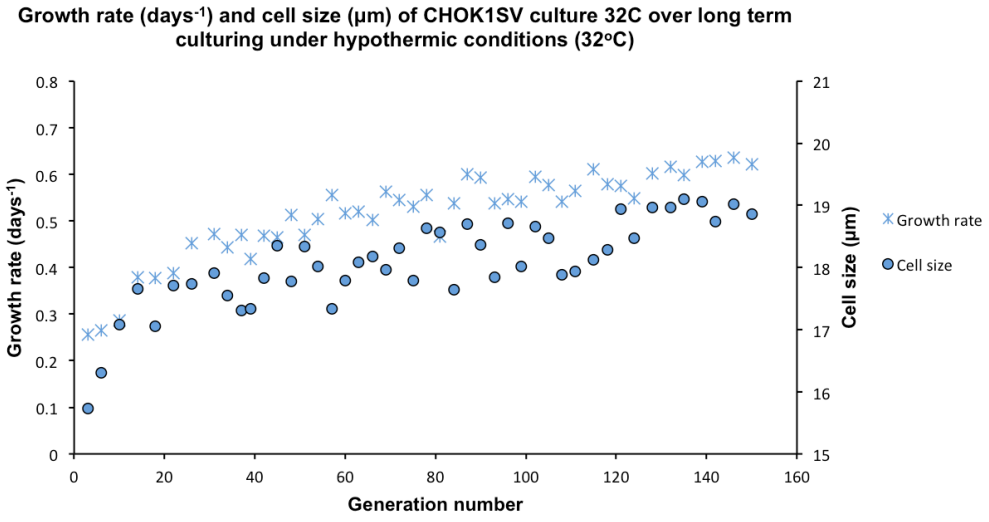

Figure 3.14 The cell size and growth rate under hypothermic conditions (32°C) of: A) culture 32A, B) culture 32B and C) culture 32C.

A)

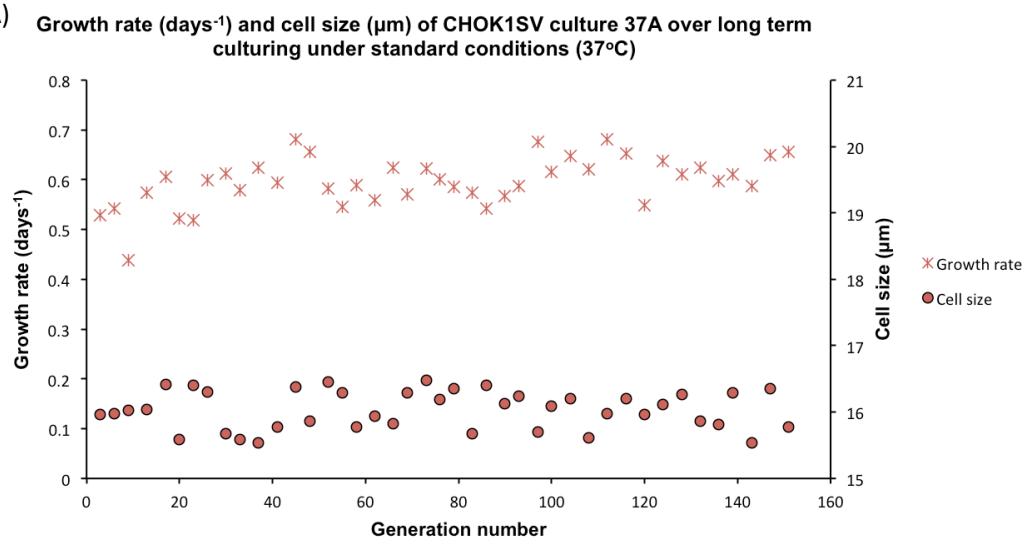

B)

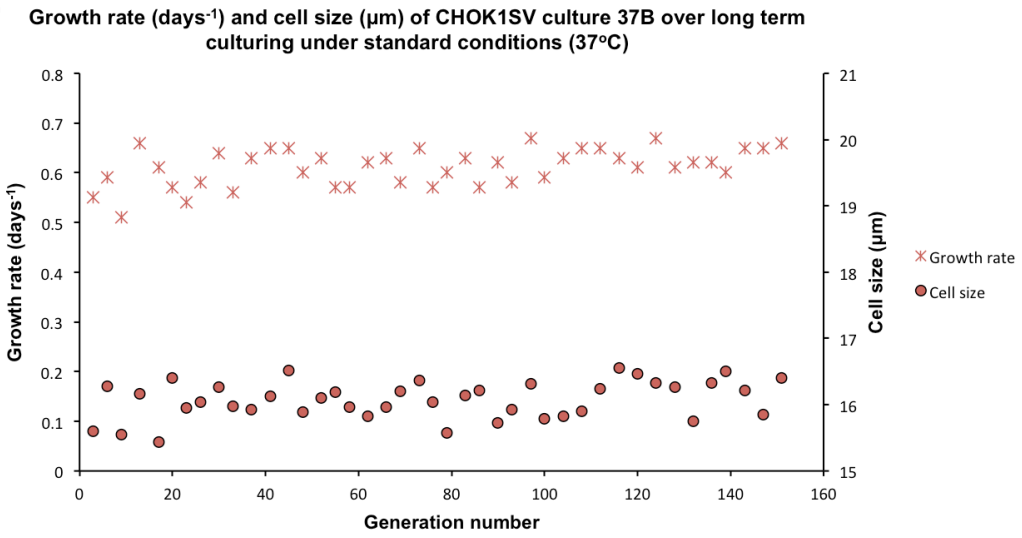

C)

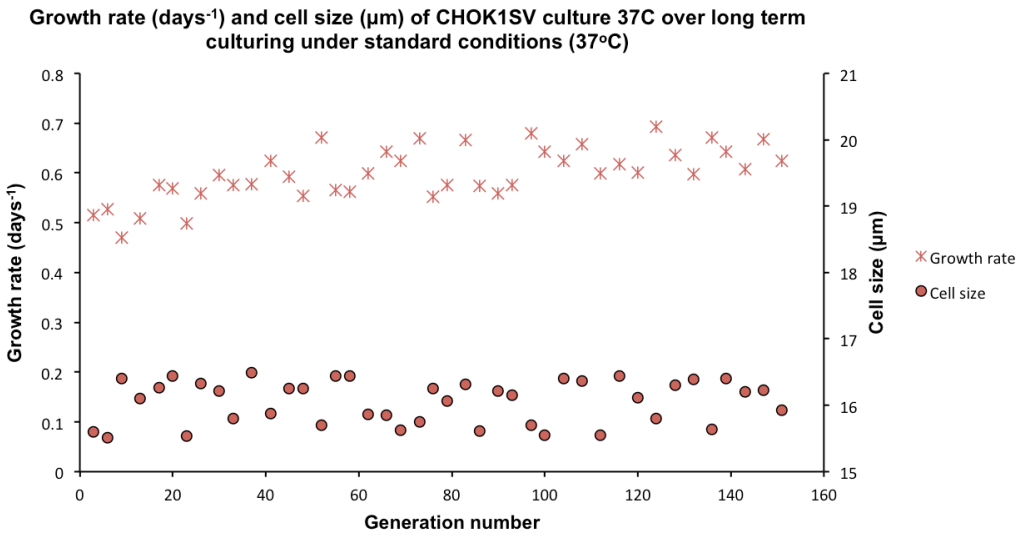

Figure 3.15 The cell size and growth rate under standard conditions (37°C) of: A) culture 37A, B) culture 37B and C) culture 37C.

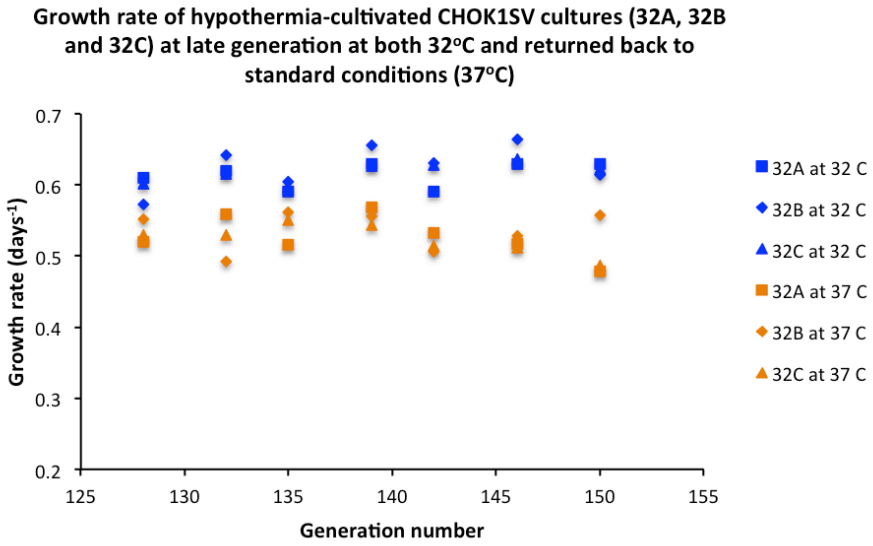

Figure 3.16 The growth rate of late generation (hypothermia adapted) 32A, 32B and 32C cultures at 32°C and when returned to standard conditions (37°C).

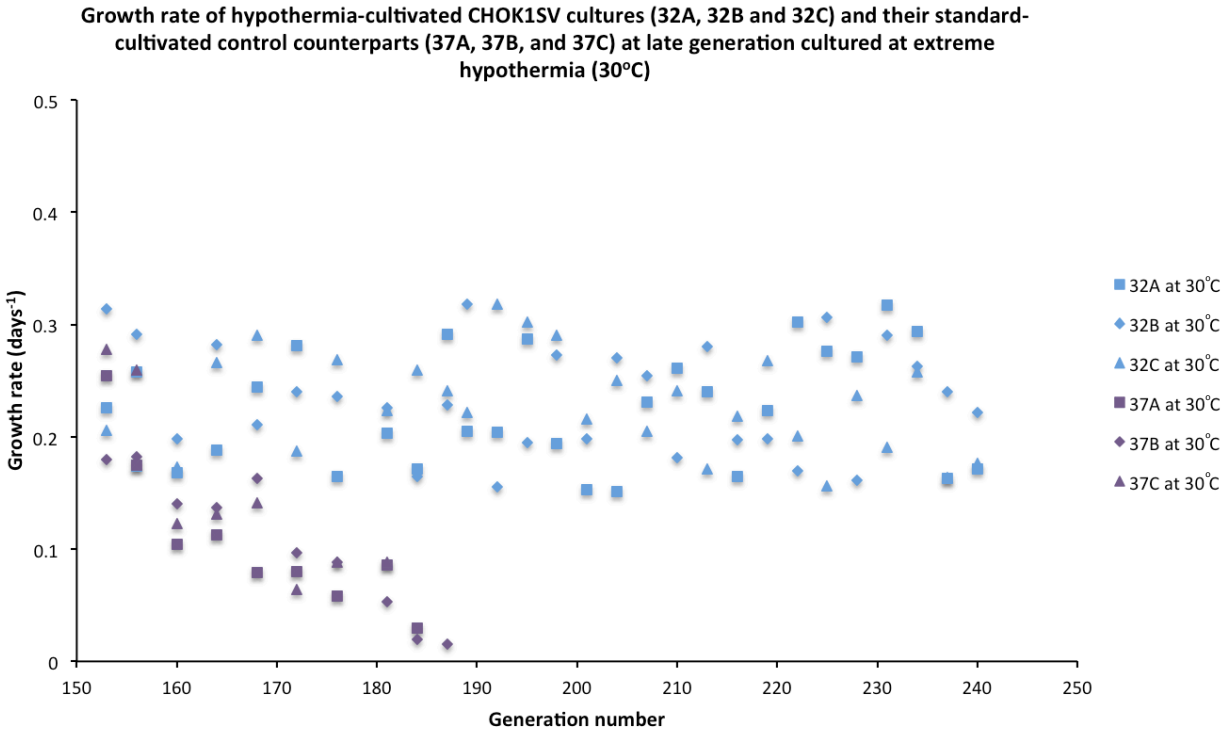

Figure 3.17 The growth rate of all late generation cultures that were subsequently subject to culturing under more extreme hypothermic conditions (30°C).

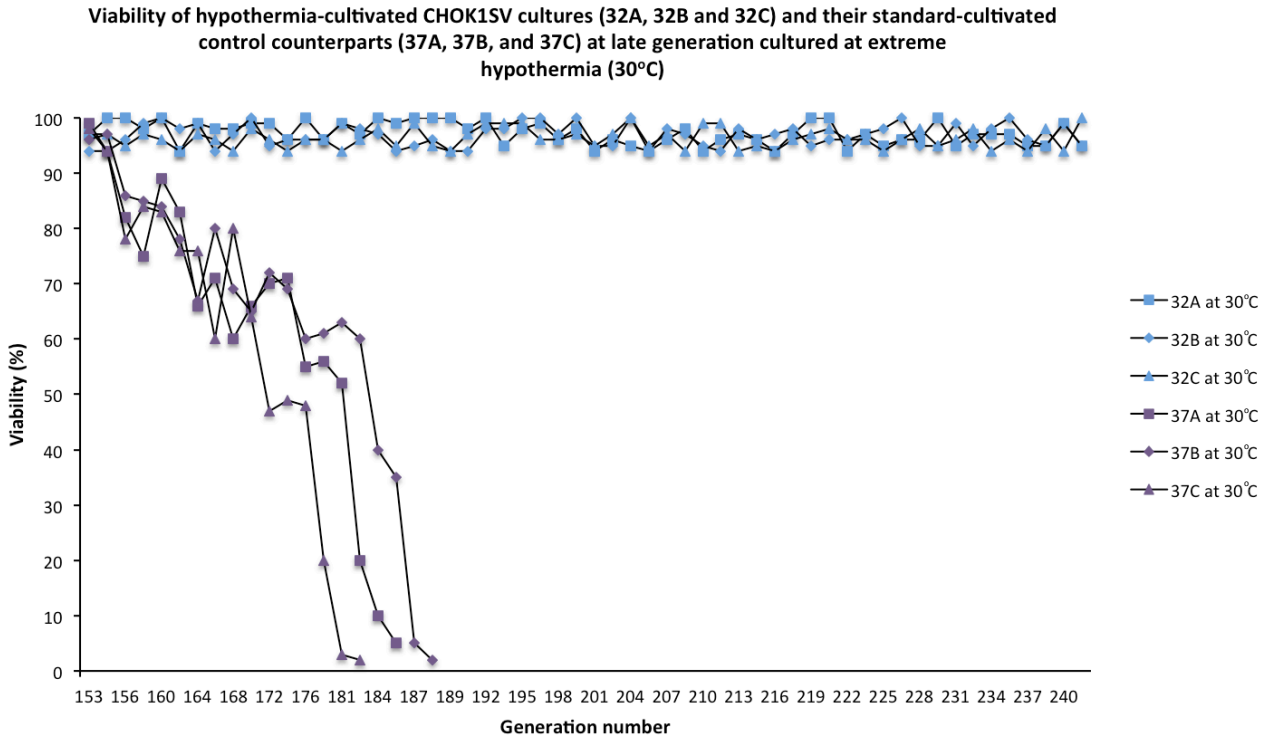

Figure 3.18 The viability of all late generation cultures that were subsequently subject to culturing under more extreme hypothermic conditions (30°C).

As can be seen in figure 3.14, after approximately 150 generations, cultures 32A, 32B and 32C achieved a growth rate of ~0.6 days^{-1}, which is in line with the growth rates exhibited by CHOK1SV cultures under standard conditions. This figure also show that all three cultures at 32°C showed an increase in cell size from ~16 μm to ~19 μm in diameter. It can also be seen in figure 3.15 that the control cultures (37A, 37B and 37C) remained relatively stable in terms of growth rate and cell size over the same number of generations. Figure 3.16 shows that when late generation cultures of 32A, 32B and 32C (that have adapted to growth in hypothermic conditions) are returned to standard conditions (37°C), growth rate continues at a lower level than corresponding cultures that remained at 32°C. All late generation cultures (32A, 32B, 32C, 37A, 37B and 37C) were subsequently subject to culturing under more extreme hypothermic conditions (30°C). As can be seen in figure 3.17, those cultures first adapted to growth at 32°C showed much

better growth rates at 30°C than cultures that had been grown under standard conditions. Figure 3.18 shows that the 32°C -adapted cultures retain high viability at 30°C whereas cultures previously grown at 37°C actually lost viability relatively quickly into exposure.

As a consequence of observing the dramatically improved growth rate and ability to rapidly proliferate under hypothermic conditions, as well as the increase in cell size, the hypothermia adapted cultures (32A, 32B and 32C), were further characterised and compared to the parental banks of cultures A, B and C (see figure 3.2) as follows:

3.3.2.2 Primary characterisation: Cell protein content

The cell size of the hypothermia adapted cultures can be seen in figure 3.14 to increase from ~16 μm (at the start of the study) to 19.5 μm in diameter. As this increase represents such a marked increase in cell volume (almost a doubling, assuming a spherical cell), the biomass (cell protein) content was measured to determine whether the cell has proportionately increased in mass or whether the increase in volume has compromised biomass density. Figure 3.19 shows the protein content of the evolved, hypothermia adapted cultures (32A, 32B and 32C) and also shows the protein content of corresponding cell cultures from the parental banks of cultures A, B and C for reference purposes (see figure 3.2, step 4 for further details). All samples were taken for analysis on the same day (day 3 post sub-culture). Figure 3.19 shows that protein content is indeed also proportionately increased in the evolved, hypothermia-adapted cell cultures compared to the parental (reference) cultures (two-way ANOVA with Tukey's multiple comparisons test, see appendix I).

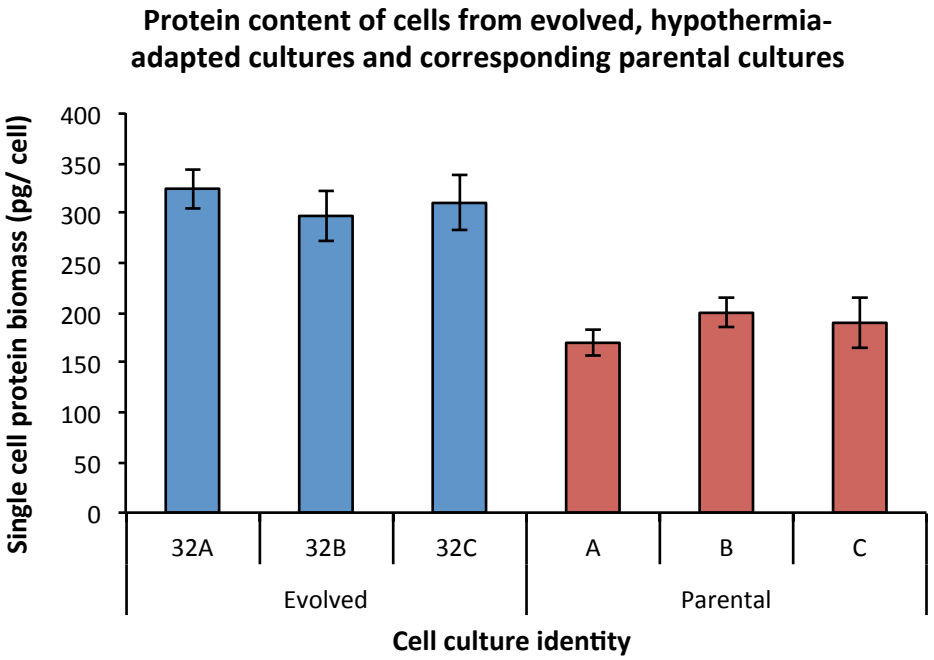

Figure 3.19 The protein content of cells from evolved, hypothermia-adapted cultures and corresponding parental cultures. Error bars, SD; N = 3.

3.3.2.3 Primary characterisation: Cell RNA content

In line with the previous results, RNA content was measured in the evolved, hypothermia-adapted cell cultures, and the parental (reference) cultures to determine whether cell RNA content per cell has proportionately increased with cell volume and protein content. Figure 3.20 shows that the RNA concentration extracted from 5 $\times 10^6$ cells is substantially and proportianally larger for cells from evolved, hypothermia-adapted cultures than it is for the same number of cells from parental cultures (two-way ANOVA with Tukey's multiple comparisons test, see appendix I).

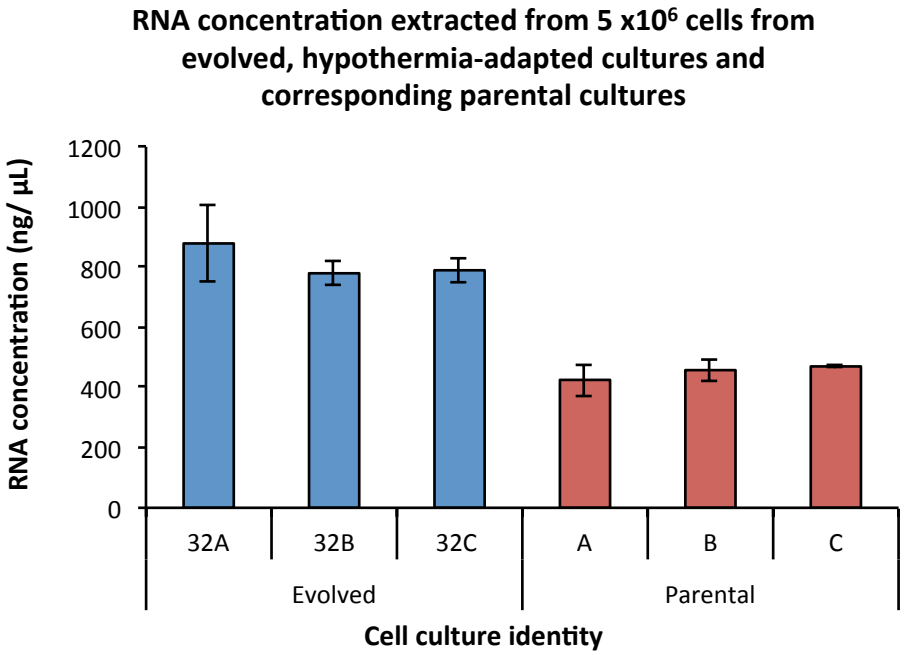

Figure 3.20 The RNA concentration extracted from 5 ×10⁶ cells from evolved, hypothermia-adapted cultures and corresponding parental cultures. Error bars, SD; N = 3.

3.3.2.4 Primary characterisation: Polyploidy assessment

The number of sets of chromosomes (ploidy) was analysed using staining and flow cytometry detection techniques. The protocol described in section 3.2.2.5 was performed for: a culture from the primary cell bank (figure 3.2, step 2) that was cultured short-term (several passages) at 37°C, the hypothermia-adapted cell cultures (32A, 32B and 32C) and also the three hypothermia-adapted cultures that were subjected to long-term culture at 30°C (hereafter termed 30A, 30B and 30C). The flow cytometry profile produced using this method provides quantitative information about the proportion of cells in a population that are in particular phase of the cell cycle, and from this, information about ploidy can also be deduced, as is explained with the aid of the schematic in figure 3.21.

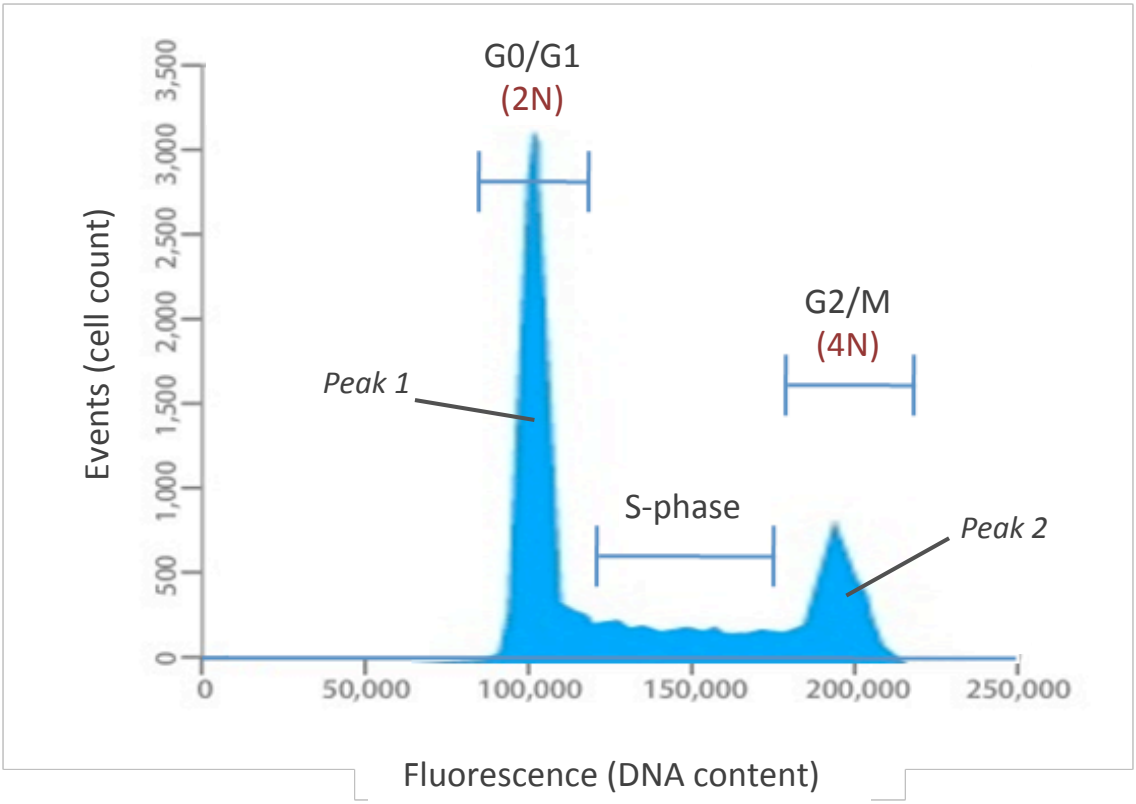

Figure 3.21 A schematic showing the expected flow cytometry cell cycle profile of a cell population with normal ploidy. The left-most peak (peak 1) in the diagram represents cells in G0/G1, where cells are defined as having two sets of chromosomes. To the right of this peak, cells in S-phase are represented, where the DNA is synthesised, and chromosome number is increasing from 2N -> 4N. The right-most peak (peak 2) represents cells in G2/M from which cells complete mitosis and the cycle starts again. Any peaks further to the right of peak 2 represents cells with abnormal numbers of sets of chromosomes.

As can be seen in figures 3.22 to 3.24, none of the evolved cultures or the parental culture from the primary cell bank exhibited polyploidy (normal profiles were observed for all cultures and no significant peaks were detected above the peak representing 4N). It can also be observed that all histograms represent growing cells (not cells arrested in G0/G1 phase of growth), and that the distribution of cells in each growth phase is similar between cell types.

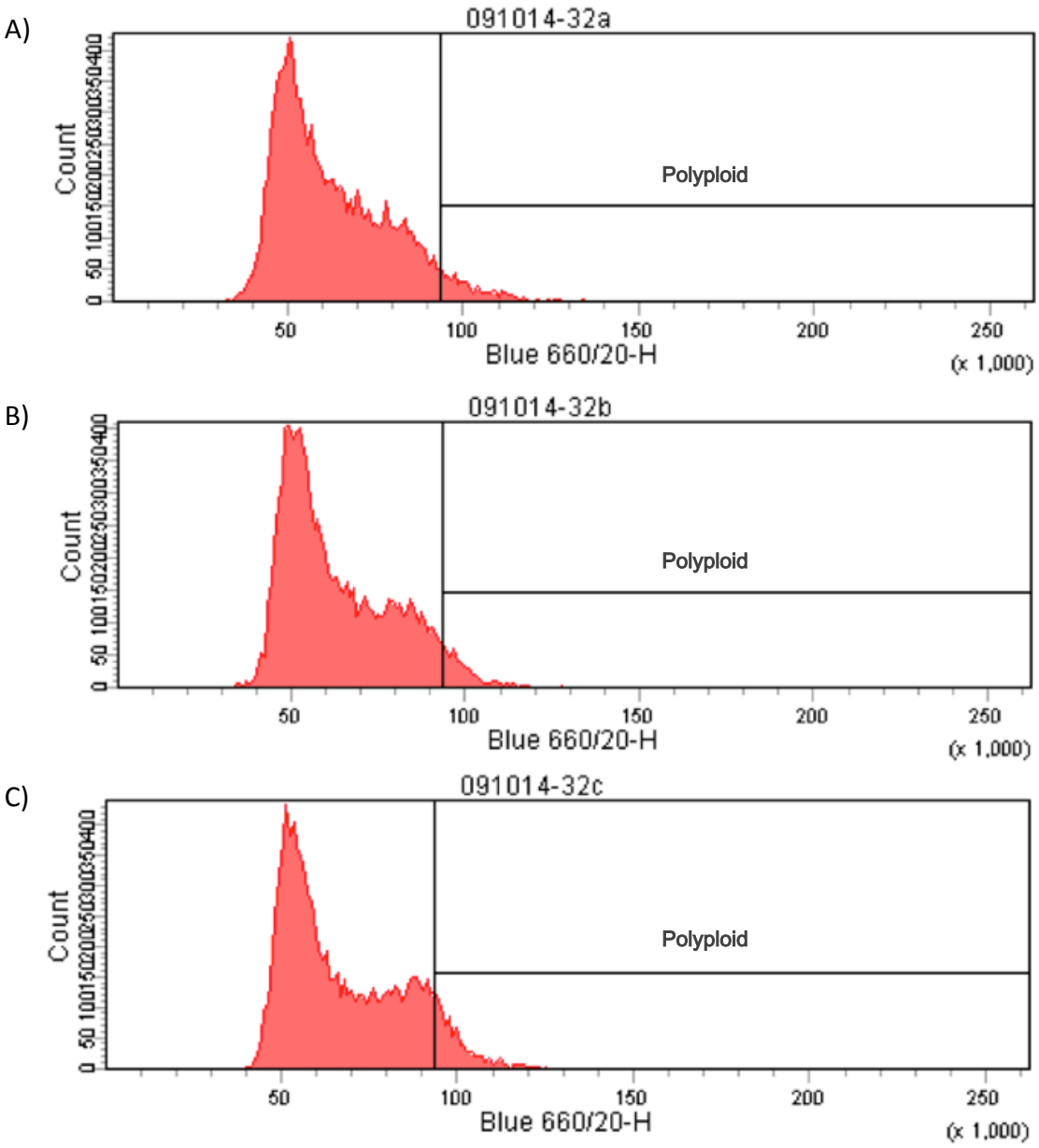

Figure 3.22 The flow cytometry cell cycle profile of A) culture 32A, B) culture 32B and C) culture 32C. The x-axis is the fluorescence intensity representing the amount of DNA. The y-axis shows the number of cells exhibiting a given fluorescence. The profile of each of the histograms (A, B and C) shows that the cells in these populations have normal ploidy as there are no significant peaks in the RHS "Polyploid" gate (as explained in figure 3.21).

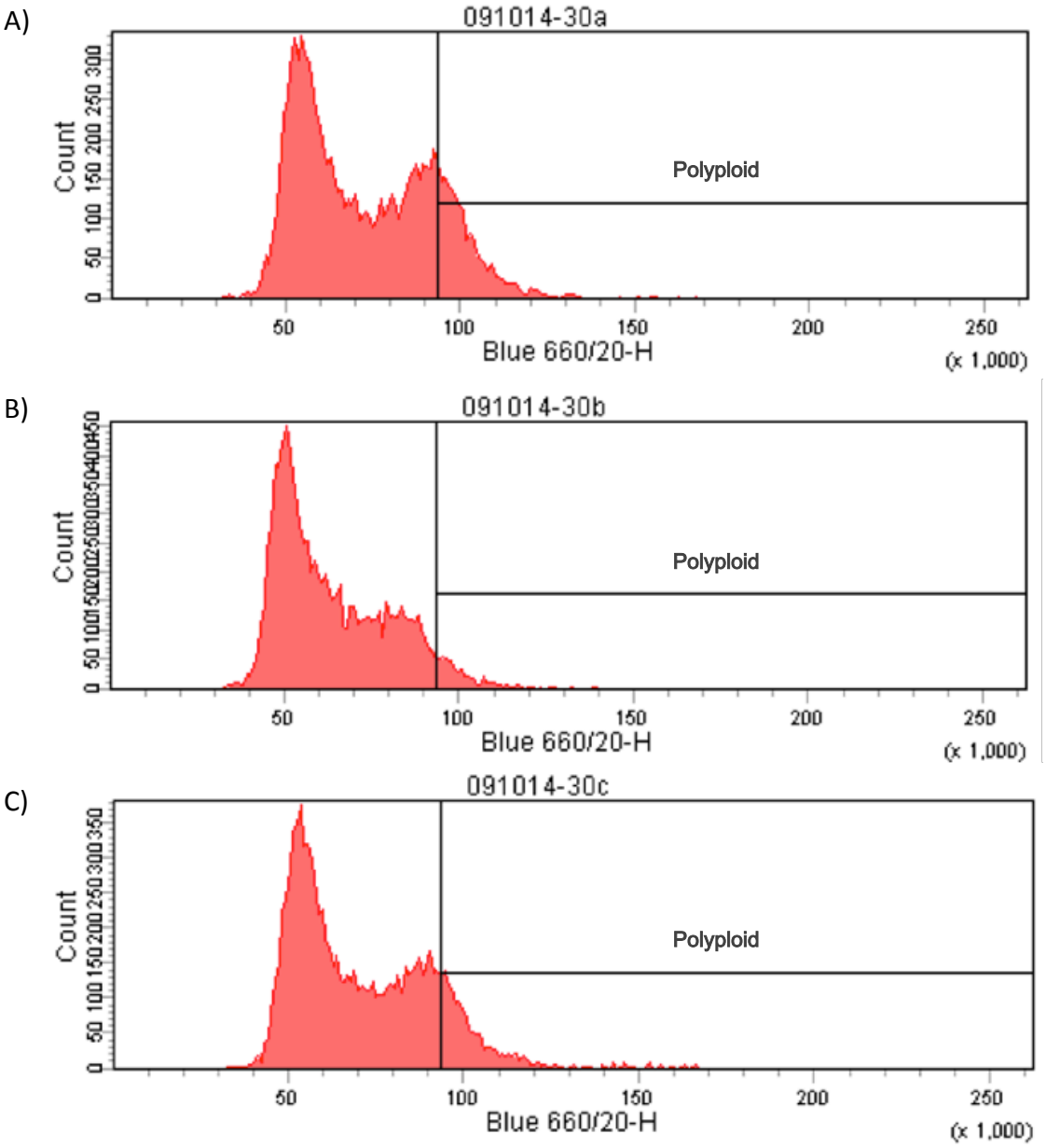

Figure 3.23 The flow cytometry cell cycle profile of A) culture 30A, B) culture 30B and C) culture 30C. The x-axis is the fluorescence intensity representing the amount of DNA. The y-axis shows the number of cells exhibiting a given fluorescence. The profile of each of the histograms (A, B and C) shows that the cells in these populations have normal ploidy as there are no significant peaks in the in the RHS "Polyploid" gate (as explained in figure 3.21).

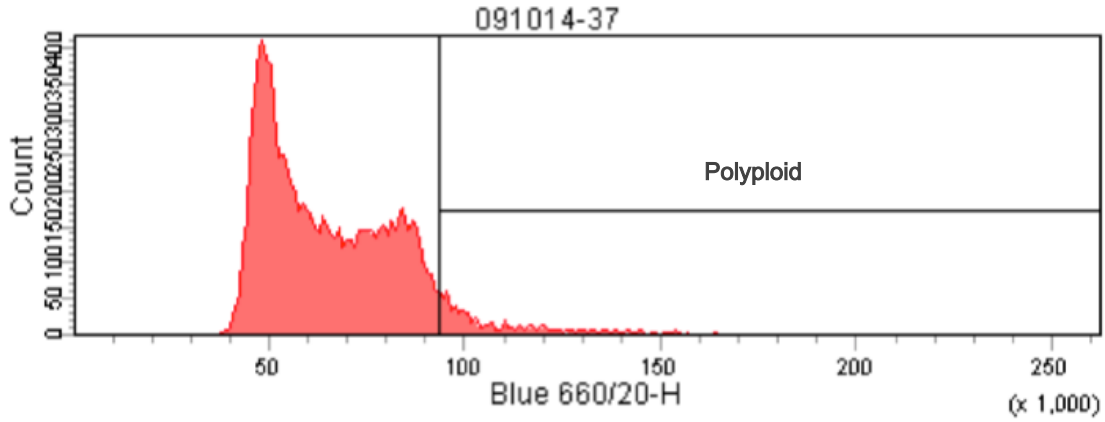

Figure 3.24 The flow cytometry cell cycle profile of a culture from the primary cell bank (figure 3.2, step 2) that was cultured short-term (several passages) at 37°C. The x-axis is the fluorescence intensity representing the amount of DNA. The y-axis shows the number of cells exhibiting a given fluorescence. The profile of the histogram shows that the cells in this population have normal ploidy as there are no significant peaks in the in the RHS "Polyploid" gate (as explained in figure 3.21).

3.3.2.5 Primary characterisation: Heritability of phenotype through cryopreservation

As the evolved, hypothermia-adapted cell cultures showed divergence in phenotype from the parental cultures (e,g, ability to rapidly proliferate at 32°C, increase in cell size) the heritability of these phenotypes through the freeze-thaw process of cryopreservation was investigated. Figure 3.25 shows that all evolved, hypothermia-adapted cultures (32A, 32B and 32C) retain their ability to proliferate under hypothermic conditions and also retain their large cell size through cryopreservation.

A)

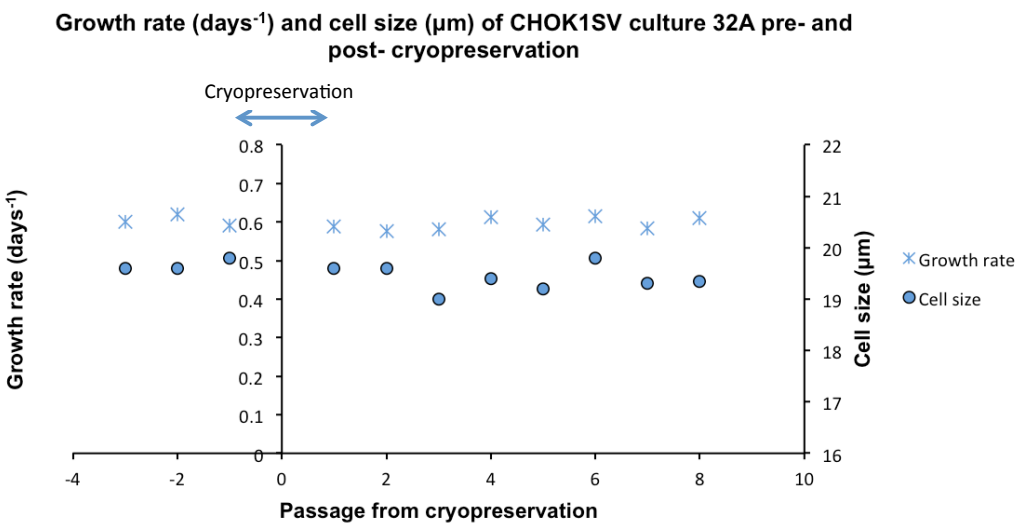

B)

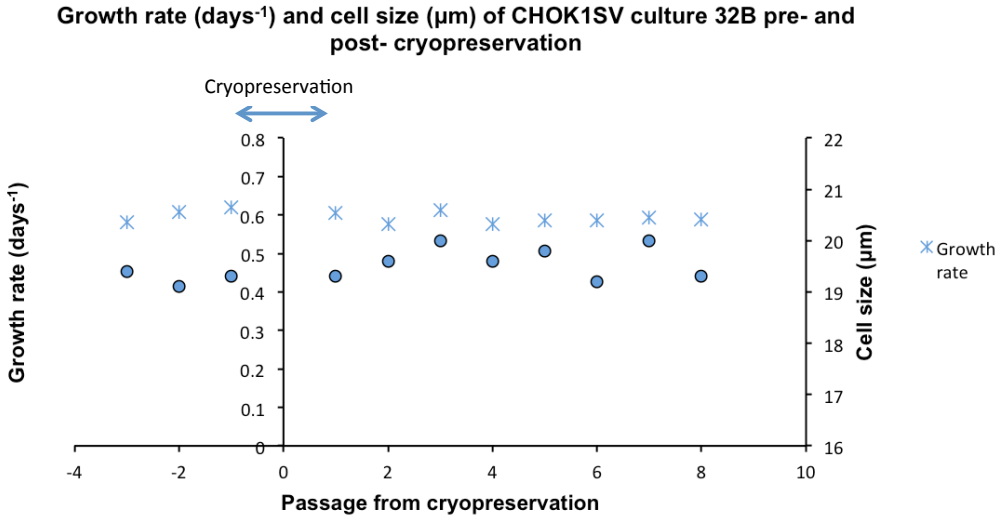

C)

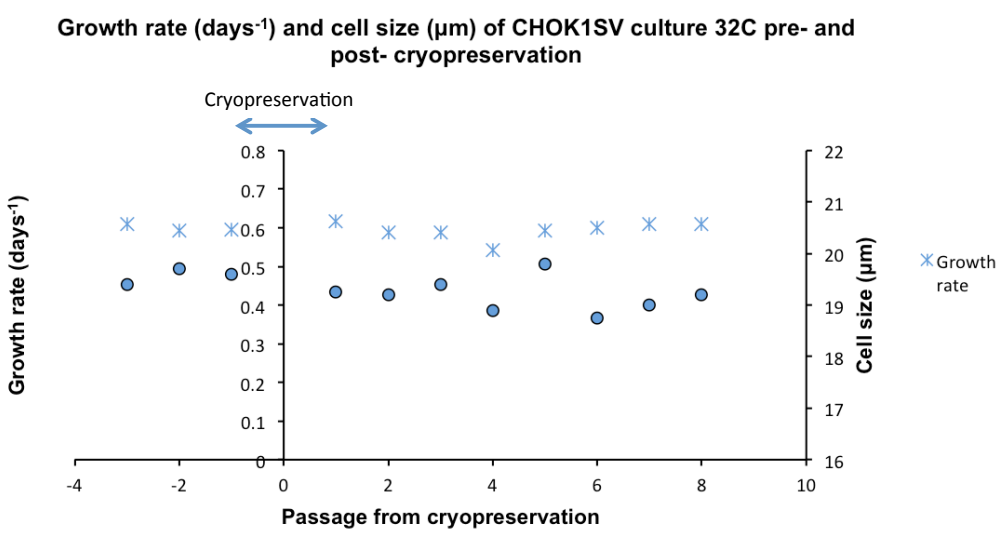

Figure 3.25 The growth rate and cell size of A) culture 30A, B) culture 30B and C) culture 30C at 32°C, pre- and post- cryopreservation. All evolved, hypothermia-adapted cultures (32A, 32B and 32C) retain their large cell phenotype and rapid growth in hypothermic conditions through the freeze-thaw process of cryopreservation.

3.4 Discussion

In the introduction to this chapter, and also more extensively reviewed in chapter 1, the advantages of directed evolution and hypothermia as a platform for improved cell line development was discussed. The research aims of this chapter were to develop an optimised cell culture regime for rapid evolution of growth rate via the manipulation of basic cell culturing parameters, and also to use directed evolution to enable the adaptation of CHOK1SV host cells to growth (exhibit normal proliferation rates) under hypothermic conditions.

The first section of work presented in this chapter showed that it is possible, via the manipulation of seeding density and passage duration (and consequently the dilution ratio at passage) to regulate the rate of change in growth rate over long-term culture. To recap, it was theorised that evolution of growth rate would be most rapid under the conditions that provided the highest number of cell divisions per unit time as this would provide more opportunity for beneficial mutations to arise at cell division when DNA is replicated. Secondly, it was also theorised that the degree of dilution at passage would affect the rate of evolution, as this factor will influence genetic drift: previous studies have suggested that a dilution ratio of 0.1 to 0.2 is most favourable for rapid evolution, as this degree of dilution has been shown to "minimise the chance that rare beneficial mutations are lost" (Whal *et al.* 2002). However, the optimal dilution ratio for rapid evolution has not been studied in the context of mammalian cells, providing an unchartered area of research to be explored here. As was seen in figure 3.12 and table 3.2, the control cultures that are seeded at 0.2 $\times 10^6$ cells/ mL and passaged every 3 or 4 days (common/ standard in-house laboratory protocol), do not largely vary in growth rate over the ~6 week study: these cultures had an average dilution ratio of ~0.11 and an average change in growth rate per day of 0.57 $\times 10^{-3}$ days^{-2}. Contrary to this, the largest average change in growth rate per day (an average of 4.46 $\times 10^{-3}$ days^{-2}) was observed in the cultures that were seeded at 3 $\times 10^6$ cells/ mL and passaged every 3 days, and the average dilution ratio for these cultures was ~0.18, supporting the dilution ratio range suggested by Wahl and colleagues (2002).

Although the control cultures have a similar dilution ratio to these cultures, there is a marked difference in the average number of cell divisions occurring per day, with control cultures providing only 0.486 $\times 10^6$ cell divisions mL^{-1} day^{-1}, while those seeded at 3 $\times 10^6$ cells/ mL and passaged every 3 days provide 4.463 $\times 10^6$ cell divisions mL^{-1} day^{-1}. The increase in the number of cell divisions, and therefore DNA replication events, could account for the larger average change in growth rate per day, as there is a larger chance that mutations in that population, such as those that could positively affect growth rate, can occur, simply due to the population size increasing. Any cells that had acquired a faster growth rate would now proliferate faster than the surrounding cell population, outcompeting slower growing cells. This result suggests that a high number of divisions per day, coupled with a dilution ratio of ~0.18 is optimum for rapid evolution.

However, there were other culturing regimes that provided relatively large values of average change in growth rate per day, these being those that were passaged every day. Cultures passaged every day and seeded at 1 $\times 10^6$ cells/ mL, 3 $\times 10^6$ cells/ mL and 5 $\times 10^6$ cells/ mL showed similar average changes in growth rates per day (values of 3.61, 4.19 and 3.75 $\times 10^{-3}$ $days^{-2}$, respectively), but understandably were largely different in the average number of cell divisions occurring per day, with values of 0.761, 2.356 and 4.02 $\times 10^6$ cell divisions mL^{-1} day^{-1}, respectively. This suggests that, contrary to the previous, a high number of cell divisions per day is not necessary for rapid evolution. In addition to this, each of these cultures provided a dilution ratio of ~0.56 at passage, meaning less than half of the population was discarded at passage and it is also a largely different ratio to that suggested by Wahl and colleagues (2002).

Interestingly, in those cultures passaged every 2 days, it was only the cultures seeded at 1 $\times 10^6$ cells/ mL and 3 $\times 10^6$ cells/ mL that showed and increase in average change in growth rates per day (albeit a small increase for 3 $\times 10^6$ cells/ mL), and those cultures seeded at and 5 $\times 10^6$ cells/ mL actually showed a decrease in growth rate over the ~6 week period, with an average change in growth rate per day of -1.19 $\times 10^{-3}$ $days^{-2}$). It is suggested here that, although preliminary studies

showed that a culture seeded at 5 $\times 10^6$ cells/ mL could be sustained in exponential growth for 2 days, over time as the cells become continuously subjected to high culture densities (reaching around 14 $\times 10^6$ cells/ mL on day 2) the conditions of stationary phase could be simulated, seeing cells reduce proliferation rates as is often observed in late phase of batch culture (Hu 2012). That said however, this would not explain why, when seeding at 3 $\times 10^6$ cells/ mL, a large average change in growth rate per day is observed in those that were passaged every one day, and then average change in growth rate is relatively reduced when passaged every two days, and then, curiously, average change in growth rate is then improved again when passaged for the longer duration of every three days. It appears there could be multiple optimal parameter combinations that can provide rapid evolution and perhaps a more systematic, design of experiments (DoE) type methodology could be implemented in the future should it be desired to fine-tune the results of this study. However, the results of this study are still valuable as it demonstrates that great improvements in growth rate can be achieved by simple manipulation of basic commonplace cell culture parameters.

In terms of practical implementation, although it has been observed here that passaging every day results in large average changes in growth rates per day, it is perhaps too labour intensive to be recommended as a directed evolution culturing platform (assuming automated culturing is unavailable, as was the case in this study). However, passaging every 3 days is much closer to conventional protocol, and it could be suggested that seeding cultures at the higher density of 3 $\times 10^6$ cells/ mL, opposed to the standard 0.2 $\times 10^6$ cells/ mL, is beneficial for experiments where rapid evolution is required.

Another principal result of this chapter, one that is central to and underpins the subsequent work described in the following chapters of this thesis, is that of the successful evolution of hypothermia-adapted CHOK1SV host cell cultures. The rationale behind this study was the notion that a host CHO cell culture that could

proliferate at normal rates under hypothermic conditions could provide a cell line that possesses the recombinant protein production capabilities observed in 'cold-shock' strategies (described in the introduction section to this chapter and in chapter 1), without the disadvantage of cell cycle arrest. As was shown in figures 3.14 and 3.15, cultures grown under hypothermic conditions (32°C) for approximately 150 generations adapt to this environment by way of improved growth rate (returning to normal growth rates observed under optimal temperature (37°C), ~0.6 $days^{-1}$), and interestingly, cultures also exhibited a substantial increase in cell size, from a diameter of approximately ~16 μm to ~19+ μm, equating to an almost doubling in cell volume assuming a spherical cell structure. Possible explanations for this size increase include it being a cell stress response, a phenomenon that has been demonstrated in mouse cardiac myocytes that increase in cellular volume as a response to various metabolic and chemical stressors (Anastacio *et al.* 2013). Another suggestion is that the increase in cell volume is a thermodynamic attempt to conserve heat in the colder environment by simply reducing the surface area to volume ratio. This change would reduce the relative heat loss by each cell and therefore improve its homoeothermic efficiency in sub-optimal temperatures (Sand *et al.* 1995).

In addition to this, protein content and RNA content were also shown to increase proportionately in the evolved, hypothermia-adapted cultures compared to their parental, unevolved counterparts. This suggests that the density of the cell constituents has not been compromised as a result of the increase in volume, meaning that the evolved cells are generating more biomass than the unevolved, parental cells, whilst growing at equivalent rates under adverse, hypothermic conditions. This could suggest that these cells do have the inherent, improved protein production and processing capabilities that was originally sought in this study – a concept that is more thoroughly examined in the succeeding chapter (chapter 4). Additionally, a feature that is necessary for any improved cell line that is to be used for industrial purposes is the heritability and preservation of those improved phenotypes through cryopreservation methods. As confirmed in figure 3.25, the evolved, hypothermia-adapted cultures do retain their fast growth rates

under hypothermic conditions and also retain their large cell size phenotype through the freeze-thaw cycle of cryopreservation and revival.

Out of interest, and to determine whether growth rate could be improved further, towards the end of the long term-culturing period, an extra set of the evolved, hypothermia-adapted cultures were created and then returned to standard culturing conditions (37°C). As was shown in figure 3.16, the growth rate of these cultures actually declined in their growth rate compared to the ones that continued to be cultured at 32°C. This shows that the evolved cultures have adapted to hypothermic conditions to the degree that these conditions have now become their optimal growth temperature and their previous native (37°C) optimum is now sub-optimal in terms of growth rate. In addition to this, the evolved, hypothermia-adapted cultures were also subjected to long-term culture at more extreme hypothermia (30°C) to determine whether they could be adapted to grow at rapid rates at even lower temperatures (for example, could they eventually grow at the same temperatures that are optimal for ectothermic insect production cell lines which has been shown to be ~27°C (Reuveny *et al.* 1993)). Presented in figures 3.17 and 3.18, results showed that while viability was maintained in the hypothermia-adapted cultures at 30°C, the growth rate did not show any improvement over the course of the long-term culturing process. However, the control cultures were also subjected to culturing at 30°C and these quickly declined in growth rate and ultimately lost all viability under these conditions.

Put together, these results show that adaptation process to 32°C has imparted a larger tolerance threshold to these cells, enabling survival in conditions that would otherwise kill ordinary CHOK1SV cultures. This suggests that, when aiming to use directed evolution to attain a cell line that is adapted to a particular condition or stress, an iterative, step-wise increase in exposure of that condition or stress may be more successful than initially introducing cultures to the most extreme levels/ concentrations. With this in mind, a hypothermia-adapted cell-line may have been attained faster in this study if the temperature was reduced in smaller increments

over time, for example, changing the temperature by -1°C initially and then once growth rates normalise, reduce by another 1°C and so on, until reaching the target temperature of 32°C.

Finally the evolved, hypothermia-adapted cultures, plus the hypothermia-adapted cultures that were subjected to growth at 30°C, as well as a parental (37°C) control culture (from the primary cell bank) were tested for polyploidy. The rationale behind this assessment came from findings in the literature that showed significant relationships between organism polyploidy (multiple sets of chromosomes) and stress adaptation (Bertier *et al.* 2013; Madlung 2013). However, as seen in figures 3.22 to 3.24, all cultures from this study were found to have normal ploidy, meaning the adaptation process was not aided by an increase in the number of sets of chromosome. Nevertheless, other studies have shown that aneuploidy (an abnormal number of chromosomes), or large-scale chromosomal rearrangements may also aid in adaptation to stress (Pavelka *et al.* 2010; Chen *et al.* 2012). However, information regarding aneuploidy and chromosomal rearrangements cannot be interpreted from this data set and more specialised analyses would need to be performed to establish whether the evolved, hypothermia-adapted cultures exhibit aneuploidy or large-scale chromosomal rearrangements. Knowing that the evolved cell lines exhibit normal ploidy (i.e. have the same number of sets of chromosomes as the parental CHOK1SV), but contain substantially more RNA than the parental cultures, implies that transcription in the hypothermia-adapted cells may be operating at significantly faster rates to account the larger disparity between DNA: RNA ratio, which could be a promising feature in terms of recombinant protein productivity. Alternatively, the increase in RNA in these cells may be a result of an increase in RNA half-life that is sometimes associated with hypothermia (Yoon *et al.* 2004).

Conclusions and future work

The initial work presented in this chapter has shown that by optimising simple cell culturing parameters, such as seeding density, passage duration and dilution ratio at passage, the evolution of rapid growth rate can be improved compared to the average rate of change observed in cultures following standard passaging protocol. These optimised regimes could be applied in directed evolution experiments where rapid increases in growth rate are required.

The rest of the work presented in this chapter forms the foundations for the subsequent chapters in this thesis. It was seen that three cultures of CHOK1SV host cells were successfully evolved over long-term culture at 32°C to become hypothermia-adapted, proliferating at similar rates to those that would be expected under optimal temperatures (37°C). As has already been highlighted, this result is particularly notable considering the literature only cites partially successful hypothermia-adaptation experiments using only stably producing cell lines (Yoon *et al.* 2006; Sunley *et al.* 2008), and there is no evidence that any laboratory has successfully adapted a host CHO cell line to hypothermic growth. The dramatic increase in cell volume, and proportionate increase in protein and RNA content is also intriguing and potentially fruitful in terms of cell recombinant protein production capabilities. The obvious future work that would be recommended from here, and is explored in the next chapter, would be to asses the evolved cell lines in terms of their transient transfection and production capabilities, their performance in fed-batch culture and also their ability to be stably transfected into stable cell lines using industrially relevant recombinant proteins.

In terms of other future work, this study may benefit from the repetition of the adaptation process but with an alternative host cell line (i.e. not CHOK1SV), to determine whether other host cell lines are able to adapt to growth at 32°C. The experiment could also be performed in different laboratories to ensure hypothermia-adapted cell lines can be obtained reliably and reproducibly. Additionally, as already alluded to, the experiment could be repeated but using an

iterative temperature reduction approach, to determine whether the adaptation process time could be reduced. The evolved, hypothermia-adapted cell lines, although found not to be polyploid, could be tested alongside the parental control cultures for aneuploidy by karyotype analysis, which would reveal information on the chromosome count and also chromosomal aberrations, highlighting any differences that may have occurred along the evolution process (Derouazi *et al.* 2006).

Chapter 4:

Functional analysis and characterisation of a hypothermia-adapted CHOK1SV cell line

The purpose of this chapter is to determine the functional attributes of the evolved, hypothermia-adapted CHOK1SV cell cultures described in chapter 3. The functional attributes include the properties of a cell line that are considered directly industrially relevant, primarily in terms of recombinant protein productivity and quality. Firstly, the three evolved, hypothermia-adapted cell cultures are assessed in terms of transient productivity using electroporation methods and the common reporter proteins, GFP and SEAP, and compared to their corresponding parental, unevolved cell lines. From here, a single culture from the three evolved, hypothermia-adapted cultures, "32A", and its corresponding parental, unevolved culture, "37A", are taken forward for further comparative analysis. These cultures are hereafter referred to simply as the evolved cell line and the parental cell line, respectively. Such further analysis includes performance in a fed-batch culturing platform, long-term transient productivity using lipofection, the ability to create stably producing cell lines, and glycan profiling of the recombinant proteins produced by the different cell lines.

4.1 Introduction

In the previous chapter it was demonstrated that hypothermia-adapted CHOK1SV host cell cultures could be attained by means of directed evolution. After long-term

culture at 32°C, the three cultures exhibited growth rates similar to those that would be expected under standard conditions (37°C). This result is a unique achievement in itself, considering there is no evidence in the literature of any other successful attempts at adapting a host CHO cell line to rapid hypothermic growth, and attempts at adapting stable CHO cell lines to hypothermic growth have been largely limited in their success, for example, becoming fragile in agitated cultures or actually decreasing in productivity as a result of the adaptation process (Yoon *et al.* 2006; Sunley *et al.* 2008). However, the hypothermia-adapted cells attained in this project have also exhibited interesting phenotypes, with an increase in cell size alongside an increase in protein and RNA content, whilst retaining the same number of sets of chromosomes as the parental cells.

There is potential promise that these evolved, hypothermia-adapted cell cultures could provide an industrial cell line that not only has the high cell specific productivity (qP) qualities that are characteristic of cells producing recombinant protein under cold-shock strategies, but the hindrance of reduced growth rate (also associated with a cold-shock strategy) has been eradicated here. For industry, this could mean that the overall titre they are able to generate may greatly be improved by using these cultures at 32°C in place of the standard CHOK1SV host cell line. However, the hypothermia-adapted cultures need first to demonstrate that they indeed do have a high qP compared to standard cultures. This chapter first examines this in terms of transient productivity, assessing both the hypothermia adapted cultures alongside parental cultures, at both 37°C and 37°C. Following this, the ability to make stable cell lines from one of the hypothermia-adapted cultures is investigated. Finally, the quality of the final recombinant protein product, a feature that can affect the half-life and efficacy of the drug (Jenkins *et al.* 1996; Croset *et al.* 2012), is analysed by glycan profiling.

4.2 Materials and methods

This section describes the materials and methods used to transfect CHOK1SV with recombinant DNA to produce a protein product, both transiently or stably. It also describes the methods and materials used to quantify said recombinant products. The reader is referred to chapter 2 for details on any other experimental techniques mentioned in this chapter.

4.2.1 Fed-batch culture optimisation for parental and evolved, hypothermia-adapted cultures

A CD CHO EfficientFeed™ Kit was used to optimise and assess fed-batch culture of the parental and evolved (hypothermia-adapted) CHOK1SV cultures at 37°C or 32°C, respectively. This kit was chosen based on the compatibility of the supplements (EfficientFeed™ A and EfficientFeed™ B) with CD CHO as the base media, which the cultures were already accustomed to. Feeds were added in volumes based on 10% of the volume of culture in the flask on that day (volume of culture was calculated by subtracting the weight of an empty 125 mL Erlenmeyer flask (Corning, Surrey, UK) from the weight of a 125 mL Erlenmeyer flask containing culture, taking 1 g as equivalent to 1 mL). The different feeds, EfficientFeed™ A and EfficientFeed™ B, were added separately or in combination, and added every two or three days, to a maximum of 4 feeds, as shown in table 4.1 below. The previously mentioned optimisation parameters were adapted from those suggested in manufacturer's guidelines. Control flasks were also included for both cell types (parental and evolved) in which no feed supplements were added. All flasks were initially seeded at 0.2 $\times 10^6$ cells/ mL and daily cell density and viability measurements were made daily using the Vi-CELL XR cell viability analyser (Beckmann Coulter, High Wycombe, UK). Prior to use, all media and feeds were warmed to 37°C or 32°C for use with the parental or evolved cultures, respectively. The best performing feed strategy was chosen based on the largest increase in integral viable cell density on the control (standard batch growth with no feed supplements).

Table 4.1 The feeding strategies used to optimise fed-batch culture in the parental and evolved, hypothermia-adapted cultures. Strategies followed a 2 or 3 day feeding pattern (to a total of 4 feeds), were added in volumes of 10% of total culture volume, and comprised of EfficientFeed™ A only, EfficientFeed™ B only or a combination of both EfficientFeed™ A and EfficientFeed™ B at a 1:1 ratio.

	Day	0	1	2	3	4	5	6	7	8	9	10	11	12
Strategy	EfficientFeeds™													
A	A			✓		✓		✓		✓				
B	A				✓			✓			✓			✓
C	B			✓		✓		✓		✓				
D	B				✓			✓			✓			✓
E	A+B			✓		✓		✓		✓				
F	A+B				✓			✓			✓			✓

4.2.2 Transfection of CHOK1SV cells

4.2.2.1 DNA vectors used in this chapter

All vectors used in this chapter contain the gene for one of the following: GFP (Green Fluorescent Protein) [phCMV C-GFP FSR Vector (Genlantis, AMS-Biotechnology, Abingdon, UK), see appendix II for map]; SEAP (Secreted Placental Alkaline Phosphatase) [gWIZ™ SEAP (Genlantis, AMS-Biotechnology, Abingdon, UK), see appendix II for map]; cB72.3 (an IgG4 mAb) (Lonza Biologics, Cambridge, UK); or Enbrel (A.K.A Etanercept, an IgG1 Fc-fusion protein, typically classed as a difficult to express (DTE) protein) (Lonza Biologics, Cambridge, UK). Vectors cB72.3 and Enbrel use the GS Gene Expression System™ (Lonza Biologics, Cambridge, UK) for stable selection and production. *Maps not available for cB72.3 and Enbrel due to IP reasons.*

4.2.2.2 Transformation of competent cells

Plasmid DNA was transfected into *E. coli* MAX Efficiency® DH5α™ competent cells (Life Technologies, Paisley, UK) according to the manufacturer's recommended protocol. 200 µL of cells were then spread onto LB agar containing antibiotic (ampicillin or kanamycin, depending on plasmid being used) which was then

inverted and incubated for ~16 hours at 37°C in order to select for successful transformants. During all stages of the transformation process, aseptic techniques were used.

4.2.2.3 Amplification of plasmid DNA

A single colony (produced via the methods described in section 4.2.1.2) was picked and inoculated in 5 mL LB broth containing antibiotic (ampicillin or kanamycin, depending on plasmid transformed). This was then incubated for ~8 hours at 37°C in a shaking incubator at 250 rpm. Following this, the cells were then used to inoculate larger cultures containing 500 mL LB medium containing antibiotic (again, ampicillin or kanamycin, depending on plasmid transformed) which were then incubated for ~16 hours at 37°C in a shaking incubator at 200 rpm. After incubation, the cells were pelleted by centrifugation at 8000 rpm for 10 minutes at 4°C. At this stage the pellet was either frozen until the purification step or purified immediately. During all stages of the amplification process, aseptic techniques were used.

4.2.2.4 Purification of plasmid DNA

After amplification, plasmid DNA was purified using either of the following commercially available kits: QIAGEN® QIAprep Spin Miniprep Kit, QIAGEN® Plasmid Plus Mega Kit or QIAGEN® Plasmid Plus Giga Kit (all QIAGEN, West Sussex, UK). All kits were used according to the manufacturer's protocols. DNA was eluted in a laminar flow cabinet to ensure DNA is sterile. Eluted DNA was then either linearised (for stable transfections) or stored in sterile TE buffer (Sigma-Aldrich, Dorset, UK) at a concentration of 400 ±50 µg/ mL.

4.2.2.5 Linearisation and solubilisation of plasmid DNA for stable transfections

For each electroporation performed, 40 µg DNA is required, however, to allow for loss, error and determination of concentration, 60 µg is linearised for each electroporation. The following reaction is set up: for every 60 µg DNA, add 10 µL

NEBuffer3, 9 µL PvuI (10U/ µL) (both New England Biolabs, Hitchin, UK), 1 µL BSA (Sigma-Aldrich, Dorset, UK), and make up to a final volume of 100 µL using d.d. H_2O. Incubate the mix for 4-6 hours in a 37°C waterbath. Following incubation, the DNA is precipitated by adding 1/10th volume 3M NaAc and 3 volumes 100% ethanol, which is mixed by pipetting and then incubated overnight at -20°C to ensure full precipitation. Next, the precipitated DNA is pelleted by centrifugation at 13000 rpm for 10 minutes. In a laminar flow cabinet, the pellet is then washed with 200 µL 70% ethanol and then centrifuged at 13000 rpm for 10 minutes. The supernatant is then removed and the pellet left to air-dry in the laminar flow cabinet for max. 15 minutes. Once all ethanol has evaporated, the pellet is resuspended in 50 µL 1×TE buffer (per 60 µg DNA) and allowed to stand for 1 hour at room temperature (remaining in the laminar flow cabinet). After this time, the DNA pellet/ TE buffer mix is pipetted gently several times to ensure the pellet is fully solubilised. The DNA concentration is then measured using a NanoDrop™ (see following section) and diluted with 1×TE buffer to a concentration of 400 µg/ mL.

4.2.2.6 NanoDrop™ quantification of DNA

The concentration of the DNA used for all transfections were assessed using a NanoDrop™ 2000 Spectrophotometer (Thermo Scientific, Loughborough, UK). Prior to sample measurements, the NanoDrop™ was blanked using 1×TE buffer. The arm was then wiped clean with lint-free microscope lens tissue and samples were added in turn, with the arm being cleaned in this way between each sample. All measurements were made in triplicate. The absorbance is read at 260 nm and 280 nm and the 260/280 ratio should be ~1.88.

4.2.2.7 Agarose gel electrophoresis for vector identity confirmation

To confirm the identity of the cB72.3 and Enbrel vectors created at Lonza Biologics (Cambridge, UK), vectors were digested using both HindIII/EcoRI and PstI. Reaction mixes were as follows per 60 µg DNA (which was ~ 1 µL):

HindIII/EcoRI: 0.5 µL HindIII, 0.5 µL EcoRI, 2 µL EcoRI Buffer (all New England Biolabs, Hitchin, UK), plus 16 µL d.d. H_2O.

PstI: 1 µL PstI, 2 µL NEBuffer3.1 (both New England Biolabs, Hitchin, UK), plus 16 µL d.d. H_2O.

Following this, DNA fragments were visualised on a 1% w/v agarose gel. Each gel block was prepared by dissolving 1 g of agarose into 100 mL 1×TBE buffer (both Sigma-Aldrich, Dorset, UK). 5 µL ethidium bromide was then streaked onto the gel pack and the agarose dissolved in TBE buffer was gently poured onto this and mixed gently using a cell spreader. Once set, the gel pack was filled with 1×TBE buffer to a level that covered the agarose gel. An equivalent volume of the 100-200 ng digested DNA mixes was combined with 4 µL loading dye (New England Biolabs, Hitchin, UK) and added to individual lane wells. Equivalent amounts of 2-log ladder (New England Biolabs, Hitchin, UK) were also loaded into end wells for reference. Gels were run at a constant voltage of 80 V for ~1.5 hours and then visualised using a UV transilluminator (ImageQuant™, GE Healthcare, Amersham, UK). All vector identities were confirmed by Lonza Biologics (Cambridge, UK) upon inspection of the gel images (see appendix II).

4.2.2.8 Electroporation – transient and stable cell line generation

Transient transfection

N.B. All of the following work is performed in a laminar flow cabinet. For each transient transfection, 10 $\times 10^6$ cells are required. Cells should be of high viability (>95%) and be from mid-exponential phase of culture growth (usually day 3). Viability and cell density of cultures is determined using the Vi-CELL XR cell viability analyser (Beckmann Coulter, High Wycombe, UK). Cell concentration is adjusted by centrifugation at 200 ×*g* for 5 minutes and the pellet of cells is resuspended in the appropriate volume of fresh, warmed, un-supplemented, CD CHO media to reach a density of 14.3 $\times 10^6$ cells/ mL. Next, 40 µg unlinearised DNA in 1×TE buffer (normally 100 µL) is added to a sterile 0.4 cm gap electroporation

cuvette (Bio-Rad, Hemel, Hempstead, UK) and then 700 µL of the 14.3 $\times 10^6$ cells/ mL cells in fresh CD CHO media is also added to the cuvette, taking care not to introduce large bubbles to this DNA-cell mix. The electroporation pulse chamber (Bio-Rad, Hemel Hempstead, UK) is then lightly sprayed with 70% ethanol and placed in the laminar flow cabinet and the cuvette is installed. The main unit of the Gene-Pulser Xcell™ is then adjusted to the following settings: 300 V, 900 µF and resistance ∞ Ω. The voltage is then applied through the cuvette, electroporating the cells. The time constant at these settings was ~18 ms, within the expected range of 12-20 ms. Control transfections should also be performed as follows: one control in which cells are added to 100 µL TE buffer *containing no DNA* and then electroporated (mock transfected). On occasion, an additional control is used in which cells are added to the DNA in TE buffer *but not electroporated*. Immediately following electroporation, cells are transferred into the desired volume of pre-warmed, 6 mM glutamine supplemented CD CHO media. With transient electroporation transfections, productivity of the recombinant protein is usually measured within 1-4 days of transfection.

Stable transfection

N.B. All of the following work is performed in a laminar flow cabinet. Stable electroporation transfection is performed as it would be for transient, however, linearised DNA is used (cB72.3 and Enbrel) and the treatment of cells post-electroporation is different, as follows: Rather than the return of the electroporated cells from the cuvette to CD CHO media supplemented with 6 mM gluatamine, cells are added to 50 mL of warmed CM55 media in a sterile T-175 flask (Nunc™, Thermo Scientific, Loughborough, UK). CM55 media is made by adding 100×HT supplement (Invitrogen, Paisley, UK) to CD CHO media. Once mixed, 25 mL of the 50 mL T-flask culture is then either transferred to a separate T-175 flask (as per Lonza Biologics SOP), or discarded (as it was in this study due to limited incubator capacity). Each T-175 flask containing 25 mL of electroporated cell culture is then placed in a 5% CO_2 static incubator at 37°C or 32°C (depending on whether the culture is of parental cells or evolved,

hypothermia-adapted cells) for 18-24 hours. Following this period of incubation, the viability and cell concentration are determined using the Vi-CELL XR cell viability analyser (Beckmann Coulter, High Wycombe, UK). Next, 75 mL of warm (37°C or 32°C according to cell type) CM55 media supplemented with 66.66 µM Methionine sulfoximine (MSX) (Sigma-Aldrich, Dorset, UK) is added to each T-flask containing 25 mL of transfected culture, resulting in a final concentration of MSX in the culture media of 50 µM. Every 3-4 days following this, viability and cell density of the cultures (including controls) is monitored using the Vi-CELL XR cell viability analyser. Once cells reach a density of 0.1 $\times 10^6$ cells/ mL, Vi-CELL XR measurements are made daily. On the day that cells reach $\sim$0.4 $\times 10^6$ cells/ mL, cultures are transferred to shake-flask culture in 125 mL vent-capped Erlenmeyer flasks (Corning, Surrey, UK) to subsequently follow a normal passaging regime as stably transfected cell cultures using CM55 media supplemented with 25 µM MSX. By this point, control cultures will have lost all viability and can now be discarded. *[N.B. cross-temperature control cultures were also created in this study (i.e. transfected parental cultures that were incubated at 32°C and transfected hypothermia-adapted cultures incubated at 37°C), however, viability of these cultures never recovered and the cells died within 1-2 weeks of static culture post-transfection].*

4.2.2.9 Lipofection: long-term (fed-batch) transient transfection

N.B. All of the following work is performed in a laminar flow cabinet. Lipofectamine-mediated transfection was conducted using Lipofectamine® LTX with PLUS™ reagent (Life Technologies, Paisley, UK). Prior to experimentation, ratio of DNA: Lipofectamine® LTX was optimised as recommended by the manufacturer. For optimisation, DNA: Lipofectamine® LTX ratios of 1:2, 1:3 and 1:4 were used and viability and GFP fluorescence were measured. The DNA load used was always 12 µg per 10 mL culture, so as an example a DNA: Lipofectamine® LTX ratio of 1:2 would contain 12 µg and 24 µL of Lipofectamine® LTX. The ideal ratio would provide intense GFP fluorescence whilst maintaining a relatively high viability of the cell culture; this ratio was then used for all following transfections. First, the

DNA and Lipofectamine® LTX are dispensed into separate sterile, 1.5 mL microcentrifuge tubes (Eppendorf, Stevenage, UK). PLUS™ reagent was added to the DNA in equivalent volume to that of DNA and mixed by pipetting. The Lipofectamine® LTX was diluted in Opti-MEM® Reduced Serum medium (Life Technologies, Paisley, UK) to a total volume of 0.5 mL, and the DNA + PLUS™ reagent mix was also diluted in Opti-MEM® Reduced Serum medium to a total volume of 0.5 mL. These two 0.5 mL volumes were then combined, mixed gently by pipetting and then allowed to stand at room temperature for 5 minutes to allow DNA-lipid complexes to form. The DNA-Lipofectamine® complex is then used immediately.

Transfection using the DNA-Lipofectamine® complex was performed as follows: One day prior to transfection, cells were passaged, scaling up to a 1 L Erlenmeyer flask and seeding at a density of 0.4 $\times 10^6$ cells/ mL. The purpose of this increased seeding density is to ensure a density of 1 $\times 10^6$ cells/ mL after ~24 hours. Once a density of 1 $\times 10^6$ cells/ mL had been established, 10 mL aliquots of this culture were then added to each 50 mL CultiFlask (Sartorius, Thermo Scientific, Loughborough, UK). To each of these aliquots, 1 mL of the DNA-Lipofectamine® complex is added and mixed gently. Mock-transfected controls were also set up in which no DNA was added but Lipofectamine® was. Cultures were then incubated at 37°C or 32°C (depending on whether the culture is of parental cells or evolved, hypothermia-adapted cells, plus cross-temperature controls), at 170 rpm under 5% CO_2. All cultures were then fed 10% culture volume (~1 mL) of EfficientFeed™ A and EfficientFeed™ B at a 1:1 ratio on days 3, 6 and 9. A sample of cells transfected with GFP were taken on day 4 (3 days post-transfection) to assess transfection efficiency using flow cytometry. Supernatant samples from all cultures were taken at early and mid exponential phase as well as late stationary phase of growth.

4.2.3 Recombinant protein quantification and purification

4.2.3.1 Secreted Alkaline Phosphatase (SEAP) reporter protein assay

Relative secreted alkaline phosphatase (SEAP) reporter protein was measured using a colorimetric Anaspec SensoLyte® pNPP Secreted Alkaline Reporter Gene Assay Kit (Cambridge Bioscience, Cambridge, UK). The hydrolysis of paranitrophenyl phosphate (pNPP) to paranitrophenol is catalysed by alkaline phosphatase. Paranitrophenol has a yellow colour, which is measured spectrophotometrically at 405 nm, therefore measuring absorbance at 405 nm is a proxy of measuring SEAP activity and concentration. In a clear, 96-well microplate, 50 µL of pNPP was added to 50 µL of supernatant. If required, supernatant should be diluted (with fresh media) and all samples should be diluted by the same factor. The absorbance was measured using kinetic readings (to ensure in linear range) at 405 nm using a PowerWave™ spectrophotometer plate reader (BioTek, Potton, Bedfordshire, UK). Values were then normalised to the lowest producing transfection condition (parental cells cultured at 37°C post-transfection) to show the % increase in production on other transfection conditions (parental cells cultured at 32°C post-transfection, hypothermia-adapted cells cultured at 37°C post-transfection and hypothermia-adapted cells cultured at 32°C post-transfection).

4.2.3.2 GFP intensity and transfection efficiency using flow cytometry

Intracellular green fluorescent protein (GFP) production and transfection efficiency was measured using flow cytometry. Fluorescence intensity was measured using an Attune® Acoustic Focusing Cytometer (Life Technologies, Paisley, UK). Samples of 10,000 cells were measured and negative ('mock-transfected') control cells (without GFP plasmid but subject to the transfection process, e.g. lipofection or electroporation) were used to determine auto-fluorescence and transfection efficiency. GFP was excited using a 488 nm laser passing through a 530/30 centre/bandpass filter and data was analysed using Attune® Cytometric software: The cell population was gated for granularity and

size (to exclude cell debris) and a daughter plot was generated to assess GFP expression. Median fluorescence intensity was measured and transfection efficiency was calculated in terms of % fluorescing cells out of the total cells in the gated transfected population. An example histogram showing how transfection efficiency is determined is given in figure 4.1.

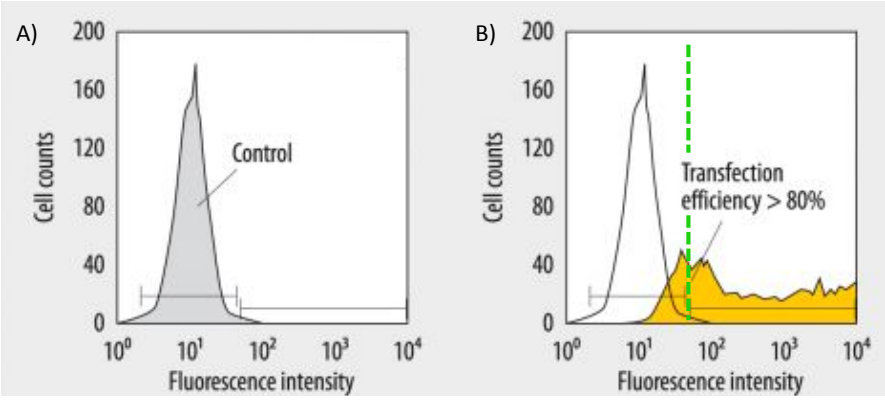

Figure 4.1 Example histograms to show the determination of transfection efficiency using GFP and flow cytometry. A) Shows the histogram for control (mock transfected) cells. B) Shows the superimposed histograms of the control cells and a transfected cell population. A gate is fitted at the top 1% fluorescing control cells (green dashed line) and transfection efficiency is calculated as the % of the transfected cell population that fluoresce with higher intensity than this marker. For example, a transfected cell population with no overlap across this marker line would be regarded as transfected with 100% efficiency.

4.2.3.3 Quantification of cB72.3 and Enbrel by FastELISA®

Production of cB72.3 and Enbrel was measured using a FastELISA® Human IgG Quantification kit (RD-Biotech, Besançon, France), according to the manufacturer's protocol. All samples were diluted 1 in 500 in the sample diluent (supplied). Absorbance of each sample at 450 nm was measured using a PowerWave™ spectrophotometer plate reader (BioTek, Potton, Bedfordshire, UK). Absorbances of the human IgG standards (supplied, concentrations ranging from 0 to 1000 ng/

mL) were plotted against actual concentrations to generate a standard curve. The unknown concentration of IgG in the sample supernatant could then be deduced via this standard curve.

4.2.3.4 Protein A purification of cB72.3 and Enbrel

Recombinant IgG protein (cB72.3 and Enbrel) was purified from cell culture supernatants using HiTrap Protein A HP prepacked columns (GE Healthcare, Buckinghamshire, UK). Prior to application to the column, supernatant was filtered through 0.22 μm syringe filters (Sigma-Aldrich, Dorset, UK). The manufacturer's recommended concentration ranges/ pH ranges were used and recommended protocol for operation with syringe was followed. The specific volumes, concentrations and pH as were used as follows, according to recommendation from Lonza Biologics (Cambridge, UK): binding buffer, 20 mM sodium phosphate, pH 7; elution buffer, 0.1 M citric acid, pH 3.5; neutralisation buffer in collection vial, 150 μL Tris-HCL. Eluted, purified protein was stored in sterile PBS at 4°C (short-term) or -20°C (long-term).

4.2.3.5 Quantification of purified cB72.3 and Enbrel by NanoDrop™

The concentrations of the purified protein samples of cB72.3 and Enbrel were assessed using a NanoDrop™ 2000 Spectrophotometer (Thermo Scientific, Loughborough, UK). This was performed using the "Other protein (E 1%)" setting when defining protein type. Using the absorbance at 280 nm and using the extinction coefficients of 14.3 and 11.6 for cB72.3 and Enbrel, respectively, the concentration of protein in each sample can be determined. Prior to measurements, the NanoDrop™ was blanked using 1 μL PBS from the same batch that was used for protein storage. The arm was then wiped clean with lint-free microscope lens tissue and samples were added and analysed in turn, with the arm being cleaned in this way between each sample. The concentrations were then used as a guide in performing SDS-PAGE to confirm the identity of the proteins.

4.2.3.6 SDS-PAGE identity confirmation of cB72.3 and Enbrel

SDS-PAGE was performed using the purified protein samples of cB72.3 and Enbrel to ensure correct banding profile of each protein. Reduced and non-reduced proteins were run, the former using NuPAGE® Sample Reducing Agent (Thermo Scientific, Loughborough, UK). First, 5 µg of protein sample was diluted in d.d. H_2O to a volume of 10 µL. To this, 2.5 µL NuPAGE® LDS Sample Buffer (Thermo Scientific, Loughborough, UK) was added to all samples. To create a reduced protein sample, 1 µL of NuPAGE® Sample Reducing Agent was added and this was then heated at 70°C for 10 minutes. The non-reduced protein sample was left at ambient temperature for the same duration. Next, 10 µL aliquots of reduced and non-reduced proteins were added to wells of Novex™ 4-12% Bis-Tris Protein Gels (pre-cast) (Thermo Scientific, Loughborough, UK) in NuPAGE® MOPS SDS Running Buffer (Thermo Scientific, Loughborough, UK). Alongside the wells containing protein sample, 10 µL of NuPAGE® Sharp Pre-Stained Protein Standard Thermo Scientific, Loughborough, UK)) was added to create a size reference ladder. The gel was then run at 180 V for approximately 1 hour. The proteins were then stained using Instant*Blue*™ Ultrafast Protein Stain (Sigma-Aldrich, Dorset, UK) and the banding profile was analysed.

4.2.4 Glycan profiling of cB72.3 and Enbrel

Protein samples of cB72.3 and Enbrel, from both the parental cell and the hypothermia-adapted cells, produced via both stable production (batch culture) and transient fed-batch Lipofection methods were analysed in terms of their glycosylation profile. Purified protein samples were provided to Lonza Biologics (Slough, UK), at a concentration of >1 mg/ mL. The major N-glycoforms (G0, G0F, Man5, G1Fa, G1Fb and G2F) were determined using UPLC.

4.3 Results

4.3.1 Relative SEAP productivities of evolved, hypothermia-adapted cultures and parental cultures incubated at both 32°C and 37°C post-transfection

All evolved (hypothermia-adapted) cultures and parental (unevolved) cultures (32A, 32B, 32C, 37A, 37B and 37C) were transfected with SEAP via electroporation. Six electroporations were performed for each culture, 3 replicates that were incubated at native temperatures (i.e. at 32°C for the evolved, hypothermia adapted cultures and 37°C for the parental cultures) post-transfection, and 3 that were incubated at non-native temperatures (i.e. at 37°C for the evolved, hypothermia adapted cultures and 32°C (a "cold-shock") for the parental cultures). A one-way ANOVA with Tukey's multiple comparisons test (comparison test between mean % increase to all other mean % increase) was performed on the data, see appendix II. As can be seen in figure 4.2, the evolved cultures incubated at 32°C post-transfection showed the largest SEAP productivities, with an average increase of ~100% on the lowest producing conditions (parental cultures at 37°C), followed by the parental cultures at 32°C which exhibited an average increase of ~50% on the lowest producing conditions. There was little observed between cultures when incubated at 37°C.

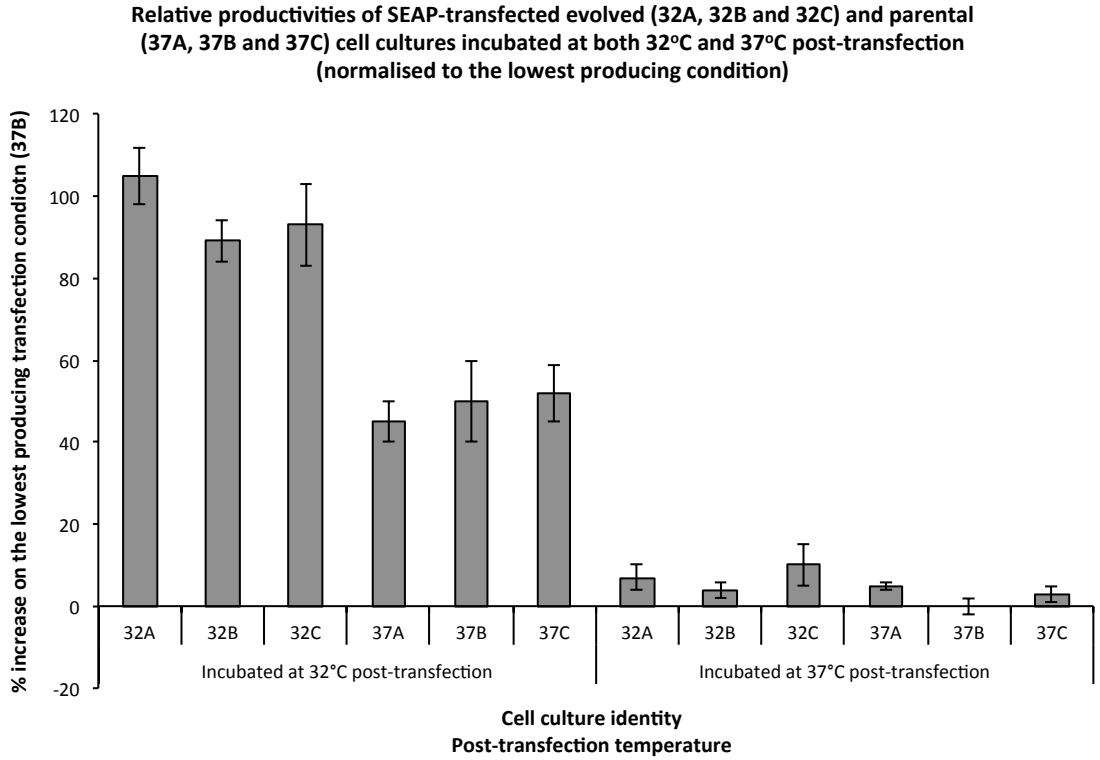

Figure 4.2 Relative SEAP productivities (24 hours post-transfection) of evolved and parental cultures incubated at both 32°C and 37°C post-transfection. Error bars, SD; N = 3.

4.3.2 GFP fluorescence of evolved, hypothermia-adapted cultures and parental cultures incubated at both 32°C and 37°C post-transfection to determine relative GFP productivities and transfection efficiencies

All evolved (hypothermia-adapted) cultures and parental cultures (32A, 32B, 32C, 37A, 37B and 37C) were transfected with GFP via electroporation. Six electroporations were performed for each culture, 3 replicates that were incubated at native temperatures (i.e. at 32°C for the evolved, hypothermia adapted cultures and 37°C for the parental cultures) post-transfection, and 3 that were incubated at non-native temperatures (i.e. at 37°C for the evolved, hypothermia adapted cultures and 32°C (a "cold-shock") for the parental cultures). Results were obtained by flow cytometry: median fluorescence values represent the relative amount of intracellular GFP produced by the cell and transfection efficiency (i.e. the % fluorescing cells) represents the % of the population that has been

successfully transfected with GFP (and is therefore producing the recombinant GFP protein). An example histogram showing typical transfection efficiency achieved from electroporation is given in figure 4.3 - this is chiefly for contrast purposes to the typical transfection efficiencies achieved via lipofection (which is usually not as well-defined and transfection efficiencies tend to be much lower than equivalent transfections using electroporation methods, see figure 4.6).

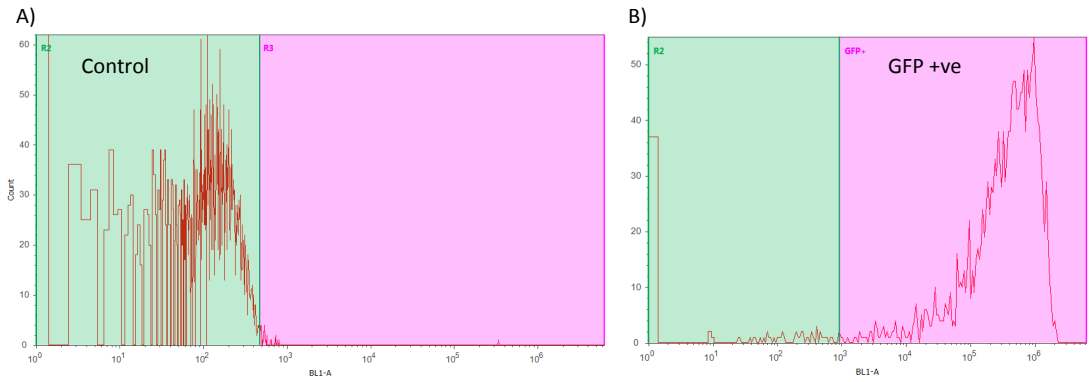

Figure 4.3 Example histograms to show the typical transfection efficiency profile achieved by electroporation transfection. A) Shows the histogram for control (mock transfected) cells and B) shows the histogram for the GFP transfected cell population.

As can be seen in figures 4.4 and 4.5 below, the evolved cell cultures (32A, 32B and 32C) show both higher median fluorescence values and higher transfection efficiencies than that of their equivalent parental cultures (37A, 37B and 37C). A one-way ANOVA with Tukey's multiple comparisons test was performed on this data set to determine where significant differences lie (see appendix II).

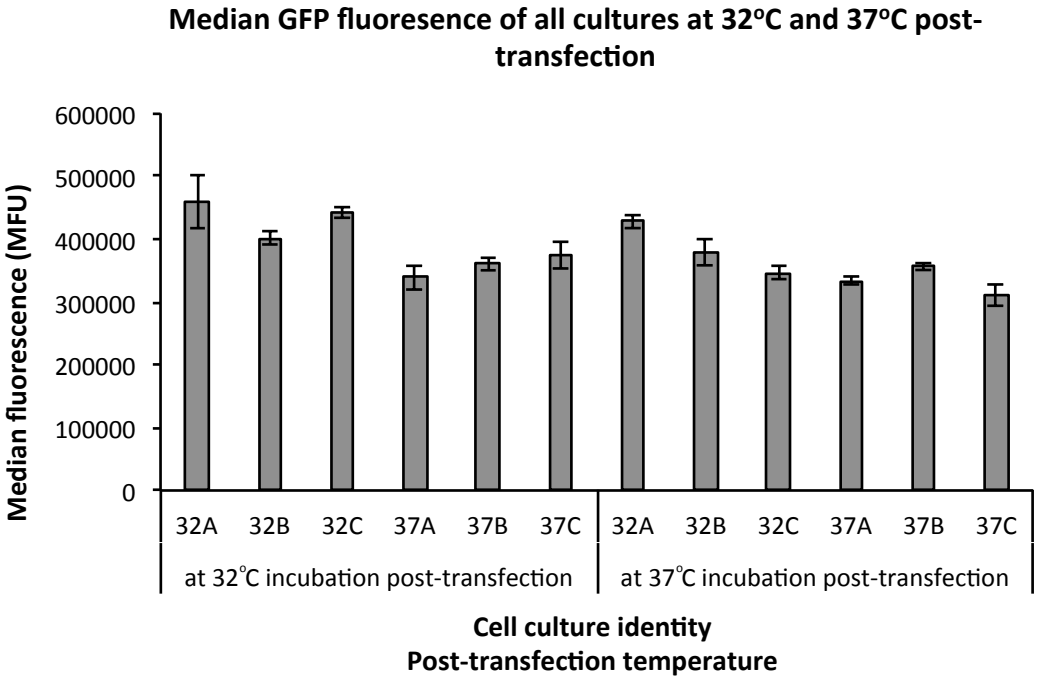

Figure 4.4 The median fluorescence (24 hours post-transfection) of all cell cultures (32A, 32B, 32C, 37A, 37B and 37C) transfected (via electroporation) with GFP and incubated post-transfection at both 32°C and 37°C. Mock-transfected controls not shown. Error bars, SD; N = 3.

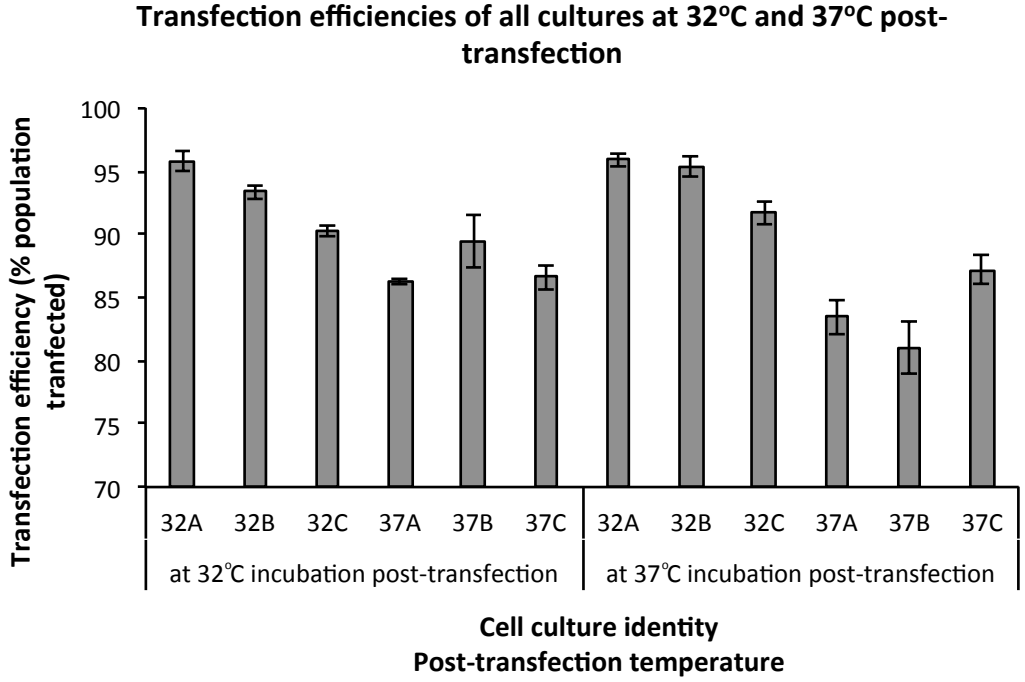

Figure 4.5 The transfection efficiencies (24 hours post-transfection) of all cell cultures (32A, 32B, 32C, 37A, 37B and 37C) transfected (via electroporation) with GFP and incubated post-transfection at both 32°C and 37°C. Error bars, SD; N = 3.

4.3.3 Explanatory statement regarding all subsequent presented data in this chapter and chapter 5

Considering the intentions for the advancement of this project combined with limited resource availability, only one of the evolved cell cultures (and its parental, unevolved counterpart) is taken forward for further productivity analysis, stable cell line generation and subsequent product quality analysis by glycan profiling. The evolved cell culture taken forward was 32A for the following reasons: 1) 32A showed the most interesting phenotype by way of exhibiting both consistent large cell size and the highest growth rate out of the three cultures - while 32B was marginally smaller in size but maintained an adequate growth rate and 32C was as large as 32A but exhibited marginally slower growth rates; 2) When assessing preliminary productivity data (both with SEAP and GFP), 32A was the highest producing evolved culture out of the three; 3) Transfection efficiency was highest in 32A out of the three evolved cultures.

For simplicity, cultures 32A and 37A are hereafter commonly referred to as the 'evolved cell line' and the 'parental (or unevolved) cell line', respectively. Unless stated, the evolved cell line is always cultured at 32°C and the parental cell line is always cultured at 37°C.

4.3.4 Lipofection

4.3.4.1 Optimisation of DNA:Lipofectamine® LTX ratios and fed-batch feeding strategy

The ratio of DNA: Lipofectamine® LTX for use in Lipofection studies was optimised in terms of transfection efficiency, cell culture viability and median fluorescence of intracellular GFP. An example histogram showing typical transfection efficiency achieved from lipofection is given in figure 4.6 below - this is chiefly for contrast purposes to the typical transfection efficiency histogram achieved via electroporation (which was shown in figure 4.3).

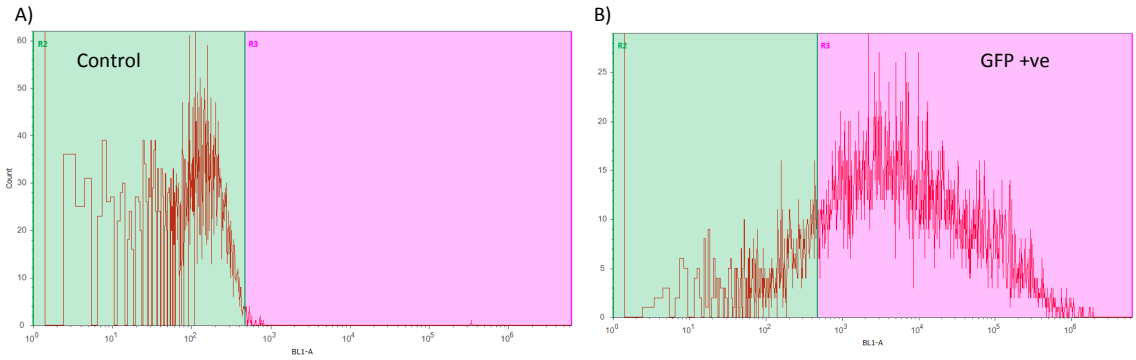

Figure 4.6 Example histograms to show the typical transfection efficiency profile achieved by lipofection transfection. A) Shows the histogram for control (mock transfected) cells and B) shows the histogram for the GFP transfected cell population.

As can be seen in figures 4.7 to 4.9, a DNA: Lipofectamine® LTX ratio of 1:2 is optimal for high transfection efficiency, median fluorescence and retaining high culture viability. Although a high median fluorescence of GFP is seen with a ratio of 1:3, this is roughly similar to that achieved with a ratio at 1:2, however, a ratio of 1:3 has unfavourable effects on culture viabilities and transfection efficiencies. N.B. optimisation studies were performed at native temperatures (i.e. i.e. at 32°C for the evolved cultures and 37°C for the parental cultures).

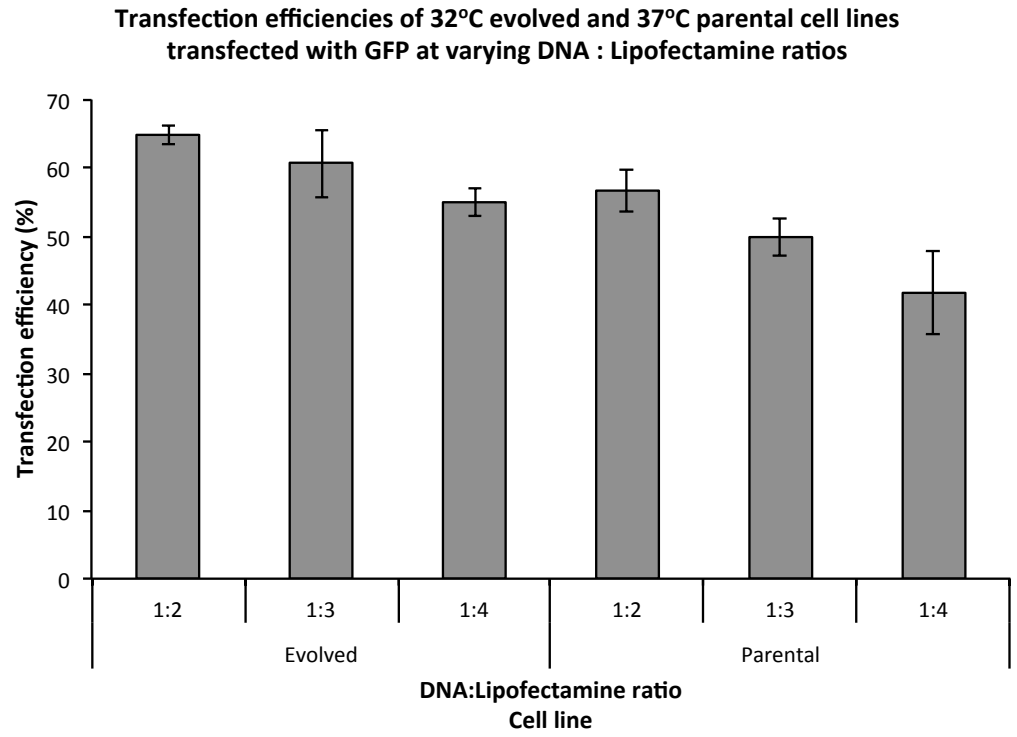

Figure 4.7 Transfection efficiencies (24 hours post-transfection) of evolved and parental cell lines, at their native temperatures, transfected (via lipofection) with GFP according to different DNA: Lipofectamine ratios. Error bars, SD; N = 3.

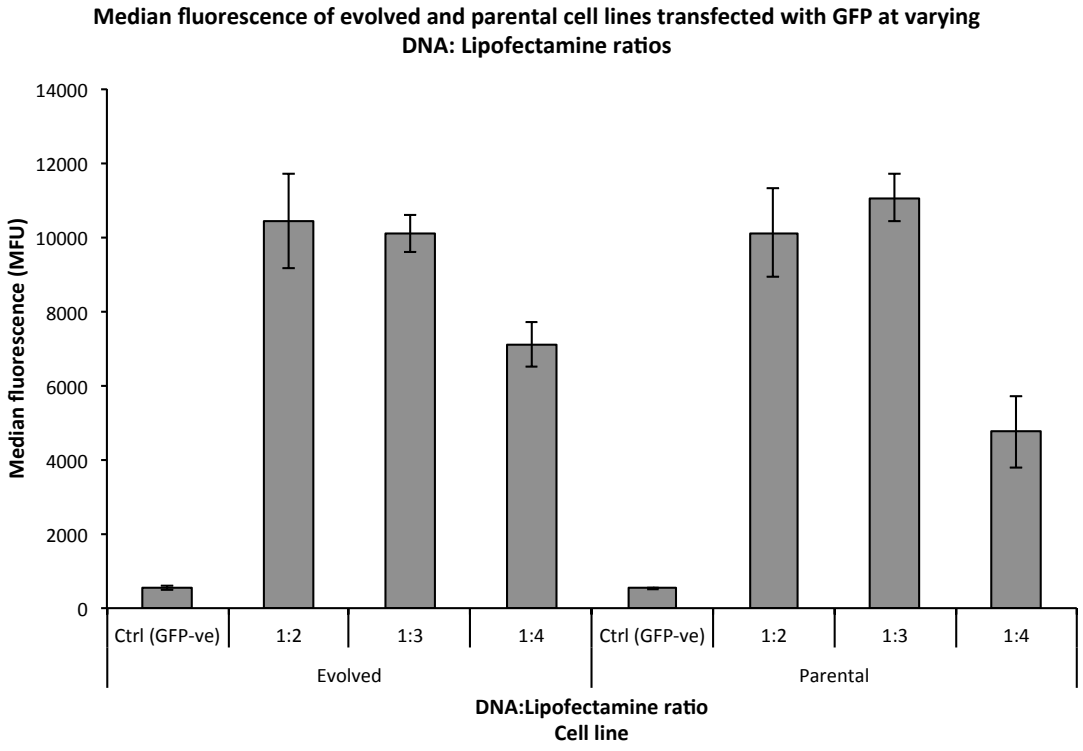

Figure 4.8 Median fluorescence values (24 hours post-transfection) of evolved and parental cell lines, at their native temperatures, transfected (via lipofection) with GFP according to different DNA: Lipofectamine ratios. Error bars, SD; N = 3.

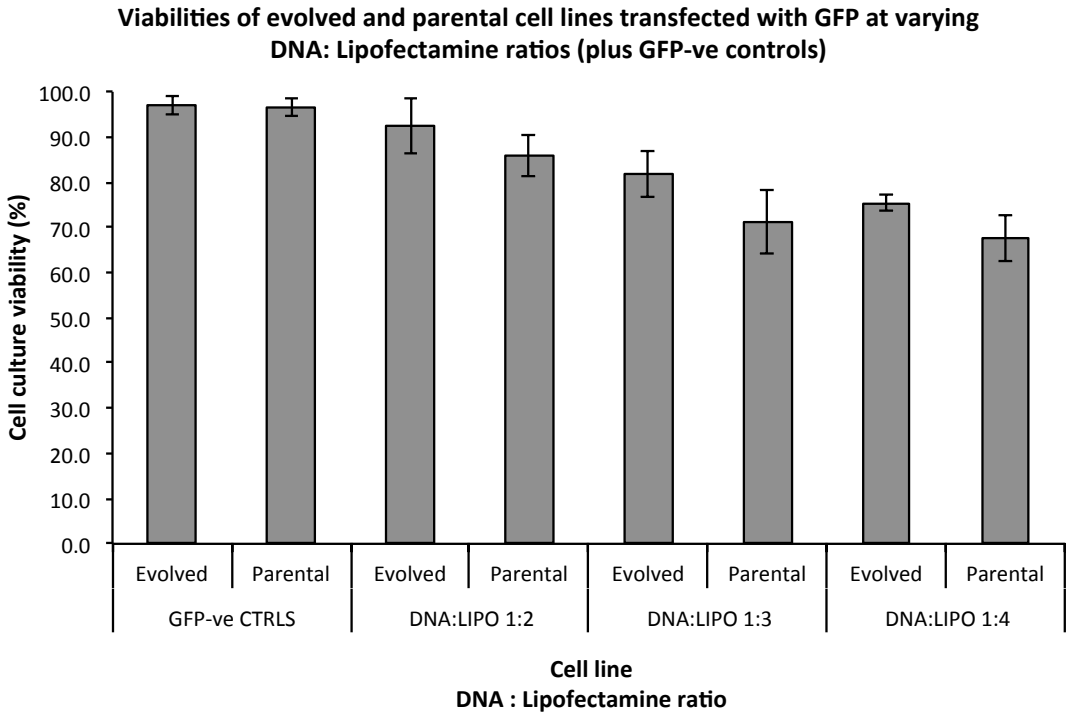

Figure 4.9 Culture viability (24 hours post-transfection) of evolved and parental cell lines transected (via lipofection) with GFP according to different DNA: Lipofectamine ratios. Error bars, SD; N = 3.

In addition to optimising the DNA: Lipofectamine ratio for transfection, the feeding strategy for fed-batch culture was also optimised as recommended by the manufacturer of the feeds. The optimal strategy was chosen based on the largest increase in IVCD on the control (un-fed, batch culture), which was strategy D - EfficientFeed™ B every three days (see appendix II).

4.3.4.2 Production of GFP, cB72.3 and Enbrel in a long-term transient, fed-batch platform

Using both FastELISA® (for cB72.3 and Enbrel) and flow cytometry (for GFP), the productivities by the evolved and parental cell lines in a long-term transient fed-batch platform were assessed. This was performed at both 32°C and 37°C for both evolved and parental cell lines. Figure 4.10 and 4.11 show the viable cell densities over time for all fed-batch lipofections and also show the feed and sampling time-points. Figure 4.12 shows the cB72.3 and Enbrel titres achieved by day 10 by the

evolved and parental cell lines in a long-term transient fed-batch platform at both 32°C and 37°C. As can be seen in this figure, generally speaking Enbrel titre is higher than cB72.3 titre in each condition. It can also be seen that, when at their native temperatures (i.e. the evolved cell line at 32°C and the parental cell line at 37°C), the evolved cell line achieves higher titres of both recombinant IgG proteins (cB72.3 and Enbrel) than the parental cell line (one-way ANOVA with Tukey's multiple comparisons test, see appendix II).

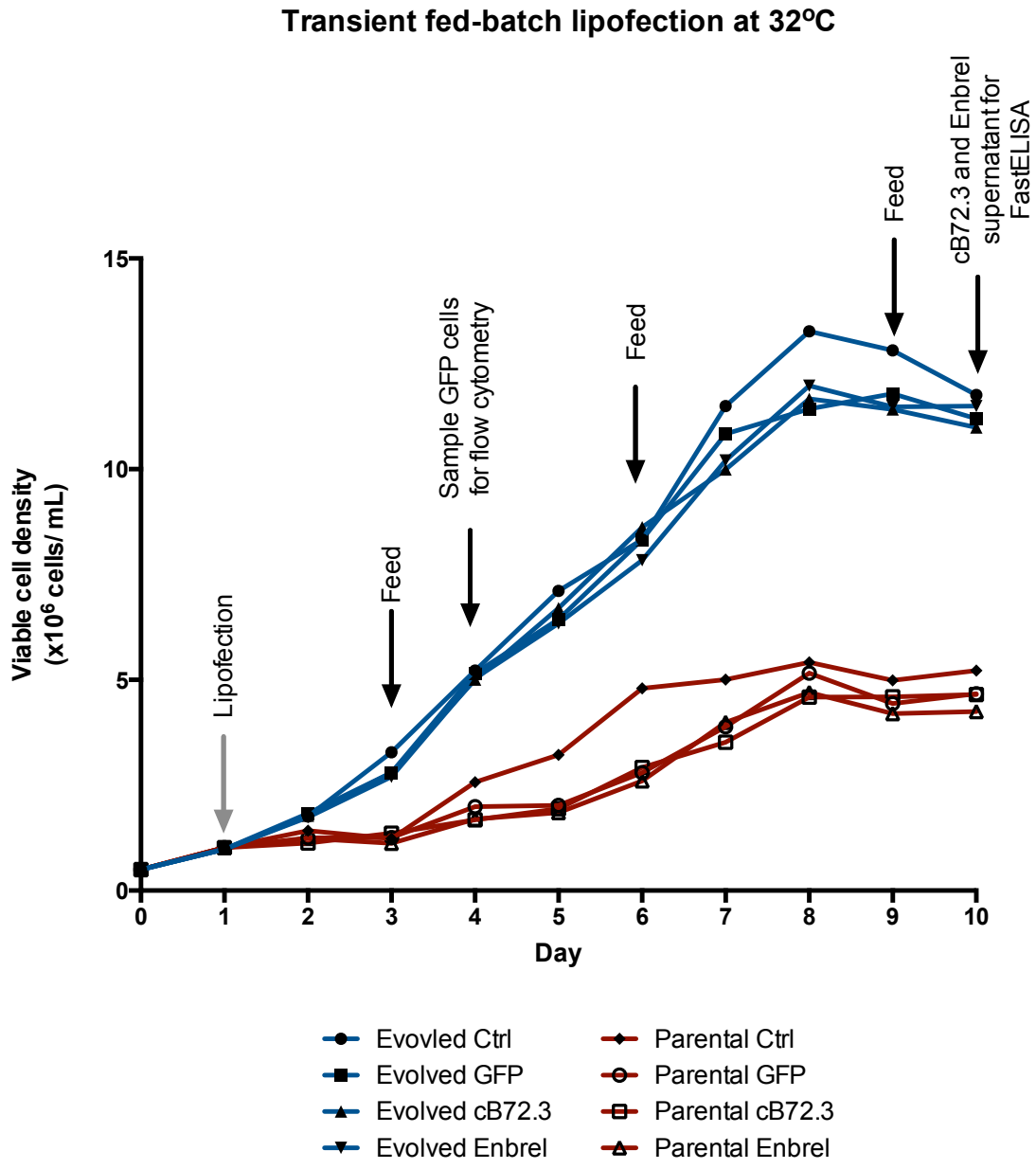

Figure 4.10 The viable cell density of the evolved and parental cell lines in a long-term transient fed-batch platform at 32°C. Lipofection, feed and sampling time points are also annotated. Error bars omitted for clarity purposes, N = 3.

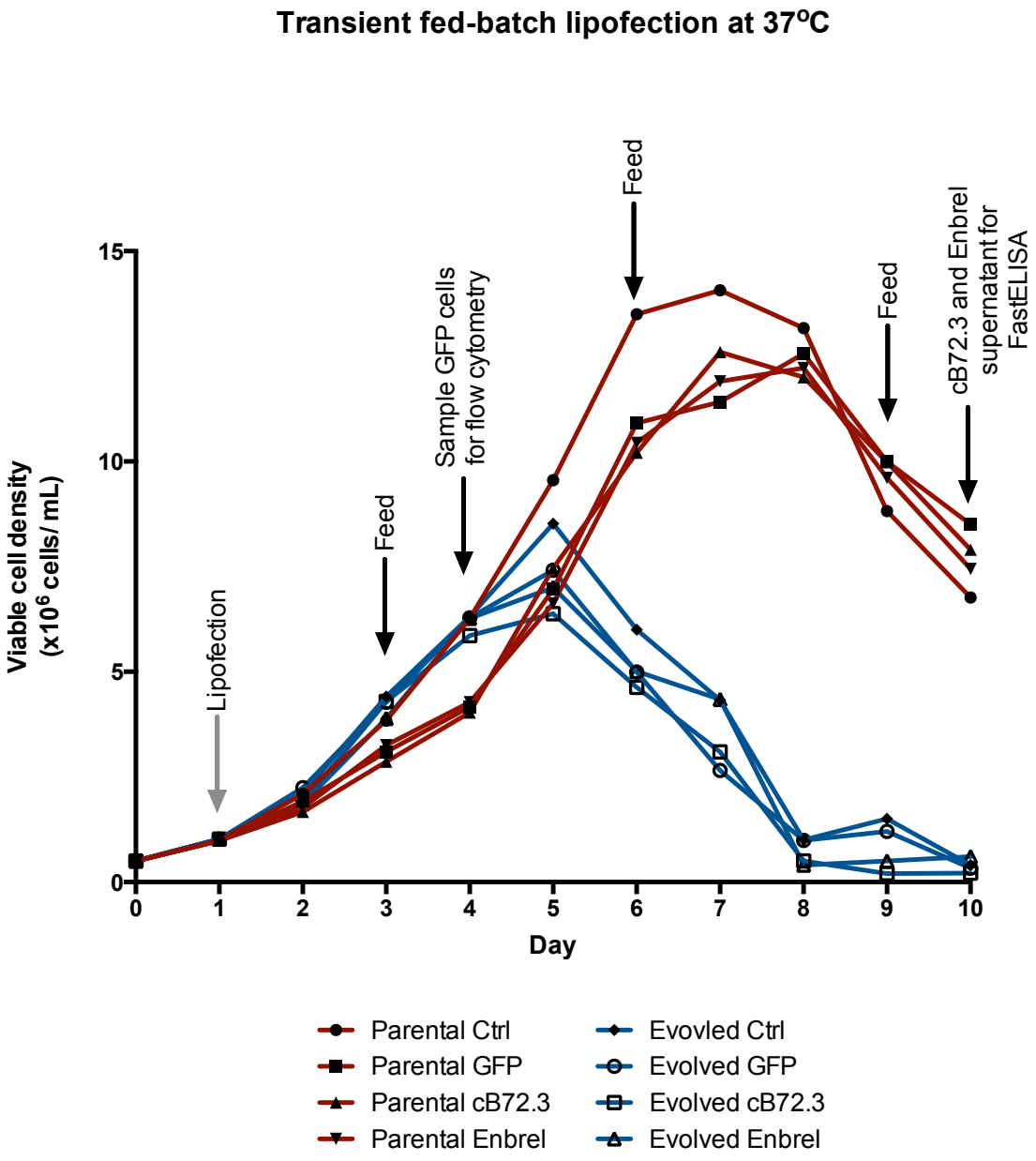

Figure 4.11 The viable cell density of the evolved and parental cell lines in a long-term transient fed-batch platform at 37°C. Lipofection, feed and sampling time points are also annotated. Error bars omitted for clarity purposes, N = 3.

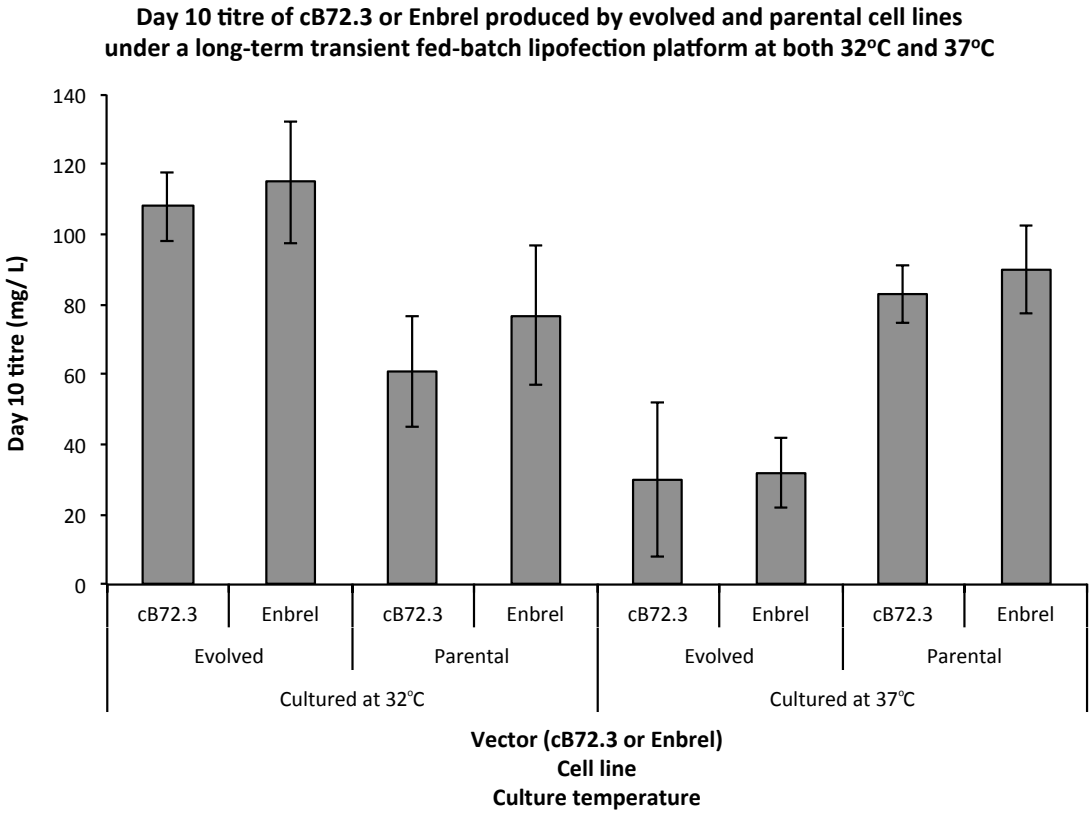

Figure 4.12 Day 10 titre of cB72.3 and Enbrel from the evolved and parental cell lines in a long-term transient fed-batch platform at both 32°C and 37°C. Error bars, SD; N = 3.

In addition to lipofection with cB72.3 and Enbrel, cultures lipofected with GFP were also assessed in this platform to determine transfection efficiency (as transfection efficiency cannot be determined using cB72.3 or Enbrel). Figure 4.13 shows the transfection efficiencies and figure 4.14 shows the median fluorescence values (from intracellular GFP production) achieved by the evolved and parental cell lines in a long-term transient fed-batch platform at both 32°C and 37°C. As was also seen in the optimisation studies (figures 4.7 to 4.9), transfection efficiencies and median fluorescence values were higher in the evolved cells (when cultured at their native temperature, 32°C).

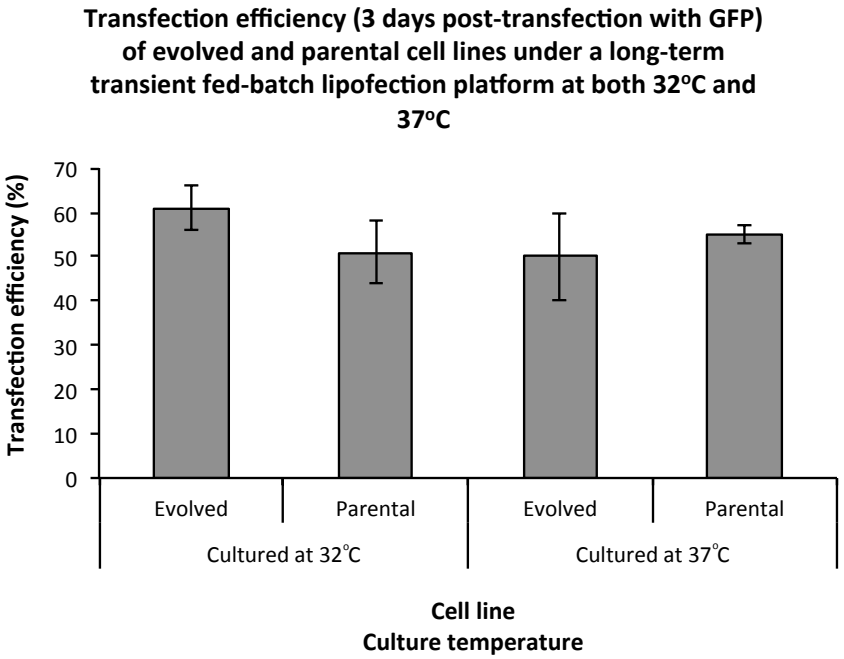

Figure 4.13 Day 4 (3 days post-transfection) transfection efficiencies of evolved and parental cell lines under a long-term transient fed-batch platform at both 32°C and 37°C. Cells were transfected with GFP via lipofection. Error bars, SD; N = 3.

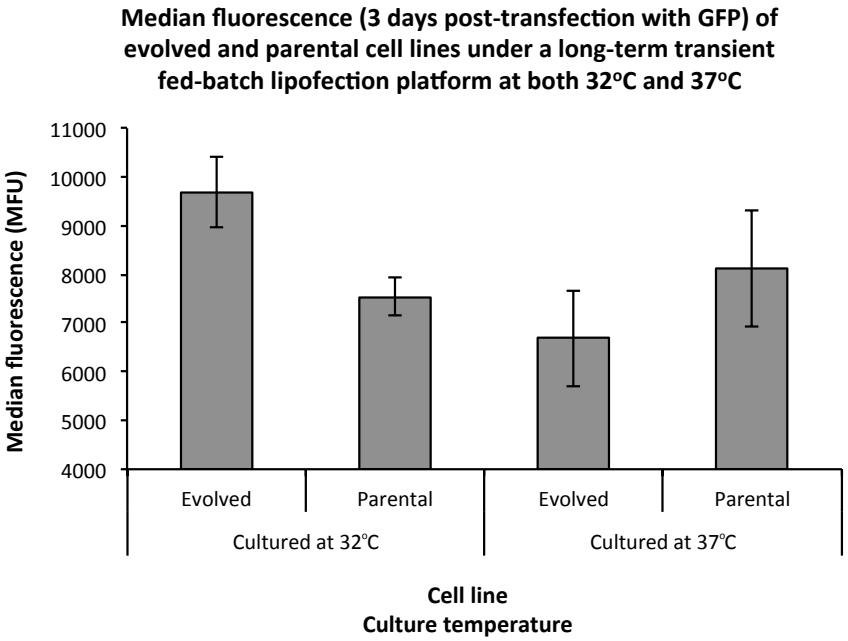

Figure 4.14 Day 4 (3 days post-transfection) median fluorescence of evolved and parental cell lines under a long-term transient fed-batch platform at both 32°C and 37°C. Cells were transfected with GFP via lipofection. Error bars, SD; N = 3.

4.3.5. Generation of cB72.3 and Enbrel stably producing cell lines from the evolved and parental cell lines

After testing negative for mycoplasma, vials of evolved and parental cells were transported to Lonza Biologics (Cambridge, UK) where work to generate stably producing cell lines from these cells was performed (by the author with supervision from Lonza staff) as outlined in the methods section. The process of stable cell line generation took ~4 weeks from transfection to transfer from static T-flask culture to agitated Erlenmeyer culture. As already stated, cross-temperature control cultures were also created at the onset of this study (i.e. transfected parental cultures that were incubated at 32°C and transfected hypothermia-adapted cultures incubated at 37°C), however, viability of these cultures never recovered and the cells died within 1-2 weeks of static culture post-transfection. Stable pools were then grown in large-scale (1 L) fed-batch cultures and supernatant was harvested at the end of culture so that recombinant protein could be purified by protein A affinity, identified by SDS-PAGE and quantified using a NanoDrop™ in synergy with known extinction coefficients. Following this, glycan profiling was performed on the purified proteins (section 4.3.7).

4.3.5.1 Concentration of protein A purified cB72.3 and Enbrel from stable pools

Protein A columns were used to purify the recombinant proteins from cell culture supernatant. Using extinction coefficients of 14.3 and 11.6 for cB72.3 and Enbrel, respectively, the concentration of purified protein was assessed using the Nanodrop™ and back-calculated to determine the true culture titre (i.e. taking into account the volume of supernatant the proteins were purified. These values summarised in table 4.2 and the titre data presented in figure 4.15. It can be seen that the evolved cell line producing Enbrel achieved the largest titre, followed by the evolved cell line producing cB72.3, followed by the parental cell line producing cB72.3, and lastly the lowest titre was achieved by the parental cell line producing Enbrel (one-way ANOVA with Tukey's multiple comparisons test, see appendix II).

Table 4.2 The average protein concentration in protein A purified cB72.3 and Enbrel samples from stably producing evolved and parental cultures and the back-calculated protein titres for those stable cell cultures. Samples were taken at the end of a complete fed-batch culture (once cells <50% viability). All evolved cultures were cultured at 32°C and all parental cultures were cultured at 37°C.

Protein name:	cB72.3		Enbrel	
Cell line:	Evolved	Parental	Evolved	Parental
Average protein concentration in sample after purification (mg/ mL)	1.521	1.500	1.314	1.220
Average culture protein titre (back-calcluated to account for volume of supernatant purified) (mg/ L)	310	272	348	303

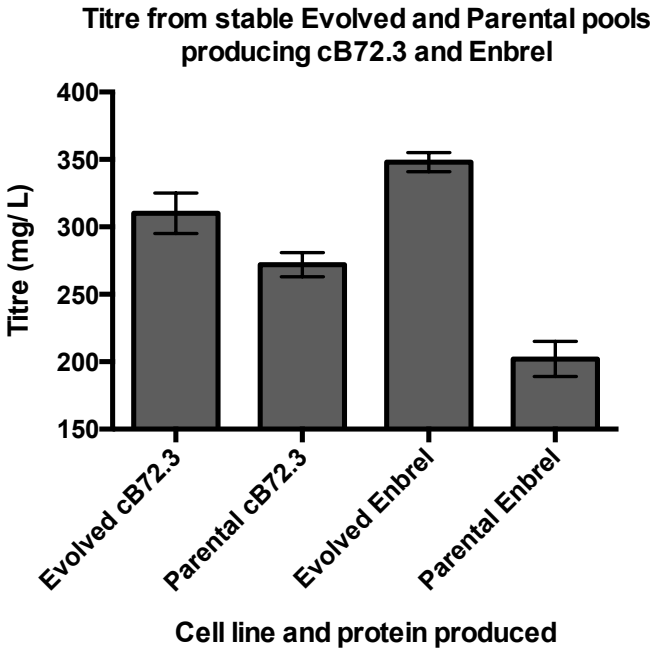

Figure 4.15 Titre from evolved and parental pools stably transfected with cB72.3 or Enbrel. Samples were taken at the end of a complete fed-batch culture (once cells <50% viability). All evolved cultures were cultured at 32°C and all parental cultures were cultured at 37°C. Error bars, SD; N = 3.

4.3.6 SDS-PAGE identification of purified cB72.3 and Enbrel from stable pools as well as from a transient (lipofection) fed-batch platform

It was important to confirm the identity of the stably produced recombinant proteins before they were analysed for glycan profiling. Reduced and non-reduced forms of both the cB72.3 and Enbrel purified proteins (produced from both stably transfected cells and from transient lipofected cultures in a fed-batch platform) were analysed using SDS-PAGE. The banding profiles should be as follows:

- cB72.3 (reduced): 2 prominent bands at ~50 kDa (heavy chain) and ~25 kDa (light chain)
- cB72.3 (non-reduced): A most prominent band at >150 kDa
- Enbrel (reduced): A most prominent band at ~70 kDa
- Enbrel (non-reduced): A most prominent band at >180 kDa

As can be seen in figure 4.16, the banding profiles for each protein are as would be expected by the manufacturer (based on previous experience), giving confidence in their identity.

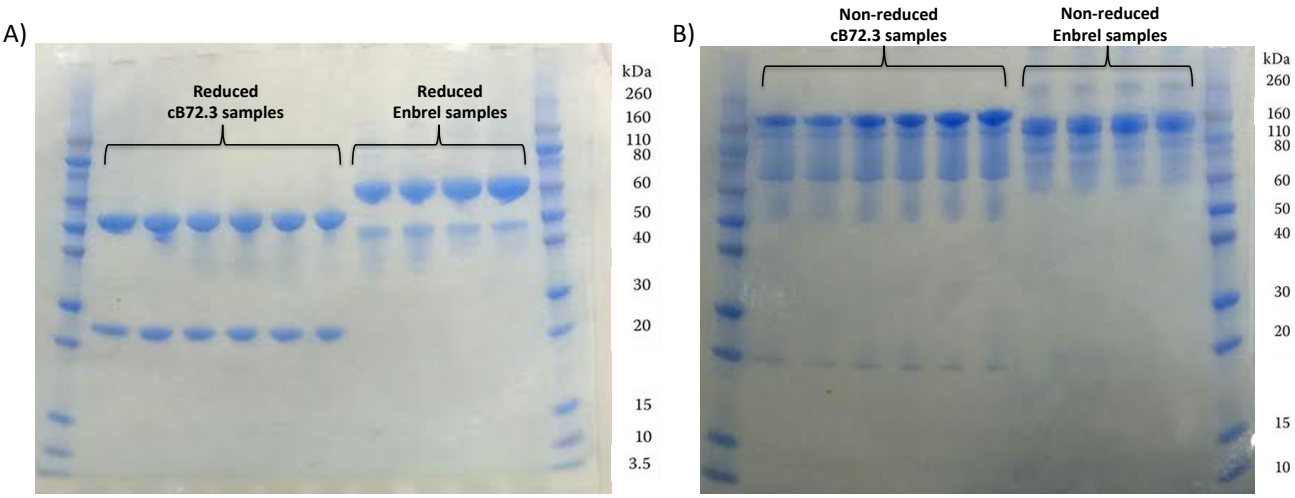

Figure 4.16 SDS-PAGE images of A) reduced cB72.3 and reduced Enbrel samples and B) reduced cB72.3 and non-reduced Enbrel samples. For the reduced samples, it can be seen that cB72.3 has prominent bands at ~50 kDa and ~25 kDa, as expected, and Enbrel has a prominent band ~70 kDa, as expected. For the non-reduced samples it can be seen that cB72.3 has a prominent band at >150 kDa, as expected, and Enbrel has a prominent band >180 kDa, as expected. N.B. For samples of cB72.3 (for both reduced and non reduced), the three leftmost lanes are from the parental cell line and the three rightmost lanes are from the evolved cell line. For samples of Enbrel (for both reduced and non reduced), the two leftmost lanes are from the parental cell line and the two rightmost lanes are from the evolved cell line.

4.3.7 Glycan profiling of cb72.3 and Enbrel in transient (fed-batch lipofection) and stable production.

Recombinant cB72.3 and Enbrel protein was purified from both stably transfected cells and from transient lipofected cultures in a fed-batch platform. Samples were sent to Lonza Biologics (Slough, UK) and N-glycan profiling was performed by their Research and Technology department. Results were returned as % of total N-glycan and are shown in figure 4.17. For cB72.3 (figure. 4.17 part A), glycan profiling largely matched the profiling observed by Lonza Biologics in their analysis of cB72.3 produced by CHOK1SV and derived host clones (O'Callaghan *et al.* 2015). It can also be seen that the largest differences in % of total N-glycan are seen when making comparisons of the same protein from the same cell line *between the two production platforms* (stable versus transient), rather than *between parental and evolved cell lines within the same production platform*. This suggests that the evolution process has not interfered with the glycan processing capabilities of the cell, and it may suggest that glycan processing capabilities are very slightly affected by the production platform used. That said, when comparing the variation between cell lines, there is more variation between evolved and parental in a transient platform than stable pools (in which there is almost no variation). Nevertheless, the variation between all samples analysed here, regardless of cell line/ production platform, is less than that is observed in the CHOK1SV clones in the work conducted by O'Callaghan *et al.* (2015). However, to have full confidence in these deductions an N of ≥3 would be required (a requirement that was not possible within the financial bounds of this project).

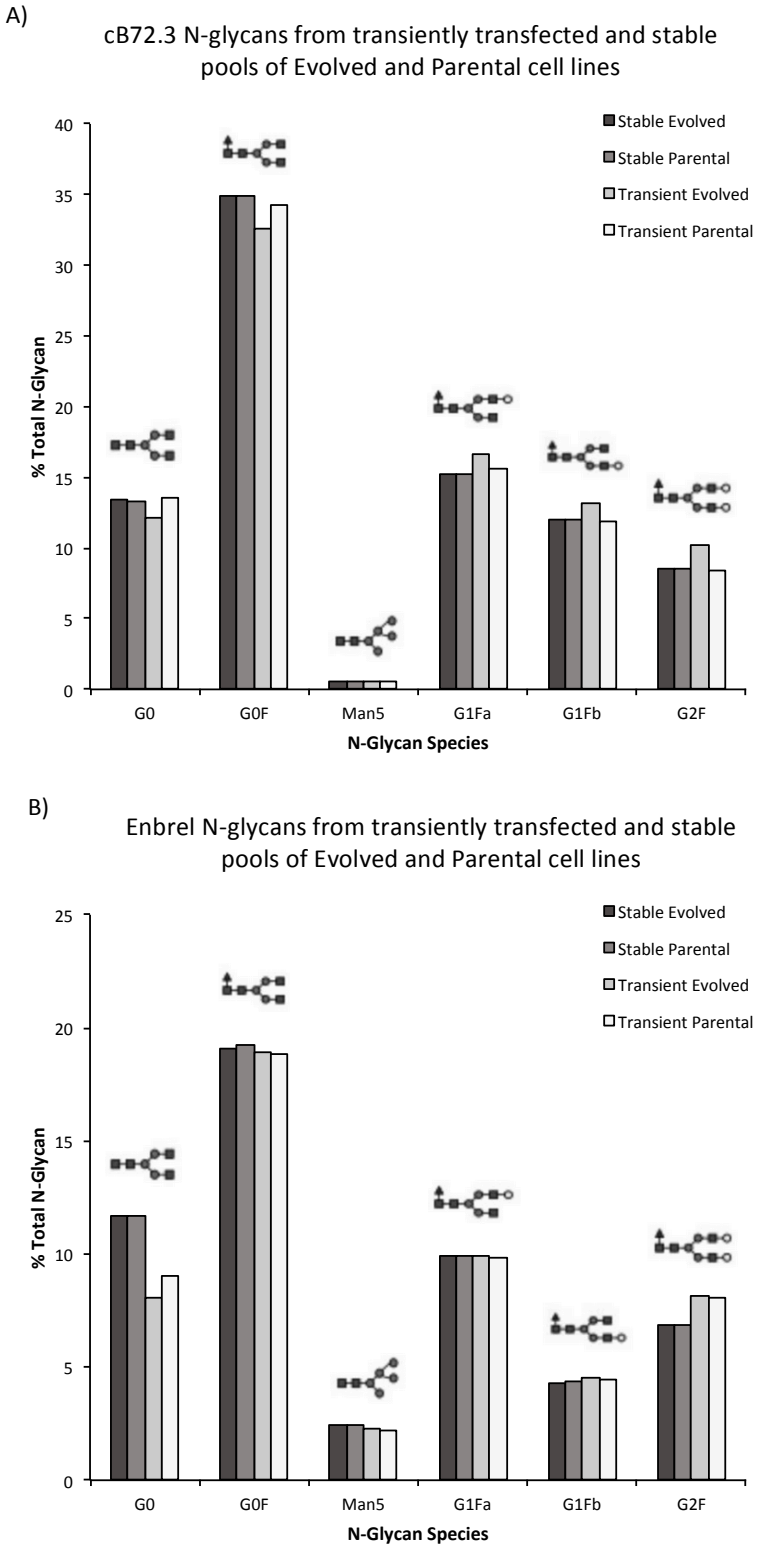

Figure 4.17 N-glycans of recombinant proteins: A) cB72.3 and B) Enbrel, produced via either stably transfected pools of evolved or parental CHOK1SV cells, or evolved or parental CHOK1SV cells in a fed-batch transient lipofection platform. Schematics above bars represent the n-glycan forms, G0, G0F, Man5, G1Fa, G2Fb or G2F (where the shapes represent the following: triangle: fucose, square: n-acetylglucosamine, clear circle: galactose, shaded circle: mannose). N = 1.

4.4 Discussion

The work presented in this chapter was conducted to address the question of whether or not the evolved, hypothermia-adapted cell cultures (that were generated as described in chapter 3) make a suitable industrial host cell line in terms of the following: their transient productivity and transfection efficiency, their performance in a fed-batch transient lipofection platform, their ability to be stably transfected to create stable cell lines producing industrially relevant protein products, and finally the quality of the protein products by glycan profiling. These investigations were performed with comparison to an unevolved, parental counterpart at all times. Initially, this included three evolved cultures being compared to three parental counterparts, however, as the analysis deepened and resources became limited, only one evolved culture was taken forward for further assessment (along with it's parental counterpart). As mentioned, these cultures were then simply termed "evolved" and 'parental" cell lines.

As was described in section 4.3.1 of this chapter, it is clear to see that the evolved cell cultures exhibit a production advantage over their parental counterparts: here it was seen that, as would be expected and has been demonstrated in the literature numerous times (Slikker *et al.* 2001; Kumar *et al.* 2008; Becerra *et al.* 2012), when parental cell cultures were exposed to hypothermia (32°C) post-transfection, their productivity is increased markedly as was observed for SEAP production (fig. 4.2). However when the evolved, hypothermia-adapted cells (that were already being cultured at 32°C) are then subjected to the same hypothermic conditions, their productivity is further increased again. This shows that there is an increased production advantage that is inherent to the evolved cell cultures. Although it has been shown in the literature that hypothermia-adapted CHO cells show significant increased in productivity (Sunley et al. 2008), this has only been demonstrated with stably producing cell lines that were subsequently adapted to hypothermia, rather than host cell lines that were subsequently transfected, as was the case here.

Following this, a study into the transfection efficiencies of the evolved and parental cultures was undertaken. This study was performed, as it was not known what effect, if any, the difference in cell size between the two culture types may have on the physical processes of electroporation (Bio-Rad 'Post-Transfection Analysis of Cells' Bulletin 5969, 2010). As demonstrated in section 4.3.2, the evolved cultures showed higher transfection efficiencies as well as higher median GFP fluorescence than the parental cultures. This would suggest (assuming the cell types have the same bio-physical composition) that the increase in size of the evolved cells has lead to improved transfection efficiencies, which may also account for the improved median fluorescence (a proxy of GFP production). However, as has been previously discussed there are numerous reasons why you might expect better productivity at lower temperatures (for example, increased mRNA half-life leading to persistence in the cell (Yoon *et al.* 2004)). That said, when the parental cell cultures are incubated at 32°C post transfection, there is no general increase in median fluorescence or transfection efficiency.

With this data alone, it is difficult to state for certain whether the differences in transfection efficiency are cell size-specific. To confirm or reject this potential relationship one could FACS sort the cells of each culture type based on size and then compare the transfection efficiencies of populations of the same cell size. Should any differences remain once cell size has been accounted for then it could be assumed that the differences are inherent to the cell type. Along a similar vein, the increased viabilities during the optimisation of lipofection conditions (section 4.3.4.1) that were observed in the evolved cell line compared to the parental may also be related to cell size due to the disproportionate cell surface area: volume ratios between the two cell lines. However, to establish this relationship, a deeper practical examination of the kinetics of DNA-Lipofectamine complexes in relation to cell membrane area would be required.

The evolved and parental cell lines were then examined in terms of productivity with larger, more industrially relevant recombinant proteins, these being cB72.3 (an IgG4 mAb) and Enbrel (A.K.A Etanercept, an IgG1 Fc-fusion protein). The

sponsors of this project, Lonza Biologics, use both proteins in early cell line development assessment phases and the latter (Enbrel) is typically classed as a difficult to express (DTE) protein. DTE proteins are often characterised by low yields or expensive downstream processing costs, both of which increase the cost of goods and time-to-market (Pybus *et al.* 2013). Naturally, to be equipped with a cell line that is inherently more able to express such DTE proteins would be a desirable asset in industry.

The day 10 yields achieved in a transient fed-batch production platform (section 4.3.4.2) were comparable to the yields achieved by Pybus and colleagues (2013) who used an equivalent transient fed-batch production platform to produce a series of DTE mAbs. As mentioned in section 4.3.4.2, the highest producing condition was achieved by the evolved cells when cultured at 32°C. The parental cells did not perform well at 32°C (as they might normally do in a "cold-shock" set-up) but this is most likely due to the consistent low growth rate and resulting low IVCD. An unusual and unexpected result of the transient fed-batch production study was that titres for Enbrel were consistently higher than titres for cB72.3 (when produced by the same cell line at the same temperature). However, this result is not reflected in the titres observed in stably producing evolved and parental cell lines, in which case the evolved cell line produces a higher titre of Enbrel than titre of cB72.3, and the parental cell line produces a higher titre of cB72.3 than titre of Enbrel. In any case, the evolved cell line is always the highest stable producer of each protein. This result is not trivial considering that all other attempts at evolving a stable cell line to become hypothermia-adapted for high productivity have either ultimately failed at scale up (Sunley *et al.* 2008), or high productivity has been lost as a result of the evolution process (Yoon *et al.* 2006). It would appear that the key element in successfully generating a high producing hypothermia-adapted stable cell line (as has been demonstrated in this chapter), lies in the order of operation, i.e. the process of adaptation to hypothermia should be performed *prior* to stable transfection.

It was seen during glycan profiling of transient and stably produced cB72.3 and Enbrel from evolved and parental cell lines that there was little variation between samples and glycan profiling largely matched the profiling observed by Lonza Biologics in their analysis of cB72.3 produced by CHOK1SV and derived host clones (O'Callaghan *et al.* 2015). For example cB72.3 Man5 was relatively low (>5%) in both the work presented in this chapter and in the work by O'Callaghan *et al.* (2015). Low Man5 glycans (relative to other glycoforms) have been directly associated with reduced clearance of IgG antibodies in humans, which can ultimately mean that time between intravenous doses of therapeutic drugs can be extended as the drug persists in the body for longer. This is more convenient for the patient and also reduces universal costs as the total mg administered over treatment can be reduced (Goetze *et al.* 2011). The main difference in the glycan profiling of cB72.3 between this work and that of O'Callaghan *et al.* (2015) is noted in the G0 proportion being higher in this study (in both evolved and parental cell lines) and the proportion of G0F is lower (in both the parental and evolved cell lines). In line with this, it is regularly documented that afucosylated therapeutic antibodies exhibit increased antibody-dependent cell-mediated cytotoxicity (ADCC) (Satoh *et al.* 2006; Jefferis 2007; Raju & Jordan 2012). Although a thorough conclusive discussion cannot justly be given regarding glycan profiling due to an N of 1 being used for each sample, it is important to note that, even with a sample size of 1, there were no major differences observed between the evolved and parental cell lines for each glycan species measured. This is important as it shows that the hypothermia-adaptation process has not altered or compromised the glycan processing capabilities. In addition to this, the fact that this is true for every glycan species profiled adds confidence in the result despite N being 1. The obvious future work that could be conducted in this area, funding permitting, would be to repeat the analysis with a larger sample size. Alternatively, one could perform clonal selection on the stable pools to try and identify and isolate high producing clones whose recombinant proteins demonstrated the preferred glycan profile. It could also be informative to investigate sialilation modifications between proteins produced from the two cell lines to determine whether the increased

degree of sialilation that is observed in "cold-shock" strategies is conserved in the cells that are now accustomed to hypothermia (Nam *et al.* 2008).

Conclusions and future work

Not only has the evolved cell line performed well as a stable producer, something that would be mandatory for it even to be considered as a production cell line in industry, it has also shown merits in transient transfection where small scale production is required in a short time-frame, for example in the early stages of drug development. In terms of future work, as already alluded to, the degree that cell size accounts for the disparity in transfection efficiency and viability post-transfection could be investigated. However, in some respects, from an industrial relevance perspective, this is likely not to be too imperative. Additionally, to fully confirm whether this cell line could be taken forward from an academic exercise into an industrial setting, a full technology readiness level (TRL) assessment would need to be performed, most likely in collaboration with Lonza Biologics. This may also include bioreactor scale-up to evaluate how the larger cell phenotype of the evolved cell line performs under bioreactor stress (higher shear, etc.). Additionally, using clonal selection one could identify and isolate a high producing clone whose recombinant proteins demonstrate the preferred glycan profile.

As previously mentioned, to further the preliminary product quality investigation, glycan profiling could be carried with at least three replicates if funding could justify this, however, as stated, the fact that the findings are the same for each of the six glycans profiled adds confidence to the finding that there appears to be no difference between evolved and parental cell lines. In addition to this, more stable cell lines could be generated from the evolved cell line to produce other DTE proteins or, for example, proteins that have a high propensity to aggregate. This would determine whether the evolved cell line consistently outperforms the parental cell lime, or whether the results presented in this chapter are specific to only cB72.3 and Enbrel. To complement further investigation into cell line performance and functionality, it could be highly beneficial to attain a more mechanistic understanding of the evolved cell line, determining what key

biological changes have occurred as a result of becoming hypothermia-adapted. Being quipped with this information could enable reverse engineering techniques to be developed, or it could lead to the generation of hypothermia-adapted cell lines in a more rapid manner. This kind of mechanistic understanding is a topic that is explored further in the following chapter.

This page is intentionally left blank.

Chapter 5:

Mechanistic analysis and characterisation of a hypothermia-adapted CHOK1SV cell line

This chapter addresses the final aim of analysing the biology that may underpin the fundamental differences (and interesting similarities) between the parental cell line and the hypothermia adapted (evolved) cell line. Experiments to investigate specific hypotheses were conducted, as well as experiments that would be informative in a hypothesis-free manner, such as comparative transcriptomics and amino acid flux analysis. From the findings, possible engineering targets are proposed as well as suggestions for potentially beneficial future work.

5.1 Introduction

As demonstrated in the previous chapters, the hypothermia-adapted, evolved cell line has undergone major phenotypic changes as well as demonstrating impressive functional feats in terms of industrial performance abilities: Compared to the parental cell line, the evolved cell line has not only reached equivalent growth rate, approximately doubled in biomass, become twice as transcriptionally active and increased in transient productivity, it has also exhibited comparable resilience during stable cell line production delivering improved titres and has also displayed similar glycosylation capabilities. Such performance changes are particularly

notable when considering that the hypothermic environment initially and ordinarily halts the cell cycle and prevents cell growth and proliferation.

This cell line has clearly advanced substantially along the evolution process, resulting in many industrially desirable qualities. However, the underlying modifications that underpin these observable transformations are as yet largely undetermined. As stated, the purpose of this chapter is to explore this area in depth, with intention to identify and characterise the cellular mechanistic differences between the hypothermia-adapted and parental cell lines. Included in this chapter is work that investigates both specific hypotheses as well as more global examinations of the evolved cell line, in the areas of: mitochondrial function, oxidative stress, amino acid flux and transcriptomics. The rationale behind undertaking this analysis is that it could lead to the isolation of specific targets that may be used to engineer, rather than evolve (which can be a reasonably lengthy process), an equivalent cell line. Alternatively the analysis could lead to information that could assist in and speed up the hypothermia-adaptation process.

As was discussed in chapter 1, the cellular responses of CHO cells that are subjected to a temperature phase shift to enhance production have been studied extensively. The pervasive findings are that transcriptional and translational process change within hours of temperature reduction. For example, commonly cited in the literature, cold-inducible RNA binding protein (CIRP) is found to be preferentially transcribed during mild hypothermia (Nishiyama *et al.* 1997; Fuller 2003). In addition to this, evidence of targeted post-translational modifications has also been identified as a cellular response, such as tyrosine phosphorylation of proteins in CHO cells (Kaufmann *et al.* 1999). There is indication that the ability of cells to respond to hypothermia can be enhanced by 'pre-conditioning' them to up-regulate their stress response, i.e. in the case for biopharmaceutical production this would mean using cells that have had prior exposure to hypothermic conditions (Vogt *et al.* 2000; Fuller 2003). The ability of the hypothermia-adapted cell line to perform successfully could be supported by constitutive or even higher

expression of the stress-response genes that have been presented in the literature so far regarding cold-shock strategies. The lengthy evolution process may have worked as iterative pre-conditioning, continuously re-regulating stress response thresholds.

It is also considered that the hypothermia-adapted cell line may have developed orthogonal solutions to sub-optimal temperatures, such as heat conservation or producing heat on a cellular level via thermogenesis. As presented in chapter 3, a characteristic of the evolved cell line is its significant increase in cell size. In Zoology, Bergmann's rule states that there is an intra-species tendency in homeothermic organisms to have increasing body size with decreasing ambient temperature. This is due to simple thermodynamics: a small surface area to volume ratio reduces relative heat loss (Sand *et al.* 1995). An increased cell size in the hypothermia-adapted cell line would therefore improve its homoeothermic efficiency in sub-optimal temperatures.

There are a number of methods by which the cell could also be generating additional heat to overcome the effects of the surrounding hypothermic environment. Firstly, adaptive non-shivering thermogenesis is a process that is present in all eutherian mammals (a clade to which Chinese hamsters belong) (Hayward & Lisson 1992). In contrast to classical non-shivering thermogenesis, which is facultative and acts within minutes when an organism acutely requires extra heat, adaptive thermogenesis takes multiple weeks for an increase in capacity to develop. Non-shivering thermogenesis activity usually occurs in brown adipose tissue and adaptive non-shivering thermogenesis ordinarily corresponds to the recruitment of such tissue (Cannon & Nedergaard 2011). As the name suggests, non-shivering thermogenesis was originally defined as a cold-inducible increase in heat production not associated with the muscle activity of shivering (Himms-Hagen 1984). It is in fact a metabolic process involving an adaptation of the inner membrane of the mitochondrion in which the permeability (conductivity) of the membrane is increased, allowing protons pumped by the respiratory chain to return to the mitochondrial matrix via the proton motive

force, dissipating energy as heat (Rial & Zardoya 2009). A family of transporters belonging to the mitochondrial carrier protein superfamily known as uncoupling proteins (UCPs) provide the pathway for this proton re-entry and ATP-synthase is bypassed. These UCPs have been found to be activated by long-chain fatty acids (LCFAs) (Fedorenko *et al.* 2012). This adaptation originally evolved as a mechanism to allow organisms living in oxygen-rich environments to overcome the dangers posed by 'reactive oxygen species' (ROS) - these are highly reactive, oxygen-derived free radicals that can cause damage to the cell known as oxidative stress. It is widely known that the mitochondrial respiratory chain is a major site of ROS and an increase in respiration due to UCP-mediated uncoupling has been found to correlate with reduced ROS formation and increased protection against subsequent oxidative stress (Rial & Zardoya 2009). Oxidative costs have been found to greatly differ depending on whether ATP-synthase or UCPs are driving respiration (Stier *et al.* 2014). Once this latter mechanism to increase respiration evolved to become operative, it was subsequently co-opted to fulfil other physiological roles, such as the generation of heat. Now, the UCPs are so recognised for their thermogenic capacity that one specific uncoupling protein, UCP1 has been alternatively termed *thermogenin* (Palou *et al.* 1998; Rial & Zardoya 2009)

A second means of cellular non-shivering heat generation that has evolved primarily to maintain physiological temperatures involves the cycling of Ca^{2+} by the membrane bound sarco/endoplasmic reticulum Ca^{2+}-ATPases (SERCA). SERCA are pumps that are able to transport Ca^{2+} ions upon hydrolysis of ATP to ADP + Pi which also generates heat energy (Kozak & Young 2012). The cytosolic ADP generated by this process consequently stimulates mitochondrial respiration, resulting in further increased heat production (de Meis 2001). Furthermore, mutations in the gene encoding for the ryanodine receptor have been found to result in uncontrolled leakage of Ca^{2+} into the cytoplasm, generating heat as Ca^{2+} moves along its concentration gradient (MacLennan & Phillips 1992). Related to these aforementioned processes, it has been shown that thermogenesis is contributed to by metabolic systems known as *futile cycles*. Futile cycles, also

known as substrate cycles, occur when two metabolic pathways run simultaneously in opposing directions with no apparent overall purpose or effect other than to dissipate heat energy (Qian & Beard 2006). Concurrent glycolysis and gluconeogenesis would be an example of an uneconomical futile cycle in which a large amount of chemical energy is dissipated as heat (Nelson *et al.* 2008).

This chapter describes the experimental studies that were undertaken to investigate the theory that the hypothermia-adapted cell line could be undergoing thermogenesis as a mechanism to thrive in sub-physiological conditions. Differential gene expression analysis is also used to further explore this hypothesis as well as examining global transcriptome changes in a hypothesis-free manner. In addition to this, as it is already evident that the evolved cell line has become physically distinct from the parent phenotype (size, RNA content), the utilisation of amino acids is comparatively examined.

5.2 Materials and methods

This section describes the materials and methods used for oxidative stress analysis, mitochondrial function analysis, amino acid analysis, RNA sample preparation and subsequent analysis by Affymetrix arrays. The reader is referred to chapter 2 for details on other experimental techniques required for this chapter (such as routine cell culturing).

5.2.1 CellROX® oxidative stress assay

Oxidative stress assays were performed using CellROX® Oxidative Stress Reagents (Molecular Probes, Life Technologies, Paisley, UK). CellROX® Deep Red Reagent specifically was used due to its absorption/emission maxima being ~644/665 nm. Parental CHOK1SV (at 37°C) and hypothermia-adapted CHOK1SV (at 32°C) cultures were grown in 6-well plates in humidified (%) static incubators at % CO_2). On day 3 (mid-exponential growth), CellROX® Deep Red Reagent was added to

each culture at a final concentration of 5 μM and incubated at room temperature for 30 minutes. For each cell type this was performed in triplicate and unstained controls of each were also incubated for the same time period. After incubation, cell cultures were centrifuged at 200 ×*g* for 5 minutes, supernatant was aspirated and the cell pellet resuspended in room temperature PBS. This was repeated another two times to thoroughly wash the cells. Cells were then fixed according to the PFA fixing method described in chapter 2. The fixed cell samples (stained and unstained) were then analysed on the BD LSRII Flow Cytometer (BD, Oxford, UK) using the Red 660 nm laser configuration. The cell-permeant Deep Red Reagent is non-fluorescent while in a reduced state and brightly fluoresces upon oxidation by reactive oxygen species (ROS).

5.2.2 Mitochondrial bioenergetics

5.2.2.1 Measurement of oxygen consumption and extracellular acidification rates

Oxygen consumption rate (OCR) and extracellular acidification rate (ECAR) were measured using the metabolic analyser Seahorse XF24 system (Seahorse Biosciences, North Billerica, MA, USA). This system uses the XF24 FluxPak which comprises of a sensor cartridge component along with a XF24 Tissue Culture Plate. The sensor cartridge component must be hydrated with XF Calibrant for at least 24 hours before use. Prior to experimentation, the evolved and parental CHOK1SV cell lines were cultured every 4 days in 125 mL vent-capped Erlenmeyer flasks (Corning, Surrey, UK) using 30 mL of CD CHO medium (Life Technologies, Paisley, UK) supplemented with 6 mM glutamine. On day 3 post sub-culture (mid-exponential growth phase), cells were sampled to assess density and viability using the Vi-CELL XR cell viability analyser (Beckmann Coulter, High Wycombe, UK). Following this, 2×10^6 cells were centrifuged at 200 ×*g* for 5 minutes, the supernatant removed and the cell pellet resuspended in fresh CD CHO medium supplemented with 6 mM glutamine at a final cell density of 1.2×10^6 cells mL^{-1} [N.B. *This cell density is specified as a result of optimisation work performed on a CloneSelect™ Imager (Molecular Devices, Sunnyvale, California, USA) that*

determined the concentration of cells in 100 µL that would provide cell confluence across the surface of an individual XF24 Tissue Culture Plate well (Seahorse Biosciences, North Billerica, MA, USA): A range of cell densities were analysed for both the evolved and parental cell lines and for both cell types a density of 1.2 × 10^6 cells mL^{-1} was consistently deemed confluent by the analysis software. In addition to this, after simulation of the BD Cell-Tak™ plate preparation treatment (see below), BCA Protein assays (Thermo Scientific, Loughborough, UK) confirmed that a comparable protein biomass content between cell types remained adhered to each well, meaning potential OCR biomass normalisation steps were not necessary]. 100 µL aliquots of each cell type (evolved and parental) were then dispensed in triplicate into separate wells of XF24 Tissue Culture Plate that had been previously treated with BD Cell-Tak™ cell and tissue adhesive (BD Biosciences, Oxford, UK) (see section below for details). Duplicate plates were generated for analysis at both 37°C and 32°C, to serve as temperature controls. Plates were then incubated at 37°C or 32°C, under 5% (v/v) CO_2 atmosphere in static incubators for 30 minutes to allow cell attachment to the well bottom. After this time, an inversed light microscope was used to confirm cell attachment and visually check cell confluence across the surface. Next, the CD CHO in which the cells had been suspended was carefully removed, leaving the cells attached to the well bottom. As quickly as possible, 600 µL of un-buffered XF Media (Seahorse Biosciences, North Billerica, MA, USA) supplemented with 2mM glutamine and 16.74 mM glucose at pH 7.4 was then applied to each well (glutamine and glucose were supplied at these concentrations as these has been shown to be representative of conditioned media from mid-exponential growth (Martell 2015, unpublished data)). The plates were then incubated for 45 minutes at 37°C or 32°C in CO_2 free incubators to allow for pH and temperature equilibration before transfer to the XF^{e}24 Extracellular Flux Analyser (Seahorse Biosciences, North Billerica, MA, USA). The XF^{e}24 Extracellular Flux Analyser was then run using a protocol set to run in cycles of 8 minutes, each containing: mix for 3 minutes, wait for 2 minutes then measure for 3 minutes. Oxygen consumption rate (OCR) and extracellular acidification rate (ECAR) are the measurements made by this analyser. After measuring basal OCR and ECAR rates, the cells are sequentially treated with different chemical inhibitors/effectors

through separate injection ports located on sensor cartridge component of the FluxPak, which fits complimentary to the XF24 Tissue Culture Plate. The Seahorse injection ports were loaded as follows, in this order:

- Port A: 75 µL (10X concentration) of Oligomycin (synthase inhibitor) in Assay media, to result in a final concentration in the well of 1.5 µM.
- Port B: 82.5 µL (10X concentration) of FCCP (electron transport chain accelerator) in Assay media, to result in a final concentration in the well of 0.75 µM.
- Port C: 91.6 µL (10X concentration) of Antimycin A / Rotenone (electron transport chain inhibitors) in Assay media, to result in a final concentration in the well of 1 µM.

The XF^{e}24 Extracellular Flux Analyser was run at both 37°C or 32°C according to the treatment of the cells up to the point of analysis. Once complete, the XF24 Tissue Culture Plate was removed and immediately the cells were viability checked using CyQUANT® NF Cell Proliferation Assay (see section 5.2.2.3 below).

5.2.2.2 Preparation of Cell-Tak™ coated plates for XF24 mitochondrial assays

At least 4 days prior to any assay an XF24 Tissue Culture Plate would need to be treated with BD Cell-Tak™ cell and tissue adhesive (BD Biosciences, Oxford, UK). To prepare one plate, 19.4 µL of BD sterile stock solution (adhesive), 1270.9 µL of NaHCO3 neutral buffer solution adjusted to pH 8.0 and 9.7 µL of NaOH 1N were mixed together in a laminar flow cabinet. The buffer solution and NaOH were sterile filtered prior to this. Once thoroughly combined, 50 µL of this solution was added to each well of the XF24 Tissue Culture Plate and left to sit at room temperature in the laminar flow cabinet for 20 minutes. Next, a multichannel pipette was used to remove all of the solution, with extra care being taken not to scratch and therefore destroy the adhesive coating now formed on the well bottom. Following this, to ensure traces of bicarbonate are washed off, 200 µL of Cell Culture Grade Water (Sigma-Aldrich, Dorset, UK) was added to each well then

removed with a multichannel pipette. The plates are then left to sit in the laminar flow cabinet for a further 20 minutes to ensure plats are fully dried. After this time, plates are securely covered with parafilm and stored at 4°C until required for use.

5.2.2.3 Post-XF24 analysis cell viability measurements using CyQUANT® NF Cell Proliferation Assay

Removal of XF24 assay media containing chemical inhibitors/effectors should be performed as soon as possible after analysis. For one XF24 Tissue Culture Plate, 8.4 µL of 500X CyQUANT NF dye reagent (component A) and 8.4 µL 500X Dye delivery reagent (component B) are mixed and added to 2.8 mL 1X HBSS buffer (component C diluted in deionised water), to create a dye binding solution. 100 µL of this dye binding solution is dispensed into each well of the XF24 Tissue Culture Plate using a multichannel pipette. The plate is then covered and incubated at 37°C or 32°C (according to the treatment of the cells up to this point of analysis) for 30 minutes. The fluorescence intensity of each sample is measured using a fluorescence microplate reader with excitation at ~485 nm and emission detection at ~530 nm. The fluorescence intensity of the cells that have undergone XF24 analysis is compared to the fluorescence intensity of control cells that are known to be of high viability (>95% viable), confirmed by the Vi-CELL XR cell viability analyser. The CyQUANT® NF Cell Proliferation Assay was chosen over other proliferation assay kits as it measures independent of metabolic status.

5.2.3 Affymetrix® GeneChip® CHO Gene 2.0 ST Array

The methods defined in this section include preparatory procedures, technical summary of the Affymetrix® Array workflow and the analytical approaches applied to the generated dataset.

5.2.3.1 Sample collection for Affymetrix® Array analysis

Triplicate samples of 5×10^6 viable cells were collected from both the evolved and parental cell lines during mid-exponential growth phase (day 3). To wash the cells,

samples were centrifuged at 200 ×*g* for 5 minutes, supernatant was aspirated, the cell pellet resuspended in room temperature and then re-centrifuged at 200 ×*g* for 5 minutes and the supernatant aspirated once again. Cell pellets were then snap frozen on dry ice before being stored at -80°C until required for RNA extraction.

5.2.3.2 RNA extraction for Affymetrix® Array analysis

An RNeasy® Mini Kit (QIAGEN, Manchester, UK) was used to extract total RNA from cell samples. The cells were first disrupted (membranes lysed) using Buffer RLT and homogenised (reducing the viscosity of the lysate by shearing high-molecular weight genomic DNA and other high-molecular weight components) by passing the lysate through a QIAshredder. The lysate then was centrifuged at maximum speed (13000 rpm) in a benchtop centrifuge and the supernatant carefully removed by pipetting. 1 volume of 70% ethanol was then added to this supernatant and thoroughly mixed by pipetting, this creates conditions that promote selective binding of RNA to the RNeasy spin column. This mixture is then applied to the RNeasy spin column (up to 700 µL at a time) placed in a 2 mL collection tube. This is the centrifuged for 15 seconds at 8000 ×*g* and the flow-through is discarded.

At this point, an optional on-column DNAse I digestion was performed using the RNase-Free DNase set to remove any contaminating genomic DNA. In brief, this step required:

1) Adding 350 µL Buffer RW1 to the RNeasy spin column, centrifuging for 15 seconds at 8000 ×*g* and discarding the flow-through
2) Gently combining 10 µL of the DNase I stock solution with 70 µL Buffer RDD by inverting the tube and adding this solution mixture directly to the RNeasy spin column membrane
3) Incubate at room temperature for 15 minutes
4) Add another 350 µL Buffer RW1 to the RNeasy spin column and centrifuge for 15 seconds at 8000 *g*, discarding the flow through.

Following this, 500 µL of Buffer RPE was added to the RNeasy spin column and centrifuged for 15 seconds at 8000 *g*, again, discarding the flow through. Another 500 µL of Buffer RPE was then added and the column centrifuged for 2 minutes at 8000 *g*. At this point, the RNeasy spin column is placed in a new 2 mL collection tube, 50 µL of RNase-free water is added directly to the spin column membrane and column plus collection tube is centrifuged for 1 minute at 8000 ×*g* to elute the RNA.

5.2.3.3 NanoDrop™ RNA purity and concentration assessment

The purity and concentration of the extracted RNA samples were assessed using a NanoDrop™ 2000 Spectrophotometer (Thermo Scientific, Loughborough, UK). Prior to sample measurements, the NanoDrop™ was blanked using 1 µL RNase-free water. The arm was then wiped clean with lint-free microscope lens tissue and samples were added and analysed in turn, with the arm being cleaned in this way between each sample. All measurements were performed in triplicate. Purity is assessed using the ratio of absorbance at 260 nm and 280 nm ($A_{260/280}$) and at 260 nm and 230 nm ($A_{260/230}$), which can indicate carry over of contaminants from RNA extraction, such as guanidine salts. All RNA samples were free of contaminants so were taken forward for integrity assessment.

5.2.3.4 RNA integrity assessment

The integrity of each RNA sample was assessed using a 2100 Bioanalyzer (Agilent Technologies, Cheshire, UK). This work was carried out at the Sheffield Institute for Translational Neuroscience (SITraN) core facility at the University of Sheffield. In short, this is a microfluidic device that separates RNA samples according to their molecular weight and automatically inspects features associated with 18S and 28S ribosomal RNA peaks. An algorithm is used to generate an RNA Integrity Number (RIN) that is graded on a scale of 1 to 10, 1 being totally degraded and 10 being completely intact. All samples had an RIN of 10 so could be taken forward for analysis (an RIN of >7 is stipulated for Affymetrix® Array analysis).

5.2.3.5 Affymetrix® GeneChip® CHO Gene 2.0 ST Array analysis

Affymetrix® GeneChip® CHO Gene 2.0 ST Arrays were run at the Sheffield Institute for Translational Neuroscience (SITraN) core facility at the University of Sheffield following the standard Affymetrix® protocols. Briefly this comprises preparing cDNA from reverse transcribing the total extracted mRNA. This cDNA is then used in an *in vitro* transcription (IVT) reaction to generate biotinylated cRNA. After fragmentation of cRNA, it is then applied to the array and incubated with agitation for 16 hours to allow hybridisation of the fragments to complimentary DNA probes on the chip. The probes on the chip are designed to cover the entire genome (in this case the CHO genome). The chip is then washed to remove any un-hybridised fragments and then stained with PE-conjugated streptavidin (fluorescent stain solution) that binds to the biotin with high affinity. The chip is then scanned and the fluorescence at each location is measured to produce a reading of relative expression of the corresponding gene at that given location. Following this, the data was extracted and preliminary analysis was performed using the Affymetrix® software packages *Expression Console* and *Transcriptome Analysis Console*. The former software package was used to perform quality control measures and to extract raw fluorescence values for each transcript on the array, while the latter was used to perform differential gene expression analysis between the evolved cell line and the parental. Sets of differentially expressed genes were extracted using significance thresholds of both $p \leq 0.05$ and $p \leq 0.01$ (FDR [False Discover Rate] corrected ANOVA), fold change thresholds could also be applied if required for certain data sets. Further data analysis and manipulation was performed using Microsoft Excel.

5.2.3.6 Functional classification of differentially expressed transcripts

Significantly differentially expressed transcripts ($p < 0.01$ FDR corrected ANOVA) with a fold change of ≥2 were classified into one of 14 categories, each representing a biological function. These were based on Reactome pathway categories (accessible at http://reactome.org) and modified where necessary (for

example, certain categories, such as Reproduction, would not be of relevance for this analysis). The number of differentially expressed transcripts that were assigned to each category was recorded according to whether that gene was increased in the evolved cell line or increased in the parental cell line. Table 5.1 shows the functional classification categories used.

Table 5.1 Functional groups used in the classification of differentially expressed transcripts.

Functional classification
Apoptosis/ cell killing
Cell cycle
Cell-cell communication
Cellular responses to stress
Chromatin organisation
DNA repair
DNA replication
ECM organisation/ cytoskeletal
Gene expression
Membrane trafficking
Metabolism
Organelle biogenesis + maintenance
Signal transduction/ signalling
Other/ miscellaneous

5.2.3.7 KEGG pathway analysis

In order to perform KEGG pathway analysis on the differentially expressed genes, *Mus musculus* UniProt IDs were assigned to the transcripts. Due to the incomplete annotation of the *Cricetulus griseus* genome it was not used for this analysis. UniProt IDs were then linked with a colour that represented the direction of differential gene expression, i.e. increased in the evolved cell line or increased in the parental cell line: a UniProt ID with an increased expression in the evolved cell line was assigned blue, and a UniProt ID with increased expression in the parental cell line was assigned red. This list of colour-associated UniProt IDs was then mapped onto pathways using the KEGG 'Search&Color' function.

5.2.4 Amino acid analysis of parental and evolved cell lines in fed-batch culture

Samples of spent culture media were taken from 3 replicates cultures of both the evolved and parental cell lines. Samples were taken on day 0, then every 3 days pre- and post- feeding with 10% culture volume EfficientFeedB™ (Life Technologies, Paisley, UK). Samples were then sent to Abingdon Health (Birmingham, UK) for concentration quantification. Briefly the analysis at Abingdon Health comprised of vortexing the sample thoroughly and 100 µL diluted to a total volume of 1 mL with TCA and centrifuged to precipitate out the proteins, then 25 µL was injected into the ion exchange chromatography analyser (with ninhydrin detection). Amino acid concentrations were then normalised to cell number and comparisons between cell lines through culture were made. N.B. Direct correspondence with Abingdon Health has given the following comment on method accuracy: "the techniques we use result in a highly reproducible analysis, therefore the differences observed are likely to be due to the sample type rather than the method of analysis used".

5.3 Results

5.3.1 Oxidative stress in the hypothermia adapted cell line versus the parental

Using flow cytometry and CellROX® Oxidative Stress Deep Red Reagent, the amount of reactive oxygen species in each cell could be inferred using the fluorescence intensity. The autofluorescence (unstained sample) of each cell line was first measured and was found to be comparable to each other, as expected (see figures 5.1 A and B). The flow cytometry data in figures 5.1 C and D also again shows a clear difference in cellular sizes between the parental and evolved cell lines: the Forward Scatter parameter along the x-axis (FSC-A) is a measurement of the amount of the laser beam that passes around the cell, giving a relative indication of cell size. In the same figures the Y-axis is the Side Scatter parameter (SSC-A), which is a measurement of the amount of light that bounces off

particulates inside the cell. This measurement can be used to infer viability information on the samples: the small clusters the bottom left of the R1 gates in figures 5.1 C and D represent the dead cells in the population. As can be seen from the small size of this cluster, very few cells die as a result of the treatment with CellROX® Oxidative Stress Deep Red Reagent (N.B figures shown are exemplary of one three repeats).

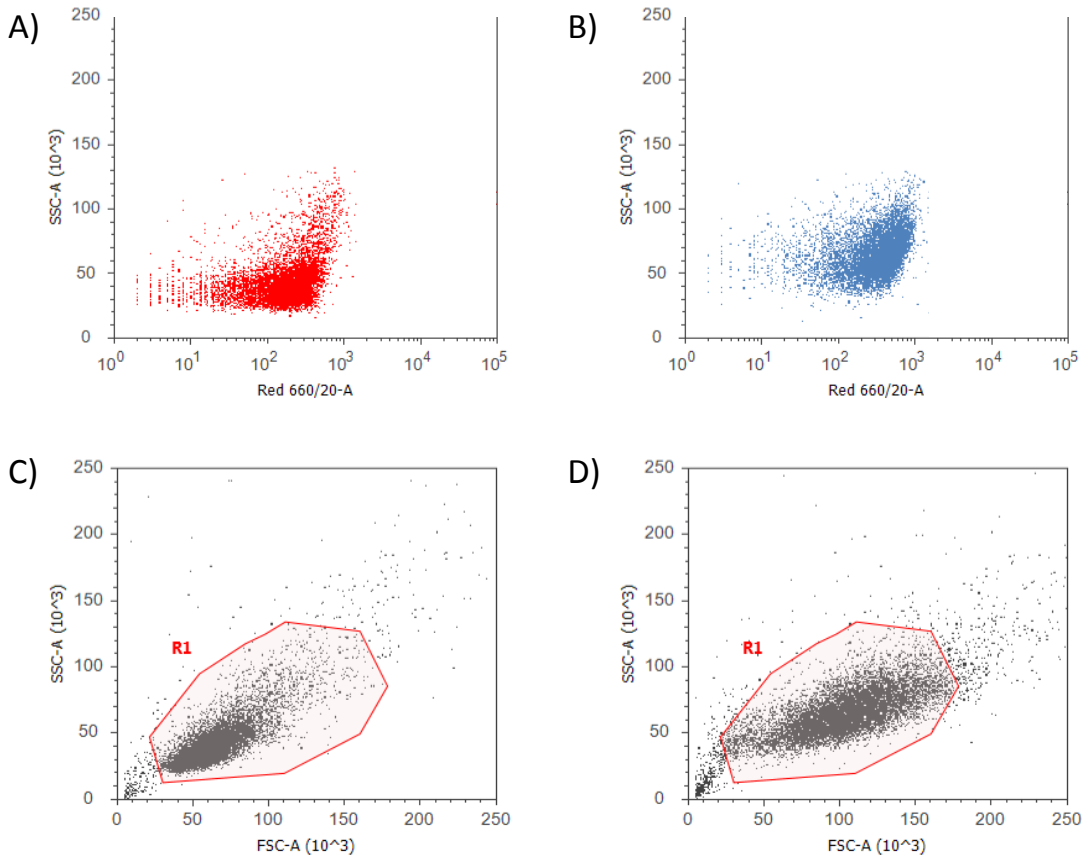

Figure 5.1 Autofluorescence of unstained samples for A) parental cells and B) evolved cells, and Forward Scatter (FSC-A) and Side Scatter (SSC-A) information for C) CellROX® Oxidative Stress Deep Red Reagent treated parental cells and D) CellROX® Oxidative Stress Deep Red Reagent treated evolved cells. As can be seen from figures 5.1 A and 5.1 B, the two cell lines have similar autofluorescence, as expected. Figures 5.1 C and 5.1 D show that there is little cell death in both cell lines from treatment with CellROX® Oxidative Stress Deep Red Reagent (small sub-populations with low SSC-A to the LHS of the R1 gates). Cells from the parental cell line are smaller than those from the evolved cell line, as can be seen from the population of cells in figure 5.1 C (parental) having smaller FSC-A than those in figure 5.1 D (evolved).

When stained samples were measured for fluorescence, a clear difference was seen between the two cell lines, with the parental cell line fluorescing more intensely than the evolved cell line. There was a larger shift in median fluorescence (median fluorescence of stained samples minus the median autofluorescence) for the parental cell line than the evolved cell line (see figures 5.2 A and B), meaning that individual cells belonging to the former contain more reactive oxygen species than the latter. This data is numerically summarised for three experimental repeats in table 5.2. As is shown, the parental cell line consistently shows a larger shift in fluorescence between unstained and stained samples compared to the evolved cell line.

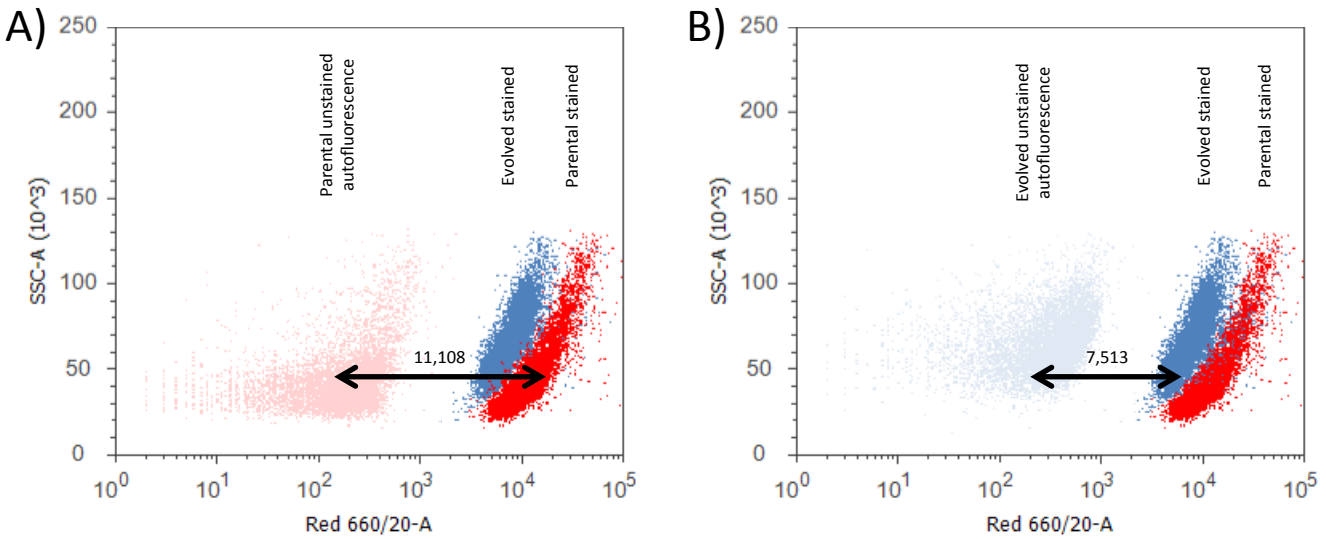

Figure 5.2 Fluorescence of parental and evolved cell lines stained with CellROX® Oxidative Stress Deep Red Reagent. Cell populations in red represent those from the parental cell line and cell populations in blue represent those from the evolved cell line. A) shows a large shift in fluorescence (11108 shift in RFU along the x-axis) from the autofluorescence of parental cells to the fluorescence of stained parental cells, where as B) shows a smaller shift in fluorescence (7513 RFU along the x-axis) from the autofluorescence of evolved cells to the fluorescence of stained evolved cells. Together, A) and B) show that there is more reactive oxygen species present in cells from the parental cell line.

Table 5.2 Numerical summary of CellROX® Oxidative Stress Deep Red Reagent flow cytometry fluorescence data. Data is shown for three experimental repeats. All data are in RFU (relative fluorescence units).

Experiment repeat no:	1		2		3	
	Cell line		Cell line		Cell line	
	Parental	Evolved	Parental	Evolved	Parental	Evolved
Median autofluorescence (unstained)	151	295	120	250	170	321
Median fluorescence (stained)	11259	7808	10885	7009	11456	7463
Fluorescence shift (stained - unstained)	11108	7513	10765	6759	11286	7142

5.3.2 Mitochondrial bioenergetics in the hypothermia adapted (evolved) cell line versus the parental

Using the Seahorse XF24 system, mitochondrial respiration was analysed in both the parental and evolved cell lines. The Seahorse XF24 system quantifies respiration by measurements of oxygen consumption rate (OCR). At the beginning of analysis cells were maintained in un-buffered XF Media, allowing basal oxygen consumption rates to be measured. As described in methods for this chapter (section 5.2.2.1), cells are then sequentially exposed to three mitochondrial inhibitors/ chemical effectors, these being: 1) Oligomycin (final concentration 1.5 μM) which inhibits ATP synthesis by blocking the proton channel of the F_o portion of ATP synthase (Complex V). This inhibitor is used to distinguish the proportion of oxygen consumption dedicated to ATP synthesis and also the proportion of oxygen consumption required to overcome the natural proton leak across the inner mitochondrial membrane (IMM); 2) FCCP (final concentration 0.75 μM) which disrupts ATP synthesis by transporting hydrogen ions across the IMM (instead of them going through the proton channel of ATP synthase (Complex V)). This collapse of mitochondrial membrane potential leads to a rapid consumption of energy and oxygen, with no generation of ATP. This step reveals the maximal respiratory capacity of the cell and also the spare respiratory capacity (defined as the quantitative difference between the initial basal OCR and the maximal uncontrolled OCR); 3) Antimycin A and Rotenone (final concentration 1 μM) are Complex III and Complex I inhibitors, respectively. Together they shut down mitochondrial respiration and allow the non-mitochondrial fraction contributing to respiration to be calculated. See figure 5.3 for a schematic representation of this information (XF24 User Manual 2013).

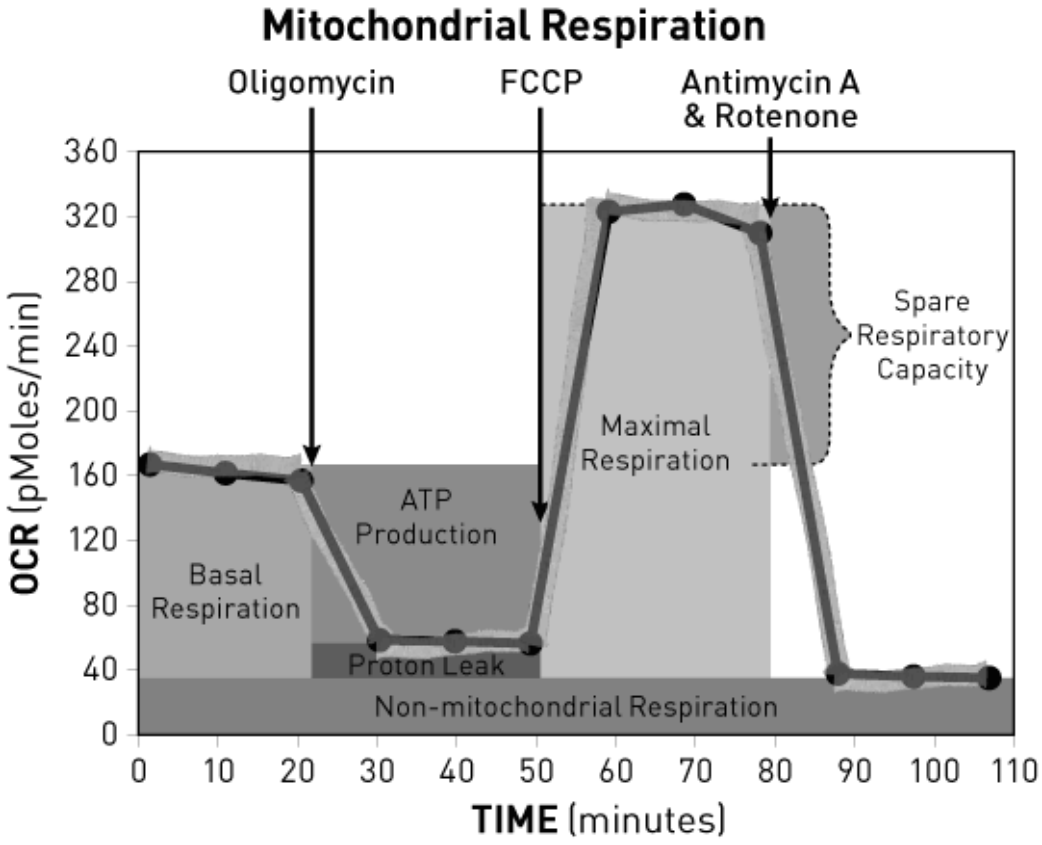

Figure 5.3 Insights into cellular mitochondrial respiration, including oxygen consumption rate from: basal respiration; ATP Production; overcoming proton leak; maximal respiration; spare respiratory capacity and also non-mitochondrial respiration, can be revealed using a sequential combination of Oligomycin, FCCP and Antimycin A & Rotenone.

To most accurately gain insights into mitochondrial metabolism using this analysis, the concentrations of Oligomycin, FCCP and Antimycin A/Rotenone stated above were first optimised to ensure complete inhibition of the target and also keep potential toxic effects to minimum. At the time of this investigation, no studies using the XF24 had been published in concert with CHO cells, so a range of concentrations were used that extended below and beyond the concentrations that other users of the XF24 had used in house, these were: 0.25 µM, 0.5 µM, 0.75 µM, 1.0 µM, 1.25 µM and 1.5 µM. Figure 5.4 shows the optimisation titrations for Oliomycin, FCCP and Antimycin A & Rotenone.

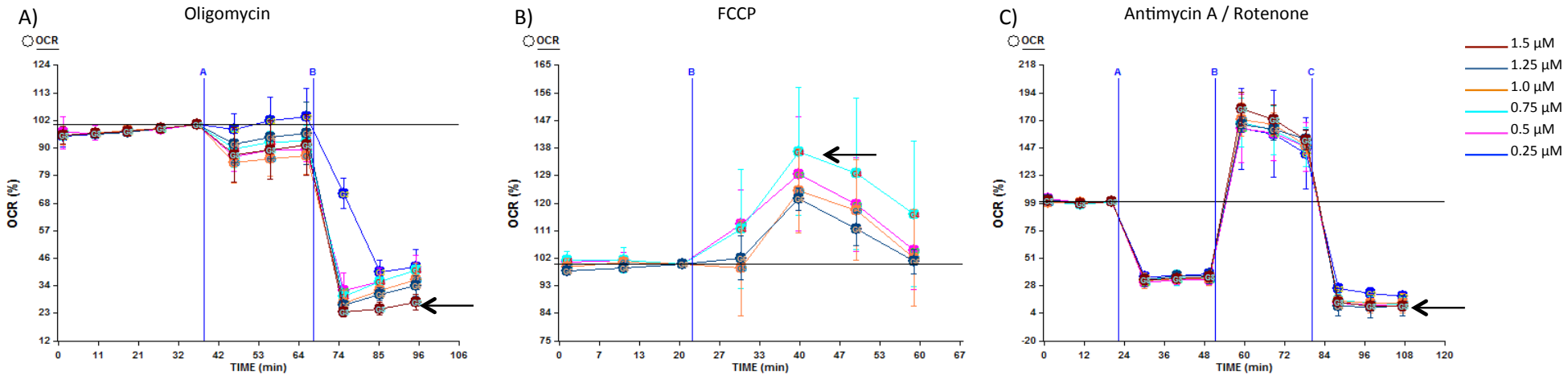

Figure 5.4 Optimisation titrations of A) Oligomycin, B) FCCP and C) Antimycin A & Rotenone for use in the XF24 Mitochondrial respiration assay system. The chemicals used in this assay had to first be titrated to optimise the concentration used in terms of keeping toxicity to a minimum and ensuring the chemical is completely inhibiting/ effecting its target. The lowest concentration of each inhibitor that supported the largest effects on oxygen consumption rate (OCR) was selected as the optimal concentration for analysis (provided this was validated in both the parental cell line and the evolved cell line at both 37°C and 32°C – data not shown). As can be seen here (indicated by black arrows), the optimal concentrations for Oligomycin, FCCP and Antimycin A & Rotenone were 1.5 µM, 0.75 µM and 1 µM, respectively.

Once the concentrations of Oligomycin, FCCP and Antimycin A & Rotenone had been optimised, the XF24 system was run in triplicate, each time using an XF24 Tissue Culture Plate containing both cells from the parental cell line and the evolved cell line, using fresh cells for each run. The assay was performed at 37°C and then 32°C to determine any differences due to machine operating temperature. It was established that machine operating temperature and sample preparation temperature on the day of assay did not affect oxygen consumption rates (appendix III), therefore data from all runs were consolidated. During the analysis, built-in software allows plate wells to be grouped according to statistical similarity to each other. Using this utility, it was determined that cells from the parental cell line and the evolved cell line exhibit distinct mitochondrial function, i.e. each of the parameters that can be inferred from this assay (basal respiration, maximal respiration, etc.) were found to be distinct between cell lines. This is represented in figure 5.5.

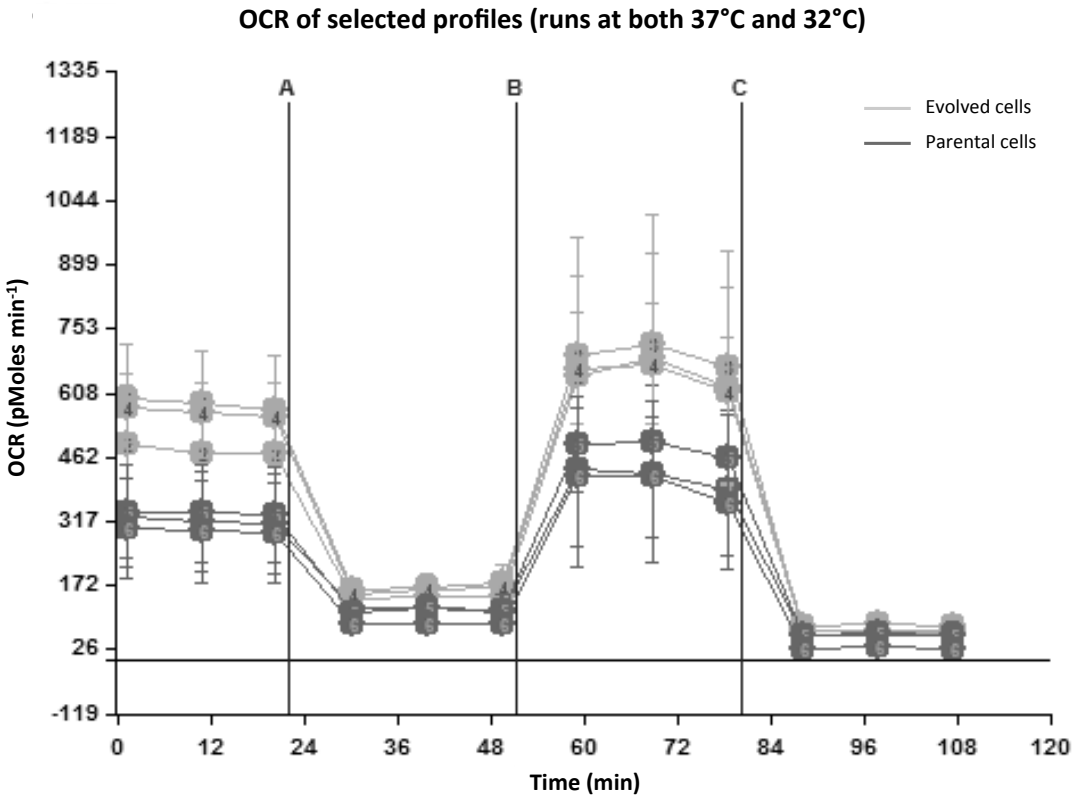

Figure 5.5 The OCR of parental and evolved cell lines over the time course of a complete XF24 mitochondrial assay. Time indicators A, B and C represent the point at which Oligomycin, FCCP and Antimycin A & Rotenone, respectively, were added to the wells. The profiles are from different runs of the assay in which the machine was operated at either 37°C and then 32°C for control purposes. Using the built in analysis software, it was determined that operating temperature did not effect OCR. Wells containing cells from either the parental or evolved cell lines were automatically grouped together by the software based on OCR similarity (denoted by matching colours). Dark grey markers represent OCR from wells that contained parental cells and light grey markers represent OCR from wells that contained evolved cells. Evolved cells show elevated OCR throughout the assay compared to parental cell.

For clarity purposes, these parameters are shown individually in figure 5.6. As can be seen, based on the oxygen consumption rate (OCR) measurements, the parental cell line has a lower basal metabolic rate and lower maximal respiration, than the evolved cell line. It can also be seen that for parental cells, less OCR is associated with ATP production than evolved cells and also less OCR is associated with proton leak than evolved cells. In addition to this, non-mitochondrial respiration was

observed to be lower in the parental cells than the evolved cells. However, the spare respiratory capacity (the difference between basal and maximal respiration) was not found to differ between parental and evolved cells.

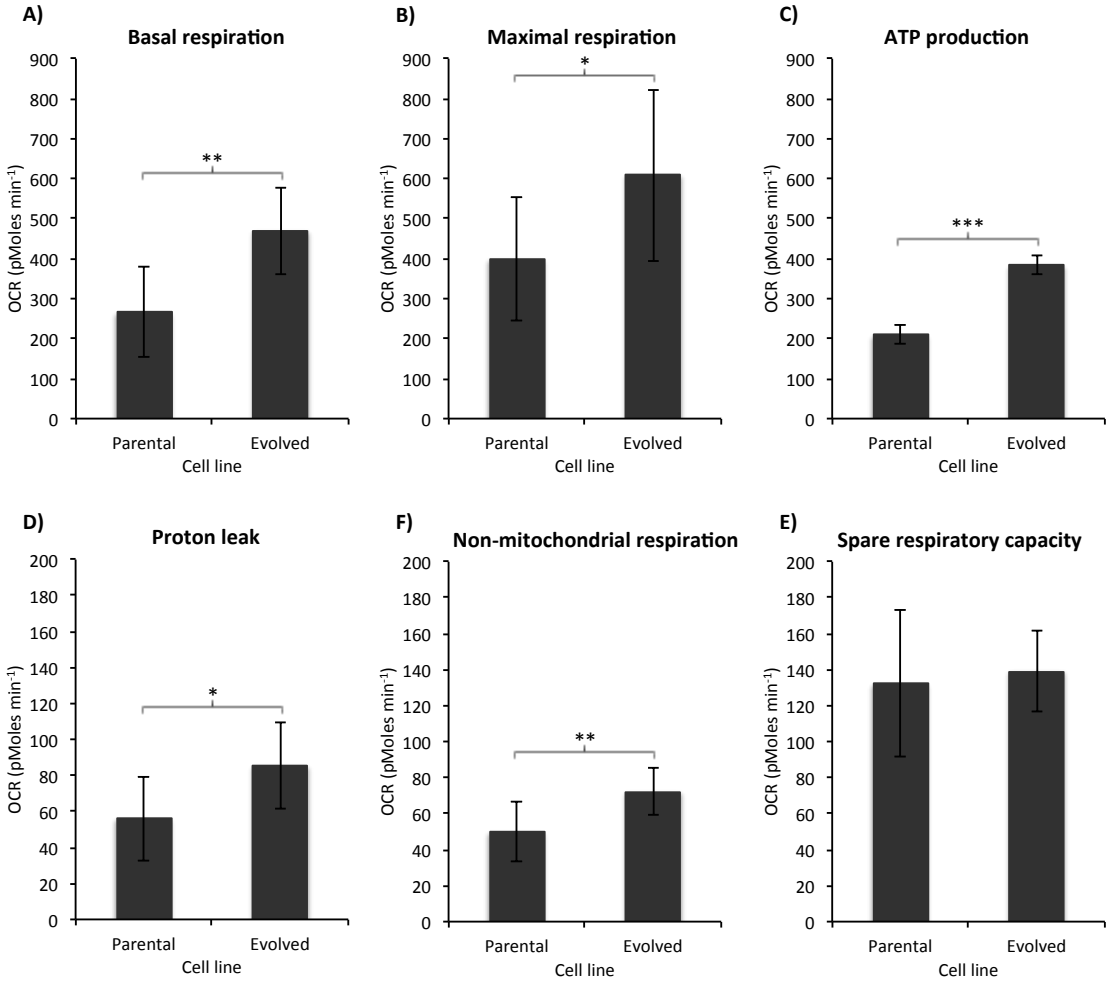

Figure 5.6 Individual parameters (basal respiration (A), maximal respiration (B), ATP production (C), proton leak (D), non-mitochondrial respiration (F) and spare-respiratory capacity (E)) that can be inferred from measurements of oxygen consumption rates (OCR) from the Seahorse XF24 mitochondrial assay. OCR is shown for cells from both the parental and evolved cell lines. The evolved cells exhibited significantly higher OCR for all parameters, except for spare respiratory capacity (E). Error bars, SD; N = 9; *, $p \leq 0.05$; **, $p \leq 0.01$; ***, $p \leq 0.001$ (Student's t-test).

Cells from the evolved cell line have increased their average basal respiration by 76%, maximal respiration by 53%, ATP production by 83%, proton leak by 53% and non-mitochondrial respiration by 45%, compared to cells from the parental cell line. There was only a 5% increase in spare respiratory capacity in the evolved cells compared to the parental. This is because despite the elevated maximal respiration in the evolved cells, they also show elevated basal respiratory rates and the difference between these two (which calculates the spare respiratory capacity) is very similar between both cell lines. However, this also means that the basal respiration in evolved cell lines works proportionately closer to their maximal levels than basal respiration in parental cells: the evolved cells basal respiration OCR is 77% of their OCR at maximal respiration, whereas the parental cells basal respiration OCR is 66% of their OCR at maximal respiration.

5.3.3 Affymetrix® GeneChip® CHO Gene 2.0 ST Array

5.3.3.1 NanoDrop™ RNA purity and concentration

Samples were collected on day 3 of culture, RNA was extracted and its purity and concentration assessed on a NanoDrop™ 2000 Spectrophotometer. Concentrations and purity indicators ($A_{260/280}$ and $A_{260/230}$ ratios) are shown in table 5.3. All samples were free from contaminants [indicated by values of ~2.0 for $A_{260/280}$ ratios and ~2.0-2.2 for $A_{260/230}$ ratios, which historically represent "pure" RNA (NanoDrop™ T042-Technical Bulletin)], so could then be assessed for integrity.

Table 5.3 Summary of Nanodrop™ data, including RNA concentration and $A_{260/280}$ and $A_{260/230}$ ratios, for the samples used in Affymetrix® GeneChip® array.

	Parental cell line			Evolved cell line		
Sample no:	1	2	3	1	2	3
Avg. conc. (ng/µl) from 5x10^6 cells	425.23	457.67	470.00	878.80	779.63	789.63
260/280 ratio	2.05	2.05	2.06	2.09	2.12	2.07
260/230 ratio	2.24	2.11	2.00	2.28	2.09	2.27

5.3.3.2 RNA integrity

The integrity of each RNA sample was assessed using an Agilent 2100 Bioanalyzer. This Bioanylzer separates RNA samples based on size and measurements are made based on fluorescence induced by a laser. Electropherograms are produced which showing peaks representing RNA species of different weights, as exemplified in figure 5.7. Good quality RNA will produce an electropherogram with two distinct peaks representing 18S and 28S ribosomal RNA, lots of other small peaks (smaller than the 18S and 28S) would indicated RNA of poor integrity. RNA Integrity Numbers (RIN) are produced by the software using an algorithm, each sample is graded on a scale of 1 (completely degraded) to 10 (completely intact). The rRNA ratio [28S/18S] can be used to check quality again – a ratio of ~2.0 represents good quality RNA. A summary of both RIN and rRNA ratios [28S/18S] for each sample is presented in table 5.4. As the integrity of all samples was graded as fully intact (RIN 10) it was deemed high enough quality to be taken forward for use in the Affymetrix® GeneChip® CHO Gene 2.0 ST Arrays.

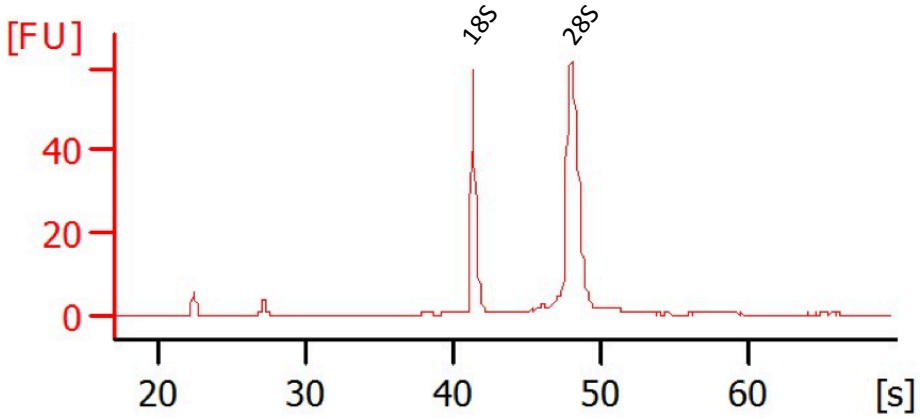

Figure 5.7 Example of an electropherogram produced by the Agilent 2100 Bioanalyzer. This particular electropherogram had an RIN of 10 and an rRNA ratio [28S/18S] of 2.2.

Table 5.4 Summary of Agilent 2100 Bioanalyzer data including RNA Integrity Numbers (RIN) and rRNA ratios [28S/18S], for the samples used in Affymetrix® GeneChip® array.

	Parental cell line			Evolved cell line		
Sample no:	1	2	3	1	2	3
RIN	10.00	10.00	10.00	10.00	10.00	10.00
rRNA ratio [28S/18S]	2.2	2.2	2.2	2.1	2.1	2.0

5.3.3.3 Affymetrix® GeneChip® Array – primary analysis

This section covers the overall outputs generated using the Affymetrix® *Transcriptome Analysis Console* (TAC) software, which was used to perform differential transcript expression analysis between samples from the evolved cell line and the parental cell line.

The Affymetrix® GeneChip® CHO Gene 2.0 ST Array measured the expression of 29,890 transcripts. Using the TAC software, the number of differentially expressed transcripts according to statistical significance and fold change threshold could be identified. For the majority of the analysis performed on the Affymetrix® data, a strong significance threshold ($p \leq 0.01$, FDR corrected ANOVA) was applied when extracting the list of differentially expressed transcripts that resulted in 2069 transcripts, of which 974 were up-regulated in the evolved cell line (*which can also be viewed as down in parental cell line*) and 1095 were up-regulated in the parental cell line (*which can also be viewed as down in evolved cell line*). This data is graphically represented as a volcano plot in figure 5.8 and also fully tabulated in appendix III. There is clear disparity in the pattern of differential transcript expression (i.e. the plot is not symmetrical) when comparing those that are up-regulated in the evolved cell line (blue markers, spreading more and further across the x-axis) compared to the parental cell line (red markers, more concentrated around lower values on the x-axis).

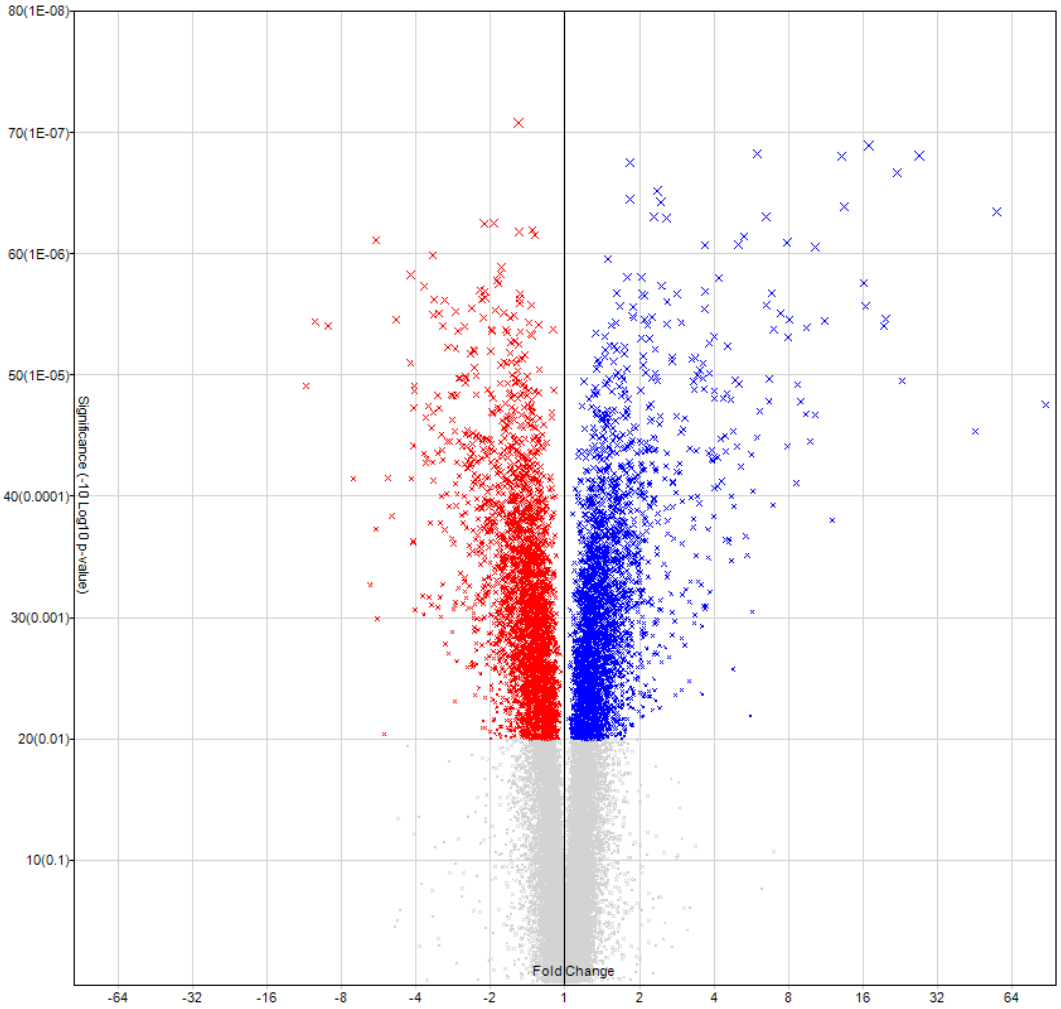

Figure 5.8 Volcano plot representing significantly differentially expressed transcripts (p ≤ 0.01, FDR corrected ANOVA). Differentially expressed transcripts below this significance threshold are shown in grey. Blue markers represent differentially expressed transcripts up-regulated in the evolved cell line and red markers represent differentially expressed transcripts up-regulated in the parental cell line. Size of markers (as well as position along the y-axis) indicates level of significance (p value), with larger markers (higher on the y-axis) representing smaller p values. Distance from the centre line on the x-axis denotes size of fold change (-ve fold changes represent those up-regulated in the parental cell line, whereas +ve fold changes represent those up-regulated in the evolved cell line).

When a fold change threshold of ≥ 2 is applied to the dataset, these numbers are reduced to 223 up-regulated in the evolved cell line and 204 up-regulated in the parental cell line, giving a total of 427 differentially expressed transcripts compared to 2069 when no fold change threshold is applied. The distribution of these fold changes according to whether they are up in the evolved cell line or the parental cell line can be seen in figure 5.9 in which all differentially expressed transcripts with a fold change of ≥ 2 are ranked consistent with size of fold change. As can be seen, the majority of transcripts with large fold changes are those that have been up-regulated in the evolved cell line. In addition to this, the largest fold change seen as up-regulated in the parental cell line is only 11.12, compared with an 87.98 fold change up-regulated in the evolved cell line.

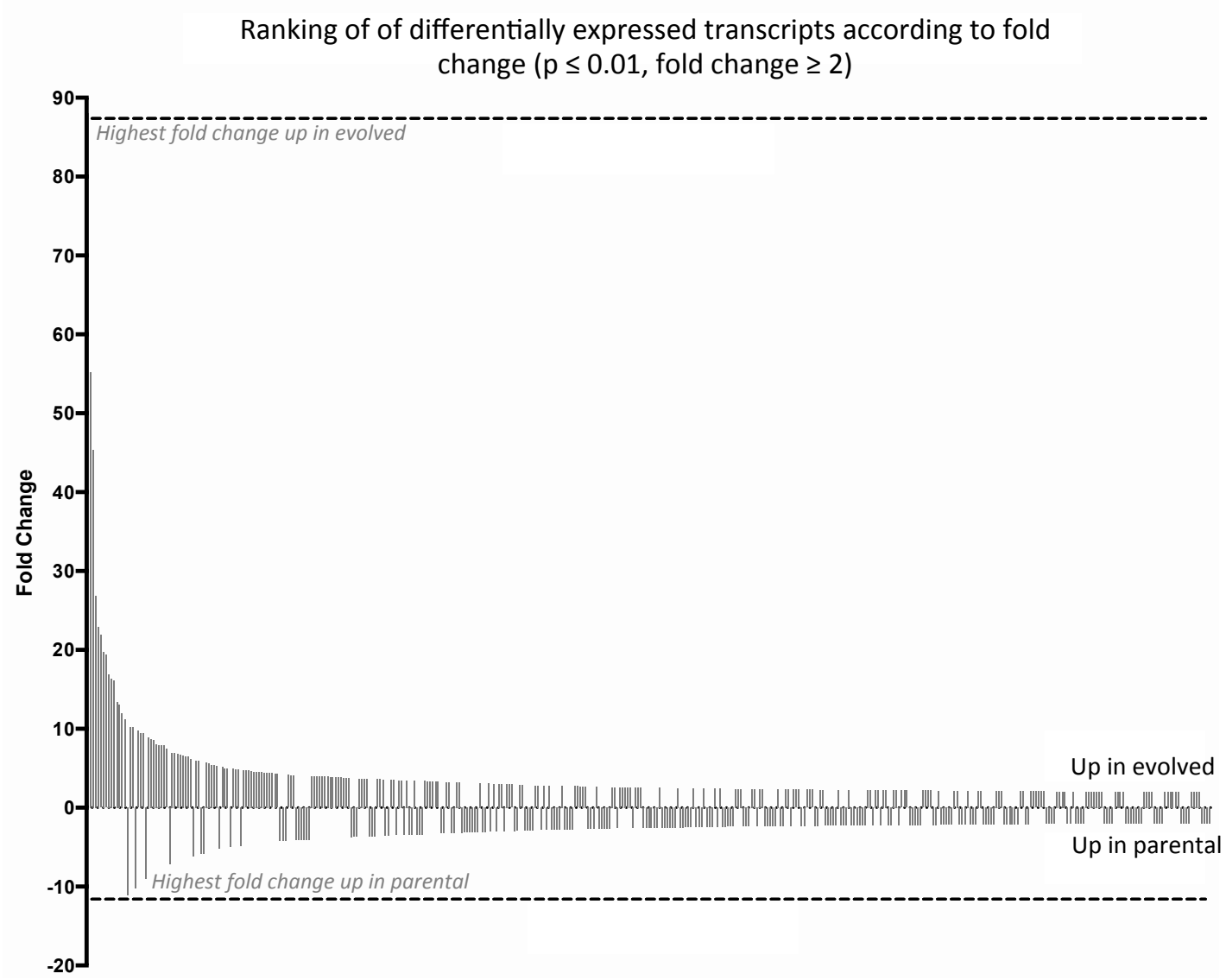

Figure 5.9 The ranked distribution of fold changes according to whether they are up-regulated in the evolved cell line (+ve fold change) or the parental cell line (-ve fold change). Transcripts that are differentially expressed with very large fold changes (i.e. ranked closer to the y-axis) tend to be those that are up-regulated in the evolved cell line. There is a marked difference between the size of the largest fold change up in the evolved cell line versus the size of the largest fold change up in the parental cell line.

For comparative purposes, the fluorescence values of all transcripts were compared between the evolved and parental cell lines. This data is shown in figure 5.10 in which normalised transcript fluorescence values were ranked for both evolved and parental cell lines and the data superimposed for comparison. As can be seen, very similar patterns in the range and distribution of relative expression levels (i.e. relative fluorescence) exist between both cell lines.

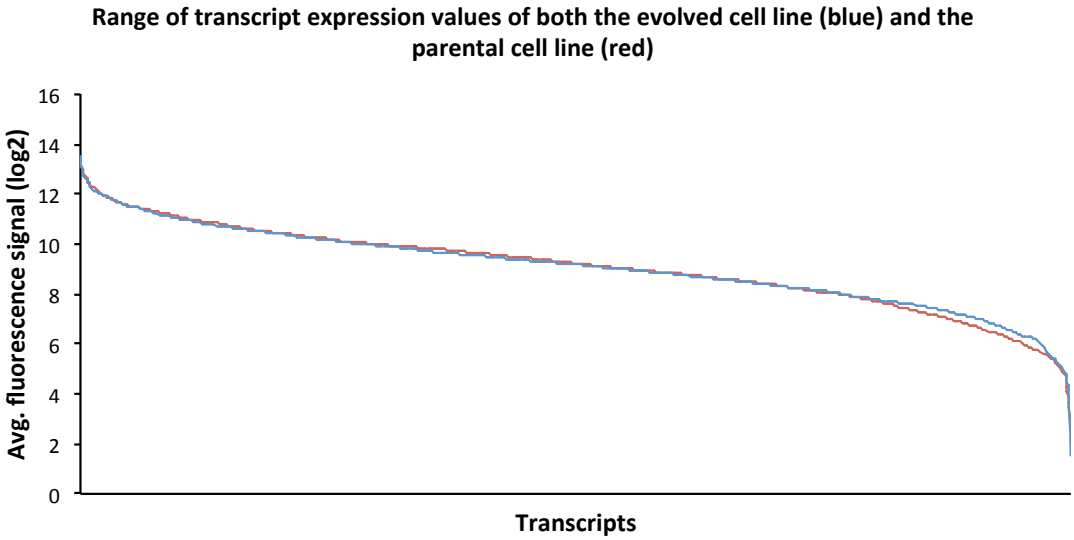

Figure 5.10 Transcript expression (Avg. fluorescence) ranges for both parental and evolved cell lines. Fluorescence values of all transcripts were ranked for both cell lines and superimposed for comparison. There is very little disparity in the distribution range between the cell lines.

5.3.3.4 Functional classification of differentially expressed transcripts

All significantly differentially expressed transcripts ($p \leq 0.01$, FDR corrected ANOVA) with a fold change of ≥ 2 were classified into 14 functional categories. The 'other/ miscellaneous' category included transcripts with unknown function or useful no chip annotation. As can be seen in figure 5.11, the categories with highest representation by differentially expressed transcripts are signal transduction/signalling and metabolism, followed by gene expression, cell cycle

and membrane trafficking. As already mentioned, when considering differentially expressed transcripts over a fold change of 2, there are 223 up-regulated in the evolved cell line and 204 up-regulated in the parental cell line (approximately equally distributed). It can also be seen in figure 5.11 that the distribution of fold changes in each category, either up-regulated in evolved or up-regulated in parental, is approximately equal, meaning that there are not particular functional categories that are being overexpressed in either cell line, more just an exchange in what is being expressed. The absence of any category containing no changes implies that there are wide, global changes between the parental cell line and the evolved cell line.

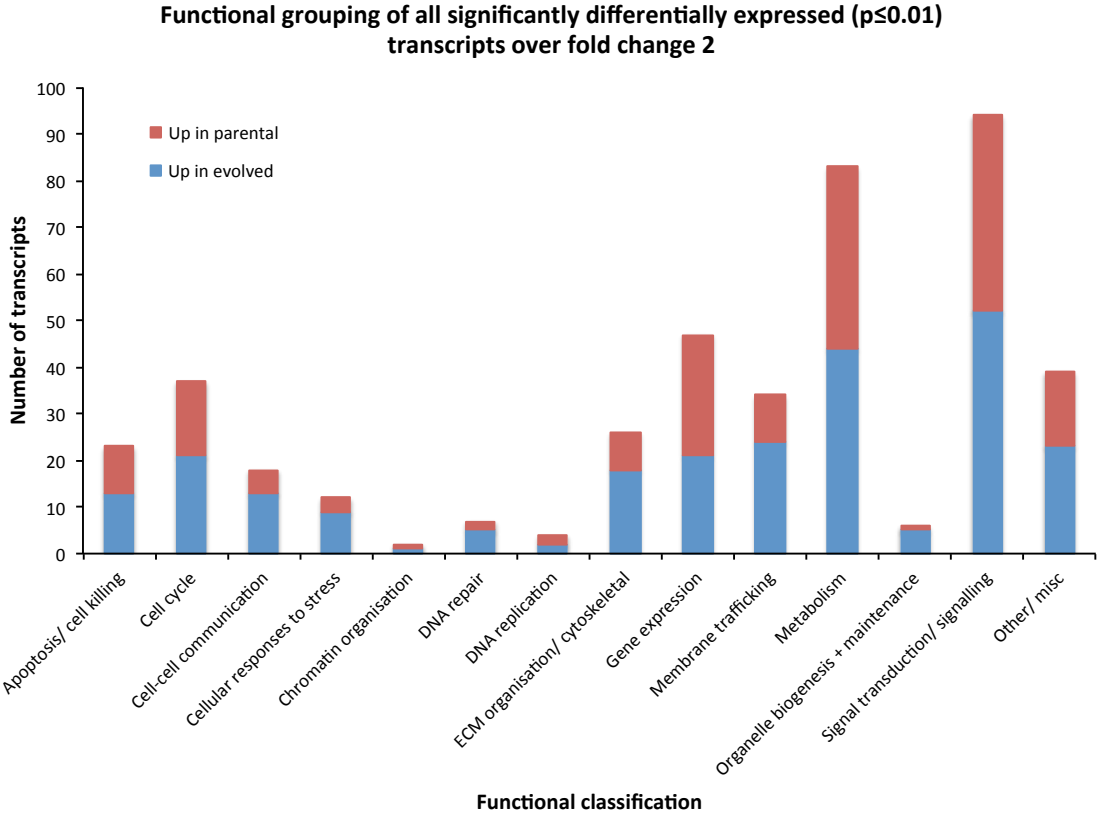

Figure 5.11 Functional grouping of significantly differentially expressed transcripts with a fold change of ≥ 2. Differentially expressed transcripts were classified into 14 functional categories. Highly represented categories include signal transduction/ signalling, metabolism, gene expression, cell cycle and membrane trafficking.

5.3.3.5 Expression conservation analysis between parental and evolved cell lines

This section of results presents expression conservation analysis between parental and evolved cell lines. In other words, it will focus on how different particular sets of related transcripts have become in terms of their expression during the process of adaptation to hypothermic conditions, or, how similar they have remained (i.e. been conserved). The sets of transcripts compared here were formed according to biological processes of interest to biopharmaceutical production (for example, transcripts associated with glycosylation), or according to hypothesis-lead notions (for example, transcripts related to oxidative stress and mitochondria due to their role in adaptive thermogenesis). The transcript expression conservation of such processes and concepts are reviewed further in the discussion section of this chapter. Here, the correlations of these sets of transcripts are presented, from which the degree of transcript conservation can be inferred (figures 5.12 to 5.21). In figures 5.12 to 5.21, the further each data point (representing one transcript) lies from the line y=x, the larger the fold change seen in that transcripts between the two cell lines. Data points below the line y=x represent transcripts that are up-regulated in the parental cell line, and data points above the line y=x represent transcripts that are up-regulated in the evolved cell line. Transcripts with a fold change of ≥ 2 are annotated within these figures and for clarity purposes are also listed in table 5.5.

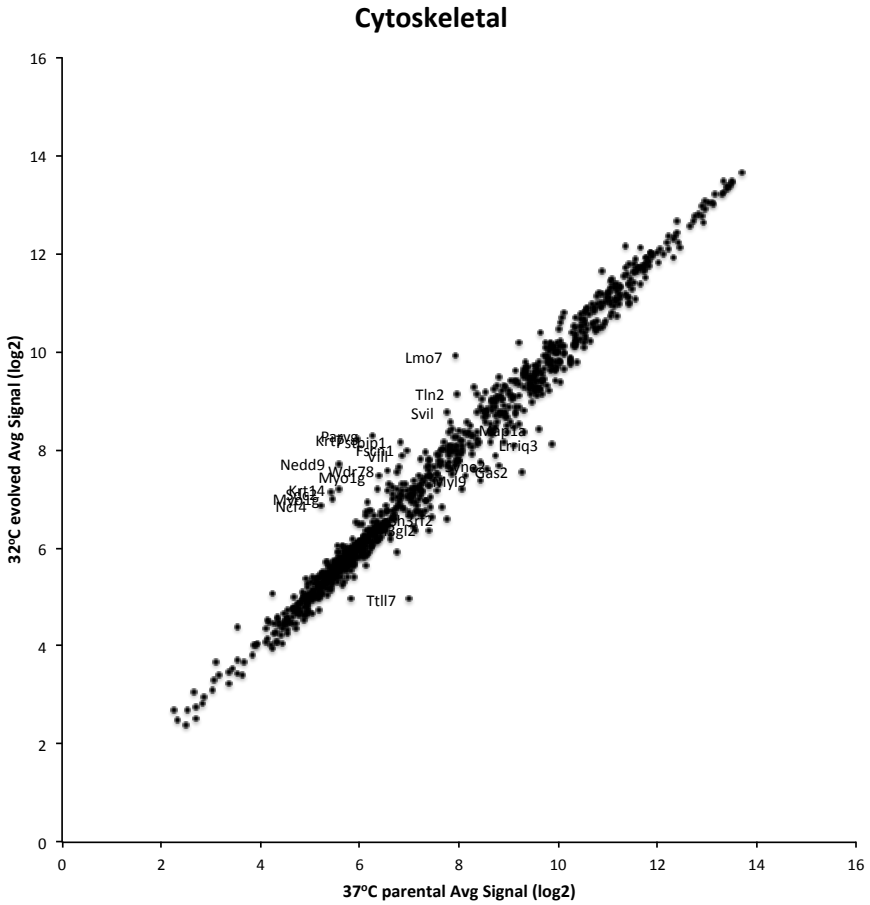

Figure 5.12 Expression of cytoskeletal–associated transcripts in the evolved cell line versus the parental cell line. Transcripts with a fold change of ≥ 2 are annotated with the gene alias.

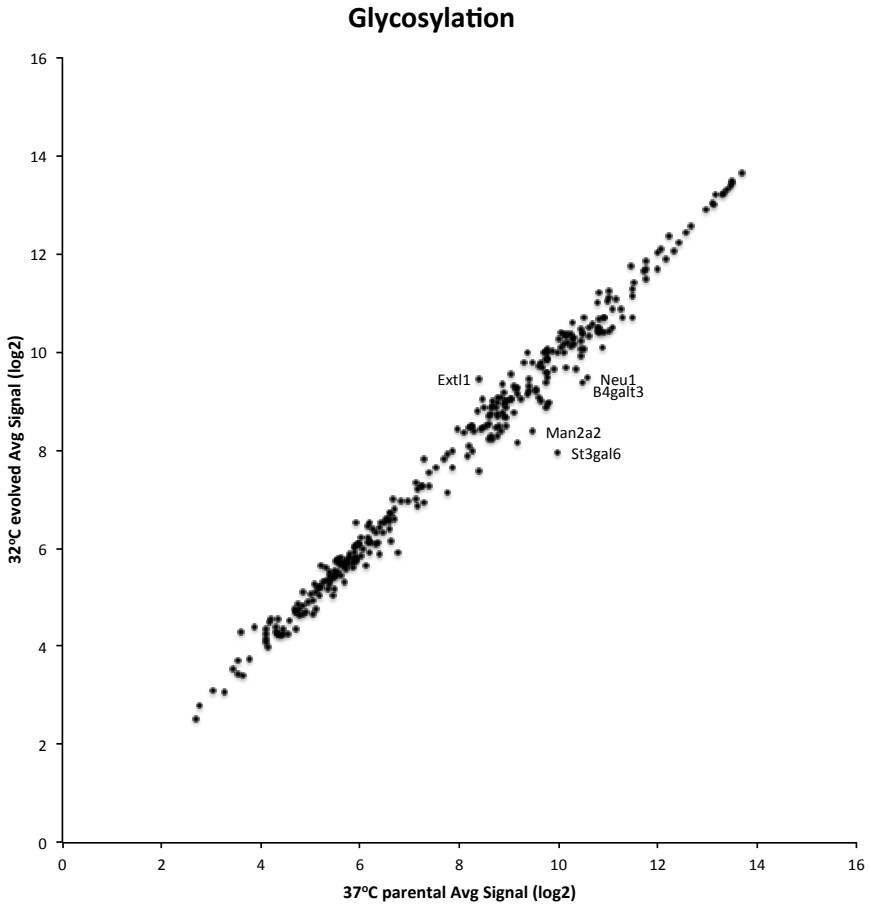

Figure 5.13 Expression of glycosylation–associated transcripts in the evolved cell line versus the parental cell line. Transcripts with a fold change of ≥ 2 are annotated with the gene alias.

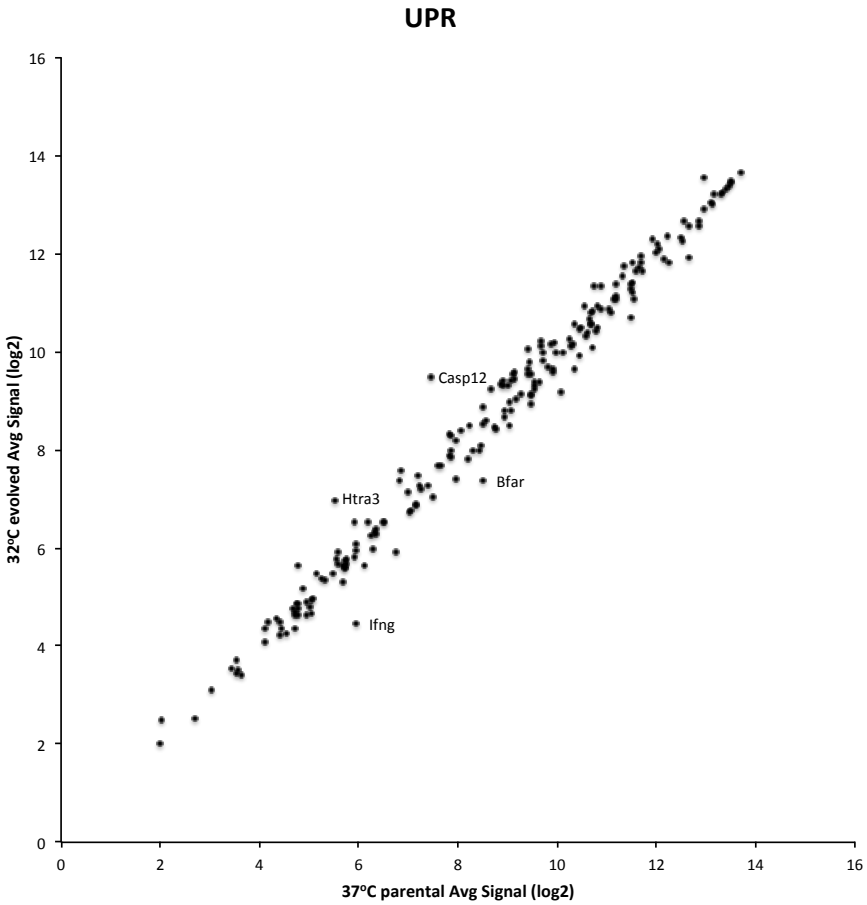

Figure 5.14 Expression of unfolded protein response (UPR)–associated transcripts in the evolved cell line versus the parental cell line. Transcripts with a fold change of ≥ 2 are annotated with the gene alias.

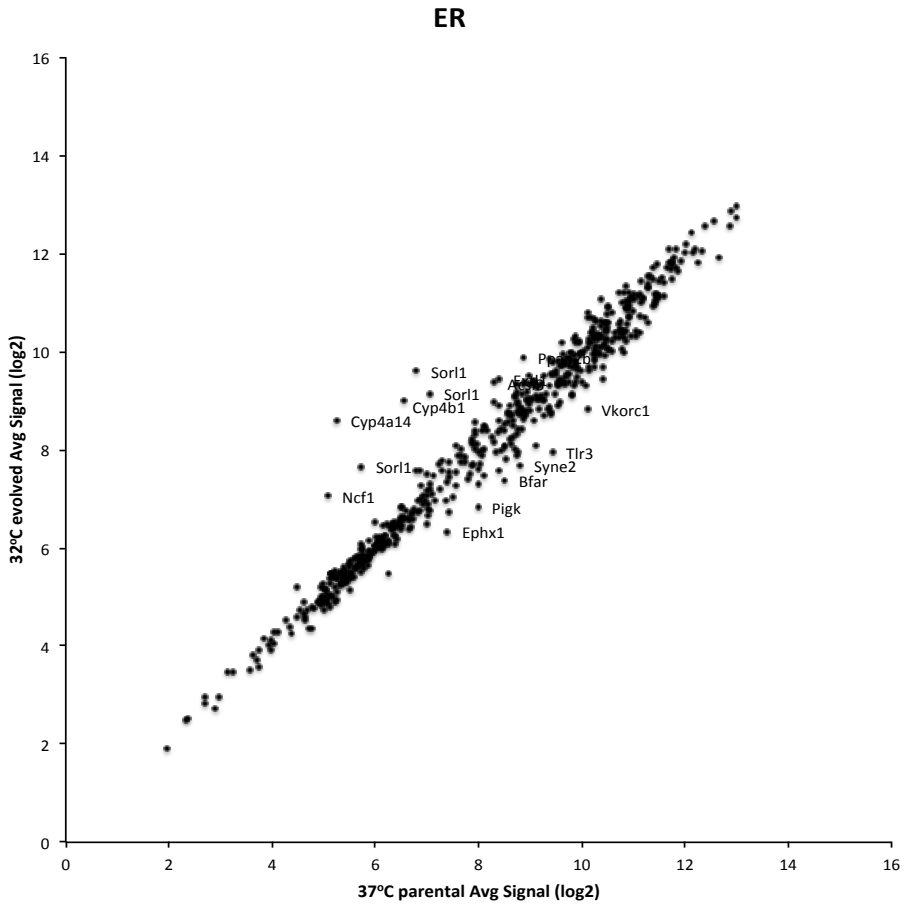

Figure 5.15 Expression of endoplasmic reticulum (ER)–associated transcripts in the evolved cell line versus the parental cell line. Transcripts with a fold change of ≥ 2 are annotated with the gene alias.

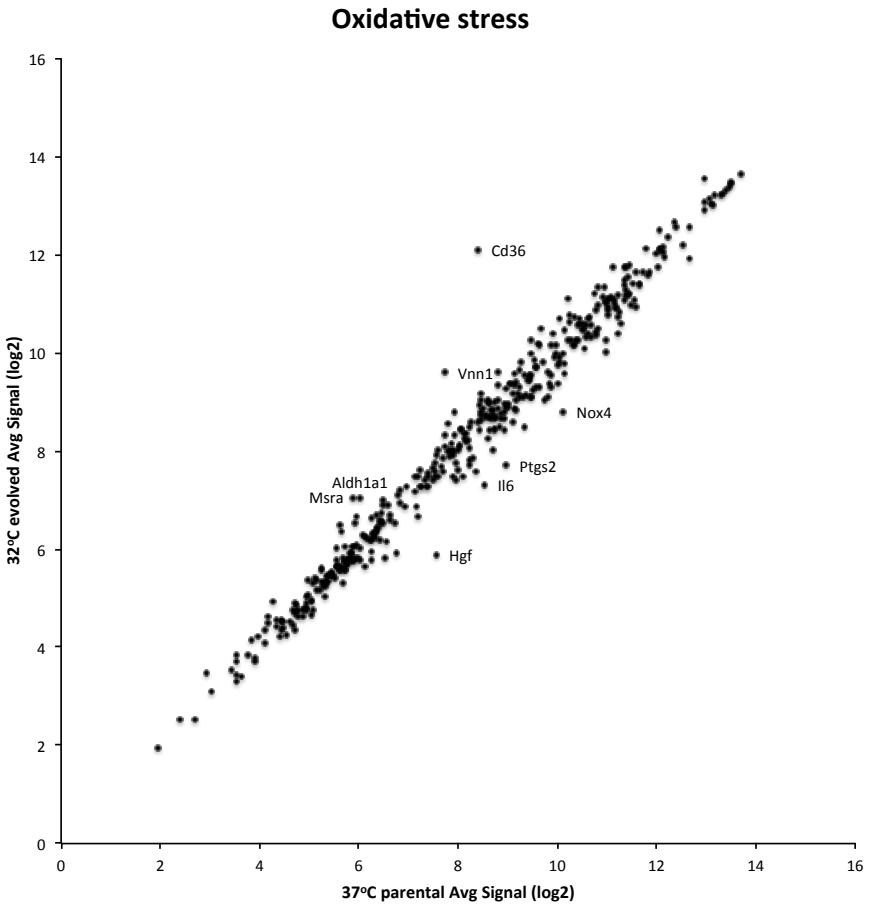

Figure 5.16 Expression of oxidative stress–associated transcripts in the evolved cell line versus the parental cell line. Transcripts with a fold change of ≥ 2 are annotated with the gene alias.

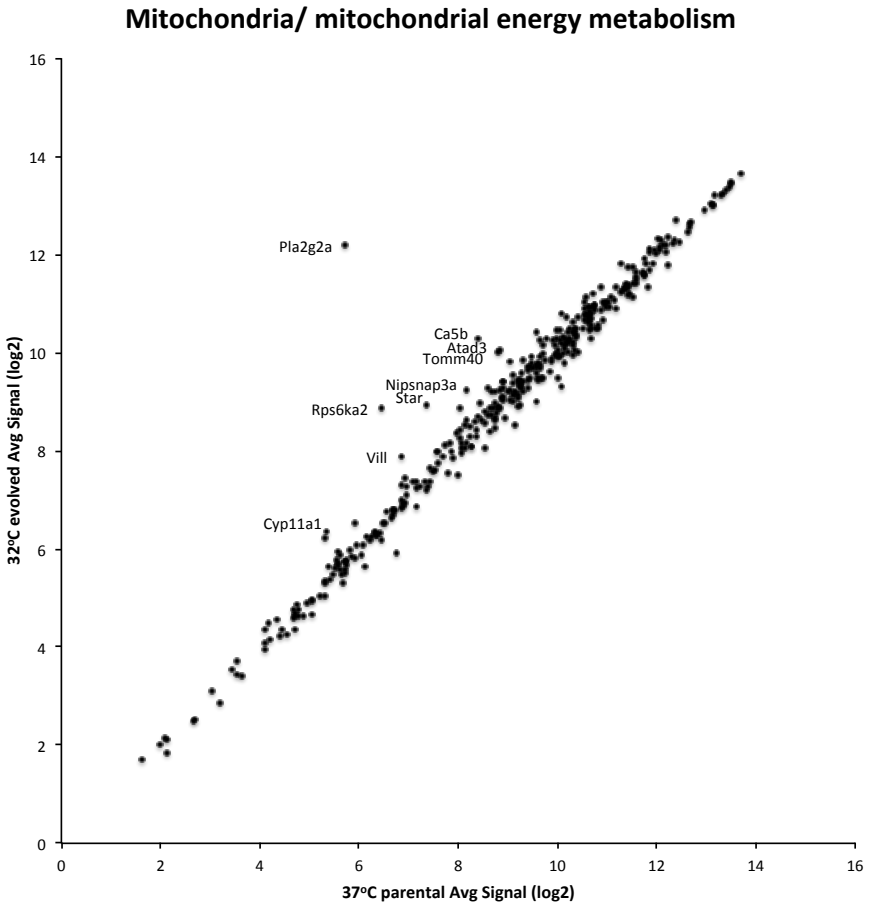

Figure 5.17 Expression of mitochondria/ mitochondrial energy metabolism–associated transcripts in the evolved cell line versus the parental cell line. Transcripts with a fold change of ≥ 2 are annotated with the gene alias.

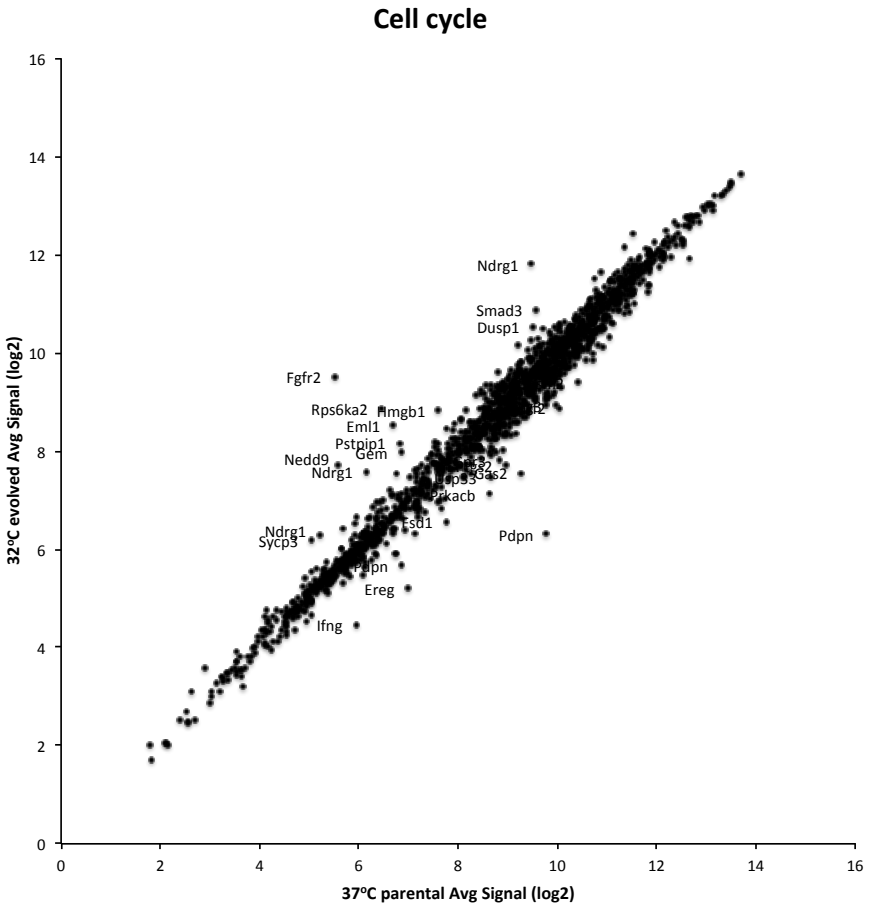

Figure 5.18 Expression of cell cycle–associated transcripts in the evolved cell line versus the parental cell line. Transcripts with a fold change of ≥ 2 are annotated with the gene alias.

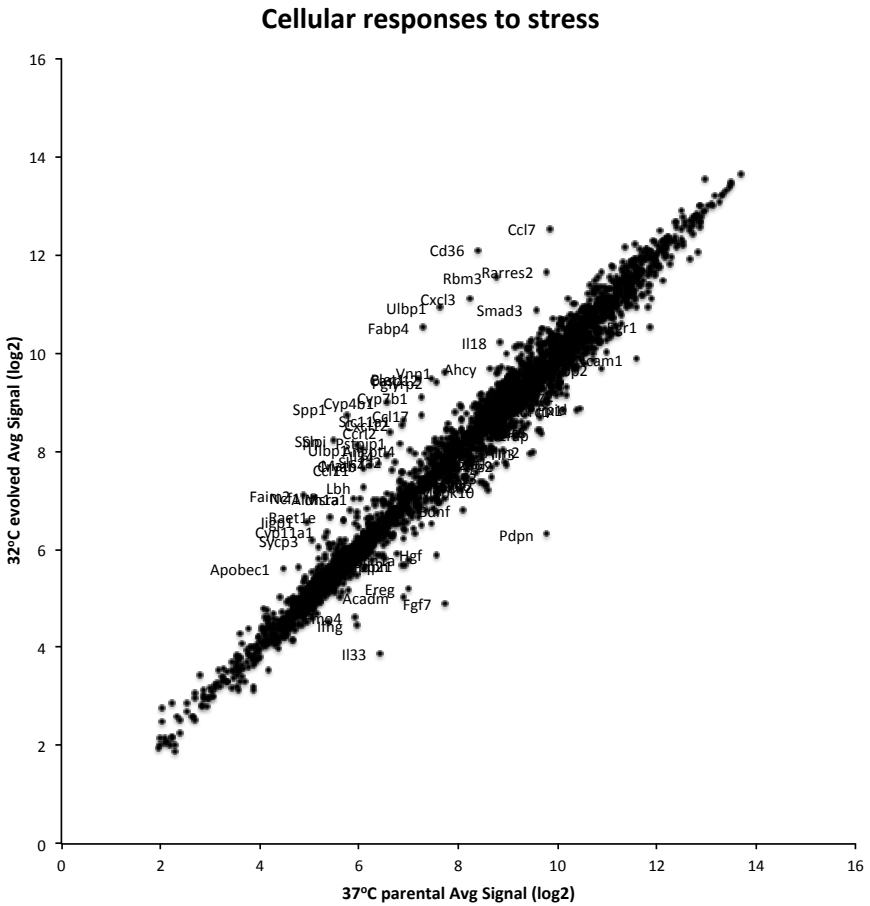

Figure 5.19 Expression of transcripts associated with cellular responses to stress in the evolved cell line versus the parental cell line. Transcripts with a fold change of ≥ 2 are annotated with the gene alias.

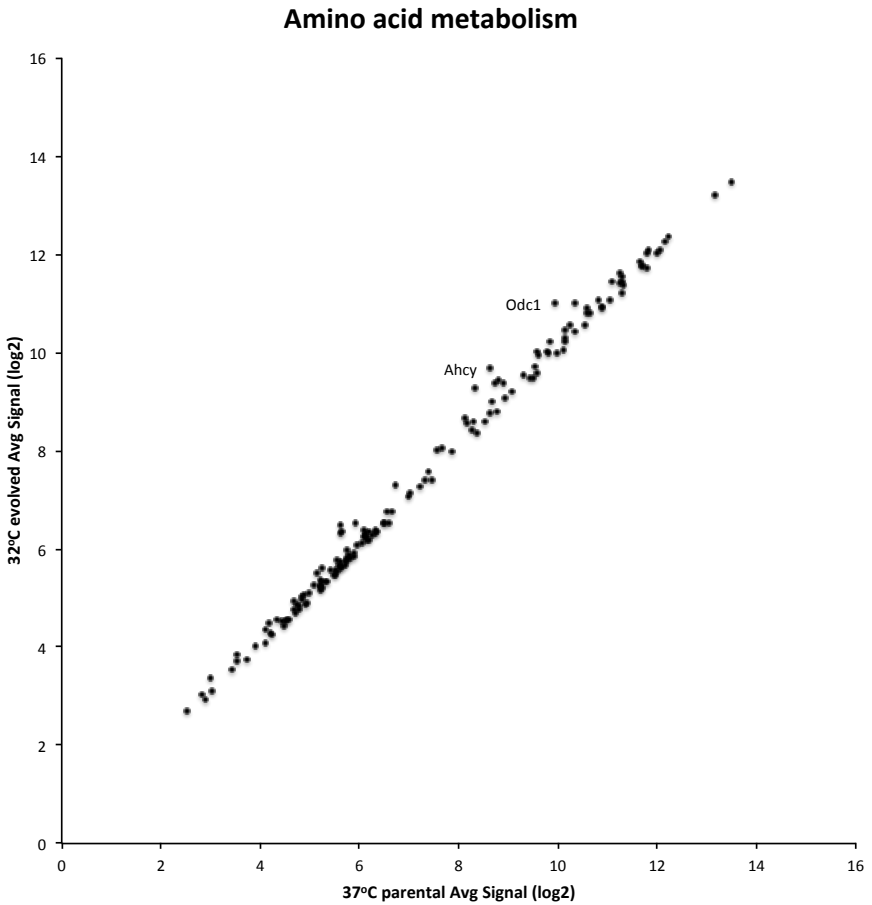

Figure 5.20 Expression of amino acid metabolism–associated transcripts in the evolved cell line versus the parental cell line. Transcripts with a fold change of ≥ 2 are annotated with the gene alias.

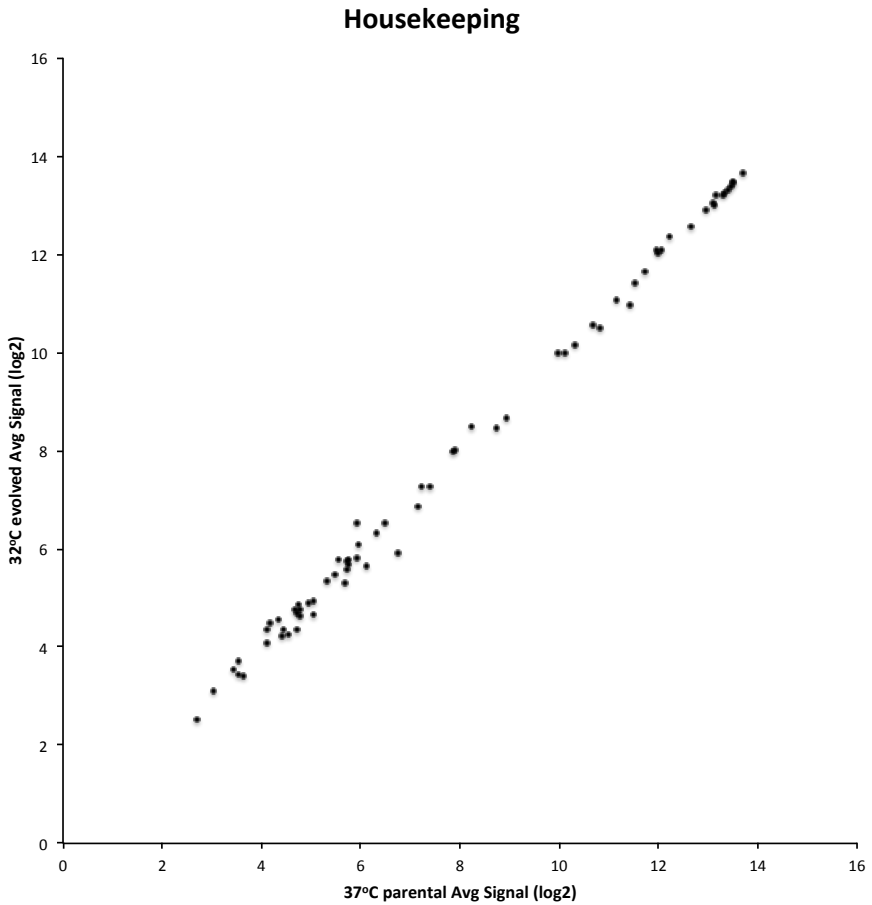

Figure 5.21 Expression of housekeeping–associated transcripts in the evolved cell line versus the parental cell line. Transcripts with a fold change of ≥ 2 are annotated with the gene alias.

Table 5.5 Summary of transcripts with a fold change of ≥ 2 according to transcript sets of interest. Lists are sub-divided according to whether the fold change direction is up-regulated in the evolved cell line or parental cell line.

Cytoskeletal		Glycosylation		UPR		ER		Oxidative stress		Mitochondria/ mito. energy metabolism		Cell cycle		Cellular responses to stress		Amino acid metabolism		Housekeeping	
Evolved	*Parental*	*Evolved*	*Parental*	*Evolved*	*Parental*	*Evolved*	*Parental*	*Evolved*	*Parental*	*Evolved*	*Parental*	*Evolved*	*Parental*	*Evolved*	*Parental*	*Evolved*	*Parental*	*Evolved*	*Parental*
Krt7	Sh3gl2	Extl1	Man2a2	Casp12	Bfar	Cyp4a14	Ephx1	Cd36	Il6	Pla2g2a	-	Fgfr2	Gpsm2	Cd36	Slc12a6	Odc1	-	-	-
Nedd9	Myl9		Neu1	Htra3	Ifng	Sorl1	Syne2	Vnn1	Ptgs2	Rps6ka2		Rps6ka2	Gpr3	Ulbp1	Fez2	Ahcy			
Parvg	Syne2		B4galt3			Cyp4b1	Bfar	Msra	Nox4	Ca5b		Ndrg1	Btg3	Fabp4	Myl9				
Lmo7	Sh3rf2		St3gal6			Ncf1	Pigk	Aldh1a1	Hgf	Star		Nedd9	Uhrf2	Spp1	Bfar				
Sdc2	Map1a					Acsl3	Vkorc1			Atad3		Eml1	Fsd1	Cxcl3	Mertk				
Ncf4	Gas2					Extl1	Tlr3			Tomm40		Pstpip1	Pdpn	Rbm3	Pdpn				
Krt14	Lrriq3					Ppap2b				Vill		Smad3	Usp33	Spn	Usp33				
Myo1g	Ttll7									Nipsnap3a		Hmgb1	Ptgs2	Ccl7	Scn1a				
Pstpip1										Cyp11a1		Sycp3	Ifng	Cyp4b1	Map1a				
Tln2												Gem	Prkacb	Plet1	Gbp2				
Vill												Dusp1	Gas2	Faim2	Il6				
Wdr78													Ereg	Slpi	Depdc5				
Fscn1														Casp12	Arpp21				
Svil														Ncf1	Tspan2				
														Vnn1	Ptgs2				
														Rarres2	Vkorc1				
														Cyp7b1	Bdnf				
														Pglyrp2	Fmo4				
														Ccrl2	Egr1				
														Slc11a1	Il1rap				
														Cxcl12	Mapk10				
														Iigp1	Tlr3				
														Ccl11	Ifng				
														Cryab	Aim2				
														Ccl17	Prrx1				
														Il18	Ppid				
														Pstpip1	Hgf				
														Il34	Ncam1				
														Matn4	Ereg				
														Smad3	Acadm				
														Raet1e	Il33				
														Lbh	Fgf7				
														Msra					
														Apobec1					
														Sycp3					
														Slc1a2					
														Ahcy					
														Cyp11a1					
														Angptl4					
														Aldh1a1					

As previously mentioned, the distance of each point in figures 5.12 to 5.21 from the line y=x, indicates the degree of change in that transcript between the parental cell line and the evolved cell line. This is numerically represented by subtracting the log2 fluorescence of a transcript from one cell line from the log2 fluorescence of that same transcript from the other cell line, giving values of log2[linear fold change]. Box plots that show the distribution of these values (i.e. the relative degree of change) for each set of transcripts in figures 5.12 to 5.21 can be seen in figure 5.22. The distribution is also shown for all transcripts on the chip, the median of which lies at 0.01 (very close to no change). Using R, notches were applied to box plots to determine whether any change in median is significantly different to the median of all transcripts. Where notches of a box do not overlap with the notches on the box for all transcripts they can be said to be significantly different to a 95% confidence interval (Chambers *et al.* 1983). As can be seen by visually inspecting notch overlaps (and as was verified in R mathematically), sets of transcripts for cytoskeletal, glycosylation, amino acid metabolism and housekeeping genes all differed significantly from the median of all transcripts. Housekeeping and glycosylation transcript sets were seen as up-regulated in the parental cell line and cytoskeletal and amino acid metabolism transcripts sets were seen as up-regulated in the evolved cell line. It is worth reiterating here that the term “up-regulated” is used for convenience, and can also imply down-regulation in the opposite condition. When inspecting outliers, it can be seen that the amino acid metabolism transcripts set only has outliers that are up-regulated in the evolved cell line, and several particularly large outliers up-regulated in the evolved cell line are also seen in the mitochondrial, oxidative stress and ER transcripts sets. Other sets of transcripts tend to be more balanced in terms of outlier distribution.

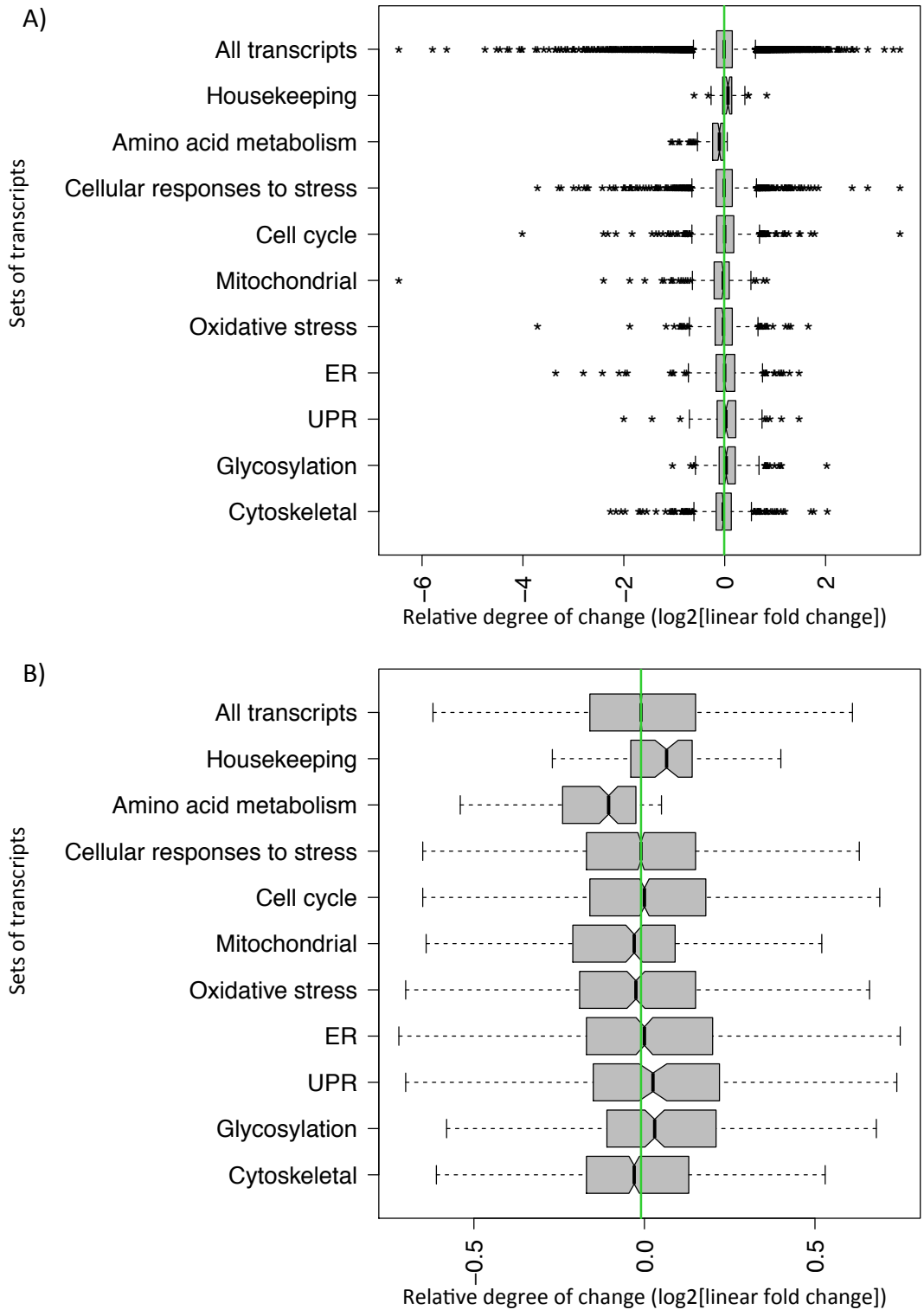

Figure 5.22 Notched box plots showing the relative degree of change of sets of transcripts between the parental and the evolved cell line. Positive changes (i.e. box skewed to the right) represent up-regulation in the parental cell line where as negative changes (i.e. box skewed to the left) represent those up-regulated in the evolved cell line. A) shows plots with outliers (defined as any point beyond 1.5 × interquartile range of that box) and B) shows the plots with outliers removed for clarity purposes. The green vertical line in A) and B) represents the median value of all transcripts, which lies at 0.01.

5.3.3.6 KEGG pathway analysis of differentially expressed transcripts

KEGG pathway analysis was used to examine whether differentially expressed transcripts ($p \leq 0.01$, FDR corrected ANOVA, no fold change threshold applied) are working in concert to affect particular cellular processes. The reader is also referred to the appendix to note the degree of fold change associated with identified/discussed transcripts, noting that certain transcripts may be found at multiple locations on the chip and there may be differences in the fold change values between these. Pathways analysed included: Metabolism; Pathways in cancer; Cell cycle and Protein processing in the endoplasmic reticulum, due to the potential to gain insights into cell line performance and also due to their high representation by differentially expressed transcripts. Differentially regulated pathways are highlighted in figures and changes described in preceding text. Other KEGG pathways are seldom referred to in the Discussion (section 5.4) but map images are not shown schematically here.

Metabolism

The KEGG pathway map for metabolism is very complex due to it representing the large numbers of metabolic process and pathways that can occur in a cell (figure 5.23). For clarity and reference purposes, a more annotated version of the map in figure 5.23 can be found in appendix III that doesn't include the colour-coded representation of differentially expressed transcripts. Fatty acid biosynthesis and fatty acid degradation are up-regulated in the evolved cell line and fatty acid elongation in mitochondria is up-regulated in the parental cell line. There is differential regulation occurring in the transcripts attributing to oxidative phosphorylation and some up-regulation in the evolved cell line of transcripts involved in the TCA cycle.

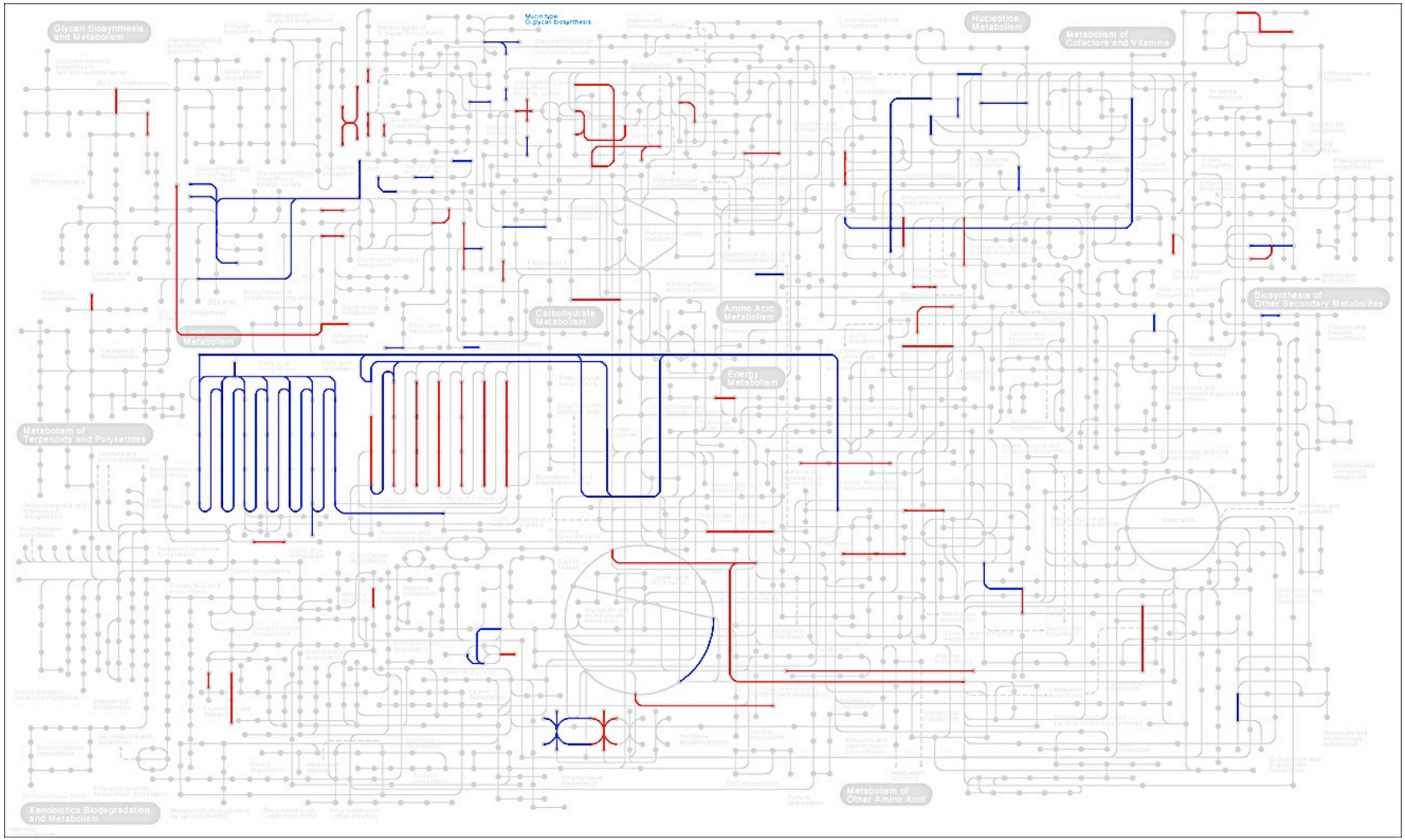

Figure 5.23 KEGG metabolism pathway. Significantly differentially expressed transcripts were mapped onto this pathway using KEGG Search&Color. Pathways in blue represent those that were up-regulated in the evolved cell line and pathways in red represent those that were up-regulated in the parental cell line. Image adapted from http://www.genome.jp/kegg/pathway.html.

Pathways in cancer

The KEGG pathway map for pathways in cancer was the second most represented pathway map, after metabolism. The map is shown in figure 5.24 with differentially expressed transcripts highlighted in blue or red. Casp8, Fzd7, Gnb5, Gng7, Mitf, Cxcl12, Tgfbr1, Tgfbr2, Traf1, Traf3, Sufu and Hdac1 were up-regulated in the evolved cell line and Col4a1, Itga3, Itgav, Lama2, Lamb1, Lamb3, Mdm2, Rock2, Akt3 and Ccdc6 were up-regulated in the parental cell line.

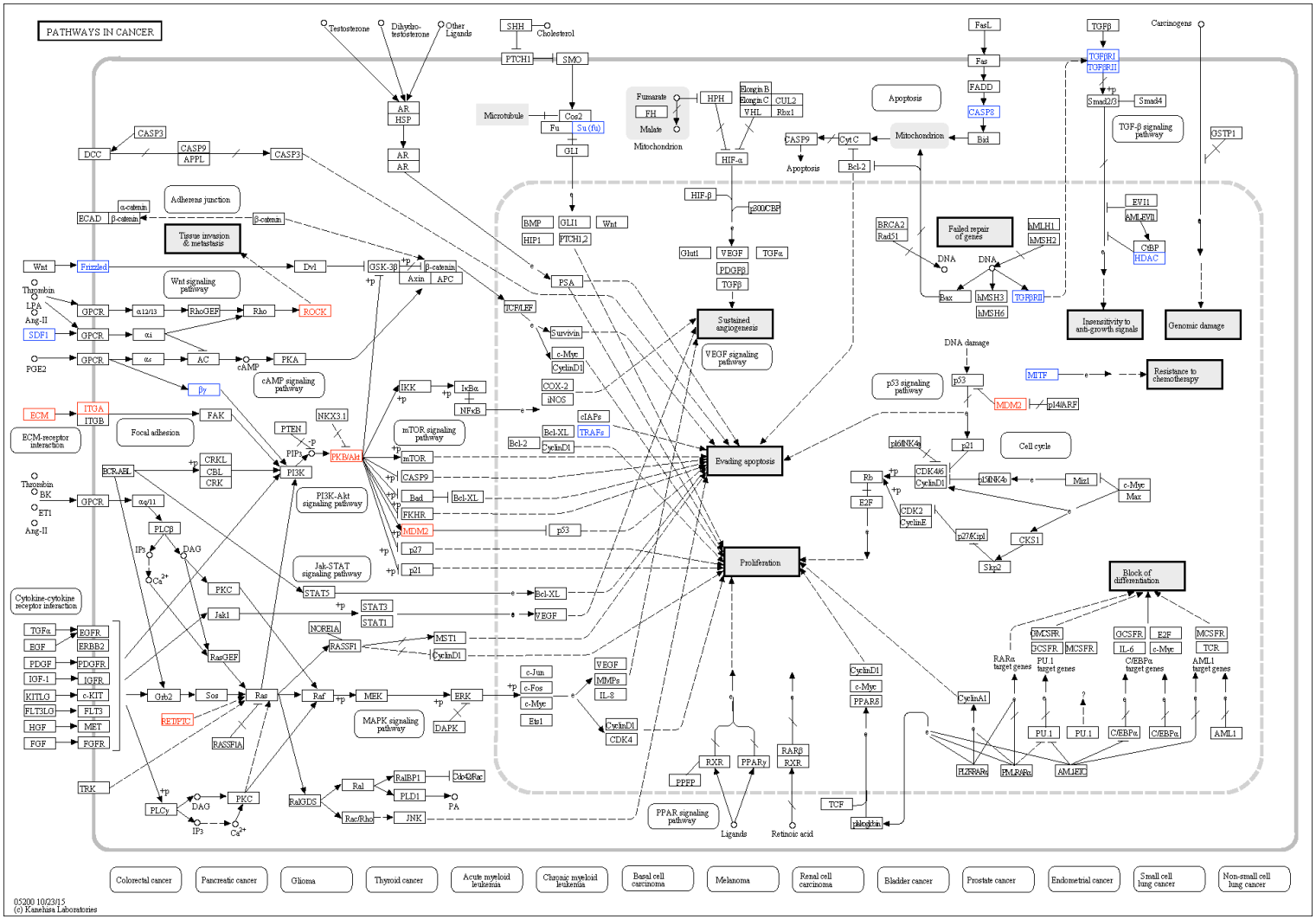

Figure 5.24 KEGG pathways in cancer. Significantly differentially expressed transcripts were mapped onto this pathway using KEGG Search&Color. Transcripts in blue represent those that were up-regulated in the evolved cell line and pathways in red represent those that were up-regulated in the parental cell line. Image adapted from http://www.genome.jp/kegg/pathway.html.

Cell cycle

The KEGG cell cycle map was not one of the most highly represented pathways but is included here due to the vast changes in cell cycle that were observed in the evolved cell line over the evolution process (i.e. very slow progression of cell cycle when first exposed to hypothermic conditions to normal growth rates once adapted). As can be seen in figure 5.25, Cdc20, Tfdp2, Tfdp1, Hdac1 and Ywhab were up-regulated in the evolved cell line and Cdkn2c, Mdm2 and Cdc27 were up-regulated in the parental cell line.

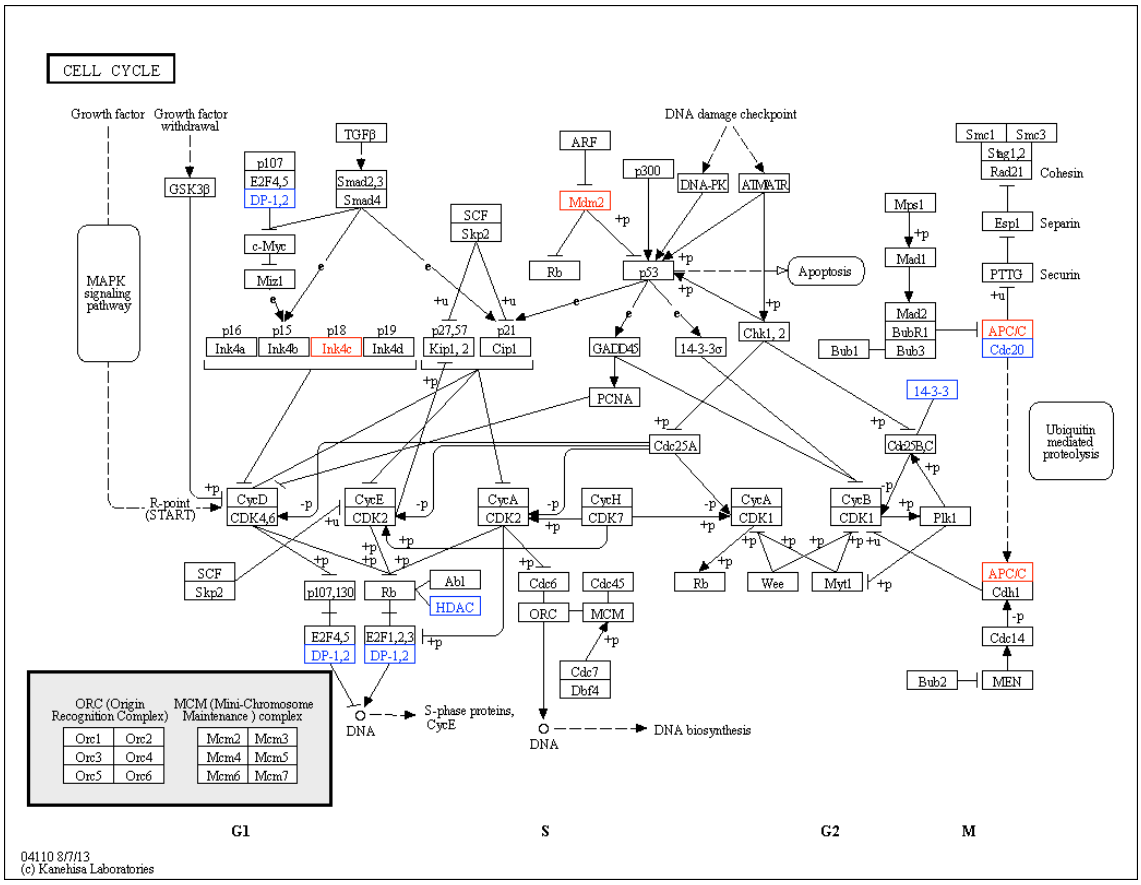

Figure 5.25 KEGG pathways in cell cycle. Significantly differentially expressed transcripts were mapped onto this pathway using KEGG Search&Color. Transcripts in blue represent those that were up-regulated in the evolved cell line and pathways in red represent those that were up-regulated in the parental cell line. Image adapted from http://www.genome.jp/kegg/pathway.html.

Protein processing in the endoplasmic reticulum

Like cell cycle pathways, protein processing in the ER was not one of the most highly represented pathways but is included out of interested due to the large differences between the evolved and parental cell line in their recombinant protein productivities. Figure 5.26 shows the KEGG pathway map for protein processing in the ER with differentially expressed transcripts highlighted in blue or red. Atf4, Casp12 and Vcp were up-regulated in the evolved cell line and Rad23a, Rpn2, Ube2d1, Edem3, Sec24d were up-regulated in the parental cell line.

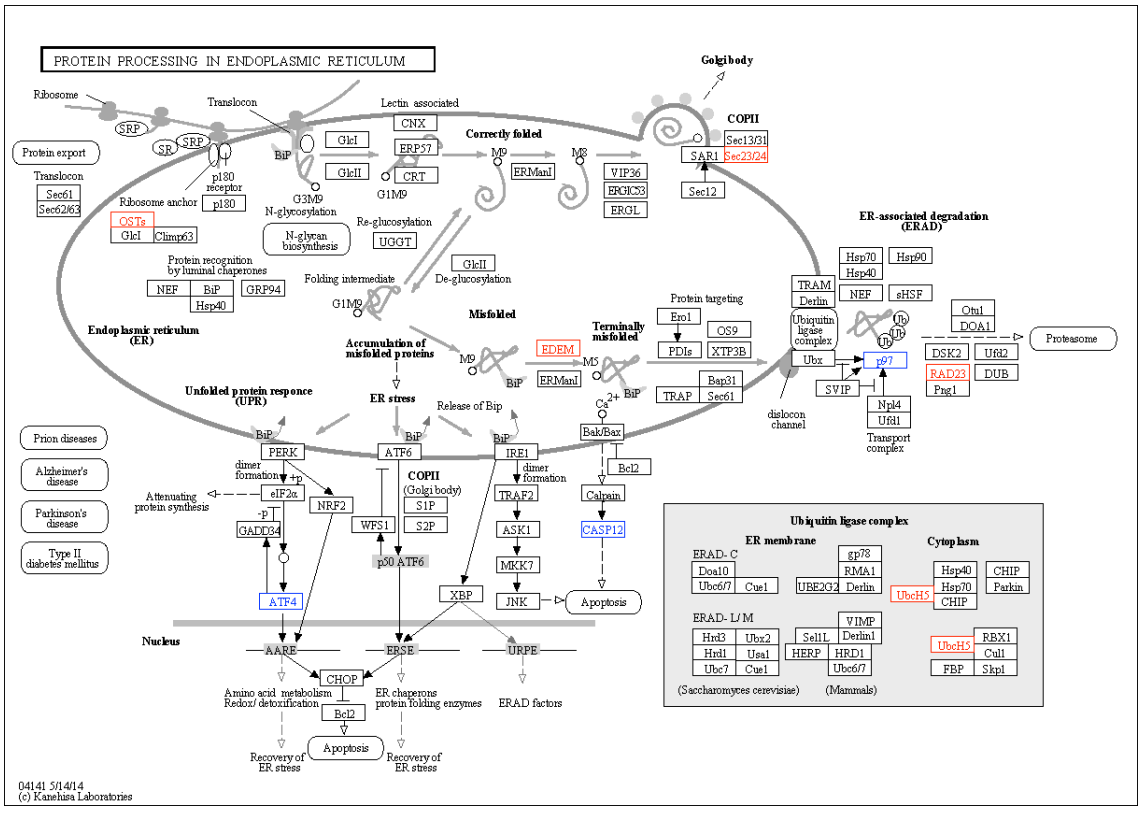

Figure 5.26 KEGG protein processing in the endoplasmic reticulum. Significantly differentially expressed transcripts were mapped onto this pathway using KEGG Search&Color. Transcripts in blue represent those that were up-regulated in the evolved cell line and pathways in red represent those that were up-regulated in the parental cell line. Image adapted from http://www.genome.jp/kegg/pathway.html.

5.3.4 Amino acid analysis through fed batch-culture

Supernatant samples were taken at the start of fed batch culture and pre- and post-addition of feed (which occurred on days 3, 6 and 9). This allowed amino acid concentrations to be measured during early exponential, mid exponential and stationary phase of growth. Samples were taken from triplicate cultures of both the parental and evolved cell line. Average absolute concentrations of each amino acid along fed batch culture are shown in figure 5.27. Specific amino acid transport rates (the amount of amino acid flux (export/production or import/consumption) normalised per cell per unit time, calculated as follows: [$pmol_{(t2)}$ – $pmol_{(t1)}$] /[$IVCD_{(t2-t1)}$]) were then analysed and compared between cell lines (see figures 5.28, 5.29 and 5.30).

A two-way ANOVA with Tukey's multiple comparisons test (comparison test between mean production/ consumption of each amino acid by each cell line at each stage of culture) was performed on the un-summed data (i.e. the data presented in figure 5.28) (see appendix III).

Notable differences were observed as follows: In early exponential phase of culture, the parental cell line exports Proline, Threonine and Tryptophan, whereas these are imported in the evolved cell line; Import rates of Lysine, Leucine, Valine, Isoleucine, Arginine, Phenylalanine and Histidine in early exponential phase are much larger in the evolved cell line than the parental cell line; Aspartic acid is exported in mid exponential phase in the evolved cell line, where as it is imported in the parental cell line; transport flux of Hydroxyproline is much higher throughout culture in the parental cell line than the evolved cell line. It can be seen in figure 5.29 that when amino acid transport rates are summed together according to import or export, the evolved cell line has higher cell specific import rates than the parental cell line in early exponential phase, whereas the parental cell line has higher cell specific export rates than the evolved cell line. Throughout the rest of culture, import and export rates remain relatively similar between the two cell lines.

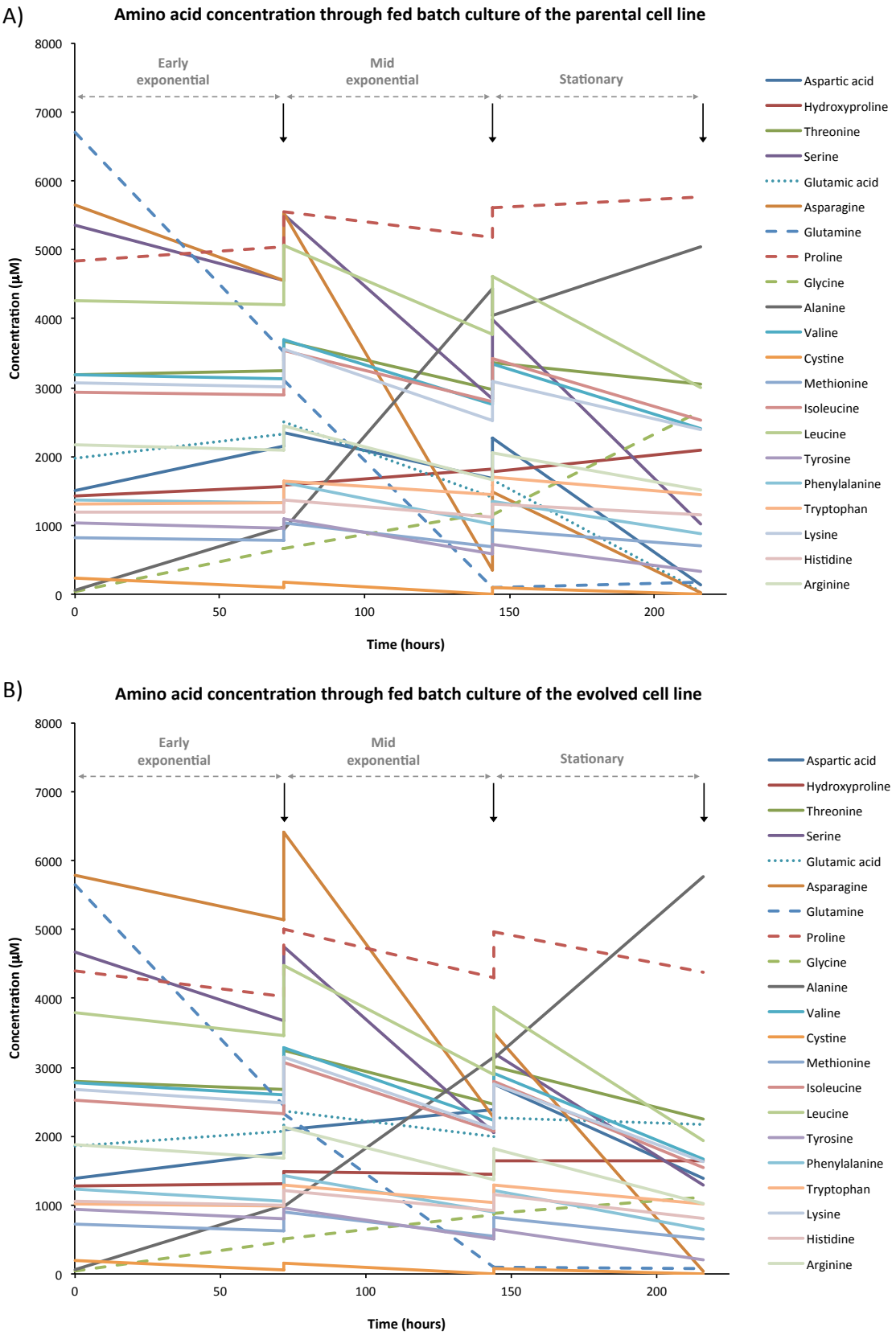

Figure 5.27 Absolute amino acid concentrations in supernatant throughout fed batch culture of the parental (A) and evolved (B) cell lines. Values shown are the average of 3 replicate samples. Error bars are not show for image clarity reasons. Time course is divided into 3 phases: early exponential, mid exponential and stationary. Vertical black arrows denote time of feed addition.

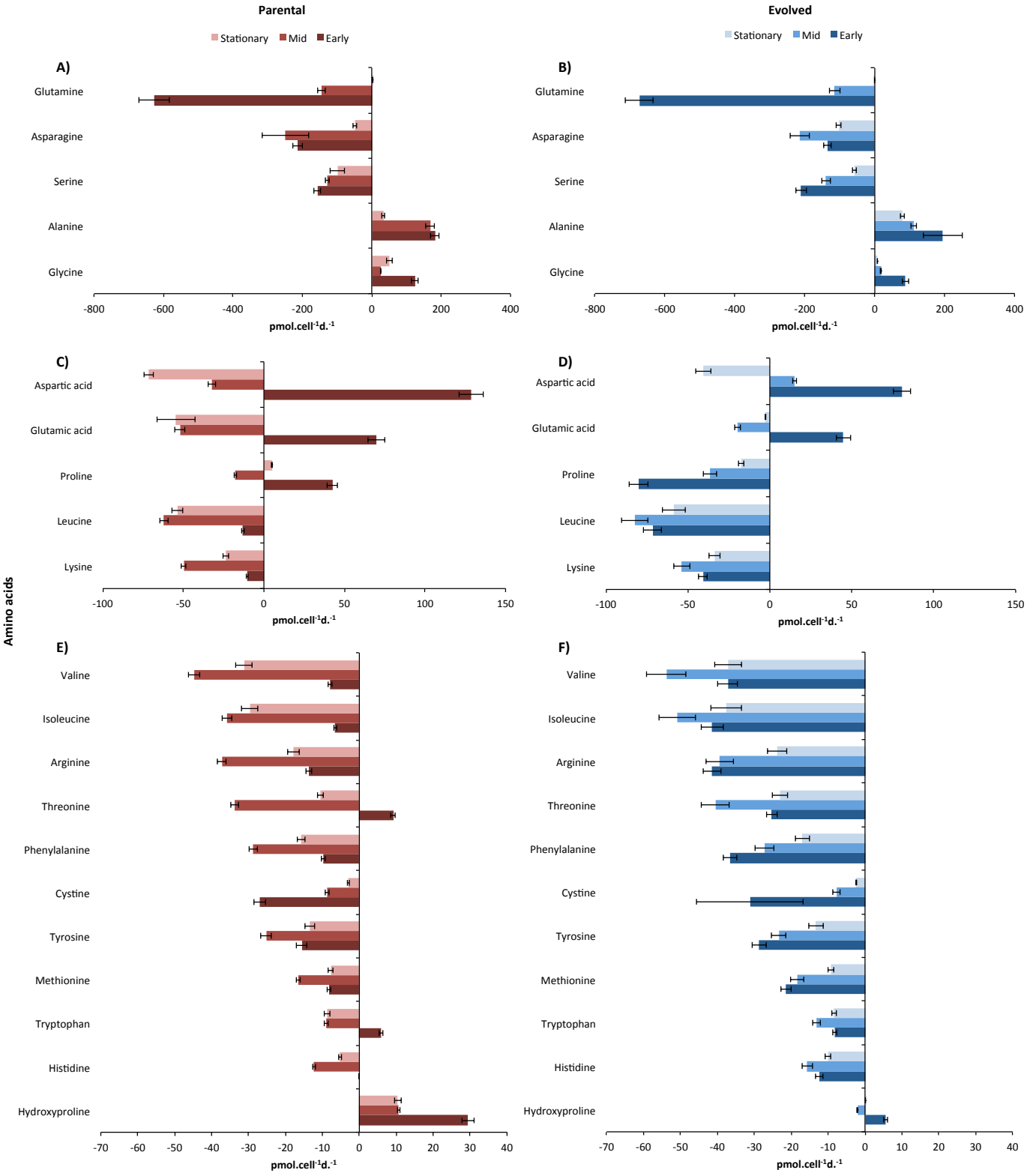

Figure 5.28 Specific amino acid transport rates of the parental and evolved cell lines through early-exponential, mid-exponential and stationary phases of fed batch culture. Negative values represent consumption of amino acid and positive values represent production/ export from the cell. A) and B) represent amino acids with large scale amino acid flux in the parental and evolved cell line, respectively; C) and D) represent amino acids with medium scale amino acid flux in the parental and evolved cell line, respectively; and E) and F) represent amino acids with small scale amino acid flux in the parental and evolved cell line, respectively. Error bars, SD; N = 3.

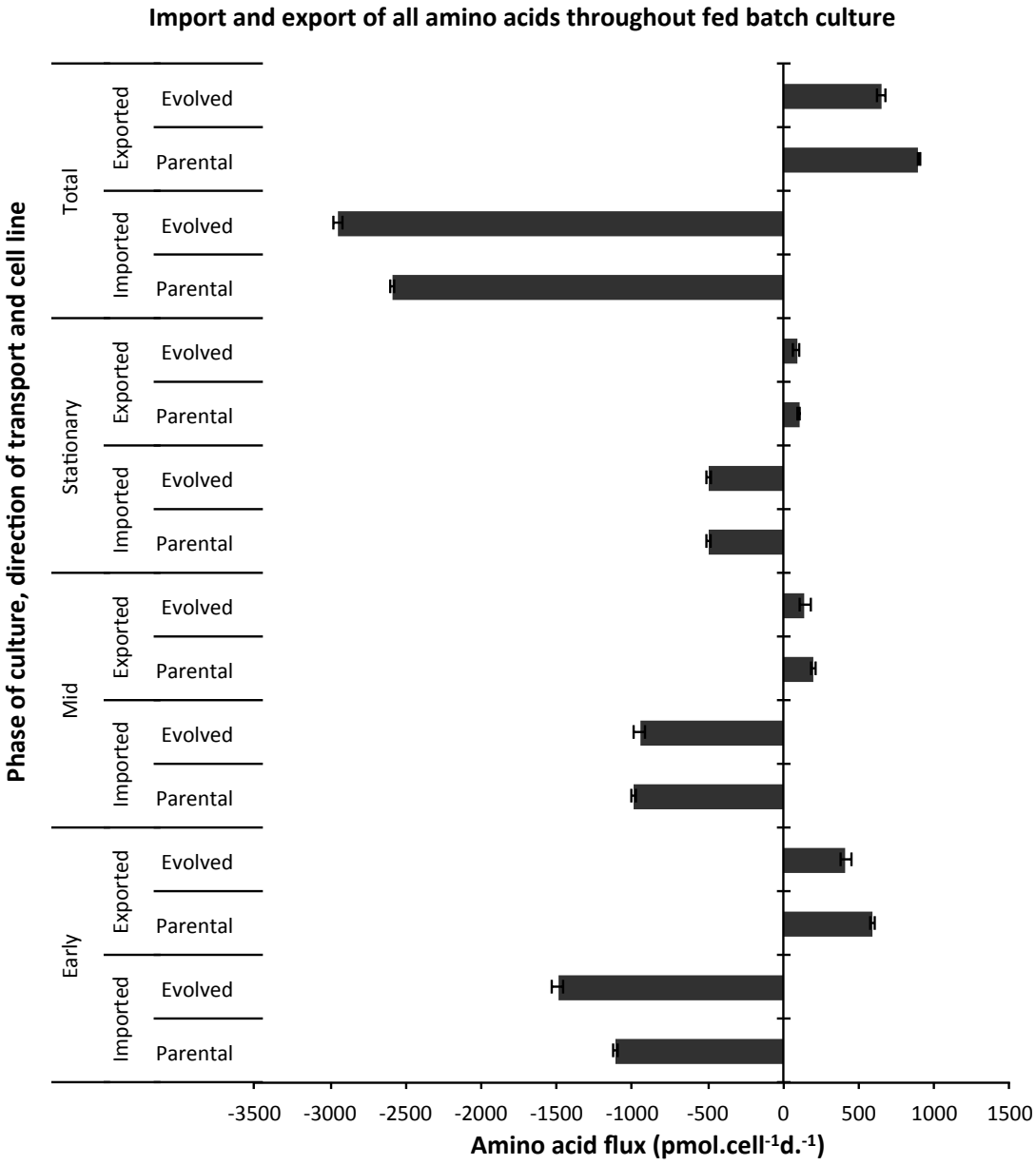

Figure 5.29 Summed specific amino acid import and export transport rates of the parental and evolved cell lines through early exponential, mid exponential and stationary phases of fed batch culture and also total transport throughout culture. All transport values for each amino acid were summed together according to transport direction (import or export) to show the total amino acid flux occurring at each phase of culture in both the parental cell line and evolved cell line. Error bars, SD; N = 3

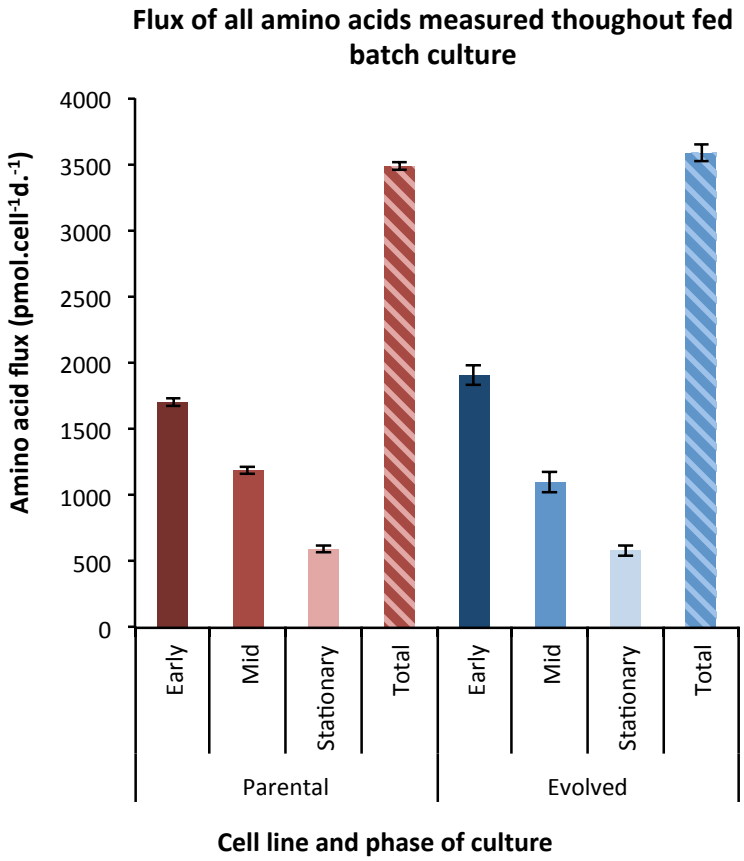

Figure 5.30 Summed directionless specific amino acid transport rates of the parental and evolved cell lines through early exponential, mid exponential and stationary phases of fed batch culture and also total transport throughout culture. All transport values for each amino acid were made positive and summed together to show the total amino acid flux occurring, i.e. the sum of all amino acids exchanged (in and out of the cell), independent of transport direction. Error bars, SD; N = 3.

5.4 Discussion

As has been highlighted throughout this thesis, numerous and marked differences have been identified between the parental and evolved cell line, namely in terms of cellular dimensions, growth rate, RNA content, and transient and stable recombinant protein production capabilities. The work and results described in this chapter aimed to provide insight into the underlying mechanistic modifications that may be underpinning the phenotypic changes and industrially relevant improvements that have been observed as a result of adaptation to hypothermic conditions through directed evolution.

This work presented in this chapter utilised experimental methods that would investigate the hypotheses that were put forward in the introduction in a "bottom-up" fashion, but also used methods that would provide information that could be analysed in a non-hypothesis lead, "top-down" manner. Taking both a bottom-up and top-down approach to this mechanistic analysis allows the pre-existing concepts to be tested as well as gaining a more complete understanding of the entire system.

As discussed in the introduction to this chapter, it was hypothesised that the evolved cell line may have adapted to growth at 32°C, i.e. overcoming the natural response which is an arrest in cell cycle, by means of generating more heat than is normal. It was mentioned that even the decrease in surface area to volume ratio, a consequence of the increase in cell size described in chapter 3, would attribute to heat conservation. Specifically, the main hypothesis considered in the introduction to this chapter was that of *adaptive non-shivering thermogenesis*: that the evolved cell line now employs a new metabolic process involving an adaptation of its mitochondrial proton circuit in order to generate heat energy. It is known from pre-described background literature the uncoupling proteins (UCPs), activated by long chain fatty acids (LCFAs), provide this modification of the mitochondrial proton circuit by allowing protons to re-enter the mitochondrial matrix, bypassing ATP-synthase and dissipating energy as heat (Fedorenko *et al.* 2012). We also know that cells that have undergone adaptive non-shivering thermogenesis exhibit

low levels of reactive oxygen species (ROS) as the adaptation primarily evolved as mechanism to allow the organism to live in oxygen rich environments by increasing respiration by UCP-mediated uncoupling which is associated with reduced ROS formation (Rial & Zardoya 2009). With this in mind, oxidative stress (ROS) levels and mitochondrial bioenergetics were investigated and compared between the parental cell line and the evolved cell line to determine whether there is any support in these areas for adaptive non-shivering thermogenesis occurring in the evolved cells. Using a reagent that fluoresces upon oxidation by reactive oxygen species and is relatively quantified by flow cytometry, it was observed that levels of reactive oxygen species were consistently higher in the parental cell line compared to the evolved cell line. This result can in some way be amplified if one takes into account that the fluorescence is measured on a per cell basis: if the evolved cells and parental cells had an equal distribution of ROS throughout the cell, it would be expected that, given that the evolved cells are almost double in volume, the evolved cells would fluoresce more intensely anyway, given that total ROS per cell would then be proportionately greater simply due to the increase in volume. However, this is not the case and the smaller, parental cells in fact fluoresce more intensely, further exaggerating the disparity in ROS levels when thought of in a per unit volume basis. Because the results were so definitive in this way, the need for positive flow cytometry controls that would allow quantification of absolute ROS values and subsequent normalisation to cell volume was not deemed necessary to address the intended purposes of this experiment.

To further probe these findings, an investigation into mitochondrial bioenergetics was performed using the Seahorse XF24 system, an instrument that assays mitochondrial respiration by using chemical inhibitors and effectors. The results showed that basal respiration levels of cells from the evolved cell line were 76% greater than basal respiration levels of cells from the parental cell line. These findings support the adaptive non-shivering thermogenesis hypothesis, as it is known that increased respiration is a feature of adaptive thermogenesis. Interestingly too, proton leak significantly differed between the two cell lines, with a 53% increase in cells from the evolved cell line. In this assay, proton leak is a

respiratory measure that is not coupled to ATP production, and elevated leakage indicates cells have increased permeability across the inner mitochondrial membrane (Kokoszka *et al.* 2001). This leakage across the membrane is the fundamental feature of adaptive non-shivering thermogenesis in which protons return to the mitochondrial matrix via the proton motive force, dissipating energy as heat (Rial & Zardoya 2009).

It was also observed during this experiment that there is no significant difference in the spare respiratory capacity between the two cell lines. This was the case because although basal respiration had significantly increased in the evolved cell line, maximal respiration levels had also significantly increased: The spare respiratory capacity is the difference between these two levels, a value that ultimately remained similar between cell lines. It has been suggested that the maintenance of some spare respiratory capacity, even under conditions of intense physiological stimulus that might demand increased respiration, is a major factor contributing to the vitality and survival of cells. The ability to satisfactorily respond to cellular stressors is associated with a large spare respiratory reserve. This capacity is determined by several factors, including the functional capacity of the enzymes involved in electron transport as well as the ability of the cell to deliver substrate to the mitochondria (Desler *et al.* 2012). This result suggests these abilities have been maintained through the evolution process suggesting these important survival mechanisms were not compromised. Despite seeing an increase in heat generating proton leak, a respiratory measure not coupled to ATP production, an increase in ATP production is also seen in the evolved cell line compared to the parental cell line. As equivalent biomass of each cell line was used, the aforementioned observation cannot be attributed to the maintenance and demands of higher protein biomass phenotype, however, one possible explanation would be that more ATP is required in the evolved cell line due to the utilisation of ATP in *futile cycles*, which, as described in the introduction section of this chapter, are metabolic pathways that run simultaneously in opposing directions with no apparent overall purpose or effect other than to dissipate heat energy (Qian & Beard 2006). Relatedly, the ATP could be utilised by SERCA transport of Ca^{2+} (also

further described in the introduction), which generates heat. Additionally the ADP produced by this process consequently stimulates mitochondrial respiration, which we have observed as elevated in the evolved cell line (de Meis 2001). This discussion assumes these differences are due to differential mitochondrial bioenergetics alone and that the density of mitochondria within the cell remains constant, however, it could also be possible that the size of mitochondria or the density of their distribution in the cell has increased in the evolved cell line to facilitate the observed bioenergetic changes.

Using the Affymetrix® GeneChip® CHO Gene 2.0 Array system, the expression of 29,890 transcripts were compared between the two cell lines. Applying a significance threshold of $p \leq 0.01$ (FDR corrected ANOVA) to the analysis, 2069 transcripts were found to be differentially expressed of which 974 were up-regulated in the evolved cell line (*which can alternatively be viewed as down in parental cell line*) and 1095 were up-regulated in the parental cell line (*which can alternatively be viewed as down in evolved cell line*). Interestingly however, despite this roughly equal divide, the majority of significantly differentially expressed transcripts with particularly high fold change values (all those with a fold change > 11.12, to a maximum fold change of 87.89) were seen as up-regulated in the evolved cell line (see figure 5.10), suggesting some major overexpression of certain transcripts could be key in the adaptation to hypothermic conditions.

It is widely known that the annotation of the CHO genome is still relatively poor (Wippermann *et al.* 2015), meaning certain transcripts on probes on the Affymetrix chip are currently without meaningful annotation, such as a gene alias. Because of this, coupled with the lack of a standardised platform that allows the analysis of such data, multiple modes of exploring the data were performed in order to derive a more accurate overview of the major mechanistic differences between the two cell lines. Such methods included: manual classification of all significantly differentially expressed (with a fold change threshold of ≥ 2) transcripts according to functional groups (determined for each transcript using Reactome.org); transcript expression conservation analysis using pre-defined sets

of transcripts from CHO cells that represent specific biological functions (transcript sets compiled by SA Bioscience) and finally KEGG pathway analysis was performed to determine whether differentially expressed transcripts were working in concert to affect particular cellular processes and pathways. An example that demonstrates the need for a standardised platform is found when probing the data set for information on cell cycle: using SA Bioscience transcript sets and KEGG pathway analysis results in largely different transcripts lists and total transcript numbers in terms of those that have been differentially expressed. It could be proposed that using only one method should be implemented but arguably that may have lead to potentially interesting information being overlooked, for example, a KEGG pathway map does not exist for glycosylation, but a transcript list has been defined for glycosylation by SA Bioscience, specifically for CHO cells.

From the functional grouping of all significantly differentially expressed transcripts over a fold change of 2, we saw that a large proportion of such transcripts were involved in cell signalling and metabolism, followed by gene expression, cell cycle, membrane trafficking and ECM/ cytoskeletal. Out of these categories, when considering other analysis performed on the rest of the data set and not just those over a fold change of two, metabolism was verified by KEGG pathway analysis as being highly regulated (discussed later), cytoskeletal transcripts were verified as being un-conserved between cell lines (figure 5.22) and there is some verification of differential membrane trafficking between cell lines from the differences observed in amino acid flux (discussed later). The distribution of direction of regulation (i.e. up in evolved or parental) is approximately equal for most categories. This indicates that no particular functional categories are being overexpressed as a whole in either cell line, more just a balanced exchange in what is being expressed. However, what is not known from this data is whether the transcripts are negative or positive regulators of their functions. Manually inspecting each transcript one by one for this information is not pragmatic for an ‘omics exercise, however, KEGG pathway analysis can reveal some indication on positive/negative regulation and can reveal

transcripts that are working in concert to affect specific pathways and processes. It is also important to remember that just because a large number of transcripts associated with a particular function may have changed, doesn't necessarily mean the you'd see observable differences in that function, or in fact the proteins that would be translated from them. For example, in contrast, the up-regulation of just a certain single transcript in a largely un-regulated functional group may have profound biological effects on the cell.

SA Bioscience transcripts sets were used to perform a conservation analysis, in other words, these pre-defined lists were used to determine whether the regulation of certain cellular systems were conserved along the evolutionary process. As was summarised in figure 5.22, out of the SA Bioscience transcript sets investigated, housekeeping (i.e. typically constitutive genes that are required for the maintenance of basic cellular function, often used for normalisation or reference purposes) and glycosylation were seen as significantly up-regulated in the parental cell line (compared to the median change of all transcripts), and cytoskeletal and amino acid metabolism were seen as up-regulated in the evolved cell line. The reader is reminded here again that "up-regulated" is used for convenience, and can alternatively imply down-regulation in the opposing cell line. One possible explanation for the apparent up-regulation in housekeeping genes in the parental cell line (or down-regulation in the evolved cell line) could be that these genes are regulated in proportion to ploidy, rather than cell size/total RNA content: the expression levels of housekeeping genes might have remained the same through evolution despite the increase in total RNA, which then as a consequence of the normalisation processes by the Affymetrix protocol (normalising to total chip fluorescence to account for cRNA load onto the chip), would perceive the housekeeping genes as down-regulated in the larger, evolved cell type, while the majority of transcripts are regulated in proportion to total cellular RNA content.

Although glycosylation is observed as up-regulated in the parental cell line, the informative importance of this result is questionable as we have seen from the

product quality analysis in chapter 4 that there is no difference in glycan profiles of the recombinant proteins between the two cell lines, when produced transiently or stably. From an industrial point of view, it could be suggested that the difference in expression of glycosylation transcripts is not as relevant as the end products are satisfactorily similar. A related study was performed in house at Lonza that looked at the expression of glycosylation genes in multiple clones and their corresponding IgG4 mAb glycosylation profiles: gene expression was highly conserved between clones but there was considerable variation in mAb product quality, showing a lack of correlation between glycosylation gene expression and glycosylation itself (O'Callaghan *et al.* 2015).

Amino acid metabolism was seen as up-regulated in the evolved cell line compared to the parental cell line, implying disparity in the utilisation of amino acids between cell lines. Phenotypically, the cell lines differ significantly in size (volume and total biomass content) so one might expect amino acid metabolism to vary, just as one might expect there to be metabolic differences between large and small organisms of the same species. On a cellular level, amino acids are exchanged through a variety of types of transporters situated in the cell membrane, however, as a cell increases in size, the surface area per unit volume is relatively reduced. This could mean that the relative proportion of amino acid transporters in the evolved cell line has been reduced; alternatively the cell may have up-regulated certain transcripts to result in a more "transporter-dense" membrane. For simplicity for the reader, further comment on amino acid metabolism transcript regulation is discussed later, in synergy with the findings from the amino acid flux through fed batch culture experiment.

As previously mentioned, cytoskeletal-associated transcripts were observed as significantly up-regulated in the evolved cell line. The profound phenotypic difference between the two cell lines in terms of cell size was itself indicative that modifications to the underlying structural elements of the evolved cell line would have occurred. The cytoskeleton creates and maintains the morphology and internal organisation of cells as well as permitting movement and division and

facilitating in trafficking and signal transduction (Amos & Amos 1991). However, cytoskeleton structural elements are also known to change in response to low temperature, for example mRNA abundance of actin and tubulin has been shown on multiple occasions to vary with reduction in temperature, as well as the spatial arrangement of the actin microfilaments (Denlinger & Lee 2010). Additionally, cytoskeletal elements have been shown to co-operate closely with molecular chaperones such as heat-shock proteins (Mounier & Arrigo 2002). From a physical viewpoint, remodelling of the cytoskeleton may be advantageous to the evolved cell line in response to increased shear stress that it would be inevitably more prone to than the parental cell line: in equivalent orbital shake flask culture, the increased cell mass will result in a larger centrifugal force against the inner flask surface and surrounding fluid. It has been shown on numerous occasions that the cytoskeleton has a role in protection against shear induced stress and cell damage (Girard & Nerem 1993; Malek & Izumo 1996; Loufrani & Henrion 2008), so it wouldn't be unreasonable to assume a similar scenario has developed in the evolved cell line.

The cytoskeleton is known to support and strengthen the cell membrane, providing a scaffold for it. Cell membrane fluidity has itself been shown to change in organisms that successfully adapt to cold environments. A common method of achieving this is to increase the proportion of unsaturated to saturated fatty acids and to increase fatty acid chain length in the membrane, changes that are accomplished by adjustments in lipid metabolism (Mansilla & Mendoza 2005). Two transcripts that were observed as significantly differentially expressed are exemplary support for membrane fluidity adjustments occurring in the evolved cell line. These are phospholipase A_2 (Pla2g2a) and desaturase (des) which both showed up-regulation in the evolved cell line, with respective fold changes of a staggering 87.98 and 3.56. Phospholipase A_2 has been shown to cold-inducibly regulate membrane unsaturation and fluidity by hydrolysing phospholipids and releasing free fatty acids and lysophospholipids from the membrane (Zeiger *et al.* 2011). Additionally, inhibition of phospholipase A_2 activity has been shown to reduce membrane fluidity (Schaeffer *et al.* 2005). Desaturase, similarly, has been

shown to enhance in expression in response to a decrease in temperature. It works by introducing double bonds into pre-existing saturated fatty acid chains, the proportional increase in unsaturated fatty acids increases the fluidity of the membrane and stabilises it under lower temperatures (Mansilla & Mendoza 2005; Bredeston *et al.* 2011).

Although not significantly different from the mean of all transcripts, mitochondrial transcripts in particular were very close to being so, and had a large bias in the distribution of outliers towards being up-regulated in the evolved cell line. When considering the results from the Seahorse XF24 studies that show vast differences between the two cell lines across multiple mitochondrial functions, it is not surprising to observe interesting distribution of outliers of mitochondrial transcripts in the evolved cell line. Upon individual inspection of some of the more differentially expressed transcripts (i.e. those with a higher fold change) several were flagged due to associations with the adaptive thermogenesis hypothesis. Firstly, Pla2g2a (phospholipase A_2), which has previously been discussed in the context of membrane fluidity and is 87.98 fold higher in the evolved cell line, is also known to have a role in thermogenesis in mitochondria: proton leak through UCP1 is activated by long-chain fatty acids which are released from the mitochondrial membrane by phospholipase A_2 (Harms & Seale 2013). Although UCPs were not found to be differentially expressed, the activity of UCPs and their role in possible thermogenesis in the evolved cell line may have been enhanced as a result of increased phospholipase A_2. Interestingly, other mitochondrial transcripts that are commonly associated with adaptive thermogenesis in brown adipose tissue (BAT) were observed as up-regulated in the evolved cell line. For example, Ca5b which is enriched 20 fold in BAT (Forner *et al.* 2009), was increased 3.68 fold in the evolved cell line, and Fabp4, Lamb3, and Rarres2 were increased 9.45, 3.83 and 3.67 fold, respectively, which are all associated with BAT differentiation (Kang *et al.* 2005; Goralski *et al.* 2007; Lee *et al.* 2013).

The following paragraphs focus on notable findings from KEGG pathway analysis and also from manual inspection of transcripts that exhibited substantial fold

changes or were simply of interest. The latter was performed as, although pragmatically 'omics studies can only be efficiently analysed on a global scale as has mostly been represented so far, there was enticing potential to identify supplementary gene targets that could potentially be used to engineer an improved CHO cell phenotype.

KEGG is a popular pathway analysis programme for analysing 'omic data, permitting 'group testing', where a list of genes can be mapped onto a particular pathway to determine whether certain function and pathways are being regulated by groups of genes (Monoli *et al.* 2006). To perform such analysis, gene lists are entered using a recognised identifier (UniProt IDs), however, we cannot assume that just because certain pathways aren't highlighted as regulated, doesn't mean they aren't being regulated. This is because the annotation of the Affymetrix data set, as previously mentioned, is not complete. This limits the conclusions that can be made; however, we can discuss the pathways/transcripts that have been highlighted as regulated on the maps.

The KEGG pathway map for pathways in cancer was the second most represented pathway map, after metabolism. As can be seen in this pathway (figure 5.24), TNF receptor associated factors (TRAFs) are highlighted as up-regulated in the evolved cell line. TRAFs are know to enable the cell to evade apoptosis (He *et al.* 2004), which is noted on the KEGG pathway map. Related to this, it can also be seen that MDM2 is up-regulated in the parental cell line (or down-regulated in the evolved cell line). p53 is an effector of the pathways for evading apoptosis and MDM2 has inhibitory effects on this effector. There is also up-regulation of effectors involved in insensitivity to anti-growth signals in the evolved cell line. Taken together, these findings could indicate that the evolved cell line has been able to not only avoid apoptosis in, but also has gained the functionality to grow rapidly in the ordinarily adverse (hypothermic) conditions by regulating these pathways.

In some way related to the pathways just discussed, KEGG pathways in cell cycle were investigated to determine whether any changes occurring in these pathways could account for the impressive growth rate characteristic of the evolved cell line

(when considering its growth-halting environment). Cdc20 was observed as up-regulated in the evolved cell line, which is known to be an essential regulator of cell division, having an important role in activating the anaphase promoting complex (APC/C) and appearing to interact with multiple other proteins throughout the cell cycle (Weinstein *et al.* 1994). Additionally, Tfdp2 was up-regulated in the evolved cell line, which is a critical cofactor required for proper cell cycle and controls the progression from G1 to S phase (Chen & Lodish 2014). In contrast, the parental cell line shows an up-regulation of Cdkn2c, a cyclin dependent kinase inhibitor that has been shown to suppress tumorigenesis and cell cycle progression (Stein *et al.* 2013). Another transcript that is mitogenic in nature but is not encompassed in the KEGG cell cycle pathway map is Rps6ka, a transcript that was up-regulated by 5.28 fold in the evolved cell line.

As stated in the results section of this chapter, protein processing in the endoplasmic reticulum was a KEGG pathway that was not particularly highly represented, but due to the large differences between the evolved and parental cell line in their recombinant protein productivities it was investigated nonetheless. The most interesting outcome from this was the finding that ATF4 was up-regulated in the evolved cell line. ATF4 is a central factor in the unfolded protein response (UPR) and overexpression of ATF4 has been shown on numerous occasions to increase the productivity of recombinant protein in CHO cells (Ohya *et al.* 2007; Haredy *et al.* 2011; Edros *et al.* 2013). It has been suggested that ATF4 enhances productivity not by increasing the level of product mRNA but by improving the translation and secretion, without effecting the transcription, of the product mRNA (Haredy *et al.* 2011). Interestingly, ATF4 has also been shown to have a role in thermogenesis (Wang *et al.* 2010).

Lastly, the KEGG pathway map for metabolism was the one that was the most represented in this analysis. The most striking observation from figure 5.23 is the number of changes over multiple areas of metabolism, which demonstrates the power of directed evolution as a strategy for host cell improvement. It is highly likely that it would not be possible to achieve so many and such diverse changes in

expression from classical gene engineering approaches. In particular, lipid metabolism was found to be highly differentially regulated between the evolved and parental cell line. It is hypothesised that this could be related to the pre-discussed role that lipid modification has in both membrane fluidity and thermogenesis (free fatty acids are hydrolysed and activate UCP1). Interesting, ATF4, already demonstrated to have links to high recombinant protein productivity and thermogenesis, has also been shown to regulate lipid metabolism (Wang *et al.* 2010). Areas of amino acid metabolism, too, are seen to be differentially regulated between cell lines: arginine, proline, glycine, serine, and threonine metabolism are marked as up in the evolved cell line, and phenylalanine, tyrosine, tryptophan and lysine biosynthesis are marked as up in the parental cell line. Pathways in cystine and methionine metabolism are differentially regulated in both directions (different pathways up in both the evolved and parental cell line). This is slightly unexpected to see as in the analysis performed using SA Bioscience transcripts sets, amino acid metabolism was seen to be up-regulated in the evolved cell line. However, out of all the transcripts in this set, only 2 transcripts had a fold change of over 2: Odc1 and Ahcy which were up-regulated in the evolved cell line.

When inspecting the actual amino acid flux data, it can be seen that largely the evolved and parental cell lines have similar total cell specific amino acid transport rates at early exponential, mid exponential and stationary phases (figure 5.30). Looking further into the data at the direction of transport, it can be seen that import and export rates are relatively similar between cell lines throughout all culture phases (figure 5.29). However, differences between cell lines were noticed at early exponential phase of growth where import rates of lysine, proline, leucine, valine, isoleucine, arginine, phenylalanine and histidine are much larger in the evolved cell line than the parental cell line. Out of interest (as RNA was extracted at early exponential phase), the transcript data set was searched for transcripts for amino acid transporters and it was found that SLC38A4 (SNAT4) and SLC43A2 (LAT4) were up-regulated in the evolved cell line with increases of 10.24 and 2.20 fold, respectively. SLC38A4 is a transporter of small, neutral amino acid transporter with broad specificity, which could account for the increased import of

histidine and proline into the evolved cell line in early exponential phase (Padmanabhan *et al.* 2012). SLC43A2 is a transporter of branched chain amino acids and could explain the increased import of leucine, isoleucine, valine and phenylalanine into the evolved cell line in early exponential phase (Wang & Holst 2015). Increased arginine import could result from the up-regulation of Odc1, which is known to have a regulatory role in arginine metabolism (Hsieh *et al.* 1990). As already mentioned, some amino acids were imported in the evolved cell line whilst actually being exported by the parental cell line; an interesting example of this is proline. It has been shown on numerous occasions that proline facilitates cold adaptation in plant, insect, bacterial, yeast and mammalian model organisms: There are numerous methods in which proline has been shown to do this including: acting as a cryoprotectant and molecular chaperone to stabilise the structure of proteins in hypothermic conditions, playing a key role in antioxidant systems by reducing ROS concentrations, influencing membrane fluidity and also maintaining osmotic balance (Kumar & Yadav 2009; Ishmayana *et al.* 2011; Hayat *et al.* 2012; Koštál *et al*. 2012; Liu *et al.* 2013). There is also evidence that increased proline uptake is a feature of hypothermia-related hibernation in mammals and recovery during arousal from hibernation (Kirstoffersson & Broberg 1986; Carey & Sills 1992).

It is interesting to note at this point that certain biological anomalies are seen in this dataset, one example being that of tryptophan and threonine which are observed as being produced by cells in the early phase of growth. This is unusual as these amino acids are essential amino acids and are not synthesised by cells. As they error rate of the analytical method was stated as negligible (direct correspondence with Abingdon Health), this puts question over the degree of experimental error introduced prior to the analytical stage. Never-the-less, the fact that, broadly speaking, amino acid flux is the same throughout culture between cell lines is indicative that the evolved cell line has become more biomass efficient, i.e. it is transporting the same amount and a similar profile of amino acids as the parental cell line, yet it is producing a cell that is roughly double in biomass

content and capable of producing significantly more recombinant protein upon transfection.

In line with the previous comment, and as has been noted throughout this discussion, a discernible feature of the evolved cell line is its significant increase in size. Whether this is a physical thermodynamic response to conserve heat, or has occurred for unidentified reasons, it is an impressive biophysical feat that would undoubtedly be difficult to intentionally engineer. During manual inspection of individual differentially expressed transcripts, it was noticed that a Nedd4-binding protein, also known as Prr16, was differentially expressed in the evolved cell line, by over 2 fold. The associated gene product was termed Largen by the authors who discovered its ability to control cell size. They found that overexpression of Prr16 resulted in increased cell size *in vivo* and also showed that Largen was also involved in mitochondrial respiration and increased ATP production, features that are also common to the evolved cell line (Yamamoto *et al.* 2014).

Conclusions and future work

From the results presented and discussed in this chapter, it is clear to see that the evolved cell line has adapted to the hypothermic environment by making changes to multiple cellular functions. We've seen that mitochondrial bioenergetics have been significantly altered, notably with increased proton leak and increased basal respiratory levels which coupled with the decrease in ROS levels in the evolved cell line, support the hypothesis that the evolved cell line is using adaptive non-shivering thermogenesis mechanisms to produce intracellular heat. Additionally, when looking at transcriptomic differences using Affymetrix technology, certain transcripts were up-regulated in the evolved cell line that are known to play roles in cellular thermogenesis, for example, Ca5b, ATF4 and Pla2g2a, the latter of which was up-regulated a staggering 87.98 fold. Large differences in the cytoskeleton were also highlighted and there is evidence that cell membrane fluidity may have been altered as a response to hypothermia.

The fact that there was contradictory findings in amino acid metabolism between KEGG pathway analysis (which mostly showed up-regulation in the parental cell line) and conservation analysis using SA Bioscience transcript sets (which showed up-regulation in the evolved cell line) highlights the need for a standardised transcriptome analysis platform that facilitates the probing of particular functional attributes. *In vitro* analysis of amino acid flux actually showed very little differences in total cell specific transport rates between cell lines, indicating that the evolved cell line has become more 'biomass efficient' when also considering its significant increased production capabilities. This also demonstrates that there would be no obvious need to generate a new, optimised, custom media for the evolved cell line as it has shown similar amino acid requirements as the parental. However, to add to the depth of these findings, it may be interesting to perform a mass balance of the protein biomass in the culture and the consumed amino acids.

It could be beneficial to validate the findings from the Affymetrix analysis with an orthogonal transcriptomic technique, such as RNA-seq. This would ensure additional confidence in the findings presented here. However, for the purposes of identifying gene-engineering targets for overexpression, this could be superfluous and costly. Potential gene engineering targets and their brief justification have been summarised in table 5.6. It is suggested that overexpression of a combination of these targets could result in a CHO cell phenotype that would posses enhanced capability to thrive in hypothermic conditions/ maintain high recombinant protein productivity. Or, should this not be directly possible, the over-expression of such targets could reduce the time frame needed to generate an equivalent evolved cell line, if some degree of hypothermic-adaptation was still required.

Table 5.6 Potential gene targets and brief justification for their use.

Gene target	Summary of justification
Pla2g2a	Largely up-regulated in the evolved cell line, has a role in membrane fluidity and adaptive non-shivering thermogenesis
Des	Up-regulated in the evolved cell line, known to increase membrane fluidity which often occurs as a hypothermic modification
Ca5b	Largely up-regulated in BAT and is up-regulated in the evolved cell line, thought to have a role in thermogenesis
Fabp4	Largely up-regulated in the evolved cell line, associated with heat-generating phenotypte of BAT
Lamb3	Largely up-regulated in the evolved cell line, associated with heat-generating phenotypte of BAT
Rarres2	Largely up-regulated in the evolved cell line, associated with heat-generating phenotypte of BAT
TRAFs	Up-regulated in the evolved cell line, have roles in cell cycle including evading apoptosis
Cdc20	Up-regulated in the evolved cell line, roles in cell cycle including promoting anaphase
Tfdp2	Up-regulated in the evolved cell line, roles in cell cycle including progression from G1 to S phase
ATF4	Up-regulated in the evolved cell line, known to have roles in lipid metabolism and thermogenesis, is also known to enhance productivity in CHO cells
Odc1	Up-regulated in the evolved cell line, has a regulatory role in arginine metabolism
SLC38A4	Up-regulated in the evolved cell line, is a transporter of small neutral amino acids
SLC43A2	Up-regulated in the evolved cell line, is a transporter of branched chain amino acids

Other suggestions for future work include investigating the size and number of mitochondria in the evolved cell line compared to the parental to determine if either of these factors have contributed to the improved mitochondrial bioenergetics observed in evolved cell line. Additionally, assessment of membrane fluidity could be investigated to see if this correlates with the indicative findings from the transcriptomic analysis. Furthermore, advances in the recently developed, but not widely available, so-called “nanothermometers” could allow for the direct measurement of internal cellular temperature, which would enable the adaptive non-shivering thermogenesis hypothesis to be explicitly confirmed or rejected depending on whether the evolved cells are indeed internally warmer than their surrounding hypothermic environment (Sokolov 2013; Wang *et al.* 2015).

A fundamental conclusion of this chapter would be that directed evolution as a strategy for cell line improvement is demonstrated here to be an extremely powerful one, achieving global cellular modifications that would undoubtedly not be conceivable through the current classical gene engineering approaches.

Chapter 6:

Concluding remarks and recommendations for future work

This chapter summarises the conclusions drawn throughout this thesis and comments on how the research presented contributes to the wider field of biopharmaceutical production. Suggested directions for future work are also considered here.

6.1 A summary of conclusions drawn from the research chapters of this thesis

This thesis has been presented in a chronological and sequential manner, with chapter 3 forming the basis of the subsequent work, and chapters 4 and 5 drawing on the results of the previous, taking these findings forward to be investigated from a different perspective. In chapter 3 it was shown that the average change in cell growth rate per day could be improved by the manipulation of simple in vitro parameters: seeding density and passage frequency. This information could be useful in directed evolution experiments where rapid increases in growth rate are required, potentially facilitating faster adaptation to particular environments or stressors. The remaining work presented in chapter 3 focussed on the adaptation of CHOK1SV host cells to hypothermia via long-term culturing at 32°C. The purpose of this study was to generate a host cell culture that could grow rapidly at 32°C whilst retaining the high production abilities that are observed during a two-phase 'cold-shock' strategies where cultures are firstly grown at 37°C to provide

initial rapid proliferation to achieve high culture density and then secondly the temperature is reduced to 32°C and proliferation is halted. As previously explained, this strategy has regularly been associated with multi-fold increased in productivity (Chuppa *et al.* 1997; Slikker *et al.* 2001; Vergara *et al.* 2014). However, titre could be improved further if cells could continue to proliferate at 32°C, which would also negate the need for a temperature phase shift strategy completely as cells could constantly be grown at 32°C. These reasons, coupled with the fact that there is no evidence of successfully adapting a host CHOK1SV cell line (only limited success with stable cell lines) to hypothermia in the literature (Yoon *et al.* 2006; Sunley *et al.* 2008), provided the rationale for this study. As was shown in chapter 3, hypothermia-adapted cultures were successfully attained through long-term adaptive evolution. Not only this, but other interesting phenotypes were observed in these hypothermia-adapted cultures such as large cell volume and corresponding increases in total cell protein biomass and RNA content. However, by this point, investigation into the productivity capabilities of these hypothermia-adapted cultures was still needed and subsequently assessed in chapter 4.

As stated, the purpose of the work described in chapter 4 was to investigate the functional attributes of the hypothermia-adapted cell cultures. The functional attributes referred to here relate essentially to those that would be of direct interest to the biopharmaceutical industry, fundamentally, addressing the question of whether the hypothermia-adapted cultures have the potential to make a suitable industrial host cell line for producing recombinant protein products. The hypothermia-adapted cultures were compared to their parental counterparts throughout. Firstly it was shown that, in terms of transient SEAP productivity, the hypothermia-adapted cell cultures (at 32°C) exhibited an impressive ~100% increase on the parental cultures (at 37°C), and also importantly showed a marked increase on the amount of SEAP produced by the parental cells that had undergone a 'cold-shock' (at 32°C) post transfection. Because of this exciting result, the hypothermia-adapted cultures were investigated in terms of transfection efficiency using transient GFP transfection and here it was again seen that the hypothermia-adapted cultures outperformed their parental counterparts. From here, a single

candidate hypothermia-adapted culture (and its parental counterpart) was taken forward for more extensive productivity analysis. Being simply termed the evolved and parental cell lines from here on, both were tested for their productivity of cB72.3 (an IgG4 mAb) and Enbrel (a difficult-to-express IgG1 Fc-fusion protein) in a long-term transient lipofection platform. The 10-day yields from this study showed that, again, the highest producing titre was achieved using the evolved cell line cultured at 32°C, and moreover this was true for both cB72.3 and Enbrel. As a result of accumulating promising transient productivity data using the evolved cell line, the next logical functional assessment was to establish stable cell lines. Separate stable pools producing cB72.3 or Enbrel were formed from both evolved and parental cell lines and again, the evolved cell line outperformed the parental in terms of titre of both proteins. Additionally, the evolved cell line unusually exhibited better titres of the difficult-to-express Enbrel than it did cB72.3, showing promise that this cell line could be used as a candidate cell line for producing higher titres of other difficult-to-express protein products. A superficial product-quality analysis was also performed in terms of glycan profiling of cB72.3 and Enbrel produced by the two cell lines, both transiently and stably. The central result from this study was that glycan profiles are largely similar between the evolved and parental cell lines. This is valuable information as it shows that glycan processing capabilities have not been altered as a result of the long-term evolution process that was necessary to attain the hypothermia-adapted phenotype.

Now being confident that the evolved cell line is superior to the parental cell line in terms of its functional characteristics, a broad and extensive investigation into the mechanisms that could be underpinning these improved functional attributes was undertaken. This work formed the body of results presented in chapter 5. Much of this work was associated with the hypothesis that the evolved cell line could be coping with the stress of hypothermia by generating localised heat within the cell by processes such as *adaptive non-shivering thermogenesis*. To investigate this theory, a combination of specific hypothesis-testing experiments (for example those that investigated mitochondrial capacity and oxidative stress) were performed in synergy with more global exploration experiments (such as

Affymetrix® differential gene expression analysis and amino acid flux through culture). As is discussed in more detail in chapter 5, results from this work showed some interesting support for certain adaptation theories. For example, the evolved cell line showed substantially lower levels of cellular reactive oxygen species (ROS) compared to the parental cell line and there was evidence that the evolved cell line exhibits increased inner mitochondrial membrane permeability. Both of these results, coupled with the increased maximal respiratory capacity of the evolved cell line, are all key features of adaptive non-shivering thermogenesis, suggesting the cell could indeed be using this mechanism to generate heat. Indications of support for this theory were also found when comparing transcript regulation between the two cell lines: Pla2g2a (phospholipase A_2), which has a direct role in adaptive non-shivering thermogenesis, was found to be up-regulated in the evolved cells by a staggering 87.98 fold (Harms & Seale 2013). Interestingly, this transcript (along with several others that were up-regulated) is known to increase membrane fluidity and stability, which is a common cold-adaptation strategy (Schaeffer *et al.* 2005). Likewise, changes to membrane fluidity could also be inferred by the large differences in cytoskeletal transcripts between cell lines. Interesting differences were also observed in the cell cycle pathways which to some degree would be expected given that under normal circumstances hypothermia arrests cell cycle progression. In relation to the enhanced titres observed in the evolved cell line, it was noticed that ATF4, which has been shown on numerous occasions to increase the productivity of recombinant protein in CHO cells (Ohya *et al.* 2007; Haredy *et al.* 2011; Edros *et al.* 2013), was significantly up-regulated in the evolved cell line transcript dataset. In addition to this, up-regulated transcripts were also identified as being potentially responsible for the increased evolved cell line cell size.

The amino acid flux analysis in this chapter showed that, largely, the evolved and parental cell lines have similar total cell specific amino acid transport rates at early exponential, mid exponential and stationary phases. In addition to this, it was shown that import and export rates are relatively similar between cell lines throughout all culture phases, with the exception of some larger differences at

early exponential phase. Some amino acid-specific differences were observed, an interesting example given in the large import of proline in the evolved cell line whilst the parental cell line largely exported this. This was of particular bearing due to the numerous associations between proline uptake and its role in cold-adaptation, specifically by: acting as a cryoprotectant and molecular chaperone to stabilise the structure of proteins in hypothermic conditions, playing a key role in antioxidant systems by reducing ROS concentrations, influencing membrane fluidity and also maintaining osmotic balance (Kumar & Yadav 2009; Ishmayana *et al.* 2011; Hayat *et al.* 2012; Koštál *et al*. 2012; Liu *et al.* 2013).

Overall, the compilation of the findings in these research chapters show chiefly that the adaptation of hypothermia-adapted host cell line has been more successful than previous attempts that have endeavoured to adapt already stably producing cell lines. Not only this, the evolved cell lines created in this study retain high productivity through both the evolution process and the process of stable cell line generation. An investigation into the understanding of the key differences between the evolved cell line and the parental has been described and there is potential to use this information in future cell line development strategies.

6.2 A summary of future work recommendations

Although specific propositions for future work have already been suggested at the end of each research chapter, a brief summary of those are given here. One primary and basic recommendation for future work includes attempting to evolve a hypothermia-adapted cell line from an alternative host CHO cell line, for example CHO-S or DG44 cells, and if successful subsequently assessing their productivity and ability to generate stably producing cell lines. This would confirm whether the capacity to adapt to hypothermia is common across multiple parental host cell lines or unique to CHOK1SV, which contains the GS selection system. Other cell lines contain different selection systems meaning they will have varying metabolic requirements and they may require bespoke culture medium (i.e. not the CD CHO media used for this project). These factors indicate that other cell lines may respond differently, slower or faster, when subjected to long-term adaptation to

hypothermia. From a mechanistic characterisation point of view, it could be suggested that both the parental and evolved cell lines undergo karyotyping to determine whether there are any major chromosomal changes that have occurred either as a result of, or to facilitate, the adaptation process, as it is know that aneuploidy has been strongly associated with stress adaptation (Derouazi *et al.* 2006; Chen *et al.* 2012). Although chapter 4 has demonstrated that the evolved cell line has out-performed the parental cell line in terms of industrial functionality, a full industrial-grade technology readiness level (TRL) assessment may be beneficial before recommending this cell line for use in industrial biopharmaceutical production. Other studies that could be conducted to corroborate the observed industrial advantages of the evolved cell line include testing the production of other difficult-to-express proteins and those that are prone to aggregation and also testing the ability to scale-up to bioreactors or equivalent large scale vessels (a necessity for an industrial cell line). It could also be beneficially to preform clonal selection on the stable pools to isolate high producing clones.

In terms of recommended work that could build upon the findings of the mechanistic analysis (chapter 5), it could be valuable to validate the findings from the Affymetrix® study by an alternative means of differential gene expression analysis, such as RNA-Seq. Once this has been performed, any one or combination of the genes already suggested (see table 5.6) could be used as gene engineering targets for overexpression. Another suggestion could be to investigate the size and number of mitochondria in the evolved cell line compared to the parental to determine if either of these factors have contributed to the improved mitochondrial bioenergetics observed in evolved cell line. Finally, as there are many indications that cell membrane fluidity may have increased in the evolved cell line as a direct result of adaptation to hypothermia, this could be directly measured using commercially available kits (e.g. available from Abcam (Cambridge, UK) which works by measuring the ratio of monomer to excimer fluorescence).

6.3 Impact of this research on the wider field of biopharmaceutical production

The work presented in this thesis has demonstrated a novel approach to attaining a high producing, hypothermia-adapted cell line. As has been iterated throughout, any other published attempts in this vein have used cell lines that were stably producing recombinant protein prior to hypothermia adaptation and were ultimately unsuccessful either in terms of low final productivity (Yoon *et al.* 2006), or in the inherent health of the adapted cells (Sunley *et al.* 2008). Not only has the work here resulted in a potential new cell line platform that has exhibited improved manufacturing properties compared to the parental cell line, it has also offered insight into possible gene engineering targets that could be used in future cell line development strategies. However, the vast and global changes between the evolved and parental cell lines that have been observed as a result of the evolution process demonstrate the power of directed evolution as a strategy for cell line engineering compared to classical gene engineering and overexpression techniques. Such classical techniques are highly unlikely, at least within the bounds of current technology, to generate a cell line that possesses the vast amount of unique features and transcript changes that have been generated in this research using directed evolution alone. This work has strong potential to lead to more efficient and economical industrial manufacture of therapeutics through the reduced production costs and higher titres that the evolved cell line could provide. Whilst this would inevitably be of commercial value, it also perhaps more important to consider that the most significant beneficiary of this work could potentially be a patient who could soon acquire access to therapeutic protein treatment where it may have formerly not been possible.

This page is intentionally left blank.

References

Alberts, B., Johnson, A., Lewis, J., Raff, M., Roberts, K. & Walter, P. (2002). Molecular Biology of the Cell, 4th edition. Garland Science, New York, USA.

Ames, B. N., Shigenaga, M. K. & Hagen, T. M. (1993). Oxidants, antioxidants and the degenerative diseases of aging. *Proc Natl Acad Sci USA.,* **90,** 7915-7922.

Amos, L. A. & Amos, W. G. (1991). Molecules of Cytoskeleton. Gilford Press, New York, USA.

Anastacio, M. M., Kanter, E. M., Makepeace, C. M., Keith, A. D., Zhang, H., Schuessler, R. B., Nichols, C. G. & Lawton, J. S. (2013). Relationship between mitochondrial matrix volume and cellular volume in response to stress and the role of ATP-sensitive potassium channel. *Circulation,* **128,** S130-5.

Aranibar, N., Borys, M., Mackin, N., Ly, V., Abu-Absi, S., Niemitz, M., Schilling, B., Li, Z., Brock, B., Russell, R. J. II, Tymiak, A., & Reily, M. D. (2011). NMR-based metabolomics of mammalian cell and tissue cultures. *J Biomol NMR.*, **49,** 195-206.

Ballou, L. M. & Lin, R. Z. (2008). Rapamycin and mTOR kinase inhibitors. *J Chem Biol.,* **1,** 27-36.

Barton, N. H., Briggs, D. E. G., Eisen, J. A., Goldstein, D. B. & Patel, N. H. (2007). Evolution, 1st edition. Cold Spring Harbor Laboratory Press, New York, USA.

Becker, J., Hackl, M., Rupp, O., Jakobi, T., Schneider, J., Szczepanowski, R., Bekel, T., Borth, N., Goesmann, A., Grillari, J., Kaltschmidt, C., Noll, T., Puhler, A., Tauch, A. & Brinkrolf, K. (2011). Unraveling the Chinese hamster ovary cell line transcriptome by next-generation sequencing. *J Biotechnol,* **156,** 227-235.

Becerra, S., Berrios, J., Osses, N. & Altamirano, C. (2012). Exploring the effect of mild hypothermia on CHO cell productivity. *Biochemical Engineering Journal,* **60,** 1-8.

Bertier, L., Leus, L., D'hondt, L. D., de Cock, A. W. A. M. & Höfte, M. (2013). Host Adaptation and Speciation through Hybridization and Polyploidy in *Phytophthora*. *PLoSONE, **8,*** e85385.

Bilanges, B. & Vanhaesebroek, B. (2010). A new tool to dissect the function of P70 S6 kinase. *Biochem J.,* **431,** e1-e3.

Bio-Rad 'Post-Transfection Analysis of Cells' Bulletin 5969, (2010).

Bork, K., Horstkorte, R. & Weidemann, W. (2009). Increasing the sialylation of therapeutic glycoproteins: The potential of the sialic acid biosynthetic pathway. *Journal of Pharmaceutical Sciences,* **98,** 3499-3508.

Bort, J. A. H., Hackl, M., Höflmayer, H., Jadhav, V., Harreither, E., Kuman, N., Ernst, W., Hrillari, J. & Borth, N. (2012). Dynamic mRNA and miRNA profiling of CHO-K1 suspension cultures. *Biotechnology Journal,* **7,** 500-515.

Bort, J. A., Stern, B. & Borth, N. (2010). CHO-K1 host cells adapted to growth in glutamine-free by FACS-assisted evolution. *Biotechnol J.,* **5,** 1090-1097.

Borth, N., Mattanovich, D., Kunert, R. & Katinger, H. (2005). Effect of Increased Expression of Protein Disulfide Isomerase and Heavy Chain Binding Protein on Antibody Secretion in a Recombinant CHO Cell Line. *Biotechnol Prog.*, **21,** 106-111.

Bredeston, L. M., Marciano, D., Albanesi, D., De Mendoza, D. & Delfino, J. M. (2011). Thermal Regulation of Membrane Lipid Fluidity by a Two-Component System in *Bacillus subtilis*. *Biochemistry and Molecular Biology Education,* **39,** 362-366.

Brinkrolf, K., Rupp, O., Laux, H., Kollin, F., Ernst, W., Linke, B., Kofler, R., Romand, S., Hesse, F., Budach, W. E., Galosy, S., Muller, D., Noll, T., Wienberg, J., Jostock, T., Leonard, M., Grillari, J., Tauch, A., Goesmann, A., Helk, B., Mott, J. E., Puhler, A. & Borth, N. (2013). Chinese hamster genome sequenced from sorted chromosomes. *Nat Biotechnol.*, **31,** 694-695.

Butler, M. (2007). Cell Culture and Upstream Processing. Taylor & Francis Group, New York, USA.

Butler, M. & Meneses-Acosta, A. (2012). Recent advances in technology supporting biopharmaceutical production from mammalian cells. *Appl Microbiol Biotechnol.,* **96,** 885-894.

Cannon, B. & Nedergaard, J. (2011). Nonshivering thermogenesis and its adequate measurement in metabolic studies. *Journal of Experimental Biology,* **214,** 242-253.

Carey, H. V. & Sills, N. S. (1992). Maintenance of intestinal nutrient transport during hibernation. *Regulatory, Integrative and Comparative Physiology,* **263,** R517-R523.

Carlage, T., Kshirsagar, R., Zang, L., Janakiraman, V., Hincapie, M., Lyubarskaya, Y., Weiskopf, A. & Hancock, W. S. (2012). Analysis of dynamic changes in the proteome of a Bcl-XL overexpressing Chinese hamster ovary cell culture during exponential and stationary phases. *Biotechnol. Pro.,* **28,** 814-823.

Campbell, N. A. & Reece, J. B. (2004). Biology, 7th edition. Pearson, Cambridge, UK.

Canitrot, Y., Frechet, M., Servant, L., Cazaux, C. & Hoffmann, J. S. (1999). Overexpression of DNA polymerase beta: a genomic instability enhancer process. *FASEB J.,* **13,** 1107-1111.

Carmen, S. & Jermutus, L. (2002). Concepts in antibody phage display. *Briefings in functional genomics and proteomics,* **1,** 189-203.

Chambers, J. M., Cleveland, W. S., Kleiner, B. and Tukey, P. A. (1983). Graphical Methods for Data Analysis. Wadsworth & Brooks/Cole, Pacific Grove, California, USA.

Chen, C. & Lodish, H. F. (2014). Global analysis of induced transcription factors and cofactors identifies Tfdp2 as an essential coregulator during erythropoiesis. *Exp Hematol.,* **42,** 464-476.

Chen, G., Bradford, W. D., Seidel, C. W. & Li, R. (2012). Hsp90 Stress Potentiates Rapid Cellular Adaptation through Induction of Aneuploidy. *Nature,* **482,** 246-250.

Chuppa, S., Tsai, Y. S., Yoon, S., Shackleford, S., Rozales, C., Bhat, R., Tsay, G., Matanguihan, C., Konstantinov, K. & Naveh, D. (1997). Fermenter temperature as a tool for control of high-density perfusion cultures of mammalian cells. *Biotechnol Bioeng.,* **55,** 328-338.

Coco-Martin, J. M. & Harmsen. M. M. (2008). Review of Therapeutic Protein Expression By Mammalian Cells. *BioProcess International,* **S4,** 28-33.

Condreay, J. P., Witherspoon, S. M., Clay, W. C. & Kost, T. A. (1998). Transient and stable gene expression in mammalian cells transduced with a recombinant baculovirus vector. *PNAS,* **96,** 127-132.

Croset, A., Delafosse, L., Gaudry, J. P., Arod, C., Glez, L., Losberger, C., Begue, D., Krstanovic, A., Robert, F., Vilbois, F., Chevalet, L. & Antonsson, B. (2012). Differences in the glycosylation of recombinant proteins expressed in HEK and CHO cells. *J Biotechnol.*, **161,** 336-348.

Damiani, R., Almeida, B. E., Oliveira, J. E., Bartolini, P. & Ribela, M. T. (2013). Enhancement of human thyrotropin synthesis by sodium butyrate addition to serum-free CHO cell culture. *Appl Biochem Biotechnol.,* **171,** 1658-1672.

Darwin, C. (1859). On the Origin of Species by Means of Natural Selection, or the Preservation of Favoured Races in the Struggle for Life. John Murray, London, UK

Davies, S. L., Lovelady, C. S., Grainger, R. K., Racher, A. J., Young, R. J. & James, D. C. (2013). Functional heterogeneity and heritability in CHO cell populations. *Biotechnology and Bioengineering,* **110,** 260-274.

de Meis, L. (2001). Role of the Sarcoplasmic Reticulum Ca^{2+}-ATPase on Heat Production and thermogenesis. *Bioscience Reports,* **21,** 113-137.

Denlinger, D. L. & Lee, Jr., R. E. (2010). Low Temperature Biology of Insects. Cambridge University Press, Cambridge, UK.

Derouazi, M., Martinet, D., Besuchet Schmutz, N., Flaction, R., Wicht, M., Bertschinger, M., Hacker, D. L., Beckmann, J. S. & Wurm, F. (2006). Genetic characterization of CHO production host DG44 and derivative recombinant cell lines. *Biochem Biophys Res Commun.,* **340,** 1069-1077.

Desler, C., Hansen, T. L., Frederiksen, J. B., Marcker, M. L., Sing, K. K. & Juel Rasmussen, L. (2012). Is there a link between mitochondrial reserve capacity and aging? *J Aging Res.,* **2012,** ID 192503

DeYoung, M. P., Horak, P., Sofer, A., Sgroi, D. & Ellisen, L. W. (2008). Hypoxia regulates TSC1/2-mTOR signaling and tumor suppression through REDD1-mediated 14-3-3 shuttling. *Genes & Development,* **22,** 239-251.

Dorai, H., Kyung, Y. S., Ellis, D., Kinney, C., Lin, C., Jan, D., Moore, G. & Batenbaugh, M. J. (2009). Expression of anti-apoptosis genes alters lactate metabolism of Chinese Hamster Ovary cells in culture. *Biotechnology and Bioengineering,* **103,** 592-608.

Doran, P. M. (1995). Bioprocess Engineering Principles. Academic Press Limited, London, UK.

Dreesen, I. A. J. & Fussenegger, M. (2010). Ectopic Expression of human mTOR Increases Viability, Robustness, Cell Size, Proliferation and Antibody Production of Chinese Hamster Ovary Cells. *Biotech Bioeng.,* **108,** 853-866.

Edros, R. Z., McDonnell, S. & Al-Rubeai, M. (2103). Using Molecular Markers to Characterize Productivity in Chinese Hamster Ovary Cell Lines. *PLoSONE,* **8,** e75935.

Evers, P. (2010). The Future of the Biological Market. Business Insights March 2010, 1-171.

Ewens, W. (2004). Mathematical Population Genetics I. Theoretical Introduction. Interdisciplinary Applied Mathematics. Springer-Verlag, Heidelberg, Germany.

Fan, L., Kadura, I., Krebs, L. E., Hatfield, C. C., Shaw, M. M. & Frye, C. C. (2012). Improving the efficiency of CHO cell line generation using glutamine synthetase gene knockout cells. *Biotechnol Bioeng,* **109,** 1007-1015.

Fan, X., Ross, D. D., Arakawa, H., Ganapathy, V., Tamai, I. & Nakanishi, T. (2010). Impact of system L amino acid transporter 1 (LAT1) on proliferation of human ovarian cancer cells: a possible target for combination therapy with anti-proliferative aminopeptidase inhibitors. *Biochem Pharmacol.,* **15,** 811-818.

FDA Q5A Guidance Document (1998): Viral Safety Evaluation of Biotechnology Products Derived from Cell Lines of Human or Animal Origin, Federal Register, **63,** 51074. Available at http://www.fda.gov/cder/guidance/Q5A-fnl.PDF.

Federenko, A., Lishko, P. V. & Kirichok, Y. (2012). Mechanism of fatty-acid dependent UCP1 uncoupling in brown fat mitochondria. *Cell,* **151,** 400-413.

Ferrer-Miralles, N., Domingo-Espín, J., Corchero, J. L., Vázquez & Villaverde, A. (2009). Microbial factories for recomninant pharmaceuticals. *Microbial Cell Factories,* **8,** 17.

Fiore, J. V., Olson, W. P. & Holst, S. L. (1980). Methods of Plasma Protein Fractionation, Academic Press, New York, 239.

Fisher, R. A. (1930). The Genetical Theory of Natural Selection. Clarendon Press, Oxford, UK.

Forner, F., Kumar, C., Luber, C. A., Fromme, T., Klingenspor, M. & Mann, M. (2009). Proteome Differences between Brown and White Fat Mitochondria Reveal Specialized Metabolic Functions. *Cell Metabolism,* **10,** 324-335.

Fuller, B. J. (2003). Gene expression in response to low temperatures in mammalian cells: a review of current ideas. *CryoLetters,* **24,** 95-102.

Futuyma, D. J. (1998). Evolutionary Biology, 3d edition. Sinauer Associates Inc., Sunderland, MA, USA.

Gagnon, P. (1995). Purification Tools for Monoclonal Antibodies. Validated Biosystems, Tucson, Arizona, USA

Goralski, K. B., McCarthy, T. C., Hanniman, E. A., Zabel, B. A., Butcher, E. C., Parlee, S. D., Muruganandan, S. & Sinal, C. J. (2007). Chemerin, a Novel Adipokine That Regulated Adipogenesis and Adipocyte Metabolism. *The Journal of Biological Chemistry,* **282,** 28175-28188.

Gualandi-Signorini, A. M. & Giorgi, G. (2001). Insulin formulations—a review. *Eur Rev Med Pharamacol Sci,* **5,** 73-83.

Geisse, S. & Fux, C. (2009). Chapter 15 Recombinant Protein Production by Transient Gene Transfer into Mammalian Cells. *Methods in Enzymology,* **463,** 223-238.

Gillespie, J. H. (2001). Is the population size of a species relevant to its evolution? *Evolution,* **55,** 2161-2169.

Girard, P. R. & Nerem, R. M. (1993). Endothelial cell signaling and cytoskeletal changes in response to shear stress. *Front Med Biol Eng.,* **5,** 31-36.

Goetze, A. M., Liu, Y. D., Zhang, Z., Shah, B., Lee, E., Bondarenko, P. V. & Flynn, G. C. (2011). High-mannose glycans on the Fc region of therapeutic IgG antibodies increase serum clearance in humans. *Glycobiology,* **21,** 949-959.

Goldhaber, S. L., Markis, J. E., Meyerovitz, M. F., Kim, D., Dawley, D. L., Sasahara, A., Vaughan, D. E., Selwyn, A. P., Loscalzo, J., Kessler, C. M., Sharma, G. C. R. K., Grossbard, E. B. & Braunwald, E. (1986). Acute pulmonary embolism treated with tissue plasminogen activator. *The Lancet,* **328,** 886-889.

Goodman, M. (2009). Sales of biologics to show robust growth through to 2013. *Nat Rev Drug Discov.,* **8,** 837.

Graf, L. H. & Chasin, L. A. (1982). Direct demonstration of genetic alterations at the dihydrofolate reductase locus after gamma irradiation. *Mol. Cell. Biol.,* **2,** 93-96.

Grasso, L., Kline, J., Chao, Q., Routhier, E., Ebel, W., Sass, P. M., & Nicolaides, N. C. (2004). Enhancing Therapeutic Antibodies and Titer Yields of Mammalian Cell Lines. *Bioprocess International,* **2,** 58-64.

Haredy, A. M., Nishizawa, A., Honda, K., Ohya, T., Ohtake, H. & Omasa, T. (2011). ATF4 over-expression increased IgG1 productivity in Chinese hamster ovary cells. *BMC Proceedings,* **5,** O11.

Harms, M. & Seale, P. (2013). Brown and beige fat: development, function and therapeutic potential. *Nature Medicine,* **19**, 1252-1263.

Hayat, S., Hayat, Q., Alyemeni, M. N., Wani, A. S., Pichtel, J. & Ahmad, A. (2012). Role of proline under changing environments. *Plant Signal Behav.,* **7,** 1456-1466.

Hayward, J. S. & Lisson, P. A. (1992). Evolution of brown fat: its absence in marsupials and monotremes. *Canadian Journal of Zoology,* **70,** 171-179.

He, B., Chadburn, A., jou, E., Schattner, E. J., Knowles, D. M. & Cerutti, A. (2004). Lymphoma B Cells Evade Apoptosis through the TNF Family Members BAFF/BLyS and APRIL. *The Journal of Immunology,* **172,** 3268-3279.

Himms-Hagen, J. (1984). Nonshivering thermogenesis. *Brain Res Bull.,* **12,** 151-160.

Hsieh, J. T., Denning, M. F., Heidel, S. M. & Verma, A. K. (1990). Expression of human chromosome 2 decarboxylase gene in ornithine decarboxylase-deficient Chinese hamster ovary cells. *Cancer Res.,* **15,** 2239-2244.

Hu, W-S. (2012). Cell Culture Bioprocess Engineering, 1st edition. Wei-Shu Hu, University of Minnesota, USA.

Ishmayana, S., Learmonth, R. P. & Kennedy, U. J. (2011). Effects of supplementation with L-proline or inositol on yeast membrane fluidity and ethanol tolerance. 12 Conference on Methods and Applications of Fluorescence Spectroscopy, Imaging and Probes (MAF12), 11-14th Sept 2011, Strasbourg, France.

Jayapal, K. P., Wlaschin, K. F., Hu, W. S. & Yap, M. G. S. (2007). Recombinant protein therapeutics from CHO cells – 20 years and counting. CHO consortium. SBE Special Edition (October 1, 2007).

Jefferis, R. (2007). Antibody therapeutics: isotype and glycoform selection. *Expert Opin Biol Ther.,* **7,** 1401-1413.

Jenkins, N., Parekh, R. B. & James, D. C. (1996). Getting the glycosylation right: implications for the biotechnology industry. *Nature Biotechnol.,* **14,** 975-981.

Johnson, I. S. 1983. Human insulin for recombinant DNA technology. *Science,* **219,** 632-637.

Jones, D., Kroos, N., Anema, R., Van Montfort, B., Vooys, A., Van Der Kraats, S., Van Der Helm, E., Smits, S., Schouten, J., Brouwer, K., Lagerwerf, F., van Berkel, P., Opstelten, D. J., Logtenberg, T. & Bout, A. (2003). High-level expression of recombinant IgG in the human cell line per.c6. *Biotechnol Prog,* **19,** 163–168.

Jones, P. T., Dear, P. H., Foote, J., Neuberger, M. S. & Winter, G. (1986). Replacing the complementarity- determining regions in a human antibody with those from a mouse. *Nature* **321,** 522–525.

Kandpal, R. P., Saviola, B. & Felton, J. (2009). The era of 'omics unlimited.

Biotechniques, **46,** 351.

Kang, S., Bajnok, L., Longo, K. A., Petersen, R. K., Hansen, J. B., Kristiansen, K. & MacDougald, O. A. (2005). Effects of Wnt signaling on Brown Adipocyte Differentiation and Metabolism Mediated by PGC-1a. *Mol Cell Biol.,* **25,** 1272-1282.

Kao, F. T. & Puck, T. T. (1968) Genetics of Somatic mammalian cells, VII. Induction and isolation of nutritional mutants in Chinese hamster cells. *Proc. Natl. Acad. Sci. U S A,* **60,** 1257-1281.

Kaufmann, H., Mazur, X., Fussenegger, M. & Bailey, J. E. (1999). Influence of low temperature on productivity, proteome and protein phosphorylation of CHO cells. *Biotechnol Bioeng.,* **63,** 573-582.

Keightley, J. A., Shang, L. & Kinter, M. (2004). Proteomic Analysis of Oxidative Stress-resistant Cells. *Molecular & Cellular Proteomics,* **3.2,** 167-175.

Kelley, B. (2009). Industrialization of mAb production technology. The bioprocessing industry at a crossroads. *MAbs,* **1,** 443-452.

Kim, S. J., Kim, N. S., Ryu, C. J., Hong, H. J. & Lee, G. M. (1998). Characterization of chimeric antibody producing CHO cells in the course of dihydrofolate reductase mediated gene amplification and their stability in the absence of selective pressure. *Biotechnol. Bioeng.,* **58**: 73–84.

Köhler G. & Milstein C. (1975). Continuous cultures of fused cells secreting antibody of predefined specificity. *Nature,* **256,** 405-497.

Kokoszka, J. E., Coskun, P., Esposito, L. A. & Wallace, D. C. (2001). Increased mitochondrial oxidative stress in he Sod2(+/-) mouse results in the age-related decline of mitochondrial function culminating in increased apoptosis. *Proc Natl Acad Sci USA.,* **98,** 2278-2283.

Koštál, V., Šimek, P., Zahradníčková, H., Cimlová, J. & Štetina. (2012). Conversion of the chill susceptible fruit fly lava (*Drosophila melanogaster*) to a freeze tolerant organism. *PNAS,* **109,** 3270-3274.

Kozak, L. P. & Young, M. E. (2012). Heat from calcium cycling melts fat. *Nature Medicine,* **18,** 1458-1459.

Kretzschmar, T. & Rüdent, T. V. (2002). Antibody discovery: phage display. *Current Opinion in Biotechnology,* **13,** 598-602.

Kristoffersson, R. & Broberg, S. (1968). Free amino acids in blood serum of hedgehogs in deep hypothermia and after spontaneous arousals. *Experientia,* **24,** 148-150.

Kumar, N., Gammell, P., Meleady, P., Henry, M & Clynes, M. (2008). Differential protein expression following low temperature culture of suspension CHO-K1 cells. *BMC Biotechnol.,* **8,** 42.

Kumar, V. & Yadav, S. K. (2009). Proline and betaine provide protection to antioxidant and methylglyoxal detoxification systems during cold stress in *Camellia sinensis* (L.) O. Kuntze. (2009). *Acta Physiol Plant.,* **31,** 261-296.

Lai, T., Yang, Y. & Ng, S. K. (2013). Advances in Mammalian Cell Line Development Technologies for Recombinant Protein Production. *Pharmaceuticals (Basel), 6,* 579-603.

Langer, E. S. & Rader, R. A. (2014). Continuous Bioprocessing and Perfusion: Wider Adoption Coming as Bioprocessing Matures. *BioProcessing Journal,* **13,** 43-49.

Le, H., Vishwanathan, N., Jacob, N. M., Gadgil, M. & Hu, W-S. (2015). Cell line development for biomanufacturing processes: recent advances and an outlook. *Biotechnol Lett.*, **37,** 1553-1564.

Le, H., Vishwanathan, N., Kantardjieff, A., Doo, I., Srienc, M., Zheng, X., Somia, N. & Hu, W-S. (2013). Dynamic gene expression for metabolic engineering of mammalian cells in culture. *Metab. Eng.,* **20,** 212-220.

Lee, H-J., Jang, M., Kim, H., Kwak, W., Park, W., Hwang, J. Y., Lee, C-K., Jang, G. W., Park, M. N., Kim, H-C., Jeong, J. Y., Seo, K. S., Kim, H., Cho, S. & Lee, B-Y. (2013). Comparative Transcriptome Analysis of Adipose Tissue Reveals that ECM-Receptor Interaction Is Involved in the Deopt-Specifc Adipogenesis in Cattle. *PLoS ONE,* **8,** 66267.

Lengauer, C., Kinzler, K. W. & Vogelstein, B. (1998). Genetic instabilities in human cancers. *Nature,* **17,** 643-649.

Lewis, A. L., Abu-Absi, N. R., Borys, M. C. & Li, Z. J. (2016). The Use of 'Omics Technology to Rationally Improve Industrial Mammalian Cell Line Performance. *Biotechnology and Bioengineering,* **113,** 26-38.

Lewis, N. E., Liu, X., Nagarajan, H., Yerganian, G., O'Brien, E., Bordbar, A., Roth, A. M., Rosenbloom, J., Bian, C., Xie, M., Chen, W., Li, N., Baycin-Hizal, D., Latif, H., Forster, J., Betenbaugh, M. J., Famili, I., Xu, X., Wang, J. & Palsson, B. O. (2013). Genomic landscapes of Chinese hamster ovary cell lines as revealed by the *Cricetulus griseus* draft genome. *Nat Biotechnol.*, **31,** 759-765.

Levy, N. E., Valente, K. N., Choe, L. H., Lee, K. H, & Lenhoff, A. M. (2014). Identification and characterization of host cell protein product-associated impurities in monoclonal antibody bioprocessing. *Biotechnol Bioeng.*, **111,** 904-912.

Liu, M., Wilk, A. A., Wang, A., Zhou, L., Wang, R-H., Ogawa, W., Deng, C., Dong, L. G. & Liu, F. (2010). Resveratrol Inhibits mTOR Signalling by Promoting the Interaction between mTOR and DEPTOR. *The Journal Of Biological Chemistry,* **285,** 36387-36394.

Liu, W., Yu, K., He, T., Li, F., Zhang, D. & Liu, J. (2013). The Low Temperature Induced Physiological Responses of *Avena nuda* L., a Cold-Tolerant Plant Species. *ScientificWorldJournal,* **2013,** 658793.

Liu, X., Liu, J., Wright, T. W., Lee, J., Lio, P., Donahue-Hjelle, L., Ravnikar, P. & Wu, F. (2010). Isolation of Novel High-Osmolarity Resistant CHO DG44 Cells After Suspension of DNA Mismatch Repair. *Bioprocess International,* **8,** 68-76.

Lodish, H., Berk, A., Kaiser, C. A., Krieger, M., Scott, M. P., Bretscher, A., Ploegh, H. & Matsudaira, P. (2008). Molecular Cell Biology, 6th edition. W. H. Freeman and Company, New York, USA.

Lonberg, N. (2005). Human antibodies from transgenic animals. *Nature Biotechnology,* **23,** 1117-1125.

Loufrani, L. & Henrion, D. (2008). Role of the cytoskeleton in flow (shear stress)-induced dilation and remodeling in resistance arteries. *Med Biol Eng Comput.,* **46,** 451-460.

MacLennan, D. H. & Phillips, M. S. (1992). Malignant hypothermia. *Science,* **256,** 789-794.

Madlung, A. (2013). Polyploidy and its effect on evolutionary success: old questions revisited with new tools. Heredity, **110,** 99-104.

Malek, A. M. & Izumo, S. (1996). Mechanism of endothelial cell shape change and cytoskeletal remodeling in response to fluid shear stress. *J Cell Sci.,* **109,** 713-726.

Manoli, T., Gretz, N., Grone, H-J., Kenzelmann, M., Eils, R. & Brors, B. (2006). Group testing for pathway analysis impoves comparability of different microarray datasets. *Bioinformatics,* **22,** 2500-2506.

Mansilla, M. C. & Mendoza, D. (2005). The *Bascillus subtilis* desaturase: a model to understand phospholipid modification and temperature sensing. *Arch Microbiol.,* **183,** 229-235.

Masel, J. (2011). Genetic drift. *Current Biology,* **21,** 837-838

Mason, M., Sweeney, B., Cain, K., Stephens, P. & Sharfstein S. T. (2014). Reduced Culture Temperature Differentially Affects Expression and Biophysical Properties of Monoclonal Antibody Variants. *Antibodies,* **3,** 254-271.

Masterton, R. J., Roobol, A., Al-Fageeh, M. B., Carden, M. J. & Smales, C. M. (2010). Post-Translational Events of a Model Reporter Protein Proceed With Higher Fidelity and Accuracy Upon Mild Hypothermic Culturing of Chinese Hamster Ovary Cells. *Biotechnology and Bioengineering,* **105,** 215-220.

Matasci, M., Hacker, D. L., Baldi, L. & Wurm, F. (2008). Recombinant therapeutic protein production in cultivated animal cells: current status and future prospects. *Drug Discovery Today: Technologies,* **5,** 37-42.

Matsumura, M., Shimoda, M., Arii, T. & Kataoka, H. (1991). Adaptation of hybridoma cells to higher ammonia concentration. *Cytotechnology,* **7,** 103-112.

Majid, F. A., Butler, M. & Al-Rubeai, M. (2007). Glycosylation of an immunoglobulin produced from a murine hybridoma cell line: the effect of culture mode and the anti-apoptotic gene, bcl-2. *Biotechnol Bioeng.,* **97,** 156-169.

Majors, B. S., Chiang, G. G. & Betenbaugh, M. J. (2009). Protein and Genome Evolution in Mammalian Cells for Biotechnology Applications. *Mol Biotechnol.,* **42,** 216-223.

Makrides, A. C. (2003). Gene Transfer and Expression in Mammalian Cells. Elsevier Science B. V., Amsterdam, The Netherlands.

Maynard Smith, J. (1998). Evolutionary Genetics, 2nd edition. Oxford University Press, USA.

Mayr, E. (1942). Systematics and the Origin of Species, from the Viewpoint of a Zoologist. Harvard University Press, Cambridge, MA, USA.

Mayr, E. (1982). The Growth of Biological Thought: Diversity, Evolution, and Inheritance. Harvard University Press, Cambridge, MA, USA.

McCafferty, J., Griffiths, A. D., Winter, G. & Chiswell, D. J. (1990). Phage antibodies: filamentous phage displaying antibody variable domains. *Nature,* **348,** 552-554.

Michod, R. E. (2000). Darwinian dynamics: evolutionary transitions in fitness and individuality. Princeton University Press, New Jersey, USA.

Moore, A., Mercer, J., Dutina, G., Donahue, C. J., Bauer, K. D., Mather, J. P., Etcheverry, T. & Ryll, T. (1997). Effects of temperature shift on cell cycle, apoptosis and nucleotide pools in CHO cell batch cultures. *Cytotechnology,* **23,** 47-54.

Morrison, S. L., Johnson, M. J., Herzenberg, L. A. & Oi, V. T. (1984). Chimeric human antibody molecules: Mouse antigen-binding domains with human constant region domains. *Proc Natl Acad Sci USA,* **81,** 6851-6855.

Mounier, N. & Arrigo, A. P. (2002). Actin cytoskeleton and small heat shock proteins: how do they interact? *Cell Stress & Chaperones,* **7,** 167-176.

Nam, J. H., Zhang, F., Ermonval, M., Linhardt, R. J. & Sharfstein, S. T. (2008). The Effects of Culture Conditions on the Glycosylation of Secreted Human Placental Alkaline Phosphatase Produced in Chinese Hamster Ovary Cells. *Biotechnol Bioeng.,* **100,** 1178-1192.

NanoDrop™ T042-Technical Bulletin.

Negrini, S., Gorgoulis, V. G. & Halazonetis, T. D. (2010). Genomic instability – an evolving hallmark of cancer. *Nat Rev Mol Cell Biol.,* **11,** 220-228.

Nelson, P. N., Reynolds, G. M., Waldron, E. E., Ward, E., Giannapoulos, K. & Murray, P. G. (2000). Demystified… Monoclonal antibodies. *Mol Pathol,* **53,** 111-117.

Nicklin, P., Bergman, P., Zhang, B., Triantafellow, E., Wang, H., Nyfeler, B., Yang, H., Hild, M., Kung, C., Wilson, C., Myer, V. E., MacKeigan, J. P., Wang, Y. K., Cantley, L. C., Finan, P. M. & Murphy, L. O. (2009). Bidirectional Transport of Amino Acids Regulates mTOR and Autophagy. *Cell,* **136,** 521-534.

Nicolaides, N. C., Littman, S. J., Modrich, P., Kinzler, K. W. & Vogelstein, B. (1998). A naturally occurring hPMS2 mutation can confer a dominant negative mutator phenotype. *Molecular and Cellular Biology,* **18,** 1635-1641.

Nicolaides, N. C., Ebel, W., Kline, B., Chao, Q., Routhier, E., Sass, P. M. & Grasso, L. (2005). Morphogenics as a tool for target discovery and drug development. *Ann N Y Acad Sci.,* **1059,** 86-96.

Nishiyama, H., Itoh, K., Kaneko, Y., Kishishita, M., Yoshid, O. & Fujita, J. (1997). A glycne-rich RNA-binding protein mediating cold-inducible suppression of mammalian cell growth. *J Cell Biol,* **137,** 899-908.

Noh, S. M., Sathyamurthy, M. & Lee, G. M. (2013). Development of recombinant Chinese hamster ovary cell lines for therapeutic protein production. *Current Opinion in Chemical Engineering,* **2,** 391-397.

North, S. J., Huang, H. H., Sundaram, S., Jang-Lee, J., Etienne, A. T., Trollope, A., Chalabi, S., Dell, A., Stanley, P. & Haslam, S. M. (2010). Glycomics profiling of Chinese hamster ovary cell glycosylation mutants reveals N-glycans of a novel size and complexity. *J Bio Chem.*, **285,** 5759-5775.

O'Callaghan, P. M., Berthelot, M. E., Young, R. J., Graham, J. W. A., Racher, A. J. & Aldana, D. (2015). Diversity in host clone performance within a Chinese hamster ovary cell line. *Biotechnology Progress*, **31,** 1187-1200.

O'Callaghan, P. M. & James, D. C. (2008). Systems biotechnology of mammalian cell factories. *Briefings in Functional Genomics and Proteomics,* **7,** 95-110.

Ohya, T., Hayashi, T., Kiyama, E., Nishii, H., Miki, H., Kobayashi, K., Honda, K., Omasa, T. & Ohtake, H. (2007). Improved Production of Recombinant Human Antithrombin III in Chinese Hamster Ovary Cells by ATF4 Overexpresion. *Biotechnology and Bioengineering,* **100,** 317-324.

Osterlehner, A., Simmeth, S. & Gopfert, U. (2011). Promoter methylation and transgene copy numbers predict unstable protein production in recombinant Chinese hamster ovary cell lines. *Biotechnol Bioeng.*, **108,** 2670-2681.

Padmanabhan, R., Gu, S., Nicholson, B. J. & Jiand, J. X. (2012). Residue cysteine 232 is important for substrate transport of neutral amino acid transporter, SNAT. *Int J Biochem Mol Biol.,* **3,** 374-383.

Palou, A., Picó, C., Bonet, M. L. & Oliver, P. (1988). The uncoupling protein, thermogenin. *The International Journal of Biochemistry & Cell Biology,* **30,** 7-11.

Patro, S. Y., Freund, E. & Chang, B. S. (2002). Protein formulation and fill-finish operations. *Biotechnol Annu Rev.,* **8,** 55-84.

Pavelka, N., Rancati, G., Zhu, J., Bradford, W. D., Saraf, A., Florens, L., Sanderson, B. W., Hattem, G. L. & Li, R. (2010). Aneuploidy confers quantitative proteomic changes and phenotypic variation in budding yeast. *Nature,* **468,** 321-325.

Porter, A. J., Racher, A. J., Preziosi, R. & Dickson, A. J. (2010). Strategies for Selecting Recombinant CHO Cell Lines for cGMP Manufacturing: Improving the Efficiency of Cell Line Generation. *Biotechnol. Prog.*, **26,** 1455-1464.

Prentice, H., Ehrenfels, B. N. & Sisk, W. P. (2007). Improving Performance of Mammalian Cells in Fed-Batch Processes through "Bioreactor Evolution". *Biotechnology Progress,* **23,** 458-464.

Provine, W. B. (2004). Ernst Mayr: Genetics and Speciation. *Genetics,* **167,** 1041-1046.

Puck, T. T. & Kao, F. T. (1967). Genetics of somatic mammalian cells. V. Treatment with 5-bromodeoxyuridine and visible light for isolation of nutritionally deficient mutants. *Proc. Natl. Acad. Sci. USA.*, **58,** 1227-1234.

Qian, H. & Beard, D. A. (2006). Metabolic futile cycles and their functions: a systems analysis of energy and control. *IEE Proceedings – Systems Biology,* **153,** 192-200.

Rajendra, Y., Hougland, M. D., Alam, R., Morehead, T., A. & Barnard G. C. (2015). A high cell density transient transfection system for therapeutic expression based on a CHO GS-knockout cell line: Process development and product quality assessment. *Biotechnol Bioeng,* **112,** 977-986.

Raju, E. S. & Jordan, R. (2012). Galactosylation variations in marketed therapeutic antibodies. *MAbs,* **4,** 385-391.

Reuveny, S., Kim, Y. J., Kemp, C. W. & Shiloach, J. (1993). Effect of temperature and oxygen on cell growth and recombinant protein production in insect cell cultures. *Appl Microbiol Biotechnol.,* **38,** 619-623.

Rial, E. & Zardoya, R. (2009). Oxidative stress, thermogenesis and evolution of uncoupling proteins. *J Biol.,* **8,** 58.

Riechmann, L., Clark, M., Waldmann, H. & Winter, G. (1988) Reshaping human antibodies for therapy. *Nature,* **332,** 323-327.

Rupp, O., Becker, J., Brinkrolf, K., Timmerman, C., Borth, N., Pühler, A., Noll, T., & Goesmann, A. (2014). Construction of a Public CHO Cell Line Transcript Database Using Versatile Bioinformatics Analysis Pipelines. *PLoS ONE,* **9,** e85568.

Sand, H. K., Cederlund, G. R. & Danell, K. (1995). Geographical and latitudinal variation in growth patterns and adult body size of Swedish moose (*Alces alces*). *Oecologia,* **102,** 433-442.

Satoh, M., Iida, S. & Shitara, K. (2006). Non-fucosylated therapeutic antibodies as next-generation therapeutic antibodies. *Expert Opin Biol Ther.,* **6,** 1161-1173.

Schaeffer, E. L., Bassi Jr, F. & Gattaz, W. F. (2005). Inhibition of phospholipase A2 activity reduces membrane fluidity in rat hippocampus. *J Neural Transm (Vienna).,* **112,** 641-647.

Schumpp, B. & Schlaeger, E. J. (1992). Growth study of lactate and ammonia double-resistant clones of HL-60 cells. *Cytotechnology,* **8,** 39-44.

Seitz, G., Bonin, M., Fuchs, J., Poths, S., Ruck, P., Warmann, S. W. & Armeanu-Ebinger, S. (2010). Inhibition of glutathione-S-transferase as a treatment strategy for multidrug resistance in childhood rhabdomyosarcoma. *International Journal Of Oncology,* **36,** 491-500.

Seth, G., McIvor, R. S. & Hu, W-S. (2006). 17Beta-hydroxysteroid dehydrogenase type 7 (Hsd17b7) reverts cholesterol auxotrophy in NS0 cells. *J Biotechnol.*, **18,** 557-564.

Shukla, A. A. & Gottschalk, U. (2013) Single-use disposable technologies for biopharmaceutical manufacturing. *Trends in Biotechnology,* **31,** 147-154.

Shukla, A. A., Hubbard, B., Tressel, T., Guhan, S. & Low, D. (2007). Downstream processing of monoclonal antibodies – Application of platform approaches. *Journal of Chromatography B,* **848,** 28-39.

Slikker III, W., Desai, V. G., Duhart, H., Feuers, R. & Imam, S. Z. (2001). Hypothermia enhances *bcl-2* expression and protects against oxidative stress-induced cell death in Chinese hamster ovary cells. *Free Radical Biology & Medicine,* **31,** 405-411.

Sokolov, K. (2013). Tiny thermometers used in living cells. *Nature,* **500,** 36-37

Stein, J., Milewski, V. M. & Dey, A. (2013). The negative cell cycle regulators, p27(Kip1), p18(Ink4c), and GSK-3, play critical role in maintaining quiescence of adult human pancreatic β-cells and restrict their ability to proliferate. *Islets,* **5,** 156-169.

Stier, A., Bize, P., Habold, C., Bouillaud, F., Massemin, S. & Criscuolo, F. (2014). Mitochondrial uncoupling prevents cold-induced oxidative stress: a case study using UCP1 knockout mice. *J Exp Biol.,* **217,** 624-630.

Sunley, K., Tharmalingam, T. & Butler, M. (2008). CHO cells adapted to hypothermic growth produce high yields of recombinant β-interferon. *Biotechnology Progress,* **24,** 898-906.

Tan, H. K., Lee, M. M., Yap, M. G. & Wang, D. I. (2008). Overexpression of cold-inducible RNA-binding protein increases interferon-gamma production in Chinese-hamster ovary cells. *Biotechnol Appl Biochem.,* **49,** 247-257.

Templeton, N., Dean, J., Reddy, P. & Young, J. D. (2013). Peak Antibody Production is Associated With Increased Oxidative Metabolism in an Industrially Relevant Fed-Batch CHO Cell Culture. *Biotechnology and Bioengineering,* **110,** 2013-2024.

Tescione, L., Lambropoulos, j., Paranandi, M. R., Makagiansar, H. & Ryll T. (2015). Application of bioreactor design principles and multivariate analysis for development of cell culture scale down models. *Biotechnol Bioeng,* **112,** 84-97.

Tjandra, J. T., Ramadi, L. & McKenzie, I. F. C. (1990). Development of human anti-murine antibody (HAMA) response in patients. *Immunology and Cell Biology,* **68,** 367-376.

Tjio, J. H. & Puck, T. T. (1958). Genetics of somatic mammalian cells. II. Chromosomal constitution of cells in tissue culture. *J. Exp. Med.,* **108,** 259-268.

Urlaub, G. & Chasin, L. A. (1980). Isolation of Chinese hamster cell mutants deficient in dihydrofolate reductase activity. *Proc. Natl. Acad. Sci. USA.*, **77,** 4216-4220.

Urlaub, G., Käs, E., Carothers, A. M. & Chasin, L. A. (1983). Deletion of the Diploid Dihydrofolate Reductase Locus from Cultured Mammalian Cells. (1983). *Cell,* **33,** 405-412.

Urlaub, G., Mitchell P. J., Kas, E., Chasin, L. A., Funanage, V. L., Myoda, T. T. & Hamlin, J. (1986). Effect of Gamma Rays at the Dihydrofolate Reductase Locus: Deletions and Inversions. *Somatic Cell and Molecular Genetics,* **12,** 555-566.

Valente, K. N., Lenhoff, A. M. & Lee, K. H. (2014b). Expression of difficult-to-remove host cell protein impurities during extended Chinese hamster ovary cell culture and their impact on continuous bioprocessing. *Biotechnol Bioeng.*, **112,** 1232-1242.

Valente, K. N., Schaefer, A. K., Kempton, H. R., Lenhoff, A. M. & Lee, K. H. (2014a). Recovery of Chinese hamster ovary host cell proteins for proteomic analysis. *Biotechnol J.*, **9,** 87-99.

Vergara, M., Becerra, S., Berrios, J., Osses, N., Reyes, J., Rodríguez-Moyá, M., Gonzalez, R. & Altamirano, C. (2014). Differential Effect of Culture Temperature and Specific Growth Rate on CHO Cell Behavior in Chemostat Culture. *PLoS ONE,* **9,** e93865.

Vogt, S., Troitzsch, D., Abdul-Khaliq, H., Böttcher, W., L., P. E. & Moosdorf, R. (2000). Improved myocardial preservation with short hypothermia prior to cold cardioplegic ischemia in immature rabbit hearts. *Eur J Cardiothorac Surg,* **18,** 233-240.

Waldmann, T. A. (2003). Immunotherapy: past, present and future. *Nature Medicine,* **9,** 269-277.

Wahl, L. M., Gerrish, P. J. & Saika-Voivod, I. (2002). Evaluating the impact of population bottlenecks in experimental evolution. *Genetics,* **162,** 961-971.

Walsh, G. & Murphy, B. (1999). Biopharmaceuticals, an Industrial Perspective. Kluwer Academic Publishers, Dordrecht, The Netherlands.

Walsh, G. (2010). Biopharmaceutical benchmarks 2010. *Nature Biotechnology,* **28,** 917-924.

Wang, C., Huang, Z., Du, Y., Cheng, Y., Chen, S. & Guo, F. (2010). ATF4 regulates lipid metabolism and thermogenesis. *Cell Res.,* **20,** 174-184.

Wang, Q. & Holst, J. (2015). L-type amino acid transport and cancer: targeting the mTORC1 pathway to inhibit neoplasia. *Am J Cancer Res.,* **5,** 1291-1294.

Wang, Z., Ma, X., Zong, S., Wang, Y., Chen, H. & Cui, Y. (2015). Preparation of magnetofluorescent nan-thermometer and its targeted temperature sensing in applications in living cells. *Talanta,* **131,** 259-265.

Weinstein, J., Jacobsen, F. W., Hsu-Chen, J., Wu, T. & Baum, L. G. (1994). A novel mammalian protein, p55CDC, present in dividing cells is associated with protein kinase activity and has homology to the *Saccharomyces cerevisiae* cell division cycle proteins Cdc20 and Cdc4. *Mol Cell Bio.,* **14,** 3350-3356,

Wipperman, A., Rupp, O., Brinkrolf, K., Hoffrogge, R. & Noll, R. (2015). The DNA methylation landscape of Chinese hamster ovary (CHO) DP-12 cells. *Journal of Biotechnology,* **199,** 38-46.

XF24 User Manual (2013). Seahorse Bioscience. North Billerica, MA, USA.

Xu, X., Nagarajan, H., Lewis, N. E., Pan, S., Cai, Z., Liu, X., Chen, W., Xie, M., Wang, W., Hammond, S., Anderson, M. R., Neff, N., Passarelli, B., Koh, W., Fan, H. C., Wang, J., Gui, Y., Lee, K. H., Betenbaugh, M. J., Quake, S. R., Famili, I. & Palsson, B. O. (2011). The genomic sequence of the Chinese hamster ovary (CHO)-K1 cell line. *Nat Biotechnol.*, **29,** 735-741.

Yamamoto, K., Gandin, V., Sasaki, M., McCracken, A., Li, W., Silvester, J. L., Elia, A. J., Wang, F., Wakutani, Y., Alexandrova, R., Oo, Y. D., Mullen, P. J., Inoue, S., Itsumi, M., Lapin, V., Haight, J., Wakeham, A., Shahinian, A., Ikura, M., Topisirovic, I., Sonenberg, N. & Mak, T. W. (2014). Largen: A Molecular Regulator of Mammalian Cell Size Control. *Molecular Cell,* **53,** 904-915.

Yan, S-K., Liu, R-H., Jin, H-Z., Liu, X-R., Ye, J., Shan, L. & Zhang, W-D. (2015). "Omics" in pharmaceutical research: overview, applications, challenges, and future perspectives. *Chinese Journal of Natural Medicines,* **13,** 0003-0021.

Yerganian, G. (1985). The biology and genetics of Chinese hamster. Molecular Cell Genetics, John Wiley & Sons Inc., New York.

Yoon, S. K., Ahn, Y-H. & Jeong, M. H. (2007). Effect of culture temperature on follicle-stimulating hormone production by a Chinese hamster ovary cells in a perfusion bioreactor. *Applied Microbiology and Biotechnology,* **76,** 83-89.

Yoon, S. K., Hong, J. K., Choo, S. H., Song, J. Y., Park, H. W. & Lee, G. M. (2006). Adaptation of Chinese hamster ovary cells to low culture temperature: Cell growth and recombinant protein production. *Journal of Biotechnology,* **122,** 463-472.

Yoon, S. K., Hwang, S. O. & Lee G. M. (2004). Enhancing effect of low culture temperature on specific antibody productivity of recombinant Chinese hamster ovary cells: clonal variation. *Biotchnol Prog.,* **20,** 1683-1688.

Young, J. D. (2013). Metabolic flux rewiring in mammalian cell cultures. *Current Opinion in Biotechnology,* **24,** 1108-1115.

Yu, L. X. (2008). Pharmaceutical Quality by Design: Product and Process Development, Understanding and Control. *Pharmaceutical Research,* **25,** 781-791.

Zagari, F., Jordan, M., Stettler, M., Broly, H. & Wurm, F. M. (2013). Lactate metabolism shift in CHO cell culture: the role of mitochondrial oxidative activity. *N Biotechnol.,* **30,** 238-245.

Zieger, M. A. J., Gupta, M. P. & Wang, M. (2001). Proteomic analysis of cold-adaptation. *BMC Genomics,* **12,** 630.

Zhu, J. (2012). Mammalian cell protein expression for biopharmaceutical production. *Biotechnol. Adv.,* **30,** 1258-1170.

Appendix

This chapter contains supplementary material from the research chapters in this thesis. Material can be found as follows:

Appendix I: data relating to work from chapter 3
Appendix II: data relating to work from chapter 4
Appendix III: data relating to work from chapter 5

Appendix I

Average change in growth rate per day

Tukey's multiple comparisons test	Significant?	Summary	Adjusted P Value
Every1 days, seeding 1x10^6 vs. Every1 days, seeding 3x10^6	No	ns	0.4104
Every1 days, seeding 1x10^6 vs. Every1 days, seeding 5x10^6	No	ns	0.9998
Every1 days, seeding 1x10^6 vs. Every2 days, seeding 1x10^6	No	ns	0.2839
Every1 days, seeding 1x10^6 vs. Every2 days, seeding 3x10^6	Yes	****	< 0.0001
Every1 days, seeding 1x10^6 vs. Every2 days, seeding 5x10^6	Yes	****	< 0.0001
Every1 days, seeding 1x10^6 vs. Every3 days, seeding 1x10^6	No	ns	> 0.9999
Every1 days, seeding 1x10^6 vs. Every3 days, seeding 3x10^6	No	ns	0.1738
Every1 days, seeding 1x10^6 vs. Every4 days, seeding 1x10^6	Yes	***	0.0003
Every1 days, seeding 1x10^6 vs. CTRL(Every3-4 days, seeding 0.2x10^6)	Yes	****	< 0.0001
Every1 days, seeding 3x10^6 vs. Every1 days, seeding 5x10^6	No	ns	0.7618
Every1 days, seeding 3x10^6 vs. Every2 days, seeding 1x10^6	Yes	**	0.0026
Every1 days, seeding 3x10^6 vs. Every2 days, seeding 3x10^6	Yes	****	< 0.0001
Every1 days, seeding 3x10^6 vs. Every2 days, seeding 5x10^6	Yes	****	< 0.0001
Every1 days, seeding 3x10^6 vs. Every3 days, seeding 1x10^6	No	ns	0.303
Every1 days, seeding 3x10^6 vs. Every3 days, seeding 3x10^6	No	ns	0.9999
Every1 days, seeding 3x10^6 vs. Every4 days, seeding 1x10^6	Yes	****	< 0.0001
Every1 days, seeding 3x10^6 vs. CTRL(Every3-4 days, seeding 0.2x10^6)	Yes	****	< 0.0001
Every1 days, seeding 5x10^6 vs. Every2 days, seeding 1x10^6	No	ns	0.1011
Every1 days, seeding 5x10^6 vs. Every2 days, seeding 3x10^6	Yes	****	< 0.0001
Every1 days, seeding 5x10^6 vs. Every2 days, seeding 5x10^6	Yes	****	< 0.0001
Every1 days, seeding 5x10^6 vs. Every3 days, seeding 1x10^6	No	ns	0.9976
Every1 days, seeding 5x10^6 vs. Every3 days, seeding 3x10^6	No	ns	0.434
Every1 days, seeding 5x10^6 vs. Every4 days, seeding 1x10^6	Yes	****	< 0.0001
Every1 days, seeding 5x10^6 vs. CTRL(Every3-4 days, seeding 0.2x10^6)	Yes	****	< 0.0001
Every2 days, seeding 1x10^6 vs. Every2 days, seeding 3x10^6	Yes	****	< 0.0001
Every2 days, seeding 1x10^6 vs. Every2 days, seeding 5x10^6	Yes	****	< 0.0001
Every2 days, seeding 1x10^6 vs. Every3 days, seeding 1x10^6	No	ns	0.3874
Every2 days, seeding 1x10^6 vs. Every3 days, seeding 3x10^6	Yes	***	0.0008
Every2 days, seeding 1x10^6 vs. Every4 days, seeding 1x10^6	No	ns	0.067
Every2 days, seeding 1x10^6 vs. CTRL(Every3-4 days, seeding 0.2x10^6)	Yes	****	< 0.0001
Every2 days, seeding 3x10^6 vs. Every2 days, seeding 5x10^6	Yes	****	< 0.0001
Every2 days, seeding 3x10^6 vs. Every3 days, seeding 1x10^6	Yes	****	< 0.0001
Every2 days, seeding 3x10^6 vs. Every3 days, seeding 3x10^6	Yes	****	< 0.0001
Every2 days, seeding 3x10^6 vs. Every4 days, seeding 1x10^6	Yes	**	0.0041
Every2 days, seeding 3x10^6 vs. CTRL(Every3-4 days, seeding 0.2x10^6)	No	ns	0.483
Every2 days, seeding 5x10^6 vs. Every3 days, seeding 1x10^6	Yes	****	< 0.0001
Every2 days, seeding 5x10^6 vs. Every3 days, seeding 3x10^6	Yes	****	< 0.0001
Every2 days, seeding 5x10^6 vs. Every4 days, seeding 1x10^6	Yes	****	< 0.0001
Every2 days, seeding 5x10^6 vs. CTRL(Every3-4 days, seeding 0.2x10^6)	Yes	****	< 0.0001
Every3 days, seeding 1x10^6 vs. Every3 days, seeding 3x10^6	No	ns	0.1185
Every3 days, seeding 1x10^6 vs. Every4 days, seeding 1x10^6	Yes	***	0.0004
Every3 days, seeding 1x10^6 vs. CTRL(Every3-4 days, seeding 0.2x10^6)	Yes	****	< 0.0001
Every3 days, seeding 3x10^6 vs. Every4 days, seeding 1x10^6	Yes	****	< 0.0001
Every3 days, seeding 3x10^6 vs. CTRL(Every3-4 days, seeding 0.2x10^6)	Yes	****	< 0.0001
Every4 days, seeding 1x10^6 vs. CTRL(Every3-4 days, seeding 0.2x10^6)	Yes	****	< 0.0001

Protein content

Tukey's multiple comparisons test	Significant?	Summary	Adjusted P Value
A:Evolved vs. A:Parental	Yes	****	< 0.0001
A:Evolved vs. B:Evolved	No	ns	0.6377
A:Evolved vs. B:Parental	Yes	***	0.0001
A:Evolved vs. C:Evolved	No	ns	0.9591
A:Evolved vs. C:Parental	Yes	****	< 0.0001
A:Parental vs. B:Evolved	Yes	***	0.0001
A:Parental vs. B:Parental	No	ns	0.548
A:Parental vs. C:Evolved	Yes	****	< 0.0001
A:Parental vs. C:Parental	No	ns	0.8544
B:Evolved vs. B:Parental	Yes	**	0.0014
B:Evolved vs. C:Evolved	No	ns	0.9722
B:Evolved vs. C:Parental	Yes	***	0.0006
B:Parental vs. C:Evolved	Yes	***	0.0004
B:Parental vs. C:Parental	No	ns	0.9912
C:Evolved vs. C:Parental	Yes	***	0.0002

RNA concentration from 5x10^6 cells

Tukey's multiple comparisons test	Significant?	Summary	Adjusted P Value
A:Evolved vs. A:Parental	Yes	****	< 0.0001
A:Evolved vs. B:Evolved	No	ns	0.4224
A:Evolved vs. B:Parental	Yes	****	< 0.0001
A:Evolved vs. C:Evolved	No	ns	0.5279
A:Evolved vs. C:Parental	Yes	****	< 0.0001
A:Parental vs. B:Evolved	Yes	***	0.0002
A:Parental vs. B:Parental	No	ns	0.9857
A:Parental vs. C:Evolved	Yes	***	0.0001
A:Parental vs. C:Parental	No	ns	0.9447
B:Evolved vs. B:Parental	Yes	***	0.0004
B:Evolved vs. C:Evolved	No	ns	> 0.9999
B:Evolved vs. C:Parental	Yes	***	0.0006
B:Parental vs. C:Evolved	Yes	***	0.0003
B:Parental vs. C:Parental	No	ns	0.9999
C:Evolved vs. C:Parental	Yes	***	0.0005

Appendix II

Map of GFP vector used

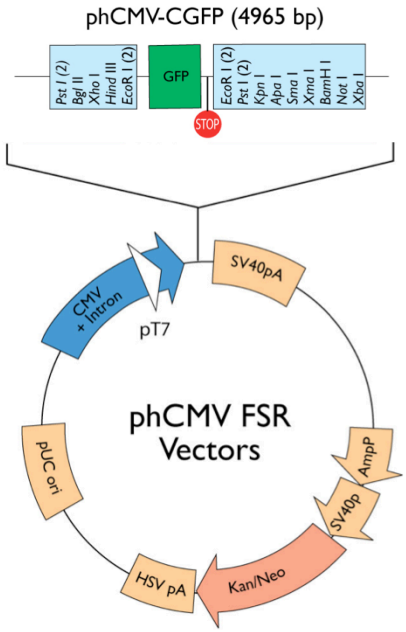

Map of SEAP vector used

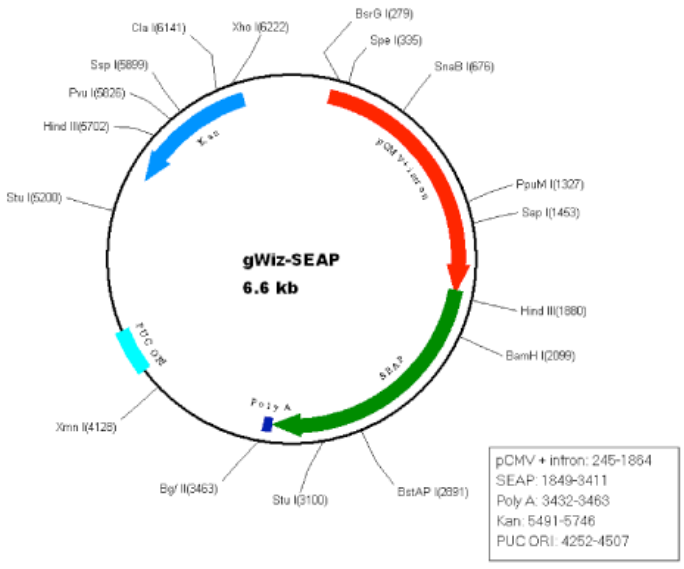

Agarose gel DNA banding profile confirming identity of cut and uncut cB72.3 and Enbrel

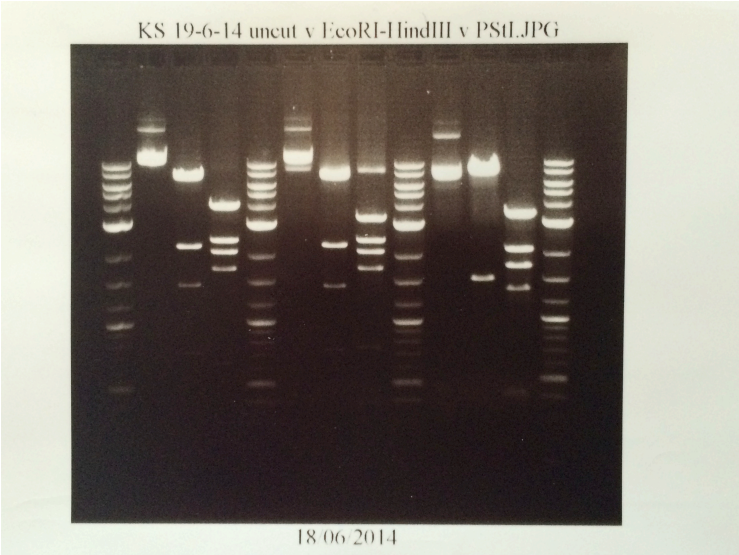

SEAP relative productivities

Tukey's multiple comparisons test	Significant?	Summary	Adjusted P Value
Culture 32A at 32°C incbuabtion vs. Culture 32B at 32°C incbuabtion	No	ns	0.0747
Culture 32A at 32°C incbuabtion vs. Culture 32C at 32°C incbuabtion	No	ns	0.3518
Culture 32A at 32°C incbuabtion vs. Culture 37A at 32°C incbuabtion	Yes	****	< 0.0001
Culture 32A at 32°C incbuabtion vs. Culture 37B at 32°C incbuabtion	Yes	****	< 0.0001
Culture 32A at 32°C incbuabtion vs. Culture 37C at 32°C incbuabtion	Yes	****	< 0.0001
Culture 32A at 32°C incbuabtion vs. Culture 32A at 37°C incbuabtion	Yes	****	< 0.0001
Culture 32A at 32°C incbuabtion vs. Culture 32B at 37°C incbuabtion	Yes	****	< 0.0001
Culture 32A at 32°C incbuabtion vs. Culture 32C at 37°C incbuabtion	Yes	****	< 0.0001
Culture 32A at 32°C incbuabtion vs. Culture 37A at 37°C incbuabtion	Yes	****	< 0.0001
Culture 32A at 32°C incbuabtion vs. Culture 37B at 37°C incbuabtion	Yes	****	< 0.0001
Culture 32A at 32°C incbuabtion vs. Culture 37C at 37°C incbuabtion	Yes	****	< 0.0001
Culture 32B at 32°C incbuabtion vs. Culture 32C at 32°C incbuabtion	No	ns	0.999
Culture 32B at 32°C incbuabtion vs. Culture 37A at 32°C incbuabtion	Yes	****	< 0.0001
Culture 32B at 32°C incbuabtion vs. Culture 37B at 32°C incbuabtion	Yes	****	< 0.0001
Culture 32B at 32°C incbuabtion vs. Culture 37C at 32°C incbuabtion	Yes	****	< 0.0001
Culture 32B at 32°C incbuabtion vs. Culture 32A at 37°C incbuabtion	Yes	****	< 0.0001
Culture 32B at 32°C incbuabtion vs. Culture 32B at 37°C incbuabtion	Yes	****	< 0.0001
Culture 32B at 32°C incbuabtion vs. Culture 32C at 37°C incbuabtion	Yes	****	< 0.0001
Culture 32B at 32°C incbuabtion vs. Culture 37A at 37°C incbuabtion	Yes	****	< 0.0001
Culture 32B at 32°C incbuabtion vs. Culture 37B at 37°C incbuabtion	Yes	****	< 0.0001
Culture 32B at 32°C incbuabtion vs. Culture 37C at 37°C incbuabtion	Yes	****	< 0.0001
Culture 32C at 32°C incbuabtion vs. Culture 37A at 32°C incbuabtion	Yes	****	< 0.0001
Culture 32C at 32°C incbuabtion vs. Culture 37B at 32°C incbuabtion	Yes	****	< 0.0001
Culture 32C at 32°C incbuabtion vs. Culture 37C at 32°C incbuabtion	Yes	****	< 0.0001
Culture 32C at 32°C incbuabtion vs. Culture 32A at 37°C incbuabtion	Yes	****	< 0.0001
Culture 32C at 32°C incbuabtion vs. Culture 32B at 37°C incbuabtion	Yes	****	< 0.0001
Culture 32C at 32°C incbuabtion vs. Culture 32C at 37°C incbuabtion	Yes	****	< 0.0001
Culture 32C at 32°C incbuabtion vs. Culture 37A at 37°C incbuabtion	Yes	****	< 0.0001
Culture 32C at 32°C incbuabtion vs. Culture 37B at 37°C incbuabtion	Yes	****	< 0.0001
Culture 32C at 32°C incbuabtion vs. Culture 37C at 37°C incbuabtion	Yes	****	< 0.0001
Culture 37A at 32°C incbuabtion vs. Culture 37B at 32°C incbuabtion	No	ns	0.9935
Culture 37A at 32°C incbuabtion vs. Culture 37C at 32°C incbuabtion	No	ns	0.9282
Culture 37A at 32°C incbuabtion vs. Culture 32A at 37°C incbuabtion	Yes	****	< 0.0001
Culture 37A at 32°C incbuabtion vs. Culture 32B at 37°C incbuabtion	Yes	****	< 0.0001
Culture 37A at 32°C incbuabtion vs. Culture 32C at 37°C incbuabtion	Yes	****	< 0.0001
Culture 37A at 32°C incbuabtion vs. Culture 37A at 37°C incbuabtion	Yes	****	< 0.0001
Culture 37A at 32°C incbuabtion vs. Culture 37B at 37°C incbuabtion	Yes	****	< 0.0001
Culture 37A at 32°C incbuabtion vs. Culture 37C at 37°C incbuabtion	Yes	****	< 0.0001
Culture 37B at 32°C incbuabtion vs. Culture 37C at 32°C incbuabtion	No	ns	> 0.9999
Culture 37B at 32°C incbuabtion vs. Culture 32A at 37°C incbuabtion	Yes	****	< 0.0001
Culture 37B at 32°C incbuabtion vs. Culture 32B at 37°C incbuabtion	Yes	****	< 0.0001
Culture 37B at 32°C incbuabtion vs. Culture 32C at 37°C incbuabtion	Yes	****	< 0.0001
Culture 37B at 32°C incbuabtion vs. Culture 37A at 37°C incbuabtion	Yes	****	< 0.0001
Culture 37B at 32°C incbuabtion vs. Culture 37B at 37°C incbuabtion	Yes	****	< 0.0001
Culture 37B at 32°C incbuabtion vs. Culture 37C at 37°C incbuabtion	Yes	****	< 0.0001
Culture 37C at 32°C incbuabtion vs. Culture 32A at 37°C incbuabtion	Yes	****	< 0.0001
Culture 37C at 32°C incbuabtion vs. Culture 32B at 37°C incbuabtion	Yes	****	< 0.0001
Culture 37C at 32°C incbuabtion vs. Culture 32C at 37°C incbuabtion	Yes	****	< 0.0001
Culture 37C at 32°C incbuabtion vs. Culture 37A at 37°C incbuabtion	Yes	****	< 0.0001
Culture 37C at 32°C incbuabtion vs. Culture 37B at 37°C incbuabtion	Yes	****	< 0.0001
Culture 37C at 32°C incbuabtion vs. Culture 37C at 37°C incbuabtion	Yes	****	< 0.0001
Culture 32A at 37°C incbuabtion vs. Culture 32B at 37°C incbuabtion	No	ns	> 0.9999
Culture 32A at 37°C incbuabtion vs. Culture 32C at 37°C incbuabtion	No	ns	> 0.9999
Culture 32A at 37°C incbuabtion vs. Culture 37A at 37°C incbuabtion	No	ns	> 0.9999
Culture 32A at 37°C incbuabtion vs. Culture 37B at 37°C incbuabtion	No	ns	0.9282
Culture 32A at 37°C incbuabtion vs. Culture 37C at 37°C incbuabtion	No	ns	0.999
Culture 32B at 37°C incbuabtion vs. Culture 32C at 37°C incbuabtion	No	ns	0.974
Culture 32B at 37°C incbuabtion vs. Culture 37A at 37°C incbuabtion	No	ns	> 0.9999
Culture 32B at 37°C incbuabtion vs. Culture 37B at 37°C incbuabtion	No	ns	0.999
Culture 32B at 37°C incbuabtion vs. Culture 37C at 37°C incbuabtion	No	ns	> 0.9999
Culture 32C at 37°C incbuabtion vs. Culture 37A at 37°C incbuabtion	No	ns	0.9935
Culture 32C at 37°C incbuabtion vs. Culture 37B at 37°C incbuabtion	No	ns	0.6056
Culture 32C at 37°C incbuabtion vs. Culture 37C at 37°C incbuabtion	No	ns	0.9282
Culture 37A at 37°C incbuabtion vs. Culture 37B at 37°C incbuabtion	No	ns	0.9935
Culture 37A at 37°C incbuabtion vs. Culture 37C at 37°C incbuabtion	No	ns	> 0.9999
Culture 37B at 37°C incbuabtion vs. Culture 37C at 37°C incbuabtion	No	ns	> 0.9999

GFP median fluorescence intensity

Tukey's multiple comparisons test	Significant?	Summary	Adjusted P Value
Culture 32A at 32°C incbuabtion vs. Culture 32B at 32°C incbuabtion	Yes	*	0.0245
Culture 32A at 32°C incbuabtion vs. Culture 32C at 32°C incbuabtion	No	ns	0.9892
Culture 32A at 32°C incbuabtion vs. Culture 37A at 32°C incbuabtion	Yes	****	< 0.0001
Culture 32A at 32°C incbuabtion vs. Culture 37B at 32°C incbuabtion	Yes	****	< 0.0001
Culture 32A at 32°C incbuabtion vs. Culture 37C at 32°C incbuabtion	Yes	***	0.0004
Culture 32A at 32°C incbuabtion vs. Culture 32A at 37°C incbuabtion	No	ns	0.6318
Culture 32A at 32°C incbuabtion vs. Culture 32B at 37°C incbuabtion	Yes	***	0.0009
Culture 32A at 32°C incbuabtion vs. Culture 32C at 37°C incbuabtion	Yes	****	< 0.0001
Culture 32A at 32°C incbuabtion vs. Culture 37A at 37°C incbuabtion	Yes	****	< 0.0001
Culture 32A at 32°C incbuabtion vs. Culture 37B at 37°C incbuabtion	Yes	****	< 0.0001
Culture 32A at 32°C incbuabtion vs. Culture 37C at 37°C incbuabtion	Yes	****	< 0.0001
Culture 32B at 32°C incbuabtion vs. Culture 32C at 32°C incbuabtion	No	ns	0.2442
Culture 32B at 32°C incbuabtion vs. Culture 37A at 32°C incbuabtion	Yes	*	0.0167
Culture 32B at 32°C incbuabtion vs. Culture 37B at 32°C incbuabtion	No	ns	0.291
Culture 32B at 32°C incbuabtion vs. Culture 37C at 32°C incbuabtion	No	ns	0.8456
Culture 32B at 32°C incbuabtion vs. Culture 32A at 37°C incbuabtion	No	ns	0.7838
Culture 32B at 32°C incbuabtion vs. Culture 32B at 37°C incbuabtion	No	ns	0.9581
Culture 32B at 32°C incbuabtion vs. Culture 32C at 37°C incbuabtion	No	ns	0.0542
Culture 32B at 32°C incbuabtion vs. Culture 37A at 37°C incbuabtion	Yes	**	0.0074
Culture 32B at 32°C incbuabtion vs. Culture 37B at 37°C incbuabtion	No	ns	0.1842
Culture 32B at 32°C incbuabtion vs. Culture 37C at 37°C incbuabtion	Yes	***	0.0002
Culture 32C at 32°C incbuabtion vs. Culture 37A at 32°C incbuabtion	Yes	****	< 0.0001
Culture 32C at 32°C incbuabtion vs. Culture 37B at 32°C incbuabtion	Yes	***	0.0006
Culture 32C at 32°C incbuabtion vs. Culture 37C at 32°C incbuabtion	Yes	**	0.0064
Culture 32C at 32°C incbuabtion vs. Culture 32A at 37°C incbuabtion	No	ns	0.9974
Culture 32C at 32°C incbuabtion vs. Culture 32B at 37°C incbuabtion	Yes	*	0.0143
Culture 32C at 32°C incbuabtion vs. Culture 32C at 37°C incbuabtion	Yes	****	< 0.0001
Culture 32C at 32°C incbuabtion vs. Culture 37A at 37°C incbuabtion	Yes	****	< 0.0001
Culture 32C at 32°C incbuabtion vs. Culture 37B at 37°C incbuabtion	Yes	***	0.0003
Culture 32C at 32°C incbuabtion vs. Culture 37C at 37°C incbuabtion	Yes	****	< 0.0001
Culture 37A at 32°C incbuabtion vs. Culture 37B at 32°C incbuabtion	No	ns	0.9496
Culture 37A at 32°C incbuabtion vs. Culture 37C at 32°C incbuabtion	No	ns	0.4512
Culture 37A at 32°C incbuabtion vs. Culture 32A at 37°C incbuabtion	Yes	***	0.0002
Culture 37A at 32°C incbuabtion vs. Culture 32B at 37°C incbuabtion	No	ns	0.273
Culture 37A at 32°C incbuabtion vs. Culture 32C at 37°C incbuabtion	No	ns	> 0.9999
Culture 37A at 32°C incbuabtion vs. Culture 37A at 37°C incbuabtion	No	ns	> 0.9999
Culture 37A at 32°C incbuabtion vs. Culture 37B at 37°C incbuabtion	No	ns	0.9887
Culture 37A at 32°C incbuabtion vs. Culture 37C at 37°C incbuabtion	No	ns	0.7274
Culture 37B at 32°C incbuabtion vs. Culture 37C at 32°C incbuabtion	No	ns	0.997
Culture 37B at 32°C incbuabtion vs. Culture 32A at 37°C incbuabtion	Yes	**	0.0062
Culture 37B at 32°C incbuabtion vs. Culture 32B at 37°C incbuabtion	No	ns	0.9693
Culture 37B at 32°C incbuabtion vs. Culture 32C at 37°C incbuabtion	No	ns	0.9987
Culture 37B at 32°C incbuabtion vs. Culture 37A at 37°C incbuabtion	No	ns	0.8242
Culture 37B at 32°C incbuabtion vs. Culture 37B at 37°C incbuabtion	No	ns	> 0.9999
Culture 37B at 32°C incbuabtion vs. Culture 37C at 37°C incbuabtion	No	ns	0.0858
Culture 37C at 32°C incbuabtion vs. Culture 32A at 37°C incbuabtion	No	ns	0.0564
Culture 37C at 32°C incbuabtion vs. Culture 32B at 37°C incbuabtion	No	ns	> 0.9999
Culture 37C at 32°C incbuabtion vs. Culture 32C at 37°C incbuabtion	No	ns	0.7738
Culture 37C at 32°C incbuabtion vs. Culture 37A at 37°C incbuabtion	No	ns	0.2705
Culture 37C at 32°C incbuabtion vs. Culture 37B at 37°C incbuabtion	No	ns	0.9795
Culture 37C at 32°C incbuabtion vs. Culture 37C at 37°C incbuabtion	Yes	**	0.0099
Culture 32A at 37°C incbuabtion vs. Culture 32B at 37°C incbuabtion	No	ns	0.1134
Culture 32A at 37°C incbuabtion vs. Culture 32C at 37°C incbuabtion	Yes	***	0.0007
Culture 32A at 37°C incbuabtion vs. Culture 37A at 37°C incbuabtion	Yes	****	< 0.0001
Culture 32A at 37°C incbuabtion vs. Culture 37B at 37°C incbuabtion	Yes	**	0.0033
Culture 32A at 37°C incbuabtion vs. Culture 37C at 37°C incbuabtion	Yes	****	< 0.0001
Culture 32B at 37°C incbuabtion vs. Culture 32C at 37°C incbuabtion	No	ns	0.5679
Culture 32B at 37°C incbuabtion vs. Culture 37A at 37°C incbuabtion	No	ns	0.1484
Culture 32B at 37°C incbuabtion vs. Culture 37B at 37°C incbuabtion	No	ns	0.9004
Culture 32B at 37°C incbuabtion vs. Culture 37C at 37°C incbuabtion	Yes	**	0.0044
Culture 32C at 37°C incbuabtion vs. Culture 37A at 37°C incbuabtion	No	ns	0.9988
Culture 32C at 37°C incbuabtion vs. Culture 37B at 37°C incbuabtion	No	ns	> 0.9999
Culture 32C at 37°C incbuabtion vs. Culture 37C at 37°C incbuabtion	No	ns	0.404
Culture 37A at 37°C incbuabtion vs. Culture 37B at 37°C incbuabtion	No	ns	0.9294
Culture 37A at 37°C incbuabtion vs. Culture 37C at 37°C incbuabtion	No	ns	0.8963
Culture 37B at 37°C incbuabtion vs. Culture 37C at 37°C incbuabtion	No	ns	0.1453

GFP transfection efficiency

Tukey's multiple comparisons test	Significan	Summary	Adjusted P Value
Culture 32A at 32°C incbuabtion vs. Culture 32B at 32°C incbuabtion	No	ns	0.3041
Culture 32A at 32°C incbuabtion vs. Culture 32C at 32°C incbuabtion	Yes	***	0.0001
Culture 32A at 32°C incbuabtion vs. Culture 37A at 32°C incbuabtion	Yes	****	< 0.0001
Culture 32A at 32°C incbuabtion vs. Culture 37B at 32°C incbuabtion	Yes	****	< 0.0001
Culture 32A at 32°C incbuabtion vs. Culture 37C at 32°C incbuabtion	Yes	****	< 0.0001
Culture 32A at 32°C incbuabtion vs. Culture 32A at 37°C incbuabtion	No	ns	> 0.9999
Culture 32A at 32°C incbuabtion vs. Culture 32B at 37°C incbuabtion	No	ns	> 0.9999
Culture 32A at 32°C incbuabtion vs. Culture 32C at 37°C incbuabtion	Yes	**	0.007
Culture 32A at 32°C incbuabtion vs. Culture 37A at 37°C incbuabtion	Yes	****	< 0.0001
Culture 32A at 32°C incbuabtion vs. Culture 37B at 37°C incbuabtion	Yes	****	< 0.0001
Culture 32A at 32°C incbuabtion vs. Culture 37C at 37°C incbuabtion	Yes	****	< 0.0001
Culture 32B at 32°C incbuabtion vs. Culture 32C at 32°C incbuabtion	No	ns	0.0734
Culture 32B at 32°C incbuabtion vs. Culture 37A at 32°C incbuabtion	Yes	****	< 0.0001
Culture 32B at 32°C incbuabtion vs. Culture 37B at 32°C incbuabtion	Yes	*	0.0102
Culture 32B at 32°C incbuabtion vs. Culture 37C at 32°C incbuabtion	Yes	****	< 0.0001
Culture 32B at 32°C incbuabtion vs. Culture 32A at 37°C incbuabtion	No	ns	0.2813
Culture 32B at 32°C incbuabtion vs. Culture 32B at 37°C incbuabtion	No	ns	0.5845
Culture 32B at 32°C incbuabtion vs. Culture 32C at 37°C incbuabtion	No	ns	0.7984
Culture 32B at 32°C incbuabtion vs. Culture 37A at 37°C incbuabtion	Yes	****	< 0.0001
Culture 32B at 32°C incbuabtion vs. Culture 37B at 37°C incbuabtion	Yes	****	< 0.0001
Culture 32B at 32°C incbuabtion vs. Culture 37C at 37°C incbuabtion	Yes	****	< 0.0001
Culture 32C at 32°C incbuabtion vs. Culture 37A at 32°C incbuabtion	Yes	**	0.0091
Culture 32C at 32°C incbuabtion vs. Culture 37B at 32°C incbuabtion	No	ns	0.9987
Culture 32C at 32°C incbuabtion vs. Culture 37C at 32°C incbuabtion	Yes	*	0.0244
Culture 32C at 32°C incbuabtion vs. Culture 32A at 37°C incbuabtion	Yes	***	0.0001
Culture 32C at 32°C incbuabtion vs. Culture 32B at 37°C incbuabtion	Yes	***	0.0005
Culture 32C at 32°C incbuabtion vs. Culture 32C at 37°C incbuabtion	No	ns	0.8869
Culture 32C at 32°C incbuabtion vs. Culture 37A at 37°C incbuabtion	Yes	****	< 0.0001
Culture 32C at 32°C incbuabtion vs. Culture 37B at 37°C incbuabtion	Yes	****	< 0.0001
Culture 32C at 32°C incbuabtion vs. Culture 37C at 37°C incbuabtion	No	ns	0.0988
Culture 37A at 32°C incbuabtion vs. Culture 37B at 32°C incbuabtion	No	ns	0.0666
Culture 37A at 32°C incbuabtion vs. Culture 37C at 32°C incbuabtion	No	ns	> 0.9999
Culture 37A at 32°C incbuabtion vs. Culture 32A at 37°C incbuabtion	Yes	****	< 0.0001
Culture 37A at 32°C incbuabtion vs. Culture 32B at 37°C incbuabtion	Yes	****	< 0.0001
Culture 37A at 32°C incbuabtion vs. Culture 32C at 37°C incbuabtion	Yes	***	0.0002
Culture 37A at 32°C incbuabtion vs. Culture 37A at 37°C incbuabtion	No	ns	0.1669
Culture 37A at 32°C incbuabtion vs. Culture 37B at 37°C incbuabtion	Yes	***	0.0004
Culture 37A at 32°C incbuabtion vs. Culture 37C at 37°C incbuabtion	No	ns	0.9929
Culture 37B at 32°C incbuabtion vs. Culture 37C at 32°C incbuabtion	No	ns	0.1554
Culture 37B at 32°C incbuabtion vs. Culture 32A at 37°C incbuabtion	Yes	****	< 0.0001
Culture 37B at 32°C incbuabtion vs. Culture 32B at 37°C incbuabtion	Yes	****	< 0.0001
Culture 37B at 32°C incbuabtion vs. Culture 32C at 37°C incbuabtion	No	ns	0.384
Culture 37B at 32°C incbuabtion vs. Culture 37A at 37°C incbuabtion	Yes	****	< 0.0001
Culture 37B at 32°C incbuabtion vs. Culture 37B at 37°C incbuabtion	Yes	****	< 0.0001
Culture 37B at 32°C incbuabtion vs. Culture 37C at 37°C incbuabtion	No	ns	0.4463
Culture 37C at 32°C incbuabtion vs. Culture 32A at 37°C incbuabtion	Yes	****	< 0.0001
Culture 37C at 32°C incbuabtion vs. Culture 32B at 37°C incbuabtion	Yes	****	< 0.0001
Culture 37C at 32°C incbuabtion vs. Culture 32C at 37°C incbuabtion	Yes	***	0.0005
Culture 37C at 32°C incbuabtion vs. Culture 37A at 37°C incbuabtion	No	ns	0.0721
Culture 37C at 32°C incbuabtion vs. Culture 37B at 37°C incbuabtion	Yes	***	0.0001
Culture 37C at 32°C incbuabtion vs. Culture 37C at 37°C incbuabtion	No	ns	> 0.9999
Culture 32A at 37°C incbuabtion vs. Culture 32B at 37°C incbuabtion	No	ns	> 0.9999
Culture 32A at 37°C incbuabtion vs. Culture 32C at 37°C incbuabtion	Yes	**	0.0063
Culture 32A at 37°C incbuabtion vs. Culture 37A at 37°C incbuabtion	Yes	****	< 0.0001
Culture 32A at 37°C incbuabtion vs. Culture 37B at 37°C incbuabtion	Yes	****	< 0.0001
Culture 32A at 37°C incbuabtion vs. Culture 37C at 37°C incbuabtion	Yes	****	< 0.0001
Culture 32B at 37°C incbuabtion vs. Culture 32C at 37°C incbuabtion	Yes	*	0.0219
Culture 32B at 37°C incbuabtion vs. Culture 37A at 37°C incbuabtion	Yes	****	< 0.0001
Culture 32B at 37°C incbuabtion vs. Culture 37B at 37°C incbuabtion	Yes	****	< 0.0001
Culture 32B at 37°C incbuabtion vs. Culture 37C at 37°C incbuabtion	Yes	****	< 0.0001
Culture 32C at 37°C incbuabtion vs. Culture 37A at 37°C incbuabtion	Yes	****	< 0.0001
Culture 32C at 37°C incbuabtion vs. Culture 37B at 37°C incbuabtion	Yes	****	< 0.0001
Culture 32C at 37°C incbuabtion vs. Culture 37C at 37°C incbuabtion	Yes	**	0.0025
Culture 37A at 37°C incbuabtion vs. Culture 37B at 37°C incbuabtion	No	ns	0.3038
Culture 37A at 37°C incbuabtion vs. Culture 37C at 37°C incbuabtion	Yes	*	0.0171
Culture 37B at 37°C incbuabtion vs. Culture 37C at 37°C incbuabtion	Yes	****	< 0.0001

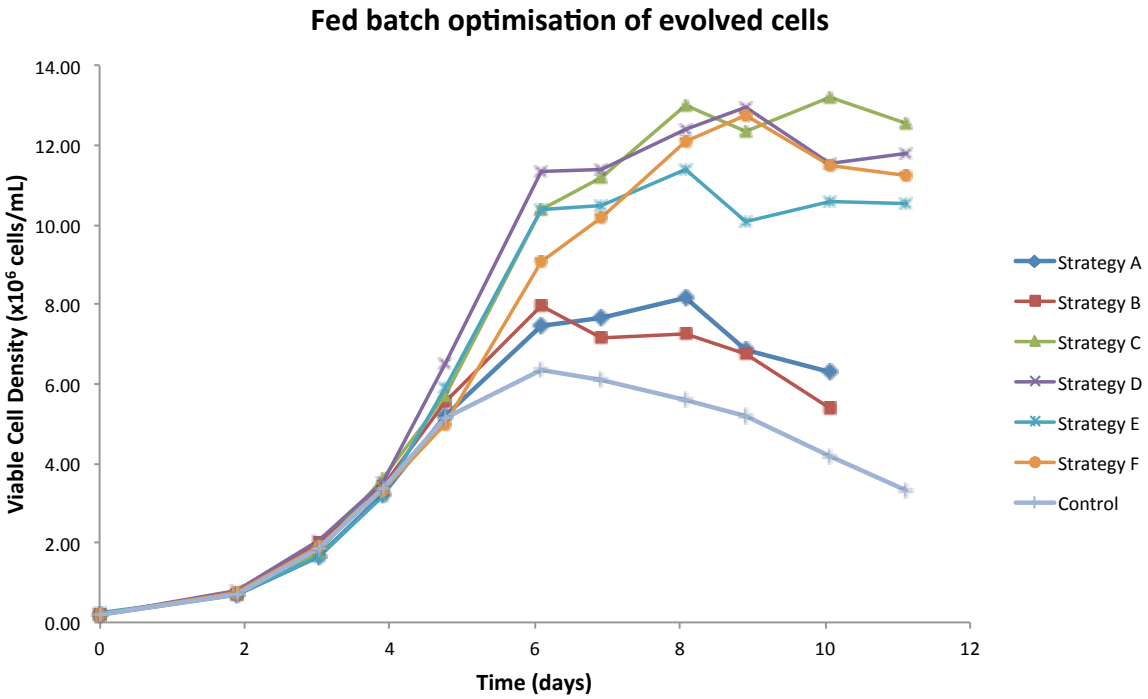

Day 10 titre cB72.3 and Enbrel

Tukey's multiple comparisons test	Significant?	Summary	Adjusted P Value
32C Evolved cB72.3 vs. 32C Evolved Enbrel	No	ns	0.9989
32C Evolved cB72.3 vs. 32C Parental cB72.3	Yes	*	0.0284
32C Evolved cB72.3 vs. 32C Parental Enbrel	No	ns	0.2703
32C Evolved cB72.3 vs. 37C Evolved cB72.3	Yes	***	0.0002
32C Evolved cB72.3 vs. 37C Evolved Enbrel	Yes	***	0.0003
32C Evolved cB72.3 vs. 37C Parental cB72.3	No	ns	0.5106
32C Evolved cB72.3 vs. 37C Parental Enbrel	No	ns	0.8263
32C Evolved Enbrel vs. 32C Parental cB72.3	Yes	**	0.0096
32C Evolved Enbrel vs. 32C Parental Enbrel	No	ns	0.1078
32C Evolved Enbrel vs. 37C Evolved cB72.3	Yes	****	< 0.0001
32C Evolved Enbrel vs. 37C Evolved Enbrel	Yes	***	0.0001
32C Evolved Enbrel vs. 37C Parental cB72.3	No	ns	0.2393
32C Evolved Enbrel vs. 37C Parental Enbrel	No	ns	0.5106
32C Parental cB72.3 vs. 32C Parental Enbrel	No	ns	0.8936
32C Parental cB72.3 vs. 37C Evolved cB72.3	No	ns	0.2703
32C Parental cB72.3 vs. 37C Evolved Enbrel	No	ns	0.3405
32C Parental cB72.3 vs. 37C Parental cB72.3	No	ns	0.6524
32C Parental cB72.3 vs. 37C Parental Enbrel	No	ns	0.3405
32C Parental Enbrel vs. 37C Evolved cB72.3	Yes	*	0.0284
32C Parental Enbrel vs. 37C Evolved Enbrel	Yes	*	0.0385
32C Parental Enbrel vs. 37C Parental cB72.3	No	ns	0.9996
32C Parental Enbrel vs. 37C Parental Enbrel	No	ns	0.9605
37C Evolved cB72.3 vs. 37C Evolved Enbrel	No	ns	> 0.9999
37C Evolved cB72.3 vs. 37C Parental cB72.3	Yes	*	0.0112
37C Evolved cB72.3 vs. 37C Parental Enbrel	Yes	**	0.0038
37C Evolved Enbrel vs. 37C Parental cB72.3	Yes	*	0.0153
37C Evolved Enbrel vs. 37C Parental Enbrel	Yes	**	0.0051
37C Parental cB72.3 vs. 37C Parental Enbrel	No	ns	0.9989

Stable titres from Evolved and Parental, cB72.3 and Enbrel pools

Tukey's multiple comparisons test	Significant?	Summary	Adjusted P Value
Evolved cB72.3 vs. Parental cB72.3	Yes	*	0.0152
Evolved cB72.3 vs. Evolved Enbrel	Yes	*	0.0152
Evolved cB72.3 vs. Parental Enbrel	Yes	****	< 0.0001
Parental cB72.3 vs. Evolved Enbrel	Yes	***	0.0002
Parental cB72.3 vs. Parental Enbrel	Yes	***	0.0003
Evolved Enbrel vs. Parental Enbrel	Yes	****	< 0.0001

Appendix III

Seahorse profile showing no difference between operating temperatures (auto-colour grouping based on similarity) - blue represent parental cells run at both 37ºC and 32ºC and green evolved cells run at both 37ºc and 32ºC

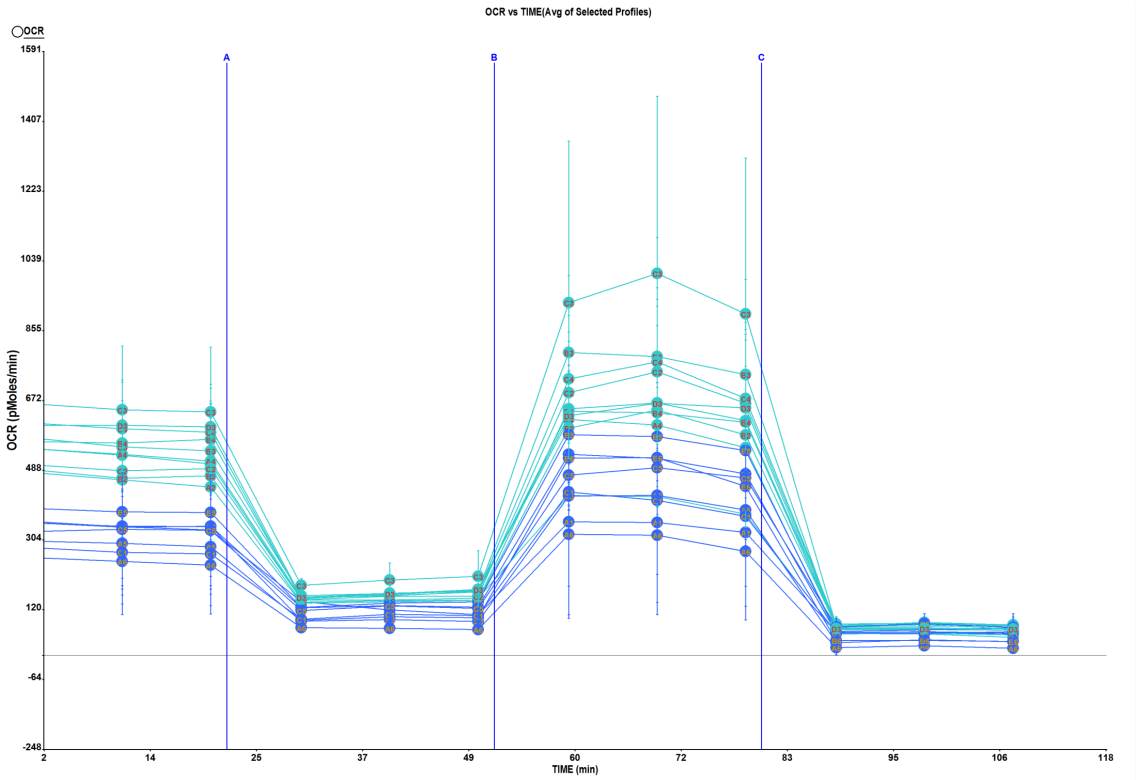

Table of Affymetrix transcript expression fold change (with p<0.01 threshold) between cell lines

Evolved: 32Condition 1.Bi.weight. Avg.Signal..log2.	Parental: 37Condition 2.Bi.weight. Avg.Signal..log2.	Fold. Change. linear	FDR. p.value	Alias	Uniprot ID	UP/ DOWN in evolved
12.19	5.73	87.98	0.00226	Pla2g2a	P31482	UP
11.61	5.82	55.23	0.001023	Fmod	P50608	UP
10.34	4.83	45.37	0.002687	Selenbp1	D6RHN2	UP
8.38	3.63	26.89	0.000921	LOC100753012	#N/A	UP
8.38	3.86	22.97	0.001947	LOC100771217	#N/A	UP
10.94	6.49	21.89	0.000946	Col6a1	Q04857	UP
8.18	3.87	19.77	0.001353	Gnat3	Q3V3I2	UP
9.34	5.07	19.36	0.001353	Vsnl1	B2L107	UP

10.77	6.7	16.87	0.000921	I79_011941	#N/A	UP
8.27	4.24	16.37	0.001353	Arhgap42	B2RQE8	UP
9.52	5.51	16.1	0.001353	Fgfr2	E9PX60	UP
11.18	7.43	13.42	0.001023	Odz2	#N/A	UP
12.1	8.39	13.1	0.000921	Cd36	Q08857	UP
10.03	6.45	11.97	0.005042	LOC100768488	#N/A	UP
8.26	4.78	11.17	0.001353	Clcn5	Q8C6W8	UP
8.6	5.25	10.26	0.002392	Cyp4a14	O35728	UP
9.54	6.18	10.24	0.001055	Slc38a4	Q9CVZ0	UP
10.92	7.63	9.74	0.002879	Ulbp1	Q3MI26	UP
10.52	7.28	9.45	0.001361	Fabp4	Q99M00	UP
8.49	5.25	9.43	0.002388	LOC100768137	#N/A	UP
9.04	5.88	8.93	0.002155	Angpt2	#N/A	UP
9.61	6.49	8.7	0.001954	I79_007854	#N/A	UP
8.92	5.81	8.6	0.003795	Angpt2	#N/A	UP
9.71	6.7	8.07	0.001353	Vcam1	Q3UPN1	UP
9.77	6.78	7.94	0.001432	Gjb5	Q91XA4	UP
8.73	5.74	7.92	0.002975	Spp1	Q3TLP1	UP
8.15	5.17	7.89	0.001055	I79_022127	#N/A	UP
11.11	8.22	7.46	0.001353	Cxcl3	#N/A	UP
9.6	6.8	6.96	0.001361	Sorl1	O88307	UP
8.7	5.91	6.93	0.004471	LOC100761143	#N/A	UP
11.54	8.76	6.86	0.001353	Rbm3	O89086	UP
8.53	5.79	6.68	0.002148	Slc38a4	Q9CVZ0	UP
8.21	5.48	6.66	0.001926	Spn	P15702	UP
12.53	9.83	6.5	0.001353	Ccl7	#N/A	UP
9.11	6.42	6.49	0.001023	Tmem176a	Q99JK9	UP
9.79	7.17	6.13	0.00235	Tmem176b	#N/A	UP
6.53	3.95	5.98	0.002841	LOC100756455	#N/A	UP
9.87	7.29	5.97	0.000921	LOC100767308	#N/A	UP
8.96	6.44	5.75	0.00405	LOC100773073	#N/A	UP
8.8	6.3	5.65	0.003051	Vcam1	Q3UPN1	UP
9.17	6.72	5.44	0.006887	Cd9	P40240	UP
8.99	6.57	5.37	0.005809	Cyp4b1	Q64462	UP
8.86	6.46	5.28	0.001055	Rps6ka2	Q7TPD5	UP
9	6.64	5.13	0.003372	I79_018773	#N/A	UP
7.92	5.59	5.03	0.001947	Tcra	P01849	UP
10.48	8.15	5	0.001055	Gpr133	B2RXV6	UP
11.8	9.49	4.94	0.002985	Ndrg1	Q545R3	UP
9.48	7.2	4.87	0.001947	Plet1	Q8VEN2	UP
8.6	6.32	4.83	0.004524	Pdzrn3	Q3UXA7	UP
8.21	5.95	4.78	0.002687	Krt7	D3Z6N5	UP
9.15	6.91	4.71	0.004216	Sema4d	Q8BJC1	UP
5.2	2.97	4.7	0.007164	Dlg5	Q9D3X0	UP

7.47	5.25	4.66	0.002104	I79_010791	#N/A	UP
7.09	4.89	4.59	0.005969	Faim2	#N/A	UP
8.39	6.2	4.57	0.006085	C10orf112	#N/A	UP
8.4	6.21	4.55	0.001551	Pla2g5	P97391	UP
7.95	5.78	4.51	0.002041	Grhl2	F6TZV3	UP
8.12	5.96	4.45	0.003	Slpi	P97430	UP
7.72	5.57	4.44	0.005969	Nedd9	#N/A	UP
6.98	4.83	4.43	0.002818	Themis	Q8BGW0	UP
8.22	6.09	4.37	0.00209	Tmcc3	Q8R310	UP
9.21	7.1	4.3	0.003738	I79_005369	#N/A	UP
9.14	7.05	4.26	0.002841	Sorl1	O88307	UP
9.73	7.67	4.18	0.001353	Traf1	P39428	UP
8.29	6.24	4.15	0.00388	Parvg	Q9ERD8	UP
9.89	7.85	4.13	0.003125	I79_025705	#N/A	UP
7.51	5.51	4.02	0.002041	I79_005372	#N/A	UP
9.47	7.46	4.02	0.00209	I79_018466	#N/A	UP
6.89	4.89	4.02	0.003103	I79_020126	#N/A	UP
7.93	5.93	4.01	0.003944	Sertad4	A7DTG3	UP
9.47	7.47	4	0.001421	Casp12	O08736	UP
8.04	6.05	3.98	0.004923	Ulbp1	Q3MI26	UP
7.08	5.1	3.95	0.003221	Myom2	Q14BI5	UP
7.06	5.09	3.92	0.003162	Ncf1	Q09014	UP
9.91	7.94	3.92	0.002995	Lmo7	Q3UPW3	UP
7.93	5.98	3.86	0.009598	I79_018190	#N/A	UP
9.05	7.11	3.83	0.001907	Lamb3	Q61087	UP
7.66	5.73	3.82	0.001529	Sorl1	O88307	UP
9.97	8.04	3.8	0.003009	S100a4	D3YUT9	UP
6.83	4.91	3.79	0.007005	LOC100757275	#N/A	UP
8.13	6.22	3.78	0.005448	Pde1c	Q64338	UP
9.6	7.72	3.68	0.001353	Vnn1	Q9Z0K8	UP
10.28	8.4	3.68	0.001055	Ca5b	#N/A	UP
11.65	9.78	3.67	0.001353	Rarres2	Q9DD06	UP
5.33	3.46	3.65	0.002041	I79_005370	#N/A	UP
9.1	7.25	3.61	0.001926	Cyp7b1	Q60991	UP
9.4	7.55	3.6	0.001715	Pglyrp2	A2TJ61	UP
8.53	6.7	3.56	0.009008	Eml1	Q05BC3	UP
11.18	9.37	3.5	0.001846	Cxcr7	#N/A	UP
7.65	5.85	3.49	0.004384	Wisp1	D3Z6X6	UP
7.45	5.66	3.45	0.00878	Susd1	E9Q3H4	UP
6.51	4.74	3.43	0.004216	Tnfsf13b	Q8BVA3	UP
8.14	6.36	3.42	0.001926	Cldn15	Q9Z0S5	UP
8.38	6.62	3.4	0.002995	Ccrl2	#N/A	UP
7.72	5.96	3.38	0.006892	I79_017897	#N/A	UP
8.99	7.24	3.36	0.001684	Fcgrt	Q6PKB0	UP

7.98	6.25	3.32	0.002041	Tnfsf15	Q5UCC2	UP
7.82	6.09	3.3	0.001947	LOC100765994	#N/A	UP
8.63	6.9	3.3	0.005006	Slc11a1	#N/A	UP
7.51	5.8	3.29	0.005373	Gjb4	Q8C677	UP
9.99	8.29	3.25	0.001713	I79_001143	#N/A	UP
7.12	5.42	3.23	0.004246	Sdc2	Q99L05	UP
8.89	7.21	3.21	0.008768	Muc13	#N/A	UP
8.54	6.86	3.19	0.002995	Cxcl12	H7BX38	UP
7.2	5.58	3.09	0.009387	Krt14	#N/A	UP
7.92	6.31	3.05	0.002392	Fam55d	#N/A	UP
9.15	7.57	3	0.002639	I79_025704	#N/A	UP
8.35	6.77	2.98	0.004355	I79_012233	#N/A	UP
8.94	7.36	2.97	0.009874	Star	P51557	UP
8.06	6.5	2.96	0.006211	Mab21l3	Q8CI17	UP
7.63	6.07	2.94	0.002736	Ccl11	#N/A	UP
9.67	8.11	2.94	0.001353	Sars2	#N/A	UP
7	5.46	2.91	0.003536	Myo1g	Q5SUA5	UP
6.92	5.39	2.9	0.003314	Enpp6	Q8BGN3	UP
7.71	6.21	2.83	0.003503	Cryab	#N/A	UP
10.22	8.72	2.83	0.001353	Sars2	#N/A	UP
7.88	6.38	2.82	0.002392	Sulf2	Q8CFG0	UP
8.25	6.77	2.8	0.004077	I79_021562	#N/A	UP
9.59	8.13	2.75	0.005927	LOC100763064	#N/A	UP
8.72	7.27	2.73	0.003757	Ccl17	F6R5P4	UP
9.21	7.76	2.73	0.003795	Gm12824	#N/A	UP
7.59	6.15	2.72	0.001684	Ndrg1	Q545R3	UP
8.53	7.09	2.72	0.00453	I79_006740	#N/A	UP
10.65	9.21	2.71	0.001715	I79_022735	#N/A	UP
7.14	5.71	2.68	0.009793	LOC100759235	#N/A	UP
8.84	7.47	2.6	0.005665	I79_021639	#N/A	UP
9.52	8.15	2.6	0.008107	LOC100761328	#N/A	UP
7.12	5.74	2.59	0.008335	Sult1a1	D3Z2P8	UP
8.14	6.77	2.59	0.005056	Tnfsf15	Q5UCC2	UP
9.98	8.61	2.58	0.001353	Gcom1	E9PZ54	UP
9.66	8.29	2.58	0.001353	Ebi3	#N/A	UP
10.08	8.71	2.58	0.003009	Gm12824	#N/A	UP
10.21	8.84	2.57	0.001023	Il18	Q80SS8	UP
8.17	6.81	2.56	0.003372	Pstpip1	P97814	UP
7.52	6.17	2.56	0.004562	I79_010833	#N/A	UP
7.73	6.4	2.53	0.003718	Matn4	O89029	UP
6.77	5.44	2.51	0.007362	Gabrb3	F6WUM4	UP
10.88	9.58	2.46	0.001353	Smad3	A2CG45	UP
10.16	8.87	2.44	0.001023	Upb1	Q8VC97	UP
7.31	6.03	2.42	0.002392	Acr	P23578	UP

7.5	6.23	2.41	0.002535	Fbn3	#N/A	UP
10.06	8.82	2.37	0.001947	Atad3	#N/A	UP
9.06	7.81	2.37	0.004788	I79_004634	#N/A	UP
7.34	6.09	2.37	0.005107	Plxna4	#N/A	UP
7.18	5.94	2.36	0.006469	LOC100757355	#N/A	UP
7.58	6.34	2.36	0.001023	LOC100768668	#N/A	UP
9.88	8.65	2.35	0.00687	I79_005883	#N/A	UP
8.22	6.99	2.35	0.001926	LOC100767926	#N/A	UP
10.09	8.88	2.33	0.003424	Xlr3a	Q60595	UP
11.26	10.05	2.32	0.002995	---	#N/A	UP
8.1	6.89	2.32	0.003478	Plxna4	#N/A	UP
6.95	5.74	2.31	0.002841	Mfng	O09008	UP
8.88	7.67	2.31	0.001575	I79_004393	#N/A	UP
9.01	7.8	2.31	0.001907	Znf667	#N/A	UP
9.7	8.51	2.29	0.001023	Retsat	F7CW61	UP
10.01	8.81	2.29	0.004307	Tomm40	G3UY77	UP
9.6	8.41	2.29	0.004384	I79_005395	#N/A	UP
7.69	6.5	2.28	0.002995	Bmpr1b	D6RET5	UP
8.69	7.49	2.28	0.004292	Pramef12	Q9D2F1	UP
9.91	8.73	2.27	0.002841	I79_005396	#N/A	UP
9.15	7.98	2.25	0.001353	Tln2	Q71LX4	UP
5.99	4.83	2.24	0.003309	Pramef18	#N/A	UP
10.01	8.84	2.24	0.002407	Prpf31	#N/A	UP
9.36	8.2	2.22	0.001926	Smg9	Q9DB90	UP
9.06	7.9	2.22	0.00226	I79_021748	#N/A	UP
9.66	8.51	2.21	0.002429	Retsat	F7CW61	UP
8.2	7.06	2.21	0.005185	Env	Q811N5	UP
7.63	6.49	2.2	0.004477	I79_003704	#N/A	UP
9.39	8.25	2.2	0.004537	I79_011079	#N/A	UP
8.64	7.51	2.19	0.003843	Slc39a2	E0CY93	UP
10.4	9.27	2.19	0.001432	Dhx33	Q80VY9	UP
6.65	5.51	2.19	0.003769	LOC100758982	#N/A	UP
6.18	5.06	2.17	0.007242	Sycp3	M0QW86	UP
7.97	6.85	2.17	0.002995	Gem	Q3U4X4	UP
7.56	6.45	2.17	0.002292	LOC100756916	#N/A	UP
8.24	7.13	2.17	0.002995	Pde1b1	#N/A	UP
6.63	5.52	2.16	0.008329	Abcg1	#N/A	UP
9.96	8.86	2.15	0.001353	Ldlrap1	Q3TEF2	UP
10.6	9.49	2.15	0.002995	Kctd20	Q8CDD8	UP
7.07	5.97	2.14	0.005532	Nnmt	O55239	UP
9.25	8.16	2.12	0.001904	Abhd6	Q8R2Y0	UP
8.85	7.76	2.12	0.002887	LOC100771057	#N/A	UP
8.82	7.75	2.11	0.005006	Gramd1b	D3YWR0	UP
7.46	6.38	2.11	0.002995	Myo1g	Q5SUA5	UP

8.41	7.33	2.11	0.005993	Plxna4	#N/A	UP
9.46	8.39	2.1	0.00415	Hmgcs2	P54869	UP
9.96	8.89	2.1	0.004302	I79_001308	#N/A	UP
8.69	7.63	2.09	0.003474	Slc27a3	B2RUG3	UP
9.36	8.29	2.09	0.001353	Acsl3	E9PUC2	UP
6.28	5.21	2.09	0.004965	Ndrg1	Q545R3	UP
10.99	9.93	2.09	0.001353	Odc1	Q8CIC5	UP
8.24	7.18	2.09	0.005185	LOC100751789	#N/A	UP
8.76	7.71	2.08	0.00411	I79_026111	#N/A	UP
9.24	8.18	2.07	0.001754	Nipsnap3a	B1AWZ3	UP
7.89	6.84	2.07	0.006015	Vill	D3YZN9	UP
10.08	9.03	2.07	0.009492	I79_003711	#N/A	UP
7.85	6.8	2.07	0.001676	I79_017685	#N/A	UP
6.6	5.56	2.06	0.00474	Enpep	P16406	UP
8	6.96	2.05	0.001353	Fscn1	F7BDR1	UP
9.68	8.65	2.05	0.009387	Ahcy	P50247	UP
7.59	6.56	2.05	0.003331	Arl11	Q6P3A9	UP
8	6.96	2.05	0.00949	Env	Q811N5	UP
8	6.96	2.05	0.00949	Env	Q811N5	UP
9.77	8.74	2.05	0.003467	Mtrr	Q8C1A3	UP
9.43	8.4	2.05	0.005727	Extl1	Q9JKV7	UP
9.13	8.1	2.04	0.003816	Pol	P10400	UP
10.53	9.51	2.04	0.001353	Dusp1	Q3UCQ6	UP
7.13	6.1	2.04	0.004095	I79_008870	#N/A	UP
10.1	9.07	2.04	0.007025	I79_026190	#N/A	UP
7.75	6.73	2.03	0.00388	N4bp2	F8VQG7	UP
7.89	6.86	2.03	0.002895	Rhoj	Q3TZU6	UP
11.1	10.08	2.03	0.002995	Ftsj1	Q8JZY1	UP
11.1	10.08	2.03	0.001432	Trmt6	#N/A	UP
6.37	5.35	2.02	0.007984	Cyp11a1	Q6NV84	UP
10.51	9.49	2.02	0.002041	Lrrc1	Q80VQ1	UP
9.89	8.88	2.02	0.003309	Ppap2b	#N/A	UP
10.79	9.78	2.01	0.003978	Agpat5	F8WGD9	UP
8.01	7.01	2.01	0.009746	Angptl4	Q3UYS5	UP
8.24	7.23	2.01	0.008824	I79_008949	#N/A	UP
8.76	7.76	2	0.006593	Svil	Q8K4L3	UP
7.03	6.03	2	0.004216	Aldh1a1	#N/A	UP
8.65	7.65	2	0.008638	LOC100754972	#N/A	UP
10.43	9.43	2	0.002879	Slc39a8	#N/A	UP
9.97	8.98	1.98	0.008209	Serpine1	D0ESZ6	UP
7.41	6.43	1.98	0.006078	Cacng4	Q9JJV4	UP
8.48	7.49	1.98	0.007345	I79_023483	#N/A	UP
6.79	5.8	1.98	0.007908	Serpinb9	#N/A	UP
8.22	7.25	1.97	0.00944	Papola	F7CXD5	UP

9.27	8.29	1.97	0.003604	Tmod2	Q9JKK7	UP
8.36	7.38	1.97	0.006774	I79_000123	#N/A	UP
9.05	8.07	1.97	0.007475	Znf540	#N/A	UP
10.12	9.15	1.96	0.007164	Ada	P03958	UP
9.98	9.01	1.96	0.005817	Ppcs	#N/A	UP
11.33	10.36	1.95	0.003005	Serpinb1a	Z4YK03	UP
8.56	7.6	1.94	0.003718	Lztfl1	Q9JHQ5	UP
9.36	8.4	1.94	0.00597	Sufu	Q9Z0P7	UP
7.5	6.55	1.94	0.006426	Plekha7	S4R243	UP
6	5.04	1.94	0.008826	I79_009161	#N/A	UP
10.77	9.82	1.94	0.004635	I79_020131	#N/A	UP
7.5	6.55	1.93	0.007164	Rplp2	P99027	UP
9.94	9	1.93	0.002597	Mitf	Q3U2D2	UP
7.85	6.91	1.93	0.008793	I79_021323	#N/A	UP
10.14	9.19	1.92	0.006887	Nupr1	Q9WTK0	UP
9.91	8.97	1.92	0.004056	I79_025541	#N/A	UP
9.02	8.08	1.92	0.003696	Rnf19a	#N/A	UP
7.86	6.92	1.92	0.006915	Znf227	#N/A	UP
9.68	8.75	1.91	0.00687	LOC100757283	#N/A	UP
9.74	8.82	1.9	0.005014	Amdhd2	Q8JZV7	UP
8.72	7.8	1.9	0.005619	I79_024095	#N/A	UP
9.66	8.73	1.9	0.005212	Nt5c3l	#N/A	UP
11.42	10.5	1.89	0.001353	Mthfd2l	D3YZG8	UP
9.26	8.34	1.89	0.007269	Gls	F6U529	UP
12.43	11.51	1.89	0.001353	Ppp2r1a	Q76MZ3	UP
9.11	8.19	1.89	0.002593	Itfg2	Q91WI7	UP
7.27	6.35	1.89	0.007273	Prelp	Q9JK53	UP
10.31	9.4	1.88	0.009628	Mthfd2l	D3YZG8	UP
8.93	8.02	1.88	0.006248	Ikbke	Q8CI55	UP
11.49	10.59	1.87	0.001353	Gag	Q7M6U4	UP
10.64	9.74	1.87	0.002867	Sufu	Q9Z0P7	UP
10.53	9.63	1.87	0.003718	Slc39a8	#N/A	UP
6.33	5.44	1.86	0.005759	I79_013110	#N/A	UP
9.83	8.94	1.85	0.005969	Rassf5	D3Z6G2	UP
6.5	5.61	1.85	0.003414	Aox1	Q3UV07	UP
7.38	6.5	1.85	0.008727	Col7a1	Q63870	UP
7.27	6.38	1.85	0.007005	I79_010496	#N/A	UP
6.99	6.11	1.85	0.002895	I79_022914	#N/A	UP
8.91	8.03	1.85	0.005651	I79_024051	#N/A	UP
6.39	5.5	1.85	0.009785	Kiaa1257	#N/A	UP
9.21	8.33	1.84	0.004363	Ttc38	A3KMP2	UP
11.09	10.21	1.84	0.004691	Hmox1	P14901	UP
10.15	9.27	1.84	0.009553	Hps1	Q3U309	UP
7.36	6.48	1.84	0.007276	Mylip	Q8BM54	UP

6.77	5.89	1.84	0.00944	Gfra2	Q9Z2A3	UP
8.77	7.9	1.83	0.003949	Tatdn2	B7ZNL9	UP
9.68	8.81	1.83	0.003949	Nuak1	F6XZX4	UP
7.3	6.43	1.83	0.002727	Thbs2	Q7TMT3	UP
11.39	10.52	1.83	0.000921	Ifrd2	Q7TSB3	UP
8.85	7.98	1.83	0.002967	Abcb8	Q9CXJ4	UP
9.43	8.56	1.83	0.001023	Cds1	#N/A	UP
6.65	5.77	1.83	0.003331	Dnajb3	#N/A	UP
8.57	7.7	1.82	0.003718	Dnajc25	A2ALW5	UP
8.79	7.93	1.82	0.003722	Pink1	Q99MQ3	UP
8.52	7.66	1.82	0.006916	I79_006743	#N/A	UP
9.4	8.54	1.82	0.006774	I79_023238	#N/A	UP
7.86	7	1.82	0.003253	I79_026033	#N/A	UP
10.62	9.76	1.81	0.006785	Scfd2	Q3UXF7	UP
8.94	8.09	1.81	0.003738	Abcc3	Q59DK8	UP
10.24	9.39	1.81	0.004151	Rab32	Q9CZE3	UP
10.97	10.12	1.81	0.008374	I79_020132	#N/A	UP
7.24	6.39	1.81	0.007396	LOC100763344	#N/A	UP
10	9.14	1.81	0.008264	LOC100767950	#N/A	UP
10.44	9.58	1.81	0.005619	Mrps22	#N/A	UP
10.96	10.1	1.81	0.004495	Pop7	#N/A	UP
10.72	9.87	1.8	0.002104	Tgfbr2	Q62312	UP
7.9	7.05	1.8	0.005401	LOC100758541	#N/A	UP
8.68	7.83	1.8	0.006532	S100a6	#N/A	UP
10.78	9.94	1.79	0.002392	Lgals3bp	F6VRP8	UP
10.92	10.08	1.79	0.006448	Eif5	P59325	UP
10.51	9.67	1.79	0.004128	Sod2	Q3U8W4	UP
8.19	7.36	1.79	0.00388	LOC100753996	#N/A	UP
8.9	8.07	1.78	0.005619	Klf4	B7ZCH2	UP
9.71	8.88	1.78	0.002298	Serpine1	D0ESZ6	UP
9.04	8.21	1.78	0.001353	Slc16a6	H9KUY0	UP
9.53	8.69	1.78	0.002985	Wbscr16	Q9CYF5	UP
8.62	7.79	1.78	0.006211	I79_010035	#N/A	UP
10.01	9.17	1.78	0.00183	I79_018215	#N/A	UP
11.08	10.25	1.78	0.005771	Mlf1ip	#N/A	UP
10.17	9.34	1.78	0.005465	Rabl2a	#N/A	UP
9.27	8.44	1.77	0.004404	Slc29a3	D6RI95	UP
7.95	7.13	1.77	0.007908	Gng7	Q3UGN1	UP
8.96	8.13	1.77	0.003565	St14	Q543E3	UP
10.18	9.35	1.77	0.00235	Tmem51	Q99LG1	UP
8.81	7.99	1.76	0.006935	Rchy1	Q8R593	UP
7.61	6.79	1.76	0.005279	Gas8	#N/A	UP
6.64	5.82	1.76	0.008608	I79_002907	#N/A	UP
8.08	7.26	1.76	0.006887	I79_006392	#N/A	UP

6.44	5.63	1.76	0.005831	LOC100771615	#N/A	UP
6.98	6.17	1.75	0.004486	Tfap2c	A2APA8	UP
9.79	8.97	1.75	0.002392	Cirbp	D3YU80	UP
11.28	10.47	1.75	0.005131	Tmc4	Q7TQ65	UP
12.17	11.36	1.75	0.009731	Ppp3ca	Q8C649	UP
9.59	8.78	1.75	0.002995	Dusp15	Q8R4V2	UP
10.23	9.43	1.75	0.009517	C1qbp	#N/A	UP
9.86	9.05	1.75	0.004216	Tsta3	#N/A	UP
9.42	8.63	1.74	0.001551	Fam120c	B7ZW94	UP
10.26	9.46	1.74	0.002041	Ercc2	Q3UKK7	UP
9.61	8.8	1.74	0.002041	Tnfaip3	Q7TQD1	UP
10.43	9.63	1.74	0.00878	Rpl14	Q9CR57	UP
9.23	8.43	1.74	0.00163	Oasl	#N/A	UP
8.51	7.71	1.74	0.003471	Slc15a3	#N/A	UP
10.7	9.91	1.73	0.005812	Pkn1	D6RH37	UP
6.95	6.17	1.73	0.009008	Lrrn4	P59383	UP
7.57	6.78	1.73	0.009969	Rnf122	Q8BP31	UP
9.25	8.45	1.73	0.006426	Xkr8	Q8C0T0	UP
9.12	8.33	1.73	0.004101	Zbtb20	Q8CAI3	UP
9.47	8.68	1.73	0.005138	LOC100766458	#N/A	UP
9.64	8.85	1.72	0.00338	Guf1	Q8C3X4	UP
11.47	10.69	1.72	0.001926	Zfp64	Q99KE8	UP
10.49	9.71	1.72	0.002995	Trip13	#N/A	UP
9.31	8.53	1.71	0.002801	Rnd3	E9Q8D7	UP
9.33	8.56	1.71	0.004677	Unc5b	Q3TYW6	UP
13.12	12.35	1.71	0.005052	Sprr1a	Q62266	UP
11.51	10.74	1.71	0.002392	Tfdp2	Q8BHD2	UP
9.8	9.03	1.71	0.00944	Ndufb3	Q9CQZ6	UP
6.59	5.81	1.71	0.009114	I79_009605	#N/A	UP
9.25	8.48	1.7	0.005532	Nfatc1	Q6P7T9	UP
11.63	10.87	1.7	0.005213	Ppp3ca	Q8C649	UP
10.51	9.75	1.7	0.008257	Exosc10	Q8K366	UP
9.22	8.45	1.7	0.004721	Pdss1	Q9CZQ1	UP
9.83	9.06	1.7	0.001926	Cdc42se2-A	#N/A	UP
10.58	9.82	1.69	0.007412	Tspan9	D3YU98	UP
7.74	6.98	1.69	0.009983	Wisp1	D3Z6X6	UP
9.33	8.57	1.69	0.007164	Mns1	Q61884	UP
10.4	9.64	1.69	0.007005	Tpm1	Q8BSH3	UP
7.6	6.85	1.69	0.007472	Ptprt	Q99M80	UP
10.64	9.89	1.69	0.005006	Clptm1	#N/A	UP
9.14	8.38	1.69	0.008121	Fbxo4	#N/A	UP
9.25	8.49	1.69	0.007039	I79_006856	#N/A	UP
9.31	8.56	1.69	0.005014	I79_023554	#N/A	UP
7.2	6.43	1.69	0.002043	I79_024424	#N/A	UP

7.03	6.27	1.69	0.004246	LOC100774241	#N/A	UP
7.7	6.95	1.68	0.009649	Plekha2	D3Z3L8	UP
8.56	7.82	1.68	0.003331	Limk2	O54785	UP
8.85	8.1	1.68	0.005552	Tgfbr1	Q64729	UP
7.78	7.04	1.68	0.008799	Dtx4	Q6PDK8	UP
12.03	11.28	1.68	0.00338	Hprt1	#N/A	UP
10.78	10.04	1.67	0.001353	Vtn	P29788	UP
8.84	8.1	1.67	0.004611	Trub2	Q91WG3	UP
7.18	6.45	1.67	0.006785	Btbd17	Q9DB72	UP
8.55	7.81	1.67	0.007462	Xpa	S4R260	UP
11.14	10.4	1.67	0.005373	I79_007599	#N/A	UP
8.96	8.23	1.66	0.005185	Polr1e	G8JL51	UP
9.36	8.63	1.66	0.005868	Slc4a2	Q7TPS4	UP
10.52	9.79	1.66	0.009755	Tbl3	Q8C4J7	UP
10.66	9.93	1.66	0.002841	Phf20l1	Q8CCJ9	UP
7.24	6.51	1.66	0.007861	Morn1	Q9D5M3	UP
9.12	8.38	1.66	0.001981	Sep-03	#N/A	UP
10.03	9.3	1.66	0.004371	---	#N/A	UP
8.91	8.18	1.66	0.003718	LOC100751805	#N/A	UP
11.47	10.74	1.65	0.003718	Cxcl1	Q5U5W9	UP
8.84	8.12	1.65	0.004302	Oscp1	Q8BHW2	UP
7.59	6.87	1.65	0.008969	Notch1	Q8BY39	UP
11.02	10.29	1.65	0.007271	Fam113a	#N/A	UP
8.38	7.67	1.64	0.009438	Prss35	Q8C0F9	UP
10.81	10.1	1.64	0.009236	Ncln	Q8VCM8	UP
7.3	6.59	1.64	0.006183	Add2	Q9QYB8	UP
7.68	6.97	1.64	0.007164	Dnah11	#N/A	UP
9.13	8.41	1.64	0.004234	Trdmt1	#N/A	UP
9.02	8.32	1.63	0.002967	Ccdc61	F6XT04	UP
10.6	9.89	1.63	0.00689	Sh3bp5l	Q3TK15	UP
9.68	8.97	1.63	0.00599	Slc43a2	Q5ND23	UP
9.17	8.46	1.63	0.001904	Lrrc1	Q80VQ1	UP
7.18	6.47	1.63	0.003894	Me3	Q8BMF3	UP
9.13	8.43	1.63	0.007122	---	#N/A	UP
11.54	10.83	1.63	0.005014	Cyr61	#N/A	UP
10.64	9.93	1.63	0.004577	I79_003401	#N/A	UP
8.07	7.36	1.63	0.004307	I79_014351	#N/A	UP
8.66	7.95	1.63	0.007942	LOC100768576	#N/A	UP
8.72	8.02	1.62	0.005151	Rbmx	A2AFI4	UP
10.4	9.7	1.62	0.004018	Eci2	E9PUY9	UP
12.12	11.42	1.62	0.003009	Dcn	P28654	UP
11.7	11	1.62	0.007382	Ncl	Q3TGR3	UP
9.16	8.47	1.62	0.001575	Lig1	Q3U4X8	UP
9.11	8.42	1.62	0.00543	Slc9a8	Q8K228	UP

8.98	8.29	1.62	0.00388	Hsd3b7	Q9EQC1	UP
8.44	7.75	1.62	0.00439	LOC100752900	#N/A	UP
8.8	8.11	1.62	0.005619	LOC100765957	#N/A	UP
8.47	7.77	1.62	0.00878	Map3k6	#N/A	UP
7.09	6.4	1.61	0.005361	Glb1l2	Q3UPY5	UP
9.5	8.81	1.61	0.002818	Brd9	Q3UQU0	UP
7.76	7.07	1.61	0.003816	Klhdc9	Q3USL1	UP
11.01	10.32	1.61	0.00436	Trim28	Q5EBP9	UP
7.63	6.95	1.61	0.009175	Col7a1	Q63870	UP
9.82	9.14	1.61	0.00884	Sympk	Q80X82	UP
8.13	7.44	1.61	0.00561	Mxd1	Q8K1Z8	UP
9.3	8.61	1.61	0.004216	Aagab	Q8R2R3	UP
9.65	8.97	1.61	0.001926	Commd5	Q8R395	UP
10.79	10.1	1.61	0.001353	Lrrc49	Q91YK0	UP
6.81	6.13	1.61	0.006731	I79_010008	#N/A	UP
8.47	7.78	1.61	0.005477	LOC100765978	#N/A	UP
9.94	9.26	1.6	0.002429	Vegfa	F8WH10	UP
8.29	7.61	1.6	0.008551	Mitf	Q3U2D2	UP
10.12	9.43	1.6	0.005783	Vps33a	Q80XK7	UP
8.33	7.65	1.6	0.00993	Xrcc6bp1	Q9CWQ3	UP
11.01	10.34	1.6	0.005889	Adh5	#N/A	UP
7.46	6.79	1.6	0.00899	Hmgn4	#N/A	UP
10.58	9.9	1.6	0.009956	I79_000422	#N/A	UP
9.92	9.24	1.6	0.004677	I79_002600	#N/A	UP
10.5	9.83	1.6	0.001353	I79_010093	#N/A	UP
9.27	8.6	1.6	0.004124	Mettl19	#N/A	UP
9.27	8.59	1.6	0.007124	Nom1	#N/A	UP
10.08	9.4	1.59	0.004542	Atp6v1g2	B0V2H4	UP
6.82	6.15	1.59	0.006629	Loxl2	P58022	UP
11.77	11.1	1.59	0.003718	Bcl10	Q3THY9	UP
9.53	8.86	1.59	0.003962	Znf419	#N/A	UP
10.23	9.57	1.58	0.002324	Wdr12	D3Z369	UP
11.19	10.53	1.58	0.003853	Kcnab2	Q3UPV6	UP
9.92	9.26	1.58	0.007931	Rnf187	Q8BFX1	UP
10.28	9.62	1.58	0.005552	Osbpl2	Q8BX94	UP
10.08	9.43	1.58	0.00388	Aco1	Q8VDC3	UP
8.57	7.92	1.58	0.009028	I79_016913	#N/A	UP
8.89	8.23	1.58	0.004611	I79_022183	#N/A	UP
10.67	10.01	1.58	0.001551	Ppp6r1	#N/A	UP
10.6	9.95	1.57	0.001715	Cpped1	D3Z7F7	UP
8.98	8.32	1.57	0.00762	Rad54b	Q6PFE3	UP
9.05	8.4	1.57	0.003584	Fam116a	#N/A	UP
7.93	7.28	1.57	0.005969	I79_000228	#N/A	UP
7.71	7.06	1.57	0.005361	LOC100769258	#N/A	UP

10.81	10.16	1.57	0.006056	Rg9mtd2	#N/A	UP
10.05	9.42	1.56	0.004077	Dab2ip	D6RDE3	UP
9.78	9.13	1.56	0.007047	Ptprg	Q05909	UP
10.92	10.28	1.56	0.003718	Ppp2r1b	Q7TNP2	UP
10.29	9.65	1.56	0.002879	Samm50	Q8BGH2	UP
6.07	5.43	1.56	0.007124	Metap1	Q8BP48	UP
10.77	10.13	1.56	0.002606	Acsl4	Q8BW44	UP
10.22	9.58	1.56	0.004923	Tmem51	Q99LG1	UP
7.99	7.34	1.56	0.003949	Fiz1	Q9WTJ4	UP
7.63	6.99	1.56	0.006312	I79_001976	#N/A	UP
12.07	11.42	1.56	0.00235	I79_016573	#N/A	UP
9.37	8.73	1.55	0.008727	Loxl4	E9Q600	UP
8.14	7.51	1.55	0.004404	Figf	Q6P5N9	UP
10.94	10.31	1.55	0.004225	Pak1ip1	Q9DCE5	UP
10.45	9.82	1.55	0.006593	Dnajc15	#N/A	UP
7.91	7.27	1.55	0.007164	Gpr182	#N/A	UP
10.72	10.09	1.55	0.00474	I79_003196	#N/A	UP
9.79	9.15	1.55	0.002789	I79_024530	#N/A	UP
9.84	9.21	1.55	0.003002	Kiaa0664	#N/A	UP
7.84	7.21	1.55	0.002041	LOC100756814	#N/A	UP
8.88	8.25	1.55	0.008295	Rp2	#N/A	UP
9.51	8.88	1.54	0.008824	Med22	A2ALA4	UP
9.59	8.97	1.54	0.003795	Arrdc3	E0CZE1	UP
9.34	8.72	1.54	0.009792	Foxred1	Q3TQB2	UP
9.77	9.15	1.54	0.005783	Cerk	Q8K4Q7	UP
10.2	9.58	1.54	0.007222	I79_020563	#N/A	UP
8.46	7.83	1.54	0.005766	LOC100750991	#N/A	UP
11.29	10.67	1.54	0.001353	LOC100761050	#N/A	UP
9.08	8.46	1.53	0.004542	Farp1	F8VPU2	UP
10.26	9.65	1.53	0.005666	Yars	Q91WQ3	UP
11.17	10.55	1.53	0.004943	Jub	#N/A	UP
9.64	9.03	1.53	0.006697	LOC100770476	#N/A	UP
9.01	8.39	1.53	0.003718	Tbc1d2	#N/A	UP
13.55	12.95	1.52	0.005918	Hspb1	D3YZ06	UP
9.81	9.21	1.52	0.007782	Elof1	P60003	UP
9.58	8.98	1.52	0.009637	Irs2	P81122	UP
10.48	9.88	1.52	0.004471	Tank	Q05BS9	UP
9.67	9.06	1.52	0.002392	Wdr36	Q3TAQ9	UP
9.98	9.37	1.52	0.00388	Slc35c2	Q5GMG8	UP
11.22	10.62	1.52	0.002995	Ift46	Q9DB07	UP
8.7	8.09	1.52	0.00543	I79_007182	#N/A	UP
10.66	10.05	1.52	0.008521	Slc29a2	#N/A	UP
8.65	8.05	1.51	0.005868	Slc12a9	D3Z362	UP
7.16	6.56	1.51	0.001926	Myrip	F7CFT8	UP

10.53	9.94	1.51	0.004302	Nsun2	H3BJF3	UP
10.22	9.62	1.51	0.003051	Dnajb14	Q149L6	UP
9.34	8.75	1.51	0.007925	Sptlc1	Q3V3A0	UP
8.08	7.48	1.51	0.006887	Rdh13	Q8CEE7	UP
10.39	9.8	1.51	0.008976	Spns1	Q8R0G7	UP
9.24	8.64	1.51	0.002995	Rrp7a	Q9D1C9	UP
7.9	7.31	1.51	0.009587	I79_007740	#N/A	UP
7.7	7.1	1.51	0.009151	I79_012054	#N/A	UP
11.03	10.44	1.51	0.007345	I79_014221	#N/A	UP
9.71	9.11	1.51	0.001551	Znf703	#N/A	UP
6.26	5.67	1.5	0.009094	Lrit3	J3QNQ8	UP
9.96	9.37	1.5	0.009258	Ets2	P15037	UP
9.98	9.39	1.5	0.003372	Fig4	Q3TA31	UP
8.5	7.92	1.5	0.005532	Xpnpep2	Q8BU59	UP
10.59	10	1.5	0.003331	Ak2	Q9WTP6	UP
9.52	8.93	1.5	0.0067	I79_011118	#N/A	UP
9.36	8.79	1.49	0.00837	Nmi	O35309	UP
7.14	6.56	1.49	0.005532	Mt2	P02798	UP
8.66	8.08	1.49	0.006968	Rad50	P70388	UP
10.67	10.09	1.49	0.002463	Mcrs1	Q3TJY1	UP
9.17	8.6	1.49	0.006211	Rps6ka1	Q505N6	UP
9.08	8.5	1.49	0.00411	Tia1	Q80ZW7	UP
7.08	6.51	1.49	0.008852	Gk5	Q8BX05	UP
7.72	7.14	1.49	0.001216	Slmo2	Q9CYY7	UP
8.54	7.97	1.49	0.007164	I79_004695	#N/A	UP
9.87	9.3	1.49	0.007164	Prss27	#N/A	UP
9.53	8.97	1.48	0.007914	Pih1d1	D3Z026	UP
10.08	9.52	1.48	0.008209	Acsl1	D3Z457	UP
6.97	6.41	1.48	0.005014	Ank3	G5E8K5	UP
11.67	11.11	1.48	0.004914	Rae1	Q6PAS9	UP
9.53	8.97	1.48	0.008557	Ccdc23	Q99LQ4	UP
6.3	5.73	1.48	0.009279	Rnase6	Q9D244	UP
11.71	11.15	1.48	0.001947	Ak2	Q9WTP6	UP
8.24	7.67	1.48	0.008042	Sfrp4	Q9Z1N6	UP
9.38	8.82	1.48	0.002343	Kiaa0664	#N/A	UP
9.07	8.5	1.48	0.009753	LOC100755981	#N/A	UP
7.95	7.39	1.48	0.009175	LOC100765287	#N/A	UP
9.9	9.35	1.47	0.002372	Zcchc24	B2RVL6	UP
7.19	6.64	1.47	0.007164	Ebf4	B7ZNC0	UP
10.68	10.12	1.47	0.002567	Cyb5r4	G3UY26	UP
10.03	9.48	1.47	0.006621	Adal	Q80SY6	UP
9.75	9.2	1.47	0.009682	Pbx1	Q8BFR8	UP
9.07	8.51	1.47	0.006795	Pole3	Q9JKP7	UP
11.17	10.61	1.47	0.003139	I79_003883	#N/A	UP

9.41	8.85	1.47	0.003467	LOC100763895	#N/A	UP
10.25	9.69	1.47	0.003503	LOC100765870	#N/A	UP
10.21	9.66	1.47	0.006887	Mlst8	#N/A	UP
9.85	9.3	1.47	0.006477	Nop14	#N/A	UP
8.89	8.33	1.47	0.006584	Selrc1	#N/A	UP
9.85	9.3	1.46	0.001575	Rhbdd2	D6RCZ4	UP
10.94	10.4	1.46	0.002392	Ppip5k2	E9Q9J4	UP
9.15	8.6	1.46	0.009604	Nsd1	O88491	UP
9.97	9.42	1.46	0.005138	Casp8	O89110	UP
10.07	9.52	1.46	0.005373	Zhx2	Q3TZR8	UP
8.62	8.07	1.46	0.008042	Fbxo25	Q3UYF5	UP
8.47	7.92	1.46	0.009439	Arl9	Q6IMB2	UP
9.66	9.11	1.46	0.005727	Rufy2	Q8BR30	UP
10.58	10.04	1.46	0.007833	Gas2l1	Q8JZP9	UP
9.01	8.47	1.46	0.009638	Nav1	Q8K1B1	UP
8.57	8.02	1.46	0.007524	Klhl36	Q8R124	UP
10.17	9.62	1.46	0.002521	Rilpl2	Q99LE1	UP
10.74	10.2	1.46	0.003718	Drg2	Q9QXB9	UP
9.86	9.31	1.46	0.008163	---	#N/A	UP
9.32	8.77	1.46	0.009992	Actr2	#N/A	UP
8.73	8.19	1.46	0.005825	Antxr1	#N/A	UP
9.64	9.1	1.46	0.00643	Eepd1	#N/A	UP
11.99	11.45	1.46	0.0091	Hnrnpab	#N/A	UP
6.5	5.95	1.46	0.007336	I79_003590	#N/A	UP
9.95	9.4	1.46	0.009688	LOC100756440	#N/A	UP
6.43	5.89	1.46	0.00687	LOC100766020	#N/A	UP
8.56	8.01	1.46	0.007122	LOC100767137	#N/A	UP
10.73	10.18	1.46	0.009846	LOC100774657	#N/A	UP
9.8	9.26	1.45	0.001421	Prkcd	Q1MX42	UP
11.27	10.73	1.45	0.002856	Dhx9	Q3TEB2	UP
8.69	8.15	1.45	0.008264	Abcd2	Q3TU16	UP
10.65	10.11	1.45	0.005727	Bclaf1	Q3UDL9	UP
9.34	8.8	1.45	0.001676	Ercc2	Q3UKK7	UP
8.67	8.13	1.45	0.005392	Gad2	Q3URJ3	UP
11.47	10.94	1.45	0.007396	Bola3	Q8CEI1	UP
10.78	10.24	1.45	0.005052	Higd2a	Q9CQJ1	UP
6.56	6.03	1.45	0.002995	C1ql3	#N/A	UP
8.79	8.25	1.45	0.001954	Dcaf13	#N/A	UP
8.41	7.87	1.45	0.006915	Dmap1	#N/A	UP
12.04	11.51	1.44	0.0067	Eif6	D6RJJ3	UP
12.17	11.64	1.44	0.00523	Eif5	P59325	UP
10.27	9.74	1.44	0.002635	Gnb5	P62881	UP
8.15	7.62	1.44	0.0067	Atg16l1	Q3TQX8	UP
10.03	9.51	1.44	0.004898	Hccs	Q8BP79	UP

8.63	8.11	1.44	0.00565	Sdcbp2	Q99JZ0	UP
10.46	9.93	1.44	0.003415	I79_007848	#N/A	UP
10.7	10.18	1.43	0.006915	Glul	D3YVK1	UP
8.61	8.09	1.43	0.00481	Fam198b	D3YXF7	UP
9.5	8.99	1.43	0.007124	Dtx3l	I6L9G8	UP
10.43	9.92	1.43	0.008969	Pmm1	O35621	UP
11.85	11.33	1.43	0.00474	F2r	Q3UK34	UP
9.68	9.17	1.43	0.006597	Kiaa1551	Q5DTW7	UP
8.03	7.52	1.43	0.00388	Tpp2	Q64514	UP
8.53	8.01	1.43	0.006887	Commd10	Q8JZY2	UP
10.77	10.25	1.43	0.005006	C15orf44	#N/A	UP
10.55	10.03	1.43	0.004324	Gpam	#N/A	UP
12.04	11.53	1.43	0.006282	I79_018556	#N/A	UP
8.58	8.07	1.43	0.008542	I79_023830	#N/A	UP
6.78	6.26	1.43	0.006822	LOC100760249	#N/A	UP
9.5	8.99	1.42	0.008007	Dock11	A2AF65	UP
10.35	9.84	1.42	0.005014	Lrrfip1	A6H5U5	UP
11.21	10.7	1.42	0.006406	Glul	D3YVK1	UP
5.43	4.92	1.42	0.009397	Rsad2	D6RJ49	UP
11.02	10.52	1.42	0.004055	Ddx46	Q05C73	UP
10.38	9.87	1.42	0.008204	Apbb1ip	Q3TS23	UP
12.16	11.65	1.42	0.00672	Slc6a6	Q8BRX2	UP
8.35	7.85	1.42	0.009258	Hoxa9	#N/A	UP
7.63	7.13	1.42	0.002372	I79_002910	#N/A	UP
12.91	12.41	1.42	0.002392	I79_013057	#N/A	UP
9.02	8.51	1.42	0.005138	Mmp23	#N/A	UP
9.45	8.95	1.42	0.008638	Slc12a7	#N/A	UP
10.13	9.62	1.42	0.002817	Tns3	#N/A	UP
10.02	9.53	1.41	0.008783	Tspan17	E9PWC3	UP
9.15	8.65	1.41	0.002428	Hfe	F7CW53	UP
9.41	8.91	1.41	0.008547	Mfn2	Q3TEX7	UP
11.33	10.84	1.41	0.006935	Noc2l	Q3UZI6	UP
11.27	10.78	1.41	0.004065	Eif4ebp1	Q60876	UP
8.22	7.72	1.41	0.006532	Gmppb	Q8BTZ7	UP
11.28	10.79	1.41	0.002995	Arrb1	Q8BWG8	UP
7.61	7.12	1.41	0.008638	Rgs3	Q9DC04	UP
11.3	10.81	1.41	0.002392	40797	#N/A	UP
10.81	10.32	1.41	0.003718	Derp6	#N/A	UP
10.12	9.63	1.41	0.002967	Eif3e	#N/A	UP
7.2	6.7	1.41	0.009638	I79_000205	#N/A	UP
7.25	6.75	1.41	0.004442	I79_010716	#N/A	UP
7.25	6.75	1.41	0.004442	I79_010717	#N/A	UP
7.25	6.75	1.41	0.004442	I79_010718	#N/A	UP
10.04	9.55	1.4	0.008594	Lrrc16a	D3Z030	UP

10.76	10.28	1.4	0.006482	Dnajc7	Q3UL32	UP
9.62	9.13	1.4	0.003738	Mapkapk3	Q3UMW7	UP
8.22	7.73	1.4	0.009279	Efnb2	Q3V1E0	UP
10.76	10.28	1.4	0.004302	Cyp20a1	Q8BKE6	UP
8.74	8.25	1.4	0.006249	Afap1	Q8BV31	UP
9.83	9.34	1.4	0.007687	Dock8	Q8C147	UP
8.83	8.35	1.4	0.004713	Phf20l1	Q8CCJ9	UP
10.16	9.67	1.4	0.005969	Mospd1	Q8VEL0	UP
9.48	8.99	1.4	0.003936	Wdr6	Q99ME2	UP
11.35	10.86	1.4	0.006457	Icmt	Q9EQK7	UP
10.35	9.86	1.4	0.00762	---	#N/A	UP
7.58	7.09	1.4	0.003894	Asap3	#N/A	UP
10.42	9.93	1.4	0.008783	I79_005240	#N/A	UP
10.19	9.7	1.4	0.007596	I79_005741	#N/A	UP
7.89	7.4	1.4	0.009731	LOC100758600	#N/A	UP
9.09	8.61	1.4	0.003191	Samd9	#N/A	UP
9.53	9.05	1.39	0.005138	Zfand2a	D3YUL0	UP
10.29	9.82	1.39	0.00982	Dnttip1	F7B2G8	UP
8.99	8.51	1.39	0.008083	Tor2a	P0C7W3	UP
9.33	8.86	1.39	0.005532	Parp16	Q7TMM8	UP
7.62	7.15	1.39	0.007717	Qrfp	Q8CE23	UP
10.12	9.65	1.39	0.009198	Tmbim4	Q8K191	UP
7.95	7.47	1.39	0.008783	Nle1	Q8VEJ4	UP
10.5	10.02	1.39	0.006774	Etfa	Q99LC5	UP
7.77	7.3	1.39	0.005929	Mageh1	Q9NWG9	UP
10.93	10.46	1.39	0.004677	Prosc	Q9Z2Y8	UP
12.12	11.65	1.39	0.005053	Csrp1	#N/A	UP
7.63	7.16	1.39	0.009874	I79_013164	#N/A	UP
9.51	9.04	1.39	0.009008	Ift27	#N/A	UP
10.39	9.92	1.39	0.003098	Mthfd1l	#N/A	UP
11.39	10.92	1.38	0.005812	Atic	B0LAC5	UP
11.21	10.75	1.38	0.007005	Aifm1	B1AU25	UP
8.99	8.53	1.38	0.007164	Rpsa	B2CY77	UP
8.83	8.37	1.38	0.007596	Blnk	D3YWR2	UP
9.31	8.85	1.38	0.007285	Gpd1l	D3Z0L6	UP
9.28	8.82	1.38	0.008465	Spsb3	D6RI75	UP
9.84	9.38	1.38	0.00313	Por	P37040	UP
8.1	7.63	1.38	0.00543	Rpl30	P62889	UP
9.33	8.87	1.38	0.00878	Urod	P70697	UP
10.03	9.56	1.38	0.009741	Anapc4	Q3TI31	UP
8.85	8.39	1.38	0.005377	Tnfaip2	Q61333	UP
6.93	6.47	1.38	0.006527	Nudt13	Q8JZU0	UP
8.84	8.38	1.38	0.009846	Toe1	Q9D2E2	UP
9.91	9.45	1.38	0.007717	Adat2	#N/A	UP

10.36	9.89	1.38	0.003497	Epdr1	#N/A	UP
9.06	8.6	1.38	0.00481	Gtf3c3	#N/A	UP
6.75	6.29	1.38	0.008952	I79_000241	#N/A	UP
8.97	8.51	1.38	0.003438	Zfp112	#N/A	UP
9.78	9.33	1.37	0.005184	Atg9a	A1A4C2	UP
8.86	8.41	1.37	0.004677	Rnf19b	B2KG08	UP
9.05	8.6	1.37	0.003718	Sash1	P59808	UP
10.28	9.83	1.37	0.0067	Nfyc	P70353	UP
10.45	9.99	1.37	0.007596	Tle3	Q3TY99	UP
10.39	9.93	1.37	0.009537	Taf5l	Q3U3C7	UP
10.13	9.67	1.37	0.009074	Cops5	Q3V0K7	UP
9.95	9.5	1.37	0.002841	Ptprm	Q3V3S2	UP
9.93	9.47	1.37	0.001715	Tnfrsf1b	Q545P4	UP
9.38	8.93	1.37	0.008763	Paqr3	Q6TCG8	UP
9.36	8.91	1.37	0.006697	Strada	Q80VZ9	UP
9.41	8.96	1.37	0.008257	Napg	Q8C1T5	UP
12.27	11.81	1.37	0.007242	Asf1b	Q9DAP7	UP
11.56	11.11	1.37	0.0091	Eif2s3	#N/A	UP
6.37	5.92	1.37	0.00643	LOC100762746	#N/A	UP
7.68	7.22	1.37	0.005138	LOC100771985	#N/A	UP
8.31	7.85	1.37	0.008952	Mtg1	#N/A	UP
8.95	8.5	1.37	0.006887	Trmt61a	#N/A	UP
11.02	10.58	1.36	0.001713	Kctd17	F7C1U0	UP
12.5	12.05	1.36	0.009436	Hdac1	O09106	UP
9.31	8.87	1.36	0.007412	Alad	O89061	UP
12.06	11.62	1.36	0.007391	Idh3g	P70404	UP
11.58	11.14	1.36	0.00715	Pes1	Q5SQ20	UP
9.48	9.04	1.36	0.008326	Stx16	Q8BVI5	UP
10.31	9.86	1.36	0.005138	Pdcd6	Q8C5M4	UP
10.76	10.32	1.36	0.005212	Gnl2	Q99LH1	UP
10.94	10.5	1.36	0.005783	Abhd5	Q9DBL9	UP
9.17	8.72	1.36	0.009992	Cyp2d10	#N/A	UP
10.47	10.02	1.36	0.005927	Ezr	#N/A	UP
10.34	9.89	1.36	0.007465	Lmf2	#N/A	UP
8.76	8.32	1.36	0.003821	LOC100755470	#N/A	UP
9.67	9.23	1.36	0.009983	Snx18	#N/A	UP
9.35	8.9	1.36	0.005249	Snx33	#N/A	UP
8.26	7.83	1.35	0.006482	Ino80b	D6RES5	UP
7.5	7.06	1.35	0.004376	Tmem222	D6RIQ5	UP
10.02	9.59	1.35	0.009279	Adsl	E9Q0A0	UP
11.07	10.64	1.35	0.007933	Rpa2	F6V8R7	UP
10.74	10.3	1.35	0.002305	Fus	P56959	UP
9.52	9.09	1.35	0.006928	Pqlc2	Q8C4N4	UP
9.51	9.08	1.35	0.004963	Vps11	Q91W86	UP

7.98	7.54	1.35	0.003051	Cenpb	Q923C5	UP
8.99	8.56	1.35	0.008969	Prpf18	Q9CYU9	UP
10.98	10.54	1.35	0.003971	---	#N/A	UP
8.25	7.82	1.35	0.002041	Agphd1	#N/A	UP
10.2	9.77	1.35	0.006429	I79_006544	#N/A	UP
11.63	11.19	1.35	0.009286	I79_026128	#N/A	UP
10.58	10.16	1.34	0.007672	Tcf25	B2ZAC8	UP
6.31	5.88	1.34	0.00183	Zan	O88799	UP
10.37	9.95	1.34	0.004542	Slc19a1	P41438	UP
8.92	8.5	1.34	0.007251	Sap25	Q1EHW4	UP
8.98	8.56	1.34	0.009279	Traf3	Q3UHJ1	UP
10.05	9.64	1.34	0.008209	Tmem164	Q6PHN7	UP
9.25	8.83	1.34	0.002392	Sdad1	Q80UZ2	UP
8.59	8.16	1.34	0.00743	Tmem161b	Q8C2L6	UP
11.17	10.75	1.34	0.009131	Arhgef6	Q8K4I3	UP
10.41	9.99	1.34	0.004216	Ankrd10	Q99LW0	UP
9.41	8.99	1.34	0.002995	Tbc1d7	Q9D0K0	UP
11.21	10.78	1.34	0.005056	Ppih	Q9D868	UP
8.6	8.18	1.34	0.005731	Arhgef40	S4R1Y4	UP
10.73	10.3	1.34	0.005588	---	#N/A	UP
9.19	8.77	1.34	0.008933	Fam204a	#N/A	UP
8.68	8.26	1.34	0.005373	LOC100757796	#N/A	UP
8.34	7.93	1.34	0.009541	Nadkd1	#N/A	UP
9.21	8.79	1.34	0.008925	Nod1	#N/A	UP
8.42	8	1.34	0.007412	Pgap3	#N/A	UP
10.05	9.63	1.34	0.007261	Trpv2	#N/A	UP
11.64	11.23	1.33	0.006006	Mybl2	A2A5P3	UP
9.87	9.46	1.33	0.004635	Aspscr1	A2AC01	UP
9.03	8.61	1.33	0.005817	Tada2b	D3YW26	UP
8.88	8.47	1.33	0.003967	Cc2d1b	H3BKI0	UP
12.9	12.49	1.33	0.002041	Ccl2	Q3U5S8	UP
10.12	9.71	1.33	0.002372	Rapgef1	Q3UGX8	UP
9.55	9.14	1.33	0.009279	Srpx2	Q8R054	UP
11.86	11.44	1.33	0.006651	Ywhab	Q9CQV8	UP
10.26	9.85	1.33	0.008319	Tlr9	Q9EQU3	UP
10.13	9.72	1.33	0.007448	Mncb-2990	Q9JJ93	UP
8.66	8.25	1.33	0.009741	Dph2	V9GX25	UP
9.9	9.49	1.33	0.001383	I79_006203	#N/A	UP
10.78	10.37	1.33	0.007267	LOC100751988	#N/A	UP
10.67	10.26	1.33	0.006593	Taf1d	#N/A	UP
9.88	9.48	1.32	0.00822	Slc1a5	F7CEQ5	UP
11.74	11.35	1.32	0.006043	Atf4	Q06507	UP
9.23	8.83	1.32	0.005035	Anapc4	Q3TI31	UP
7.8	7.41	1.32	0.002967	Daam1	Q8BPM0	UP

10.26	9.86	1.32	0.005139	Lmbrd2	Q8C561	UP
10.92	10.51	1.32	0.002016	Ddx41	Q91VN6	UP
10.11	9.71	1.32	0.006035	Tars	Q9D0R2	UP
9.01	8.61	1.32	0.009236	Hinfp	#N/A	UP
10.85	10.45	1.32	0.007005	I79_006202	#N/A	UP
7.11	6.71	1.32	0.007908	I79_016672	#N/A	UP
9.26	8.86	1.32	0.006887	I79_021809	#N/A	UP
8.65	8.25	1.32	0.002736	Shcbp1	#N/A	UP
8.59	8.2	1.31	0.003103	Mecr	A2A845	UP
10.73	10.34	1.31	0.002041	Srxn1	A2AQU8	UP
11.47	11.08	1.31	0.0091	Mcm7	D3Z0J6	UP
8.58	8.19	1.31	0.008422	Trmu	E0CZ49	UP
11.89	11.5	1.31	0.004943	Rnaseh2b	E9PYC5	UP
10.7	10.31	1.31	0.007164	Nhp2l1	E9PZS4	UP
10.45	10.05	1.31	0.006074	Wipf1	F6QWW7	UP
9.63	9.24	1.31	0.008369	Bag5	Q8CI32	UP
9.71	9.33	1.31	0.007672	Ptcd2	Q8R3K3	UP
10.2	9.81	1.31	0.008413	Cstf1	Q99LC2	UP
9.59	9.2	1.31	0.004376	Rhobtb1	Q9DAK3	UP
9.63	9.25	1.31	0.007596	Exoc1	#N/A	UP
10.38	9.99	1.31	0.005279	Golm1	#N/A	UP
7.45	7.05	1.31	0.008105	LOC100761549	#N/A	UP
9.35	8.97	1.31	0.007717	Sp110	#N/A	UP
10.02	9.64	1.31	0.004677	Ube2e1	#N/A	UP
10.09	9.71	1.3	0.006785	Tfe3	A2AEW0	UP
9.11	8.73	1.3	0.006915	Pcbp4	P57724	UP
9.83	9.46	1.3	0.004234	Sh3pxd2b	Q3TDV5	UP
10.35	9.97	1.3	0.005986	Tbc1d1	Q3U3T9	UP
8.89	8.51	1.3	0.0091	Mar-08	Q3U7P8	UP
11.45	11.07	1.3	0.003949	Wars	Q4FJZ4	UP
10.93	10.55	1.3	0.002597	Insig1	Q8BGI3	UP
8.74	8.37	1.3	0.004923	Gtf2f2	Q8R0A0	UP
11.33	10.94	1.3	0.006892	Txnip	Q91X82	UP
10.01	9.64	1.3	0.003821	Btf3l4	Q9CQH7	UP
9.16	8.79	1.3	0.006774	Gemin7	Q9CWY4	UP
9.32	8.94	1.3	0.004843	I79_006441	#N/A	UP
2.28	1.91	1.3	0.003414	I79_019636	#N/A	UP
5.75	5.38	1.3	0.008339	LOC100770473	#N/A	UP
9.27	8.89	1.3	0.008319	Mrps31	#N/A	UP
9.41	9.02	1.3	0.00702	Rnf14	#N/A	UP
8.17	7.79	1.3	0.00949	Tceanc2	#N/A	UP
10.37	10	1.29	0.008557	Lpar1	A2AMJ0	UP
10.9	10.53	1.29	0.005783	Mtdh	F6ZSG0	UP
7.82	7.45	1.29	0.002841	Slc2a8	Q2TK27	UP

10.17	9.8	1.29	0.009279	Cpsf1	Q3U1X8	UP
8.87	8.5	1.29	0.008654	Tap2	Q3UA79	UP
12.1	11.73	1.29	0.004537	Gdi2	Q3UUX9	UP
10.21	9.85	1.29	0.009874	Heatr1	Q3V1X6	UP
9.37	9.01	1.29	0.003718	Fmr1	Q6AXB7	UP
9.08	8.72	1.29	0.00932	Gypc	Q78HU7	UP
9.78	9.42	1.29	0.006916	Dctn4	Q8CBY8	UP
10.61	10.24	1.29	0.005268	Tcea1	Q9JMB4	UP
12.28	11.92	1.29	0.002995	Tcp1	W0TYI4	UP
7.7	7.34	1.29	0.006205	Bend3	#N/A	UP
8.12	7.75	1.29	0.007994	Ffr	#N/A	UP
11.33	10.97	1.29	0.007941	I79_001984	#N/A	UP
9.57	9.2	1.29	0.008295	LOC100763885	#N/A	UP
10.78	10.42	1.29	0.005665	Sord	#N/A	UP
8.28	7.93	1.28	0.007122	Per2	O54943	UP
11.98	11.63	1.28	0.003949	Arhgap1	Q5FWK3	UP
8.39	8.04	1.28	0.002292	Mfsd3	Q5U419	UP
10.27	9.91	1.28	0.009095	Grk6	Q792R0	UP
11.18	10.82	1.28	0.008107	Psmd6	Q99JI4	UP
9.84	9.49	1.28	0.003912	Lcmt1	Q9D963	UP
9.51	9.15	1.28	0.004292	Acox3	Q9EPL9	UP
10.39	10.03	1.28	0.003797	Pigb	Q9JJQ0	UP
11.88	11.52	1.28	0.005006	---	#N/A	UP
9.3	8.95	1.28	0.007047	LOC100769365	#N/A	UP
9.3	8.94	1.28	0.007462	LOC100770616	#N/A	UP
11.31	10.95	1.28	0.006578	Rlim	#N/A	UP
11.92	11.57	1.27	0.005927	Ifrd1	E9PZB9	UP
8.75	8.4	1.27	0.007596	Slc2a9	Q3T9X0	UP
10.74	10.4	1.27	0.006426	Psme4	Q5SSW0	UP
11.29	10.94	1.27	0.00436	Acly	Q91V92	UP
9.91	9.56	1.27	0.008598	Adrm1	#N/A	UP
9.87	9.52	1.27	0.00455	Cdc42ep1	#N/A	UP
10.22	9.88	1.27	0.007462	Ppan	#N/A	UP
9.56	9.21	1.27	0.008326	Rbfox2	#N/A	UP
10.63	10.29	1.27	0.004225	Sar1b	#N/A	UP
8.52	8.17	1.27	0.006345	Slc10a3	#N/A	UP
9.56	9.23	1.26	0.005969	Fam171a1	A2ATK9	UP
11.46	11.12	1.26	0.008783	Nop56	F6USW7	UP
9.54	9.2	1.26	0.008209	Gabpb2	P81069	UP
10.46	10.13	1.26	0.0098	Ddx10	Q80Y44	UP
9.52	9.18	1.26	0.007645	Hus1	Q8BQY8	UP
10.85	10.52	1.26	0.009956	Pabpc4	Q91YZ8	UP
11.76	11.43	1.26	0.005541	Ndufa10	Q99LC3	UP
11.19	10.86	1.26	0.008295	---	#N/A	UP

6.03	5.7	1.26	0.008563	Hes3	#N/A	UP
9.38	9.05	1.26	0.006774	I79_015825	#N/A	UP
10.81	10.47	1.26	0.004302	LOC100765868	#N/A	UP
10.53	10.19	1.26	0.008169	LOC100766729	#N/A	UP
10.02	9.7	1.25	0.008393	Rrn3	B2RS91	UP
9.52	9.2	1.25	0.006963	Erbb2ip	B7ZNX6	UP
11.15	10.83	1.25	0.00949	Serinc1	E9Q553	UP
11.71	11.39	1.25	0.007086	Zmpste24	I7HIP5	UP
12.53	12.22	1.25	0.009441	Ptma	P26350	UP
6.9	6.58	1.25	0.003949	Nudt15	Q3TH44	UP
9.45	9.13	1.25	0.008204	Insig1	Q8BGI3	UP
9.59	9.27	1.25	0.006687	Acad9	Q8JZN5	UP
10.55	10.23	1.25	0.007064	Rragc	Q99K70	UP
10.19	9.86	1.25	0.005014	---	#N/A	UP
10.6	10.28	1.25	0.009413	Akr7a2	#N/A	UP
10.5	10.18	1.25	0.00209	Ecm29	#N/A	UP
8.72	8.4	1.25	0.007164	I79_013111	#N/A	UP
12.11	11.79	1.25	0.003005	Serinc3	#N/A	UP
10.77	10.44	1.25	0.004355	Tmem185a	#N/A	UP
5.05	4.74	1.24	0.008209	Rpsa	B2CY77	UP
9.69	9.38	1.24	0.006333	Micall2	E9PZD2	UP
9.01	8.7	1.24	0.009008	Hdac7	E9PZG4	UP
9.84	9.53	1.24	0.009876	Ascc2	Q3UG63	UP
10.6	10.28	1.24	0.004355	Net1	Q3USZ7	UP
11.18	10.87	1.24	0.004545	Dusp14	Q542U4	UP
10.77	10.46	1.24	0.00432	Utp15	Q8C7V3	UP
9.08	8.77	1.24	0.007862	B3galt6	Q91Z92	UP
9.37	9.06	1.24	0.00671	LOC100754521	#N/A	UP
8.34	8.04	1.23	0.009114	Igdcc4	E9QAQ0	UP
8.71	8.41	1.23	0.003718	Znf512b	F6PYY4	UP
11.77	11.47	1.23	0.008459	Prmt5	F6QQQ6	UP
10.84	10.54	1.23	0.009973	Mprip	F6S5I0	UP
9.39	9.09	1.23	0.009114	Rpusd3	Q14AI6	UP
9.86	9.56	1.23	0.008684	Cnot10	Q8BH15	UP
7.92	7.62	1.23	0.006248	Cables2	Q8K3M5	UP
10.84	10.54	1.23	0.008976	Atp6v0b	Q91VS4	UP
11.96	11.66	1.23	0.003502	Ccni	Q9Z2V9	UP
11.46	11.17	1.22	0.009874	Mbnl2	D0EX61	UP
11.46	11.17	1.22	0.008927	Rps2	D3YVC1	UP
10.84	10.55	1.22	0.008264	Zeb2	H3BLE2	UP
10.18	9.88	1.22	0.006333	Ppfibp1	Q3UJ84	UP
10.67	10.38	1.22	0.005041	Fam149a	Q8CFV2	UP
9.97	9.69	1.22	0.008848	Spg21	Q9CQC8	UP
10.67	10.38	1.22	0.006785	I79_025871	#N/A	UP

7.05	6.76	1.22	0.007844	LOC100754083	#N/A	UP
8.86	8.59	1.21	0.006272	Txlng	A2AFJ4	UP
9.29	9.02	1.21	0.009106	Map3k7	A2AP93	UP
11.51	11.24	1.21	0.004814	Ctnnb1	E9Q6A9	UP
11.27	10.99	1.21	0.005989	Plaa	F7D1R5	UP
7.65	7.37	1.21	0.009911	Fzd7	Q61090	UP
8.67	8.39	1.21	0.009196	Kri1	Q8VDQ9	UP
9.64	9.37	1.21	0.004355	Tacc3	Q99LH8	UP
11.66	11.39	1.21	0.003478	Kpna3	Q9CT07	UP
8.55	8.27	1.21	0.00313	Ctu1	#N/A	UP
5.6	5.33	1.21	0.008326	LOC100757919	#N/A	UP
12.28	12.01	1.21	0.007251	Prelid1	#N/A	UP
8.8	8.53	1.21	0.007242	Slc24a6	#N/A	UP
10.49	10.23	1.2	0.006887	Chek1	G3UYC5	UP
10.65	10.39	1.2	0.007122	Tfdp1	Q08639	UP
11.19	10.93	1.2	0.005361	Hp1bp3	Q3TEA8	UP
10.13	9.86	1.2	0.002632	Wbp11	Q3U6Q1	UP
11.3	11.04	1.2	0.008903	Calm1	Q3UKW2	UP
10.05	9.79	1.2	0.003002	Galnt2	Q6PB93	UP
7.74	7.48	1.2	0.009874	Pik3c3	Q6PF93	UP
8.17	7.9	1.2	0.004814	I79_013783	#N/A	UP
8.66	8.4	1.2	0.008851	I79_016332	#N/A	UP
10.3	10.03	1.2	0.009755	Nup50	#N/A	UP
11.28	11.02	1.2	0.008851	Serpinb6	#N/A	UP
12.98	12.72	1.19	0.007164	Eif5a	P63242	UP
10	9.76	1.19	0.007171	Sppl2b	Q3TD49	UP
11.13	10.88	1.19	0.001947	Gnl3	Q3TK27	UP
9.89	9.63	1.19	0.009731	Ehd1	Q8K1X5	UP
8.61	8.36	1.19	0.009114	Stap2	Q8R0L1	UP
11.87	11.62	1.19	0.009637	Cdc20	Q9JJ66	UP
8.58	8.34	1.18	0.008442	Nbn	A2AMG5	UP
8.86	8.63	1.18	0.007921	Vcp	Q01853	UP
10.52	10.29	1.18	0.004511	Ccnc	Q62447	UP
10.32	10.08	1.18	0.008326	Coq2	Q66JT7	UP
11.43	11.19	1.18	0.009667	Ubl7	Q91W67	UP
11.39	11.14	1.18	0.008123	Vta1	Q9CR26	UP
7.86	7.62	1.18	0.007717	I79_014916	#N/A	UP
7.86	7.62	1.18	0.007717	I79_023585	#N/A	UP
12.08	11.85	1.18	0.005783	Nsmce2	#N/A	UP
7.46	7.21	1.18	0.008209	Ppp6r2	#N/A	UP
10.17	9.94	1.17	0.005843	Ranbp9	E9Q5D6	UP
8.4	8.18	1.17	0.002284	Ksr1	Q5SXE1	UP
10.75	10.52	1.17	0.009983	Gpr176	#N/A	UP
11.22	11	1.17	0.007939	LOC100769531	#N/A	UP

12.06	11.84	1.17	0.009309	Naa11	#N/A	UP
11.74	11.53	1.16	0.003757	Med14	A2BDP0	UP
10.82	10.6	1.16	0.007242	Ap2a1	F6TPX8	UP
11.47	11.26	1.16	0.008264	Fasn	P19096	UP
9.13	8.92	1.16	0.008159	Edrf1	Q6GQV7	UP
12.75	12.53	1.16	0.008673	Gja1	Q6T9D4	UP
8.55	8.33	1.16	0.006078	Qpctl	Q8BH73	UP
8.69	8.47	1.16	0.007939	Epc1	Q8C9X6	UP
11.07	10.86	1.16	0.009962	Pak2	Q8CIN4	UP
8.95	8.74	1.16	0.009983	Ccdc22	#N/A	UP
7.12	6.9	1.16	0.009846	Znf304	#N/A	UP
11.74	11.53	1.15	0.004371	Akt1	D3Z783	UP
8.25	8.05	1.15	0.005623	Fubp3	Q3TIX6	UP
12.63	12.43	1.15	0.006785	Eif4g2	Q3U9U9	UP
9.59	9.4	1.15	0.009943	Usp30	Q3UN04	UP
10.38	10.18	1.15	0.005138	Thap4	Q6P3Z3	UP
11.59	11.39	1.15	0.005488	Oxa1l	Q8BGA9	UP
11.85	11.64	1.15	0.009753	Acat2	Q8CAY6	UP
8.53	8.33	1.15	0.003718	Emilin1	Q99K41	UP
9.69	9.49	1.15	0.008161	Dido1	#N/A	UP
7.4	7.2	1.15	0.009541	Tmsb10	#N/A	UP
10.43	10.22	1.15	0.007157	Topbp1	#N/A	UP
9.75	9.56	1.14	0.002995	Slc25a16	D3YVC9	UP
9.97	9.78	1.14	0.005212	Mtmr14	Q8VEL2	UP
12.98	12.8	1.13	0.004335	Tsc22d1	H3BLI9	UP
11.62	11.44	1.13	0.009131	Cd81	Q3UWG5	UP
11.7	11.52	1.13	0.008209	Ccnb1	Q68EM3	UP
9.23	9.04	1.13	0.004216	Tmem205	Q91XE8	UP
11.01	10.83	1.13	0.003103	LOC100758537	#N/A	UP
13.26	13.08	1.13	0.004124	Tuba	#N/A	UP
11	10.84	1.12	0.009428	Aaas	P58742	UP
9.18	9.03	1.11	0.00878	Mst1r	#N/A	UP
8.1	7.95	1.11	0.009637	Znf180	#N/A	UP
5.05	4.92	1.1	0.003949	Myo3b	Q1EG27	UP
9.87	9.73	1.1	0.008727	Stam2	Q3YEC8	UP
7.95	7.81	1.1	0.009583	Gtf2ird1	Q6PD35	UP
8.42	8.29	1.1	0.009983	Bcdin3d	Q91YP1	UP
12	11.87	1.09	0.007861	Surf4	Q3U7E6	UP
10.66	10.53	1.09	0.007267	Zswim1	Q9CWV7	UP
9.38	9.26	1.09	0.009839	Znf828	#N/A	UP
5.79	5.68	1.08	0.009846	I79_021715	#N/A	UP
12.09	11.99	1.07	0.00481	Atp6v0c	Q8C1D9	UP
11.22	11.35	-1.09	0.006896	Osbpl9	Q5FWX7	DOWN
7.47	7.6	-1.1	0.009793	Safb2	Q80YR5	DOWN

5.4	5.54	-1.1	0.004216	Tspan8	Q8R3G9	DOWN
8.91	9.06	-1.1	0.005759	I79_008571	#N/A	DOWN
5.52	5.67	-1.11	0.004721	Prr16	A3KMN5	DOWN
10.57	10.72	-1.11	0.008319	Atp6v1b2	B0LAC8	DOWN
10.47	10.62	-1.11	0.009399	Lin54	E9PV28	DOWN
12.1	12.26	-1.11	0.007994	Pigt	Q3U5R2	DOWN
12.58	12.73	-1.11	0.008183	Kiaa0100	Q5SYL3	DOWN
11.08	11.23	-1.11	0.002041	Prc1	Q99K43	DOWN
6.54	6.7	-1.12	0.008159	Papln	Q9EPX2	DOWN
9.67	9.83	-1.12	0.001361	Panx1	Q9JIP4	DOWN
9.94	10.11	-1.12	0.004923	Ppp6r3	#N/A	DOWN
11.52	11.7	-1.13	0.003926	Got1	P05201	DOWN
8.96	9.13	-1.13	0.002364	Uhrf1bp1	Q3UNI3	DOWN
11.28	11.45	-1.13	0.006025	Ogdh	Q6P8I7	DOWN
11.78	11.95	-1.13	0.002392	Pxk	Q8BX57	DOWN
10.81	10.99	-1.13	0.004246	Anxa6	Q8CEX0	DOWN
6.69	6.86	-1.13	0.008329	Acbd6	Q9D061	DOWN
10	10.18	-1.13	0.006248	I79_014469	#N/A	DOWN
11.45	11.65	-1.14	0.004963	Fkbp10	F6W360	DOWN
10.76	10.95	-1.14	0.003705	Dcxr	Q91X52	DOWN
8.55	8.74	-1.14	0.009587	Rev1	#N/A	DOWN
9.31	9.51	-1.15	0.009317	Ncapg	B2RQA7	DOWN
12.21	12.41	-1.15	0.003718	Arf4	P61750	DOWN
11.12	11.32	-1.15	0.007251	Tmem127	Q8BGP5	DOWN
8.54	8.74	-1.15	0.007164	Cecr5	Q91WM2	DOWN
10.56	10.76	-1.15	0.009139	Csnk1g2	Q99JQ5	DOWN
9.93	10.13	-1.15	0.009236	Ap1s2	Q9DB50	DOWN
8.73	8.92	-1.15	0.008799	I79_002830	#N/A	DOWN
9.01	9.22	-1.16	0.003949	Tmem106a	Q8VC04	DOWN
9.62	9.84	-1.16	0.009874	Usp16	Q99LG0	DOWN
11.65	11.87	-1.16	0.0063	Glrx	#N/A	DOWN
10.11	10.33	-1.17	0.009197	Kif2a	F6RLL5	DOWN
9.69	9.91	-1.17	0.00932	Vti1b	F6T4B9	DOWN
11.14	11.37	-1.17	0.00904	Hadha	Q8BMS1	DOWN
8.25	8.48	-1.17	0.008969	Ttc26	Q8BS45	DOWN
11	11.24	-1.17	0.005224	Rbm14	Q8C2Q3	DOWN
5.4	5.62	-1.17	0.007833	I79_011405	#N/A	DOWN
9.59	9.82	-1.17	0.008952	LOC100757451	#N/A	DOWN
7.99	8.22	-1.17	0.007782	Wbp7	#N/A	DOWN
9.02	9.26	-1.18	0.008092	Setdb1	D3YYC3	DOWN
8.23	8.46	-1.18	0.006929	Aplf	Q9D842	DOWN
10.4	10.65	-1.18	0.009549	Kctd13	#N/A	DOWN
10.68	10.93	-1.19	0.007717	Alg3	D6RCW8	DOWN
11.92	12.17	-1.19	0.007848	Ube2d1	P61080	DOWN

10.54	10.8	-1.19	0.008118	Ap2a2	Q3U7X9	DOWN
11.48	11.73	-1.19	0.005544	N4bp1	Q99KT2	DOWN
11.42	11.66	-1.19	0.005532	Cuta	Q9CQ89	DOWN
10.65	10.91	-1.19	0.007113	Mrpl14	Q9D1I6	DOWN
12.06	12.31	-1.19	0.00565	Rpn2	Q9DBG6	DOWN
9.36	9.61	-1.19	0.008547	Tm9sf1	Q9DBU0	DOWN
10.17	10.43	-1.19	0.007947	Epb41	#N/A	DOWN
10.96	11.2	-1.19	0.004677	I79_026136	#N/A	DOWN
10.86	11.12	-1.19	0.00949	Rnf2	#N/A	DOWN
11.49	11.74	-1.19	0.004495	Tmed10	#N/A	DOWN
10.38	10.64	-1.19	0.002887	Zfand6	#N/A	DOWN
11.47	11.74	-1.2	0.004302	St3gal1	Q3UU61	DOWN
5.47	5.74	-1.2	0.009094	Tbc1d9	Q6PGG9	DOWN
10.21	10.46	-1.2	0.004511	Cog6	Q8BRB0	DOWN
8.85	9.11	-1.2	0.006114	Daglb	Q91WC9	DOWN
7.85	8.12	-1.2	0.009587	Dcaf12l2	#N/A	DOWN
9.72	9.98	-1.2	0.008547	Mettl21b	#N/A	DOWN
10.58	10.86	-1.21	0.008739	R3hdm1	B9EHE8	DOWN
11.23	11.5	-1.21	0.005373	Ak3	F6RP11	DOWN
7.03	7.31	-1.21	0.00949	Pknox1	O70477	DOWN
11.76	12.04	-1.21	0.00599	Top2a	Q3TTG4	DOWN
10.4	10.67	-1.21	0.008209	Spag5	Q7TME2	DOWN
9.94	10.22	-1.21	0.005552	Snx27	Q8BYM0	DOWN
9.15	9.43	-1.21	0.0091	Arfip2	Q8K221	DOWN
8.96	9.25	-1.22	0.009198	Lepre1	A2A7Q5	DOWN
7.32	7.61	-1.22	0.009787	Usp20	A2AQ35	DOWN
10.99	11.28	-1.22	0.002552	Tjp1	B9EHJ3	DOWN
8.8	9.09	-1.22	0.003672	Sp3	O70494	DOWN
9.28	9.57	-1.22	0.007164	Klc2	O88448	DOWN
11.51	11.8	-1.22	0.008103	Rras2	P62071	DOWN
11.22	11.51	-1.22	0.0067	Ccnd1	Q3TC96	DOWN
10.16	10.45	-1.22	0.008796	Usp15	Q3TQV7	DOWN
12.56	12.85	-1.22	0.005532	Hspa5	Q3TUS2	DOWN
8.53	8.81	-1.22	0.009414	Cbx2	Q3URA3	DOWN
9.21	9.49	-1.22	0.004344	Slc33a1	Q3UXZ5	DOWN
9.53	9.82	-1.22	0.002995	Prepl	Q8BKS6	DOWN
11.12	11.4	-1.22	0.007014	Hnrnpcl1	#N/A	DOWN
9.92	10.22	-1.23	0.008952	Slc45a1	B0QZL3	DOWN
10.9	11.2	-1.23	0.007325	Ccdc6	D3YZP9	DOWN
10.74	11.03	-1.23	0.008257	Fam3c	E9Q6F0	DOWN
11.19	11.49	-1.23	0.005788	Micu1	F6Z1Z9	DOWN
9.46	9.76	-1.23	0.007242	Trak2	G3UZH5	DOWN
11.18	11.48	-1.23	0.004302	Setd8	Q2YDW7	DOWN
10.26	10.56	-1.23	0.004666	Cdc42bpa	Q3TSA3	DOWN

10.25	10.55	-1.23	0.009114	Ppa2	Q91VM9	DOWN
10.74	11.04	-1.23	0.008209	Dennd5a	#N/A	DOWN
7.91	8.21	-1.23	0.009151	Fam86a	#N/A	DOWN
7.29	7.59	-1.23	0.006224	I79_007603	#N/A	DOWN
7.04	7.33	-1.23	0.005164	I79_016537	#N/A	DOWN
8.22	8.51	-1.23	0.006312	I79_021646	#N/A	DOWN
10.95	11.26	-1.24	0.007086	Lasp1	A2A6G0	DOWN
9.13	9.44	-1.24	0.006896	Adm	P97297	DOWN
5.2	5.51	-1.24	0.007149	Lhfp	Q8BM86	DOWN
8.47	8.79	-1.24	0.00944	Rassf8	Q8CJ96	DOWN
12.43	12.74	-1.24	0.009907	Plac8	Q9JI48	DOWN
8.28	8.59	-1.24	0.004588	Kcnk5	Q9JK62	DOWN
12.63	12.94	-1.24	0.004923	Arpc1b	Q9WV32	DOWN
11.6	11.91	-1.24	0.002801	Qki	#N/A	DOWN
10.03	10.35	-1.25	0.002967	Smurf2	A2A5Z6	DOWN
9.8	10.11	-1.25	0.008118	Cdc27	A2A6Q5	DOWN
9.59	9.9	-1.25	0.009839	Lrp10	B0LAD7	DOWN
11.67	11.99	-1.25	0.006916	Gnptab	D3YXC6	DOWN
9.92	10.24	-1.25	0.006078	Orc5	D3Z0X3	DOWN
9.46	9.78	-1.25	0.004151	Nsun5	E9QAY1	DOWN
9.32	9.64	-1.25	0.003967	Rptor	F6U5L3	DOWN
11.13	11.46	-1.25	0.003565	Rangrf	Q05D49	DOWN
10.42	10.74	-1.25	0.007921	Jmjd8	Q3TA59	DOWN
7.66	7.98	-1.25	0.009945	Mar-09	Q3TZ87	DOWN
9.2	9.52	-1.25	0.008046	Cenpc1	Q3UUX2	DOWN
9.54	9.86	-1.25	0.008654	I79_020151	#N/A	DOWN
10.19	10.51	-1.25	0.004943	Trip10	#N/A	DOWN
7.52	7.86	-1.26	0.00338	Pikfyve	D3Z5N5	DOWN
8.34	8.67	-1.26	0.005636	Arhgap6	O54834	DOWN
10.44	10.78	-1.26	0.008169	Edem3	Q2HXL6	DOWN
9.37	9.71	-1.26	0.006763	Fuz	Q3UYI6	DOWN
10.46	10.79	-1.26	0.009197	Pcyt2	Q922E4	DOWN
12.08	12.41	-1.26	0.006043	Ly6e	Q9CXN2	DOWN
9.71	10.05	-1.26	0.007931	Gdap2	Q9DBL2	DOWN
11.07	11.4	-1.26	0.009846	Dedd	Q9Z1L3	DOWN
9.11	9.44	-1.26	0.003821	Acer3	#N/A	DOWN
6.77	7.1	-1.26	0.00904	LOC100753391	#N/A	DOWN
9.29	9.64	-1.27	0.003718	Fndc3a	F6TLV3	DOWN
9.25	9.6	-1.27	0.009453	Rab33b	O35963	DOWN
10.27	10.61	-1.27	0.002392	Ptpn12	P35831	DOWN
8.24	8.58	-1.27	0.005006	Taf1b	P97358	DOWN
9.93	10.28	-1.27	0.004027	Slc30a4	Q3TM66	DOWN
8.09	8.44	-1.27	0.007412	Ppp2r5b	Q3V3S8	DOWN
9.55	9.89	-1.27	0.006532	Cdkn1a	Q4FK34	DOWN

11.28	11.63	-1.27	0.001844	Tmed4	Q5SVW9	DOWN
9.53	9.87	-1.27	0.008159	Adrbk1	Q7TS64	DOWN
10.15	10.5	-1.27	0.008927	Tlcd1	Q99JT6	DOWN
8.59	8.93	-1.27	0.007994	Snx7	Q9CY18	DOWN
9.28	9.62	-1.27	0.006599	Tmem135	Q9CYV5	DOWN
10.76	11.11	-1.27	0.004569	Csnk1e	Q9JMK2	DOWN
8.54	8.89	-1.27	0.009229	Disp1	#N/A	DOWN
8.24	8.59	-1.27	0.007005	Fer	#N/A	DOWN
9.88	10.22	-1.27	0.007832	Me1	#N/A	DOWN
9.71	10.05	-1.27	0.004292	Mpzl1	#N/A	DOWN
9	9.35	-1.27	0.008283	Rilpl1	#N/A	DOWN
7.6	7.95	-1.28	0.009797	Kank1	E9Q238	DOWN
8.32	8.67	-1.28	0.002995	Clip1	F6RAY2	DOWN
8.32	8.68	-1.28	0.006837	Fam160a2	J3QP99	DOWN
10.48	10.83	-1.28	0.001353	Clock	O08785	DOWN
8.85	9.21	-1.28	0.00481	Prkar2b	P31324	DOWN
10.35	10.7	-1.28	0.002856	Pcnx	Q3TD89	DOWN
9.94	10.29	-1.28	0.007345	Sgpp1	Q3U4P6	DOWN
8.31	8.66	-1.28	0.002887	Arhgap17	Q3UIA2	DOWN
9.29	9.65	-1.28	0.004383	Mmp9	Q3UQ52	DOWN
10.29	10.64	-1.28	0.005647	Ncapd3	Q80W41	DOWN
9.86	10.22	-1.28	0.006916	Zcchc11	Q8BIZ5	DOWN
9.41	9.77	-1.28	0.006369	Scyl1	Q9EQC5	DOWN
9.61	9.97	-1.28	0.008547	Plod3	Q9R0E1	DOWN
6.53	6.88	-1.28	0.002041	Cttnbp2	R7RU63	DOWN
7.6	7.96	-1.28	0.004686	I79_018240	#N/A	DOWN
9.19	9.54	-1.28	0.009846	I79_025063	#N/A	DOWN
8.99	9.34	-1.28	0.004355	LOC100758211	#N/A	DOWN
10.19	10.56	-1.28	0.00762	LOC100766560	#N/A	DOWN
8.77	9.13	-1.28	0.006345	Mastl	#N/A	DOWN
8.36	8.72	-1.28	0.00529	Pard6b	#N/A	DOWN
9.11	9.48	-1.29	0.006399	Mapk8	A6P3E4	DOWN
10.28	10.65	-1.29	0.003811	Sec11a	D3YWT0	DOWN
10.11	10.48	-1.29	0.003309	Zc3hc1	D3Z0B2	DOWN
10.28	10.64	-1.29	0.004244	Adam17	Q3UEW9	DOWN
7.6	7.96	-1.29	0.008777	Ptbp2	Q3V328	DOWN
9.18	9.55	-1.29	0.009008	Plekhm1	Q7TSI1	DOWN
9.67	10.04	-1.29	0.007305	Tmem209	Q8BRG8	DOWN
5.53	5.9	-1.29	0.005373	Hdgfrp3	Q9JMG7	DOWN
8.72	9.08	-1.29	0.007047	C5orf25	#N/A	DOWN
7.48	7.84	-1.29	0.007164	Cep152	#N/A	DOWN
7.26	7.64	-1.3	0.009279	Otud7b	B2RUR8	DOWN
9.31	9.69	-1.3	0.004355	Fto	D3Z127	DOWN
6.96	7.34	-1.3	0.007149	Kif13b	O35063	DOWN

10.32	10.69	-1.3	0.00397	Atf2	P16951	DOWN
11.9	12.28	-1.3	0.004627	Mfge8	P21956	DOWN
9.71	10.09	-1.3	0.008325	Ctps2	P70303	DOWN
10.47	10.85	-1.3	0.003565	Brd2	Q3TH63	DOWN
9.63	10.01	-1.3	0.005955	Lrrc28	Q3TX51	DOWN
9.45	9.84	-1.3	0.004898	Foxn2	Q8BSS2	DOWN
11.59	11.96	-1.3	0.003718	Bst2	Q8R2Q8	DOWN
10.2	10.58	-1.3	0.009455	Adipor1	Q91VH1	DOWN
8.44	8.82	-1.3	0.005868	Spry2	Q9QXV8	DOWN
8.94	9.32	-1.3	0.002841	Deaf1	Q9Z1T5	DOWN
6.77	7.16	-1.3	0.009114	I79_023912	#N/A	DOWN
8.6	8.99	-1.31	0.006399	Pdpr	D3Z443	DOWN
7.13	7.52	-1.31	0.005041	Rsf1	E9PWW9	DOWN
9.64	10.03	-1.31	0.004955	Uty	P79457	DOWN
9.23	9.63	-1.31	0.008257	Ppp1r12a	Q3TS88	DOWN
8.17	8.55	-1.31	0.00481	Ttc9c	Q810A3	DOWN
7.04	7.44	-1.31	0.003718	Hectd2	Q8CDU6	DOWN
9.9	10.3	-1.31	0.009258	Sertad2	Q91VV6	DOWN
7.89	8.28	-1.31	0.008264	Dlg1	S4R2V5	DOWN
9.77	10.16	-1.31	0.006701	Tlr4	U5LL67	DOWN
11.03	11.41	-1.31	0.00605	G6pc3	#N/A	DOWN
10.34	10.72	-1.31	0.009205	Hist2h2bf	#N/A	DOWN
9.56	9.96	-1.31	0.003002	I79_006325	#N/A	DOWN
9.57	9.96	-1.31	0.007122	LOC100773978	#N/A	DOWN
9.56	9.96	-1.32	0.007005	Gpd2	A2AQR0	DOWN
10.67	11.07	-1.32	0.009495	Asxl2	D3Z112	DOWN
11.91	12.32	-1.32	0.008037	Tinagl1	H3BJ97	DOWN
10.49	10.88	-1.32	0.003478	Asap1	H3BK40	DOWN
8.53	8.93	-1.32	0.004567	Brca2	Q3TN53	DOWN
10.44	10.84	-1.32	0.004495	Alg8	Q3URN2	DOWN
6.25	6.65	-1.32	0.007266	Ltbp3	Q61810	DOWN
9.74	10.13	-1.32	0.006731	Uvrag	Q8C0K8	DOWN
7.49	7.89	-1.32	0.007832	Noxa1	Q8CJ00	DOWN
10.51	10.91	-1.32	0.002597	Gak	Q99KY4	DOWN
11.13	11.53	-1.32	0.004562	Uqcrc2	Q9DB77	DOWN
11.91	12.32	-1.32	0.004322	Pfn2	Q9JJV2	DOWN
9.65	10.05	-1.32	0.008891	Aak1	#N/A	DOWN
7.36	7.77	-1.32	0.006765	I79_014386	#N/A	DOWN
9.53	9.94	-1.32	0.009785	LOC100759120	#N/A	DOWN
9.5	9.9	-1.32	0.007396	Neurl	#N/A	DOWN
10.08	10.47	-1.32	0.008189	Rgnef	#N/A	DOWN
9.31	9.71	-1.32	0.002999	Znf187	#N/A	DOWN
9.59	10	-1.33	0.002995	Yeats2	B9EKJ4	DOWN
5.68	6.09	-1.33	0.002841	Gpr113	D3Z171	DOWN

8.34	8.76	-1.33	0.003103	Tgif1	E0CYI0	DOWN
8.2	8.61	-1.33	0.008295	Gpr137	E9Q9I0	DOWN
9.67	10.08	-1.33	0.004537	Pds5b	F8WHU5	DOWN
9.95	10.36	-1.33	0.006915	Agpat1	O35083	DOWN
9.39	9.8	-1.33	0.006833	Irf2	P23906	DOWN
10.28	10.69	-1.33	0.009028	Tnfrsf1a	Q3TVS9	DOWN
8.01	8.42	-1.33	0.002041	Athl1	Q8BP56	DOWN
8.49	8.89	-1.33	0.006887	Ccdc165	#N/A	DOWN
10.5	10.92	-1.33	0.006248	Dexi	#N/A	DOWN
7.8	8.21	-1.33	0.005138	Glt25d1	#N/A	DOWN
10.92	11.33	-1.33	0.006856	I79_001770	#N/A	DOWN
8.91	9.32	-1.33	0.006731	Kdm5b	#N/A	DOWN
10.5	10.92	-1.33	0.006928	LOC100762757	#N/A	DOWN
10.42	10.83	-1.33	0.001055	LOC100763741	#N/A	DOWN
9.36	9.78	-1.34	0.002597	Med24	A6PW47	DOWN
10.26	10.68	-1.34	0.005969	Plk4	E9PVH4	DOWN
10.84	11.26	-1.34	0.005969	Ap2b1	H3BKM0	DOWN
9.84	10.26	-1.34	0.003718	Dtnb	O70585	DOWN
9.91	10.32	-1.34	0.005076	Cpd	O89001	DOWN
10.45	10.87	-1.34	0.005783	Ptpn11	P35235	DOWN
10.86	11.28	-1.34	0.007242	Sos2	Q02384	DOWN
9.27	9.69	-1.34	0.006935	Ankrd12	Q3U569	DOWN
8.77	9.2	-1.34	0.0091	Mfhas1	Q3V1N1	DOWN
9.62	10.04	-1.34	0.006875	Map4k5	Q8BPM2	DOWN
10.3	10.73	-1.34	0.008324	Frmd6	Q8C0V9	DOWN
9.97	10.38	-1.34	0.008325	Ing3	Q8VEK6	DOWN
8.96	9.38	-1.34	0.009229	Stard13	Q923Q2	DOWN
10.13	10.55	-1.34	0.009403	Rnf111	Q99ML9	DOWN
5.2	5.62	-1.34	0.009839	Slc44a3	#N/A	DOWN
10.56	10.97	-1.34	0.005138	Ubxn7	#N/A	DOWN
9.62	10.05	-1.35	0.008209	Med24	A6PW47	DOWN
9.97	10.41	-1.35	0.002407	Dgcr2	E9QNU3	DOWN
9.92	10.36	-1.35	0.005008	Terf2	F6VIR4	DOWN
8.2	8.64	-1.35	0.003315	Fam13a	G3UYL7	DOWN
10.39	10.82	-1.35	0.004495	Cep170	H7BX26	DOWN
11.29	11.72	-1.35	0.009982	Nit1	Q8VDK1	DOWN
10.82	11.25	-1.35	0.006025	Gpx8	Q9D7B7	DOWN
8.93	9.37	-1.35	0.004675	Oma1	Q9D8H7	DOWN
9.36	9.79	-1.35	0.002867	Eps15l1	#N/A	DOWN
9.63	10.07	-1.35	0.005138	Fam168a	#N/A	DOWN
10.86	11.29	-1.35	0.009223	Kirrel	#N/A	DOWN
9.83	10.26	-1.35	0.007164	LOC100764634	#N/A	DOWN
10.25	10.69	-1.36	0.002104	Wdr46	A0A068BFS0	DOWN
9.64	10.08	-1.36	0.0091	Phf3	B2RQG2	DOWN

8.5	8.95	-1.36	0.007514	Fam111a	D3YYD2	DOWN
8.67	9.11	-1.36	0.007086	Angel2	F6SBQ6	DOWN
8.51	8.95	-1.36	0.007267	Tspyl2	J3QP69	DOWN
10.29	10.74	-1.36	0.005014	Gba	P17439	DOWN
7.55	8	-1.36	0.002372	Galc	P54818	DOWN
8.94	9.39	-1.36	0.003313	Rspry1	Q3T9K3	DOWN
8.09	8.53	-1.36	0.005996	Cog8	Q3U5F9	DOWN
10.87	11.31	-1.36	0.001055	Lman1	Q3U944	DOWN
8.69	9.13	-1.36	0.006227	Cand2	Q3UM57	DOWN
10.51	10.95	-1.36	0.003718	Ints3	Q7TPD0	DOWN
9.31	9.75	-1.36	0.006794	Prr14	Q7TPN9	DOWN
10.2	10.64	-1.36	0.005056	Itih5	Q8BJD1	DOWN
9.95	10.4	-1.36	0.009823	Naa25	Q8BKI9	DOWN
9.41	9.85	-1.36	0.004267	Rab3ip	Q8BR32	DOWN
7.59	8.04	-1.36	0.007092	Smyd3	Q8C2Y2	DOWN
10.1	10.54	-1.36	0.005516	Etfdh	Q921G7	DOWN
9.61	10.05	-1.36	0.005989	Dnajc14	Q921R4	DOWN
10.69	11.13	-1.36	0.001414	Tmem39a	Q9CYC3	DOWN
10.12	10.56	-1.36	0.005855	Acaca	Q9ESZ5	DOWN
4.7	5.14	-1.36	0.009066	Dnah12	#N/A	DOWN
9.05	9.5	-1.36	0.004843	I79_003829	#N/A	DOWN
9.19	9.63	-1.36	0.009024	I79_016242	#N/A	DOWN
8.04	8.48	-1.36	0.009279	Ppm1k	#N/A	DOWN
11.77	12.23	-1.37	0.008087	Slc25a39	B0QZI3	DOWN
9.8	10.25	-1.37	0.007242	Prkx	B1AVU1	DOWN
9.63	10.08	-1.37	0.002995	Ikzf5	D3YYG0	DOWN
11.97	12.43	-1.37	0.006935	Sparc	P07214	DOWN
8.94	9.39	-1.37	0.004442	Sass6	Q3UM73	DOWN
9.12	9.57	-1.37	0.00235	Trim6	Q8BGE7	DOWN
10.79	11.25	-1.37	0.00904	Setd5	Q8C2M5	DOWN
10.5	10.96	-1.37	0.003757	Brox	Q8K2Q7	DOWN
10.49	10.94	-1.37	0.005783	Ube3b	Q9ES34	DOWN
6.66	7.12	-1.37	0.00879	Fam164c	#N/A	DOWN
8.9	9.35	-1.37	0.006482	I79_002539	#N/A	DOWN
9.06	9.51	-1.37	0.005138	I79_016335	#N/A	DOWN
8.87	9.33	-1.37	0.005565	LOC100764678	#N/A	DOWN
9.39	9.85	-1.37	0.004843	LOC100774070	#N/A	DOWN
12.65	13.1	-1.37	0.002292	S100a11	#N/A	DOWN
9.26	9.72	-1.37	0.001353	Slc30a7	#N/A	DOWN
4.72	5.18	-1.37	0.008295	Tuba1c	#N/A	DOWN
10.21	10.67	-1.37	0.006248	Wwtr1	#N/A	DOWN
8.17	8.63	-1.38	0.00643	Fbxl8	D6RGN0	DOWN
8.44	8.9	-1.38	0.005565	Btaf1	E9QAE3	DOWN
11.05	11.51	-1.38	0.009325	Atp6v1f	F7B2B4	DOWN

9.68	10.15	-1.38	0.005465	Uggt1	G3UY73	DOWN
11.57	12.04	-1.38	0.001383	Mfge8	P21956	DOWN
9.84	10.31	-1.38	0.007947	Pros1	Q3V0M0	DOWN
11.38	11.84	-1.38	0.006426	Bre	Q8K3W0	DOWN
8.57	9.03	-1.38	0.004923	Kif18a	Q91WD7	DOWN
9.53	9.99	-1.38	0.00949	Mllt3	Q9D2P1	DOWN
12.57	13.04	-1.38	0.002557	---	#N/A	DOWN
10.75	11.21	-1.38	0.007852	Dcaf12	#N/A	DOWN
9.54	10	-1.38	0.009036	Gdf11	#N/A	DOWN
9.26	9.72	-1.38	0.003438	Herc2	#N/A	DOWN
8.01	8.47	-1.38	0.005993	I79_025753	#N/A	DOWN
10.85	11.31	-1.38	0.00397	Isyna1	#N/A	DOWN
10.73	11.19	-1.38	0.007242	Map1b	#N/A	DOWN
8.72	9.2	-1.39	0.003221	Ctnnal1	B1AZA7	DOWN
9.46	9.94	-1.39	0.006332	Pgs1	F8WI04	DOWN
10.22	10.69	-1.39	0.005178	Mdm2	P23804	DOWN
10.13	10.61	-1.39	0.009983	Brca1	P48754	DOWN
9.65	10.12	-1.39	0.006599	Vangl1	Q3UXU7	DOWN
9.14	9.61	-1.39	0.00338	Prune	Q8BIW1	DOWN
9.84	10.31	-1.39	0.008877	Tbck	Q8BM85	DOWN
9.83	10.31	-1.39	0.003372	Gtf3c1	Q8K284	DOWN
8.74	9.22	-1.39	0.004814	Uxs1	Q91XL3	DOWN
9.57	10.04	-1.39	0.002291	Gpr108	Q9CU01	DOWN
10.63	11.1	-1.39	0.008105	Skp2	Q9Z0Z3	DOWN
11.63	12.11	-1.39	0.006887	Ddr2	#N/A	DOWN
7.83	8.31	-1.39	0.004611	I79_020071	#N/A	DOWN
8.64	9.12	-1.39	0.004168	I79_021515	#N/A	DOWN
7.6	8.07	-1.39	0.00643	Klhl28	#N/A	DOWN
10.08	10.55	-1.39	0.006929	LOC100762576	#N/A	DOWN
9.72	10.19	-1.39	0.004569	LOC100763193	#N/A	DOWN
9.13	9.61	-1.39	0.003002	Znf770	#N/A	DOWN
7.55	8.03	-1.4	0.008557	Ston1	D3Z0U0	DOWN
8.64	9.13	-1.4	0.00762	Agtpbp1	E9PXA7	DOWN
8.49	8.98	-1.4	0.005008	Clip1	F6RAY2	DOWN
7.41	7.89	-1.4	0.004477	Pol	P10400	DOWN
9.47	9.96	-1.4	0.008727	Tmem231	Q3U284	DOWN
10.04	10.52	-1.4	0.005969	Cln5	Q3UMW8	DOWN
8.91	9.39	-1.4	0.004065	Srgap2	Q3UPB8	DOWN
10.78	11.27	-1.4	0.005212	Acd	Q5EE38	DOWN
10.73	11.21	-1.4	0.003936	Mef2a	Q60929	DOWN
9.54	10.03	-1.4	0.00671	Casc4	Q6P2L7	DOWN
9.89	10.37	-1.4	0.00911	Prdm4	Q80V63	DOWN
8.13	8.62	-1.4	0.001353	Sec62	Q8CIK3	DOWN
8.28	8.76	-1.4	0.005491	Mgat5	Q8R4G6	DOWN

8.49	8.98	-1.4	0.006915	Pygl	Q9ET01	DOWN
9.34	9.83	-1.4	0.009141	Foxf1	#N/A	DOWN
8.64	9.13	-1.4	0.007191	I79_014905	#N/A	DOWN
8.95	9.43	-1.4	0.004384	LOC100758878	#N/A	DOWN
8.25	8.74	-1.41	0.002392	Spg20	D3Z3F8	DOWN
10.06	10.55	-1.41	0.008209	Atxn2	E9QM77	DOWN
8.78	9.28	-1.41	0.007672	Tsc1	F2Z3X2	DOWN
9.53	10.02	-1.41	0.002041	Kdm5c	F6WXI0	DOWN
9.69	10.19	-1.41	0.009674	Jmjd1c	G3UZM1	DOWN
9.44	9.94	-1.41	0.003696	Dnmt3a	O88508	DOWN
8.83	9.33	-1.41	0.002535	Cant1	Q8VCF1	DOWN
11.47	11.97	-1.41	0.004692	Gatad2b	Q8VHR5	DOWN
8.38	8.88	-1.41	0.006664	Stat2	Q9WVL2	DOWN
10.61	11.11	-1.41	0.009453	Skp2	Q9Z0Z3	DOWN
7.59	8.09	-1.41	0.003103	Bcar3	#N/A	DOWN
6.26	6.75	-1.41	0.006785	I79_010558	#N/A	DOWN
9.47	9.96	-1.41	0.008264	Synj2bp	#N/A	DOWN
9.42	9.92	-1.42	0.004542	Ptprs	B0V2N1	DOWN
10.54	11.04	-1.42	0.003953	Golim4	F6RUD1	DOWN
9.15	9.66	-1.42	0.008673	Nav3	F6U6A7	DOWN
9.18	9.69	-1.42	0.006774	Fkbp14	P59024	DOWN
11.06	11.57	-1.42	0.001926	Nfe2l2	Q05DU7	DOWN
10.84	11.34	-1.42	0.002041	Cnot4	Q3TMM0	DOWN
9.38	9.89	-1.42	0.007242	Rngtt	Q3TUK6	DOWN
8.36	8.86	-1.42	0.007285	Evi5l	Q3U1G0	DOWN
11.06	11.56	-1.42	0.00226	Neo1	Q7TQG5	DOWN
8.67	9.17	-1.42	0.005532	Slc22a17	Q8C0Y4	DOWN
8.63	9.14	-1.42	0.008532	Flad1	Q8R123	DOWN
11.36	11.87	-1.42	0.004567	Rtn3	Q9ES97	DOWN
8.11	8.62	-1.42	0.00787	Pvrl3	Q9JLB9	DOWN
9.1	9.61	-1.42	0.007687	Gabbr1	Q9WV18	DOWN
11	11.51	-1.42	0.006426	I79_005363	#N/A	DOWN
10.18	10.69	-1.42	0.007388	I79_015026	#N/A	DOWN
8.39	8.9	-1.42	0.002392	Irx3	#N/A	DOWN
7.14	7.65	-1.42	0.006916	Kiaa0232	#N/A	DOWN
9	9.52	-1.43	0.00949	Ssfa2	A2AQD6	DOWN
9.63	10.14	-1.43	0.00701	Mbtps1	A3QWY0	DOWN
8.41	8.94	-1.43	0.006915	Phf3	B2RQG2	DOWN
10.78	11.3	-1.43	0.007833	Coq10a	B2RWC6	DOWN
9.52	10.04	-1.43	0.005887	Ankib1	B2RX15	DOWN
8.97	9.48	-1.43	0.007062	Fnbp1l	E9PUK3	DOWN
10.38	10.9	-1.43	0.009983	Man2a1	F6QMB7	DOWN
11.44	11.96	-1.43	0.005969	Gatad1	F7CAN4	DOWN
8.23	8.75	-1.43	0.009008	Ube2l6	Q4FJY2	DOWN

9.61	10.13	-1.43	0.005006	Sort1	Q6PHU5	DOWN
8.43	8.95	-1.43	0.006074	Mef2c	Q8CFN5	DOWN
9.15	9.67	-1.43	0.008557	Frmd4b	Q920B0	DOWN
7.26	7.77	-1.43	0.005006	Bbs12	Z4YKQ3	DOWN
10.71	11.22	-1.43	0.003331	Cers6	#N/A	DOWN
9.15	9.66	-1.43	0.007687	Flrt3	#N/A	DOWN
9.91	10.42	-1.43	0.009649	I79_000877	#N/A	DOWN
7.71	8.23	-1.43	0.005955	I79_005651	#N/A	DOWN
6.84	7.36	-1.43	0.008673	I79_019977	#N/A	DOWN
9.13	9.65	-1.43	0.006541	Isca2	#N/A	DOWN
10.37	10.88	-1.43	0.005138	Lpcat4	#N/A	DOWN
9.72	10.24	-1.43	0.003587	Znf800	#N/A	DOWN
7.91	8.44	-1.44	0.009236	Wdr47	A2AGC6	DOWN
8.89	9.41	-1.44	0.00453	Arfip1	A2RSX9	DOWN
8.24	8.77	-1.44	0.004943	Casc5	A3KGI3	DOWN
9.36	9.88	-1.44	0.005918	Tmem132a	D3Z4S6	DOWN
9.6	10.12	-1.44	0.003221	Slc35b2	Q3TJQ2	DOWN
9.73	10.26	-1.44	0.009943	Cdkn2c	Q60772	DOWN
10.15	10.67	-1.44	0.003139	Tbc1d22b	Q6PAT2	DOWN
8.33	8.86	-1.44	0.004787	Akap9	Q8C0C6	DOWN
11.12	11.64	-1.44	0.008209	Cd151	Q921J7	DOWN
10.02	10.54	-1.44	0.003821	Sgsh	Q9JHK6	DOWN
9.42	9.95	-1.44	0.003538	Dst	S4R1Y6	DOWN
9.22	9.74	-1.44	0.004719	Btbd7	#N/A	DOWN
9.03	9.56	-1.44	0.007609	I79_014653	#N/A	DOWN
7.72	8.25	-1.44	0.008608	LOC100763467	#N/A	DOWN
7.54	8.07	-1.44	0.009483	Map6	#N/A	DOWN
9.46	9.99	-1.44	0.007271	Specc1l	#N/A	DOWN
8.32	8.85	-1.44	0.008557	Zcchc2	#N/A	DOWN
10.43	10.97	-1.45	0.009279	Pcyox1	F7CIP8	DOWN
9.24	9.78	-1.45	0.00338	Tob1	Q3UQ91	DOWN
7.79	8.33	-1.45	0.002841	Mybl1	Q3ZB49	DOWN
10.52	11.06	-1.45	0.006491	Sec24d	Q6NXL1	DOWN
8.82	9.35	-1.45	0.008632	Kiaa0195	Q7TSH8	DOWN
8.28	8.82	-1.45	0.004292	Tcp11l1	Q8BTG3	DOWN
8.44	8.97	-1.45	0.007472	Klhl2	Q8JZP3	DOWN
10.43	10.97	-1.45	0.007565	Elk3	Q91W17	DOWN
7.09	7.62	-1.45	0.00804	Rabgap1l	Q9CRQ7	DOWN
10.81	11.34	-1.45	0.003912	Arl2	Q9D0J4	DOWN
12.22	12.76	-1.45	0.00671	---	#N/A	DOWN
10.16	10.7	-1.45	0.003967	Bcar3	#N/A	DOWN
7.15	7.7	-1.45	0.007921	LOC100761811	#N/A	DOWN
9.21	9.75	-1.45	0.008282	LOC100763232	#N/A	DOWN
10.68	11.21	-1.45	0.006457	LOC100766481	#N/A	DOWN

7.51	8.05	-1.45	0.007164	LOC100767949	#N/A	DOWN
11.27	11.81	-1.45	0.006915	Spcs2	#N/A	DOWN
8.02	8.57	-1.46	0.007832	Brpf3	B2KF05	DOWN
12.17	12.71	-1.46	0.003114	Capns1	D3YW48	DOWN
9.91	10.45	-1.46	0.007164	Man2a1	F6QMB7	DOWN
9.17	9.71	-1.46	0.007416	Synj1	F6XIX0	DOWN
8.6	9.15	-1.46	0.009638	Slc5a6	Q5U4D8	DOWN
6.41	6.96	-1.46	0.003894	Cp	Q61147	DOWN
9.38	9.93	-1.46	0.004562	Fbxo11	Q7TPD1	DOWN
11.06	11.61	-1.46	0.002016	Rin2	Q9D684	DOWN
10.73	11.27	-1.46	0.001651	Gpc1	Q9QZF2	DOWN
9.99	10.53	-1.46	0.005636	Ccdc56	#N/A	DOWN
10.6	11.15	-1.46	0.003718	LOC100752106	#N/A	DOWN
10.5	11.05	-1.46	0.003672	LOC100755646	#N/A	DOWN
8.32	8.87	-1.46	0.004588	Znf451	#N/A	DOWN
8.08	8.63	-1.47	0.002292	Chd2	E9PZM4	DOWN
9.9	10.46	-1.47	0.005001	Atf6b	G3UXQ6	DOWN
11.16	11.72	-1.47	0.001947	Ubash3b	H3BJB9	DOWN
8.68	9.24	-1.47	0.002597	Ipo13	Q3UDQ3	DOWN
9.58	10.14	-1.47	0.005565	Ezh2	Q6AXH7	DOWN
9.6	10.15	-1.47	0.007396	Atl2	Q8C081	DOWN
10.01	10.57	-1.47	0.009638	Dnajb9	Q9QYI6	DOWN
10.59	11.15	-1.47	0.004355	Gpc1	Q9QZF2	DOWN
8.88	9.43	-1.47	0.008083	Cd320	Q9Z1P5	DOWN
11.01	11.57	-1.47	0.00474	Ccdc80	#N/A	DOWN
6.17	6.73	-1.47	0.005101	I79_005615	#N/A	DOWN
6.82	7.38	-1.47	0.00388	I79_020153	#N/A	DOWN
9.27	9.82	-1.47	0.008799	I79_021371	#N/A	DOWN
9.54	10.09	-1.47	0.003478	LOC100766184	#N/A	DOWN
8.28	8.83	-1.47	0.009272	Wdr85	#N/A	DOWN
8.82	9.38	-1.48	0.003816	Camsap1	A2AHC3	DOWN
7.73	8.29	-1.48	0.004843	Acbd4	E0CXU7	DOWN
9.28	9.85	-1.48	0.008319	Pi4ka	E9Q3L2	DOWN
8.92	9.48	-1.48	0.009552	Xbp1	H3BLF6	DOWN
10.03	10.59	-1.48	0.002041	Clk2	O35491	DOWN
9.3	9.87	-1.48	0.00671	Rad52	P43352	DOWN
8.1	8.66	-1.48	0.008007	Cpeb1	Q059Z2	DOWN
11.05	11.62	-1.48	0.007984	Stip1	Q60864	DOWN
8.93	9.49	-1.48	0.00543	Kiaa1841	Q68FF0	DOWN
9.43	10	-1.48	0.003372	Mamdc2	Q8CG85	DOWN
9.97	10.54	-1.48	0.00397	Txndc11	Q8K2W3	DOWN
8.02	8.59	-1.48	0.00388	Mxra7	Q9D1T2	DOWN
9.38	9.94	-1.48	0.007251	Agrn	Z4YK85	DOWN
11.45	12.02	-1.48	0.003103	Gpr56	#N/A	DOWN

10.73	11.3	-1.48	0.00991	LOC100760205	#N/A	DOWN
10.05	10.62	-1.48	0.009008	Rad9a	#N/A	DOWN
10.86	11.43	-1.48	0.004326	Wdr67	#N/A	DOWN
9.48	10.06	-1.49	0.003051	Phf21a	A2AHG3	DOWN
10.01	10.58	-1.49	0.009873	Ptprs	B0V2N1	DOWN
9.65	10.23	-1.49	0.006426	Sbf2	E9Q372	DOWN
9.03	9.6	-1.49	0.009956	Mut	P16332	DOWN
8.38	8.96	-1.49	0.003718	Snx25	Q3ZT31	DOWN
8.43	9	-1.49	0.004923	Heatr6	Q6P1G0	DOWN
9.21	9.78	-1.49	0.005993	Tbc1d22b	Q6PAT2	DOWN
10.24	10.82	-1.49	0.001708	Foxk2	Q811H2	DOWN
8.24	8.81	-1.49	0.004747	Klhl24	Q8BRG6	DOWN
10	10.57	-1.49	0.009873	Tmem175	Q9CXY1	DOWN
8.99	9.57	-1.49	0.006244	Slc25a19	Q9DAM5	DOWN
9.62	10.19	-1.49	0.003718	Cab39l	Q9DB16	DOWN
9.04	9.62	-1.49	0.004322	Cd320	Q9Z1P5	DOWN
8.64	9.22	-1.49	0.008727	Ccdc76	#N/A	DOWN
7.03	7.61	-1.49	0.008833	Dclk2	#N/A	DOWN
8.22	8.79	-1.49	0.00944	I79_011251	#N/A	DOWN
8.29	8.86	-1.49	0.006224	I79_012309	#N/A	DOWN
8.81	9.38	-1.49	0.009094	LOC100753065	#N/A	DOWN
7.65	8.23	-1.49	0.006591	LOC100764227	#N/A	DOWN
9.25	9.83	-1.49	0.008598	Zfc3h1	#N/A	DOWN
10.45	11.04	-1.5	0.005005	Glg1	E9PWD8	DOWN
7.33	7.91	-1.5	0.002887	Map3k13	Q1HKZ5	DOWN
10.42	11.01	-1.5	0.002392	Dpy19l3	Q71B07	DOWN
10.11	10.7	-1.5	0.002567	Tmem184b	Q8BG09	DOWN
7.51	8.1	-1.5	0.005619	Pygl	Q9ET01	DOWN
8.69	9.28	-1.5	0.007164	Pign	Q9R1S3	DOWN
8.41	9	-1.5	0.009541	I79_007541	#N/A	DOWN
6.06	6.65	-1.5	0.003718	I79_023557	#N/A	DOWN
7.34	7.94	-1.51	0.00481	Ppm1e	B2KGP3	DOWN
8.73	9.33	-1.51	0.008527	Map3k12	E9PZU4	DOWN
7.25	7.84	-1.51	0.008739	Socs3	Q3U9J8	DOWN
9.41	10.01	-1.51	0.003587	Ddr1	Q544T2	DOWN
7.55	8.14	-1.51	0.00667	Pcyt1b	Q811Q9	DOWN
7.25	7.85	-1.51	0.002557	Phf21b	Q8C966	DOWN
8.3	8.89	-1.51	0.009602	Nrm	Q8VC65	DOWN
9.39	9.98	-1.51	0.004101	Aig1	Q9D8B1	DOWN
6.15	6.75	-1.51	0.008522	I79_003763	#N/A	DOWN
9.2	9.8	-1.51	0.004216	I79_026264	#N/A	DOWN
10.24	10.83	-1.51	0.005373	LOC100760720	#N/A	DOWN
8.13	8.74	-1.52	0.007267	Larp1b	E9PYM4	DOWN
7.91	8.52	-1.52	0.008089	Prdm15	E9Q8T2	DOWN

8.3	8.91	-1.52	0.006085	Exd2	F8WID1	DOWN
10.68	11.28	-1.52	0.005465	Fuca1	Q3TCW3	DOWN
10.55	11.15	-1.52	0.008796	Rad23a	Q3TN85	DOWN
8.36	8.96	-1.52	0.009139	Rint1	Q8BZ36	DOWN
6.96	7.57	-1.52	0.006953	Pmvk	Q9D1G2	DOWN
7.15	7.75	-1.52	0.007149	B3galnt1	#N/A	DOWN
8.38	8.98	-1.52	0.009139	Cntnap1	#N/A	DOWN
7.41	8.01	-1.52	0.001373	Heatr7a	#N/A	DOWN
8.8	9.4	-1.52	0.005373	I79_004782	#N/A	DOWN
5.2	5.81	-1.52	0.005885	I79_005205	#N/A	DOWN
5.83	6.43	-1.52	0.001353	I79_020723	#N/A	DOWN
3.47	4.07	-1.52	0.006249	Or4a15	#N/A	DOWN
9.23	9.83	-1.52	0.002041	Pot1	#N/A	DOWN
9.04	9.64	-1.52	0.00878	Rft2	#N/A	DOWN
8.79	9.39	-1.52	0.007941	Spast	#N/A	DOWN
9.78	10.39	-1.53	0.001947	Pcgf5	B7ZP24	DOWN
10.43	11.04	-1.53	0.004355	Hyou1	E0CYZ2	DOWN
8.83	9.44	-1.53	0.005007	Crtc3	F6UMS9	DOWN
7.59	8.2	-1.53	0.005821	Tmem44	F7D1Q2	DOWN
7.97	8.58	-1.53	0.008532	Trim13	Q3TSD2	DOWN
8.48	9.1	-1.53	0.003414	Lrrc58	Q3UGP9	DOWN
9.7	10.32	-1.53	0.007939	Abr	Q5SSL4	DOWN
9.44	10.05	-1.53	0.001353	Ahcyl2	Q68FL4	DOWN
7.16	7.77	-1.53	0.001713	Loxl1	Q8BP04	DOWN
10.93	11.54	-1.53	0.005588	Mamdc2	Q8CG85	DOWN
8.61	9.22	-1.53	0.0067	Cep57l1	Q9D9M1	DOWN
8.83	9.44	-1.53	0.006822	Ago61	#N/A	DOWN
10.23	10.85	-1.53	0.005623	Pycard	#N/A	DOWN
7.82	8.43	-1.53	0.001353	Tmem237	#N/A	DOWN
9.93	10.55	-1.54	0.000921	Clec16a	D3YVA1	DOWN
8.09	8.71	-1.54	0.007276	Gpt2	D6RFQ8	DOWN
9.3	9.92	-1.54	0.006599	Ubash3b	H3BJB9	DOWN
11.47	12.09	-1.54	0.001055	Rras	P10833	DOWN
8.76	9.39	-1.54	0.006918	Pja2	Q0VDX8	DOWN
9.73	10.35	-1.54	0.005373	Col5a2	Q3U962	DOWN
8.64	9.26	-1.54	0.00338	Fam135a	Q6NS59	DOWN
9.13	9.76	-1.54	0.001541	Eif4a2	Q8BTU6	DOWN
10.32	10.95	-1.54	0.00417	Minpp1	Q8C9C2	DOWN
7.15	7.77	-1.54	0.003718	Stx3	Q8CAN1	DOWN
9.56	10.18	-1.54	0.003876	Rnf183	Q8QZS5	DOWN
8.84	9.47	-1.54	0.006731	Acp5	#N/A	DOWN
9.84	10.47	-1.54	0.002841	I79_005632	#N/A	DOWN
8.73	9.36	-1.54	0.005843	I79_015611	#N/A	DOWN
9.47	10.09	-1.54	0.005138	Itfg1	#N/A	DOWN

8.69	9.32	-1.54	0.003221	Nedd1	#N/A	DOWN
9.41	10.05	-1.55	0.003004	Parp4	E9PYK3	DOWN
10.82	11.46	-1.55	0.003587	Rock2	P70336	DOWN
10.83	11.46	-1.55	0.001862	Arid5b	Q3TRJ5	DOWN
9.27	9.9	-1.55	0.003051	Lrrc58	Q3UGP9	DOWN
9.71	10.35	-1.55	0.003604	Baz2a	Q3UXC9	DOWN
7.13	7.77	-1.55	0.005212	Letm2	Q7TNU7	DOWN
9	9.63	-1.55	0.007596	Nagpa	Q8BJ48	DOWN
9.42	10.04	-1.55	0.00209	Gdpd5	#N/A	DOWN
8.32	8.96	-1.55	0.009139	Tada3	#N/A	DOWN
9.86	10.49	-1.56	0.005636	Hipk1	A0S0L5	DOWN
8.8	9.45	-1.56	0.007388	Msl1	F7CR37	DOWN
9.4	10.04	-1.56	0.007273	Pde5a	Q8BJ62	DOWN
9.83	10.47	-1.56	0.003718	Bbx	Q8C9P7	DOWN
9.24	9.88	-1.56	0.003862	Uap1	Q91YN5	DOWN
8.41	9.06	-1.56	0.007672	Phf14	Q9D4H9	DOWN
7.5	8.14	-1.56	0.005279	Slc5a3	Q9JKZ2	DOWN
9.74	10.39	-1.56	0.004495	Fam160b1	#N/A	DOWN
7.38	8.03	-1.56	0.002995	Heatr5a	#N/A	DOWN
5.7	6.35	-1.56	0.004588	I79_007835	#N/A	DOWN
6.5	7.14	-1.56	0.009214	I79_009106	#N/A	DOWN
6.68	7.32	-1.56	0.008638	I79_021705	#N/A	DOWN
5.52	6.15	-1.56	0.008927	LOC100751350	#N/A	DOWN
8.07	8.72	-1.56	0.005809	LOC100767289	#N/A	DOWN
7.45	8.11	-1.57	0.007058	Ankrd34a	B2RW11	DOWN
11.28	11.93	-1.57	0.002879	Itgb5	O70309	DOWN
10.83	11.48	-1.57	0.004562	Dcakd	Q8BHC4	DOWN
11.47	12.12	-1.57	0.001715	Scarb1	Q8BNQ0	DOWN
7.86	8.51	-1.57	0.00751	Arid4a	Q8BY40	DOWN
10.85	11.51	-1.57	0.002995	Smpd1	Q8K011	DOWN
8.48	9.13	-1.57	0.004721	Pycr1	Q922W5	DOWN
8.48	9.13	-1.57	0.003718	Tctn2	Q9D8A8	DOWN
8.71	9.36	-1.57	0.004677	Mapk1ip1	#N/A	DOWN
9.18	9.83	-1.57	0.006593	Tfap2a	#N/A	DOWN
10.6	11.27	-1.58	0.003718	Pxdn	D3Z5M7	DOWN
8.42	9.08	-1.58	0.001926	Chka	D6RG40	DOWN
7.89	8.55	-1.58	0.009222	Uspl1	Q3ULM6	DOWN
8.39	9.04	-1.58	0.002879	Eras	Q7TN89	DOWN
8.38	9.04	-1.58	0.004302	Sccpdh	Q8R127	DOWN
6.56	7.22	-1.58	0.001947	Ccrl1	#N/A	DOWN
9.3	9.96	-1.58	0.006491	Ebf2	#N/A	DOWN
9.34	10	-1.58	0.004302	Hspa2	#N/A	DOWN
6.22	6.88	-1.58	0.008422	Tbc1d8	#N/A	DOWN
10.34	11.01	-1.59	0.005887	Prkd3	D3YU02	DOWN

10.2	10.87	-1.59	0.009638	Mesdc2	D3YVR4	DOWN
9.5	10.17	-1.59	0.004216	Igsf8	D3Z4Q8	DOWN
7.62	8.29	-1.59	0.007861	Sorbs1	E9PYX6	DOWN
6.88	7.55	-1.59	0.001947	Shox2	F6UTR6	DOWN
7.81	8.49	-1.59	0.004611	Eapp	Q5BU09	DOWN
8.61	9.28	-1.59	0.009604	Boc	Q6AZB0	DOWN
6.23	6.9	-1.59	0.003503	Adck1	Q9D0L4	DOWN
10.53	11.2	-1.59	0.002343	Dcbld2	Q9D9K5	DOWN
5.67	6.34	-1.59	0.009888	Cttnbp2	R7RU63	DOWN
7.36	8.03	-1.59	0.006593	I79_019388	#N/A	DOWN
10.08	10.75	-1.6	0.002041	Cnpy3	B0V2V1	DOWN
9.13	9.81	-1.6	0.004355	Ttc17	E9PVB5	DOWN
9.37	10.05	-1.6	0.005185	Tgfb1i1	E9PYQ1	DOWN
10.63	11.31	-1.6	0.002856	Ermp1	F6TQS9	DOWN
8.67	9.35	-1.6	0.007124	Cnih2	Q3SYI8	DOWN
8.03	8.7	-1.6	0.004898	Prkca	Q3TQ39	DOWN
7.84	8.52	-1.6	0.005616	Mga	Q3ULI0	DOWN
6.15	6.83	-1.6	0.005518	Gm4952	Q5FW57	DOWN
7.38	8.06	-1.6	0.008727	Nhlrc3	Q8CCH2	DOWN
8.53	9.21	-1.6	0.005056	Scamp4	Q9JKV5	DOWN
8.59	9.26	-1.6	0.001502	I79_024494	#N/A	DOWN
9.1	9.79	-1.61	0.00984	Srpk2	O54781	DOWN
7.31	8	-1.61	0.002415	Phtf1	Q80YS3	DOWN
8.13	8.82	-1.61	0.005014	Zbtb11	Q8BXA4	DOWN
8.52	9.21	-1.61	0.003565	Sh3d19	Q91X43	DOWN
9.11	9.79	-1.61	0.004355	Itsn2	Q9CQD9	DOWN
9.12	9.81	-1.61	0.001353	Pigc	Q9CXR4	DOWN
6.97	7.66	-1.61	0.004292	I79_004233	#N/A	DOWN
9.77	10.46	-1.61	0.008209	LOC100764737	#N/A	DOWN
8.06	8.75	-1.61	0.003315	LOC100773413	#N/A	DOWN
7.47	8.15	-1.61	0.008565	Nfkbiz	#N/A	DOWN
9.21	9.9	-1.62	0.009688	Trmt1l	A2RSY6	DOWN
7.68	8.37	-1.62	0.005138	Rpgrip1l	D3Z0V3	DOWN
8.26	8.96	-1.62	0.003565	Chka	D6RG40	DOWN
8.59	9.29	-1.62	0.00411	Ptgr2	D6RGL6	DOWN
9.39	10.09	-1.62	0.002392	Plxna2	F6VSI0	DOWN
8.03	8.72	-1.62	0.008374	Ube3a	O08759	DOWN
8.58	9.28	-1.62	0.00751	Pias3	O54714	DOWN
6.57	7.26	-1.62	0.004963	Col4a1	P02463	DOWN
6.41	7.1	-1.62	0.005861	Ctsk	P55097	DOWN
6.9	7.6	-1.62	0.002817	Sdccag8	Q05DD9	DOWN
9.18	9.88	-1.62	0.006482	Etv1	Q549J8	DOWN
9.28	9.98	-1.62	0.006025	Adam23	Q5SRA0	DOWN
8.85	9.54	-1.62	0.002984	Kiaa0226	Q80U62	DOWN

8.62	9.32	-1.62	0.00701	Cacna2d1	Q8C6Y3	DOWN
8.67	9.37	-1.62	0.009552	Creld1	Q91XD7	DOWN
5.26	5.96	-1.62	0.008332	I79_003014	#N/A	DOWN
8.49	9.19	-1.62	0.007939	I79_015167	#N/A	DOWN
8.14	8.84	-1.63	0.003947	Txndc16	D3Z7P6	DOWN
8.02	8.73	-1.63	0.005565	Irf3	P70671	DOWN
8.3	9.01	-1.63	0.00878	Ttc21b	Q3TP46	DOWN
9.24	9.94	-1.63	0.00701	Cdon	Q3TZM7	DOWN
8.33	9.03	-1.63	0.005599	Fam178a	Q6P9P0	DOWN
6.72	7.42	-1.63	0.00481	Aqp11	Q8BHH1	DOWN
9.74	10.44	-1.63	0.007345	Psd3	Q8C0E9	DOWN
10.17	10.88	-1.63	0.007345	Baiap2l1	#N/A	DOWN
6.4	7.1	-1.63	0.008768	I79_010994	#N/A	DOWN
10.58	11.29	-1.63	0.004355	LOC100760682	#N/A	DOWN
8.14	8.85	-1.63	0.005185	LOC100768853	#N/A	DOWN
8.81	9.51	-1.63	0.004355	Mettl2	#N/A	DOWN
8.23	8.94	-1.63	0.001926	Pot1	#N/A	DOWN
7.43	8.13	-1.63	0.004227	Znf654	#N/A	DOWN
9.23	9.94	-1.64	0.004355	Efemp2	E9Q8E0	DOWN
10.79	11.51	-1.64	0.00671	Vgll3	P85442	DOWN
8.59	9.31	-1.64	0.004302	Fchsd2	Q3U0A9	DOWN
8.86	9.58	-1.64	0.006426	Arhgap10	Q6Y5D8	DOWN
9.04	9.75	-1.64	0.005014	Osbpl3	Q80UX3	DOWN
8.63	9.35	-1.64	0.004151	Arsj	Q8BM89	DOWN
10.27	10.98	-1.64	0.004183	Foxo1	Q8BPP2	DOWN
7.99	8.71	-1.64	0.002985	Dnase1l1	Q9D7J6	DOWN
9.3	10.01	-1.64	0.005783	Git2	Q9JLQ2	DOWN
11.49	12.21	-1.64	0.00944	I79_026010	#N/A	DOWN
10.26	10.98	-1.64	0.005224	LOC100757521	#N/A	DOWN
9.17	9.88	-1.64	0.001715	Napepld	#N/A	DOWN
7.73	8.44	-1.65	0.003769	Fblim1	A2ADE8	DOWN
6.78	7.51	-1.65	0.007947	Pcdh7	E9Q2S0	DOWN
11.51	12.23	-1.65	0.00209	Gaa	P70699	DOWN
10.12	10.85	-1.65	0.002292	Wsb2	Q3UC26	DOWN
9.52	10.24	-1.65	0.007164	Sipa1l1	Q4VBF8	DOWN
9.99	10.71	-1.65	0.00508	Sipa1	Q7TMS2	DOWN
9.5	10.22	-1.65	0.006968	Dock4	Q8BMP2	DOWN
9.03	9.75	-1.65	0.002392	Nqo1	Q99KL8	DOWN
11.61	12.33	-1.65	0.00545	---	#N/A	DOWN
8.18	8.9	-1.65	0.009695	Cnnm2	#N/A	DOWN
6.3	7.02	-1.65	0.005927	I79_010657	#N/A	DOWN
8.17	8.89	-1.65	0.005955	Wasf1	#N/A	DOWN
7.71	8.43	-1.65	0.006482	Znf318	#N/A	DOWN
7.63	8.36	-1.66	0.006968	Fam179b	B2RXS2	DOWN

9.89	10.62	-1.66	0.005518	Tgfbr3	O88393	DOWN
10.32	11.05	-1.66	0.002967	Met	P16056	DOWN
9.2	9.93	-1.66	0.003795	Nek1	P51954	DOWN
9.54	10.27	-1.66	0.001515	Etv4	Q3TYM4	DOWN
6.76	7.49	-1.66	0.008315	Ipp	Q8BY33	DOWN
8.96	9.7	-1.66	0.003471	Ctsf	Q9R013	DOWN
8.98	9.71	-1.66	0.002392	Cflar	#N/A	DOWN
7.89	8.62	-1.66	0.002429	I79_000078	#N/A	DOWN
6.08	6.81	-1.66	0.009279	I79_016894	#N/A	DOWN
10.1	10.83	-1.66	0.003331	Inm02	#N/A	DOWN
9.08	9.81	-1.66	0.008714	Ints6	#N/A	DOWN
9.03	9.76	-1.66	0.003894	LOC100752469	#N/A	DOWN
7.9	8.64	-1.66	0.006588	Ngf	#N/A	DOWN
7.22	7.96	-1.67	0.002041	Ttbk2	A2AW14	DOWN
10.71	11.46	-1.67	0.003458	Lamb1	E9QN70	DOWN
11.91	12.65	-1.67	0.001353	Thbs1	Q80YQ1	DOWN
7.82	8.55	-1.67	0.006327	Pign	Q9R1S3	DOWN
9.88	10.61	-1.67	0.003002	---	#N/A	DOWN
7.14	7.88	-1.67	0.001625	I79_013426	#N/A	DOWN
7.43	8.17	-1.67	0.002392	I79_020093	#N/A	DOWN
8.01	8.75	-1.67	0.004898	LOC100773770	#N/A	DOWN
6.5	7.25	-1.68	0.005185	Serpinf1	E9PWS2	DOWN
7.53	8.28	-1.68	0.00474	Bahcc1	E9Q7G4	DOWN
8.15	8.91	-1.68	0.008369	Nav3	F6U6A7	DOWN
9.84	10.59	-1.68	0.004355	E2f6	O54917	DOWN
7.48	8.24	-1.69	0.009945	Ctnna2	E0CXB9	DOWN
8.2	8.96	-1.69	0.006286	Atat1	F6RPX5	DOWN
10.38	11.13	-1.69	0.006332	Plod2	Q9R0B9	DOWN
10.27	11.03	-1.69	0.002567	Cachd1	Z4YK18	DOWN
9.67	10.42	-1.69	0.002041	I79_003336	#N/A	DOWN
8.22	8.98	-1.69	0.008319	I79_007417	#N/A	DOWN
9.52	10.28	-1.7	0.002392	Sh2b3	D3Z0T9	DOWN
9.56	10.32	-1.7	0.009874	Acss2	F7CU63	DOWN
9.3	10.07	-1.7	0.002995	Lrp5	H3BIY3	DOWN
7.27	8.04	-1.7	0.006915	Rap1gap2	Q5SUE5	DOWN
12.06	12.82	-1.7	0.001947	Serpinh1	Q8BVU9	DOWN
6.86	7.63	-1.7	0.009541	Cdkl2	#N/A	DOWN
8.7	9.46	-1.7	0.008267	I79_004447	#N/A	DOWN
8.69	9.46	-1.71	0.00313	Exosc9	F6Y747	DOWN
8.43	9.21	-1.71	0.002538	Fam96b	F8WHV1	DOWN
8.58	9.36	-1.71	0.004939	Abca2	Q3TMR1	DOWN
10.13	10.91	-1.71	0.001373	Anln	Q8K298	DOWN
10.57	11.34	-1.71	0.007149	---	#N/A	DOWN
8.82	9.6	-1.71	0.005969	Heatr5a	#N/A	DOWN

6.25	7.02	-1.71	0.009552	I79_015691	#N/A	DOWN
9.13	9.92	-1.72	0.004355	Cdk14	D6RHB2	DOWN
6.35	7.14	-1.72	0.003718	Zfhx4	E9Q5A7	DOWN
9.77	10.55	-1.72	0.002392	Flot1	O08917	DOWN
8.23	9.02	-1.72	0.005178	Fchsd2	Q3U0A9	DOWN
8.37	9.16	-1.72	0.009247	Hmga2	Q6NSP9	DOWN
8.66	9.44	-1.72	0.005093	Nav2	V9GXT5	DOWN
4.92	5.7	-1.72	0.006224	Areg	#N/A	DOWN
6.27	7.06	-1.72	0.005544	I79_002403	#N/A	DOWN
6.87	7.65	-1.72	0.006399	I79_003410	#N/A	DOWN
8.56	9.35	-1.72	0.008209	LOC100770196	#N/A	DOWN
11.11	11.89	-1.72	0.001715	Pdia4	#N/A	DOWN
9.67	10.46	-1.73	0.004976	Hcfc1r1	J3QPD4	DOWN
9.08	9.87	-1.73	0.007373	Dnase1l3	O55070	DOWN
9.44	10.23	-1.73	0.003718	Itfg3	Q8C0Z1	DOWN
9.34	10.13	-1.73	0.00687	Tmem50b	Q9D1X9	DOWN
8.66	9.46	-1.74	0.003718	Pdgfc	D6RGS6	DOWN
9.16	9.96	-1.74	0.001361	Usp32	G3UXQ4	DOWN
8.21	9.02	-1.74	0.007149	Brwd1	Q8BPZ1	DOWN
10	10.8	-1.74	0.008796	Akt3	Q9WUA6	DOWN
7.58	8.38	-1.74	0.008432	Epas1	#N/A	DOWN
6.25	7.06	-1.74	0.009874	Heatr4	#N/A	DOWN
5.96	6.76	-1.74	0.002687	I79_004019	#N/A	DOWN
6.6	7.4	-1.74	0.007164	I79_009797	#N/A	DOWN
9.63	10.44	-1.75	0.009236	Fhl2	O70433	DOWN
9.02	9.83	-1.75	0.006927	Mettl4	Q3U034	DOWN
10.7	11.5	-1.75	0.002222	Ganab	Q3UE86	DOWN
9.46	10.27	-1.75	0.002597	Slc38a10	Q5I012	DOWN
9.82	10.63	-1.75	0.00388	I79_022228	#N/A	DOWN
9.82	10.63	-1.75	0.00388	I79_025164	#N/A	DOWN
8.08	8.89	-1.75	0.007672	Trim34	#N/A	DOWN
10.39	11.21	-1.76	0.002841	Itgav	P43406	DOWN
10.07	10.88	-1.76	0.003672	Tiparp	Q8C1B2	DOWN
9.02	9.83	-1.76	0.001715	C7orf58	#N/A	DOWN
8.96	9.77	-1.76	0.007672	I79_024686	#N/A	DOWN
7.22	8.05	-1.77	0.003718	Kif21a	F8WGN6	DOWN
8.06	8.89	-1.77	0.007119	Tanc2	Q3UF55	DOWN
7.99	8.81	-1.77	0.007659	Ddx50	Q99MJ9	DOWN
6.83	7.65	-1.77	0.002597	Dst	S4R1Y6	DOWN
6.18	7.01	-1.77	0.001353	I79_026093	#N/A	DOWN
8.14	8.96	-1.77	0.009141	Kiaa0240	#N/A	DOWN
7.6	8.43	-1.77	0.004122	Kiaa0586	#N/A	DOWN
8.57	9.4	-1.77	0.002995	Lgr4	#N/A	DOWN
8.4	9.23	-1.78	0.00599	Fcgr3	P08508	DOWN

4.19	5.03	-1.78	0.009338	Pol	P10400	DOWN
9.99	10.82	-1.78	0.007164	P4ha1	Q60715	DOWN
7.67	8.51	-1.78	0.005868	Lrif1	Q8CDD9	DOWN
7.19	8.02	-1.78	0.005927	Gstk1	Q9DCM2	DOWN
7.61	8.44	-1.78	0.007164	I79_015359	#N/A	DOWN
7.81	8.64	-1.78	0.004691	I79_024054	#N/A	DOWN
8.35	9.18	-1.78	0.009688	LOC100751127	#N/A	DOWN
8.48	9.32	-1.79	0.003103	Abl2	B2RQ57	DOWN
9.32	10.15	-1.79	0.007242	Mov10	D3YVL0	DOWN
8.31	9.16	-1.79	0.0091	Rasal2	Q3TPW3	DOWN
7.89	8.72	-1.79	0.004719	Syne2	Q6ZWQ0	DOWN
8.95	9.79	-1.79	0.00499	Fut8	Q9WTS2	DOWN
6.62	7.46	-1.79	0.007005	I79_012982	#N/A	DOWN
7.32	8.16	-1.79	0.00701	I79_017575	#N/A	DOWN
6.36	7.2	-1.79	0.005812	LOC100766236	#N/A	DOWN
8.98	9.82	-1.8	0.004565	Dock9	B2RY08	DOWN
8.33	9.17	-1.8	0.007978	Agpat9	D3YUY8	DOWN
8.14	8.99	-1.8	0.007672	Plcd3	F7AAE0	DOWN
6.95	7.8	-1.8	0.007122	Cryba1	P02525	DOWN
7.64	8.49	-1.8	0.004384	Gpr19	Q61121	DOWN
6.62	7.47	-1.8	0.007005	Lpxn	Q99N69	DOWN
7.46	8.31	-1.8	0.005658	Mthfs	Q9D110	DOWN
10.03	10.88	-1.8	0.002429	I79_002408	#N/A	DOWN
9.02	9.87	-1.8	0.007276	I79_011822	#N/A	DOWN
7.74	8.58	-1.8	0.008595	I79_024617	#N/A	DOWN
10.53	11.39	-1.81	0.008326	Adam19	Q3UH67	DOWN
8.94	9.79	-1.81	0.004611	Dmtf1	V9GX14	DOWN
7.41	8.27	-1.81	0.003536	C1rl	#N/A	DOWN
10.3	11.16	-1.81	0.001353	LOC100772783	#N/A	DOWN
9.69	10.55	-1.82	0.002881	Ypel3	D3Z3G7	DOWN
8.59	9.45	-1.82	0.001754	Eif4enif1	Q3TS00	DOWN
9.08	9.94	-1.82	0.003051	Emsy	Q8BMB0	DOWN
8.96	9.82	-1.82	0.007692	Pofut2	Q8VHI3	DOWN
8.86	9.72	-1.82	0.004511	Arhgef5	Q922T1	DOWN
9.4	10.26	-1.82	0.006211	---	#N/A	DOWN
10.95	11.83	-1.83	0.001353	Errfi1	Q3TJN8	DOWN
6.28	7.15	-1.83	0.006448	Dhrs9	Q58NB6	DOWN
7.25	8.12	-1.83	0.006777	Galk2	Q68FH4	DOWN
7.18	8.05	-1.83	0.002298	I79_005029	#N/A	DOWN
8.3	9.17	-1.83	0.001947	LOC100755141	#N/A	DOWN
7.54	8.43	-1.84	0.004814	Vezt	Q3ZK22	DOWN
8.18	9.06	-1.84	0.003926	Snx13	Q6PHS6	DOWN
6.65	7.54	-1.85	0.007396	Swt1	Q9DBQ9	DOWN
8.92	9.81	-1.85	0.00671	I79_003457	#N/A	DOWN

8.21	9.11	-1.86	0.00338	Fam46d	B1ATX4	DOWN
7.71	8.6	-1.86	0.00762	Gstp2	K9JA74	DOWN
4.45	5.34	-1.86	0.003853	Arhgap20	Q3V0V2	DOWN
9.16	10.06	-1.86	0.004065	---	#N/A	DOWN
8.19	9.08	-1.86	0.001353	Dcaf6	#N/A	DOWN
7.36	8.25	-1.86	0.004542	I79_025169	#N/A	DOWN
8.62	9.52	-1.86	0.005812	Ndp	#N/A	DOWN
8.85	9.75	-1.86	0.003478	Poglut1	#N/A	DOWN
9.24	10.14	-1.87	0.002292	Srsf11	D3Z4B0	DOWN
9.95	10.85	-1.87	0.002345	Arhgap29	Q8CGF1	DOWN
6.85	7.76	-1.88	0.008969	Grhl1	E9QMF0	DOWN
10.52	11.43	-1.88	0.003221	Galm	Q8K157	DOWN
8	8.91	-1.88	0.003584	Aer61	#N/A	DOWN
8.63	9.54	-1.88	0.005665	I79_002570	#N/A	DOWN
8.37	9.29	-1.89	0.001353	Kif21a	F8WGN6	DOWN
8.36	9.28	-1.89	0.007562	Nbea	Q6P2L4	DOWN
5.29	6.21	-1.89	0.004442	Rpf1	#N/A	DOWN
8.19	9.12	-1.9	0.008848	Dhx57	Q6P5D3	DOWN
6.43	7.36	-1.9	0.009621	LOC100752390	#N/A	DOWN
8.7	9.63	-1.9	0.006081	Socs1	#N/A	DOWN
9.19	10.11	-1.9	0.008637	Wdr67	#N/A	DOWN
5.64	6.57	-1.91	0.009638	Vwa5a	D3Z671	DOWN
9.06	9.99	-1.91	0.001353	Mtmr10	Q7TPM9	DOWN
6.04	6.98	-1.91	0.003894	I79_001835	#N/A	DOWN
6.24	7.17	-1.91	0.004442	I79_003701	#N/A	DOWN
9.42	10.35	-1.91	0.006913	I79_026123	#N/A	DOWN
8.5	9.43	-1.91	0.005279	LOC100759025	#N/A	DOWN
8.26	9.2	-1.92	0.00543	Tnrc6c	B1ATC3	DOWN
7.81	8.75	-1.92	0.008068	Plcxd3	Q8BLJ3	DOWN
8.95	9.9	-1.92	0.004721	I79_007625	#N/A	DOWN
9.49	10.43	-1.92	0.005005	Sema3e	#N/A	DOWN
8.66	9.61	-1.93	0.003372	Mtf2	M0QWI3	DOWN
10.02	10.98	-1.93	0.002995	Mcl1	P97287	DOWN
7.63	8.58	-1.93	0.005056	Arid3b	Q3V3M5	DOWN
7.61	8.56	-1.93	0.007687	Katnal1	Q8K0T4	DOWN
8.49	9.45	-1.94	0.004404	Plcxd2	B2RXA1	DOWN
10.04	11	-1.94	0.001023	Fgfrl1	#N/A	DOWN
7.86	8.82	-1.95	0.005128	Smarca1	Q8BS67	DOWN
9.22	10.18	-1.95	0.005185	I79_011973	#N/A	DOWN
10.41	11.38	-1.96	0.002386	Fubp1	Q3TUE1	DOWN
7.81	8.79	-1.96	0.004882	Tpk1	Q9R0M5	DOWN
9.53	10.5	-1.96	0.00209	C7orf60	#N/A	DOWN
9.44	10.41	-1.96	0.009131	I79_017434	#N/A	DOWN
9.82	10.8	-1.97	0.001373	I79_009448	#N/A	DOWN

7.68	8.66	-1.97	0.00432	Ptx3	#N/A	DOWN
9.44	10.42	-1.98	0.001361	Lman2l	J3QNZ7	DOWN
6.24	7.23	-1.98	0.002356	I79_020724	#N/A	DOWN
7.35	8.34	-1.99	0.002933	Itga3	Q62470	DOWN
9.32	10.31	-1.99	0.005513	Nbea	Q6P2L4	DOWN
7.66	8.65	-1.99	0.005382	Dhx57	Q6P5D3	DOWN
8.17	9.16	-1.99	0.006074	B3gnt9	Q8VI16	DOWN
8.23	9.22	-1.99	0.002041	Epb41l5	#N/A	DOWN
8.65	9.64	-1.99	0.00327	Znf260	#N/A	DOWN
9.4	10.41	-2	0.002995	Gpsm2	A2AEL5	DOWN
7.93	8.93	-2	0.001589	Il15ra	Q60819	DOWN
8.17	9.17	-2	0.003936	Tmem2	Q8BS93	DOWN
8.51	9.52	-2	0.002867	Tmem170a	#N/A	DOWN
8.14	9.14	-2.01	0.002867	Tars2	E9Q7H6	DOWN
6.23	7.24	-2.01	0.007261	I79_003762	#N/A	DOWN
8.84	9.85	-2.01	0.005536	Kiaa2026	#N/A	DOWN
8.97	9.98	-2.01	0.005108	Nr1d1	#N/A	DOWN
10.39	11.41	-2.03	0.004355	---	#N/A	DOWN
5.56	6.59	-2.03	0.008442	I79_018889	#N/A	DOWN
5.44	6.46	-2.03	0.008326	I79_021559	#N/A	DOWN
5.13	6.16	-2.03	0.009552	LOC100772772	#N/A	DOWN
7.81	8.84	-2.04	0.004355	Gpr3	B1AUM8	DOWN
7.52	8.54	-2.04	0.003	Lama2	Q60675	DOWN
9.32	10.35	-2.04	0.002853	Ehd3	Q8R0V6	DOWN
8.96	9.99	-2.04	0.003718	Klf7	Q99JB0	DOWN
6.58	7.6	-2.04	0.006429	I79_008854	#N/A	DOWN
7.44	8.47	-2.04	0.004539	I79_011972	#N/A	DOWN
5.47	6.49	-2.04	0.00899	I79_012773	#N/A	DOWN
8.93	9.96	-2.05	0.004065	Btg3	D3Z1M9	DOWN
7.87	8.9	-2.05	0.002041	Rabggtb	P53612	DOWN
7.74	8.77	-2.05	0.005532	Slc12a6	Q3V0N8	DOWN
8.09	9.13	-2.05	0.005006	Ddx26b	Q8BND4	DOWN
8.74	9.78	-2.06	0.005565	Cybrd1	B2RVP1	DOWN
10.83	11.87	-2.06	0.002995	I79_000466	#N/A	DOWN
9.88	10.92	-2.06	0.005185	I79_004545	#N/A	DOWN
10.83	11.87	-2.06	0.002995	I79_015048	#N/A	DOWN
9.14	10.19	-2.07	0.005008	Fez2	Q6TYB5	DOWN
7.37	8.42	-2.07	0.009621	Myl9	#N/A	DOWN
7.2	8.26	-2.08	0.003098	Dusp6	Q3U786	DOWN
6.18	7.24	-2.08	0.009846	Kiaa1024	Q8K3V7	DOWN
9.21	10.27	-2.08	0.004355	Fam48a	#N/A	DOWN
8.82	9.88	-2.08	0.002841	I79_015705	#N/A	DOWN
8.54	9.61	-2.1	0.00523	Eri2	D6RE53	DOWN
8.95	10.02	-2.1	0.009667	I79_007330	#N/A	DOWN

7.76	8.84	-2.11	0.0037	Filip1l	E0CYM1	DOWN
8.39	9.47	-2.11	0.001353	Man2a2	Q7TPQ0	DOWN
9.3	10.38	-2.11	0.001353	Pgm2l1	Q8CAA7	DOWN
7.72	8.79	-2.11	0.005373	I79_009763	#N/A	DOWN
4.89	5.97	-2.11	0.004416	LOC100759368	#N/A	DOWN
9.99	11.06	-2.11	0.006918	LOC100770147	#N/A	DOWN
10.68	11.77	-2.12	0.001023	Alcam	Q61490	DOWN
8.41	9.49	-2.12	0.004292	Steap2	Q8BWB6	DOWN
9.76	10.84	-2.12	0.008547	---	#N/A	DOWN
7	8.08	-2.12	0.005411	I79_000606	#N/A	DOWN
6.95	8.03	-2.12	0.007164	I79_004971	#N/A	DOWN
9.21	10.3	-2.13	0.0091	---	#N/A	DOWN
9.34	10.44	-2.14	0.002995	Socs2	D3Z441	DOWN
6.89	7.99	-2.14	0.001353	Lama2	Q60675	DOWN
8.19	9.3	-2.15	0.002879	I79_003106	#N/A	DOWN
7.4	8.51	-2.15	0.009279	I79_003281	#N/A	DOWN
9.46	10.57	-2.15	0.002841	Neu1	#N/A	DOWN
9.65	10.76	-2.16	0.003797	Pld3	D3YY25	DOWN
8.73	9.84	-2.16	0.006248	Glcci1	E0CXI8	DOWN
8.13	9.24	-2.16	0.006774	Aff2	Q8BQB7	DOWN
8.48	9.59	-2.16	0.006074	Eif2c3	#N/A	DOWN
7.62	8.73	-2.16	0.001353	LOC100750665	#N/A	DOWN
9.83	10.95	-2.17	0.004542	---	#N/A	DOWN
4.98	6.1	-2.17	0.004569	Fam5c	#N/A	DOWN
7.38	8.51	-2.18	0.003866	Bfar	Q8R079	DOWN
9.36	10.49	-2.18	0.003139	B4galt3	Q91YY2	DOWN
8.51	9.63	-2.18	0.006482	---	#N/A	DOWN
7.78	8.92	-2.19	0.006508	Mertk	Q8C584	DOWN
6.25	7.39	-2.19	0.007386	I79_013812	#N/A	DOWN
9.76	10.89	-2.2	0.001353	Idua	P48441	DOWN
8.33	9.47	-2.21	0.005415	Six4	H3BL91	DOWN
8.97	10.11	-2.21	0.004542	Sel1l3	#N/A	DOWN
9.12	10.27	-2.22	0.006426	LOC100774774	#N/A	DOWN
8.88	10.04	-2.24	0.002841	Uhrf2	Q3T995	DOWN
6.13	7.3	-2.25	0.003221	Arhgef16	Q3U5C8	DOWN
6.82	7.99	-2.25	0.003707	Pigk	Q9CXY9	DOWN
8.8	9.97	-2.25	0.00573	---	#N/A	DOWN
6.05	7.22	-2.25	0.003696	I79_005425	#N/A	DOWN
8.78	9.96	-2.25	0.009839	I79_010455	#N/A	DOWN
6.58	7.75	-2.25	0.005008	Sh3rf2	#N/A	DOWN
7.81	8.99	-2.27	0.004594	Cryz	P47199	DOWN
8.82	10	-2.27	0.002818	---	#N/A	DOWN
7.47	8.65	-2.27	0.004302	I79_017673	#N/A	DOWN
7.4	8.59	-2.28	0.002041	Txndc16	D3Z7P6	DOWN

8.62	9.81	-2.28	0.006588	Plac1	Q9JI83	DOWN
5.37	6.56	-2.28	0.00327	I79_007192	#N/A	DOWN
6.18	7.37	-2.28	0.006831	I79_007718	#N/A	DOWN
7.41	8.6	-2.28	0.001926	I79_016813	#N/A	DOWN
7.46	8.66	-2.29	0.003816	Usp33	D6RES0	DOWN
8.35	9.55	-2.29	0.002817	Tmeff1	Q6PFE7	DOWN
8.62	9.82	-2.3	0.005955	Mtf2	M0QWI3	DOWN
8.42	9.62	-2.31	0.003718	Map1a	#N/A	DOWN
7.81	9.03	-2.32	0.001813	Ssx2ip	Q8VC66	DOWN
9.67	10.89	-2.33	0.003584	Gbp2	Q9Z0E6	DOWN
9.53	10.75	-2.33	0.001589	Mllt11	#N/A	DOWN
8.25	9.48	-2.34	0.001575	Grb14	Q9JLM9	DOWN
8.51	9.74	-2.35	0.005532	Adamts6	D3Z1A5	DOWN
10.27	11.51	-2.35	0.002738	Igfbp4	Q8BSM9	DOWN
9.24	10.48	-2.35	0.003795	Ccnjl	#N/A	DOWN
9.24	10.47	-2.35	0.003162	I79_011371	#N/A	DOWN
8.41	9.65	-2.36	0.003009	Depdc5	Q6GQV2	DOWN
11	12.25	-2.37	0.001353	Tnfsf9	Q3TEQ6	DOWN
7.9	9.15	-2.37	0.00666	I79_006727	#N/A	DOWN
8.7	9.94	-2.37	0.002948	Sel1l3	#N/A	DOWN
7.9	9.14	-2.38	0.003949	I79_007724	#N/A	DOWN
7.7	8.97	-2.4	0.003309	Ptgs2	Q3UMR6	DOWN
7.29	8.56	-2.4	0.002995	Tspan2	Q922J6	DOWN
7.39	8.65	-2.41	0.003103	Dsel	Q0VBN2	DOWN
9.18	10.45	-2.41	0.001629	Ccnjl	#N/A	DOWN
7.68	8.96	-2.42	0.003331	Thsd7a	D3YWC4	DOWN
7.58	8.86	-2.43	0.0091	Lphn2	Q3UQ39	DOWN
8.82	10.11	-2.44	0.006863	Vkorc1	Q9CRC0	DOWN
9.76	11.04	-2.44	0.002817	I79_009395	#N/A	DOWN
6.14	7.43	-2.45	0.006327	LOC100754382	#N/A	DOWN
8.89	10.19	-2.46	0.004376	I79_006177	#N/A	DOWN
10.03	11.33	-2.46	0.003414	Wls	#N/A	DOWN
8.7	10.01	-2.48	0.003221	Ttc3	D3Z330	DOWN
9.63	10.94	-2.48	0.003385	I79_024475	#N/A	DOWN
8.81	10.12	-2.49	0.002658	Nox4	S4R1R3	DOWN
8.99	10.31	-2.51	0.002977	Gng5	D3Z7Q3	DOWN
7.08	8.41	-2.51	0.005373	Socs5	Q3UXZ1	DOWN
10.54	11.87	-2.52	0.002789	Egr1	Q544D6	DOWN
7.83	9.16	-2.52	0.001926	Senp7	Q9CQN9	DOWN
8.35	9.69	-2.53	0.003315	Il1rap	Q61730	DOWN
10.1	11.44	-2.53	0.001926	Crim1	Q9JLL0	DOWN
6.78	8.12	-2.53	0.00474	I79_007053	#N/A	DOWN
5.76	7.1	-2.53	0.001947	Rundc3b	#N/A	DOWN
6.6	7.94	-2.54	0.00878	Syde2	E9PUP1	DOWN

5.76	7.11	-2.54	0.009587	Slc14a1	Q8VHL0	DOWN
6.75	8.1	-2.54	0.00837	I79_002524	#N/A	DOWN
10.2	11.55	-2.55	0.004216	---	#N/A	DOWN
8.02	9.37	-2.55	0.001353	I79_012737	#N/A	DOWN
6.73	8.09	-2.56	0.008547	I79_017183	#N/A	DOWN
6.73	8.09	-2.58	0.005138	Tspan12	D3YW00	DOWN
9.3	10.68	-2.6	0.002985	Rps4	#N/A	DOWN
7.19	8.59	-2.62	0.004843	Mapk10	Q3TQZ7	DOWN
5.27	6.67	-2.65	0.008083	Serpini1	E0CYW0	DOWN
9.77	11.19	-2.67	0.001926	Crim1	Q9JLL0	DOWN
7.54	8.97	-2.68	0.002879	I79_013538	#N/A	DOWN
6.32	7.74	-2.68	0.003696	I79_025946	#N/A	DOWN
7.78	9.21	-2.69	0.001926	Arhgef4	Q3TDW8	DOWN
6.58	8.01	-2.7	0.009258	Thsd7a	D3YWC4	DOWN
7.87	9.31	-2.71	0.001373	Ccdc92	D6RJ58	DOWN
6.62	8.08	-2.74	0.004151	Gls2	E0CYF7	DOWN
5.38	6.83	-2.74	0.003275	I79_005625	#N/A	DOWN
7.02	8.48	-2.75	0.004495	Env	Q811N5	DOWN
7.73	9.19	-2.75	0.002041	C4orf49	#N/A	DOWN
8.18	9.64	-2.76	0.001353	Zzz3	Q6KAQ7	DOWN
9.13	10.6	-2.77	0.003816	Nab2	Q61127	DOWN
7.95	9.43	-2.78	0.001575	Tlr3	Q99MB1	DOWN
6.14	7.62	-2.79	0.002687	Fst	P47931	DOWN
4.81	6.31	-2.82	0.006223	Chrdl1	Q6NXY0	DOWN
7.12	8.62	-2.83	0.002041	Prkacb	Q8CBP8	DOWN
6.43	7.95	-2.86	0.005927	Pol	P10400	DOWN
7.99	9.51	-2.87	0.002041	Aim2	D3Z341	DOWN
7.2	8.72	-2.87	0.002419	Env	Q811N5	DOWN
8.84	10.37	-2.89	0.002041	Prrx1	Q3TMI4	DOWN
8.06	9.6	-2.92	0.002879	LOC100773320	#N/A	DOWN
5.19	6.75	-2.94	0.004537	Sema3a	E9Q668	DOWN
8	9.57	-2.97	0.001554	Elovl4	Q9EQC4	DOWN
8.88	10.46	-3	0.002879	Ppid	Q9CR16	DOWN
8.62	10.21	-3.01	0.004122	I79_004992	#N/A	DOWN
5.21	6.82	-3.06	0.005472	I79_000888	#N/A	DOWN
6.46	8.08	-3.06	0.001353	I79_020713	#N/A	DOWN
6.28	7.91	-3.11	0.008976	Cnksr2	Q3URG0	DOWN
5.38	7.02	-3.12	0.003198	Calcr	Q60755	DOWN
7.54	9.19	-3.13	0.001353	I79_005383	#N/A	DOWN
8.1	9.75	-3.14	0.002995	Pirt	Q8BFY0	DOWN
6.27	7.92	-3.15	0.002804	Fpgt	Q2TB53	DOWN
6.81	8.47	-3.15	0.004216	I79_015692	#N/A	DOWN
6.2	7.88	-3.19	0.005138	I79_010946	#N/A	DOWN
9.19	10.88	-3.23	0.001353	Pol	P10400	DOWN

7.83	9.51	-3.23	0.002298	I79_014723	#N/A	DOWN
9.87	11.58	-3.27	0.002041	Ncam1	Q61946	DOWN
7.56	9.27	-3.27	0.003005	Gas2	Q9D699	DOWN
5.59	7.35	-3.39	0.001353	I79_000889	#N/A	DOWN
7.05	8.82	-3.4	0.002368	Ugt1a7c	D3YZ96	DOWN
4.33	6.1	-3.4	0.003718	I79_007567	#N/A	DOWN
8.45	10.22	-3.41	0.001353	Ltbp1	Q8CG19	DOWN
8.11	9.88	-3.42	0.001185	Lrriq3	#N/A	DOWN
5.38	7.16	-3.43	0.00327	Murc	A2AMM0	DOWN
6.45	8.25	-3.46	0.002597	I79_004541	#N/A	DOWN
6.83	8.65	-3.52	0.005138	Env	Q811N5	DOWN
5.9	7.73	-3.56	0.002284	LOC100752107	#N/A	DOWN
7.42	9.28	-3.62	0.003147	LOC100754872	#N/A	DOWN
5.02	6.88	-3.65	0.00329	Acadm	P45952	DOWN
7.57	9.44	-3.65	0.002392	Cnksr2	Q3URG0	DOWN
9.01	10.91	-3.71	0.003009	Ankrd13c	Q3UX43	DOWN
7.73	9.62	-3.71	0.001353	Depdc1a	Q8CIG0	DOWN
5.97	7.88	-3.75	0.009963	I79_005407	#N/A	DOWN
7.33	9.35	-4.06	0.002041	Ptprz1	B9EKR1	DOWN
8.99	11.02	-4.08	0.001977	Tp53	#N/A	DOWN
7.96	9.99	-4.09	0.002296	St3gal6	A6X952	DOWN
7.83	9.87	-4.1	0.002967	Ccl27	#N/A	DOWN
4.96	7	-4.11	0.006127	Ttll7	A4Q9F0	DOWN
7.05	9.09	-4.11	0.006025	Lrrc40	Q9CRC8	DOWN
8.23	10.3	-4.19	0.003718	I79_001952	#N/A	DOWN
6.52	8.59	-4.21	0.001353	Ctbs	Q8R242	DOWN
4.37	6.45	-4.23	0.001715	Dctd	Q8K2D6	DOWN
10.02	12.29	-4.83	0.001353	Env	Q811N5	DOWN
4.3	6.62	-5	0.004898	Cyp11b1	Q3TG86	DOWN
6.51	8.89	-5.19	0.003718	LOC100759571	#N/A	DOWN
3.89	6.42	-5.8	0.00543	Il33	Q8BVZ5	DOWN
9.88	12.42	-5.81	0.001055	Efemp1	F6ZFS0	DOWN
1.51	4.13	-6.13	0.00901	---	#N/A	DOWN
4.89	7.73	-7.17	0.003718	Fgf7	#N/A	DOWN
4.86	8.03	-9.05	0.001353	LOC100757172	#N/A	DOWN
6.33	9.68	-10.23	0.001353	Sgce	O70258	DOWN
6.31	9.79	-11.12	0.001977	Pdpn	A8Y5F6	DOWN

Appendix

Fully annotated KEGG pathway of metabolism

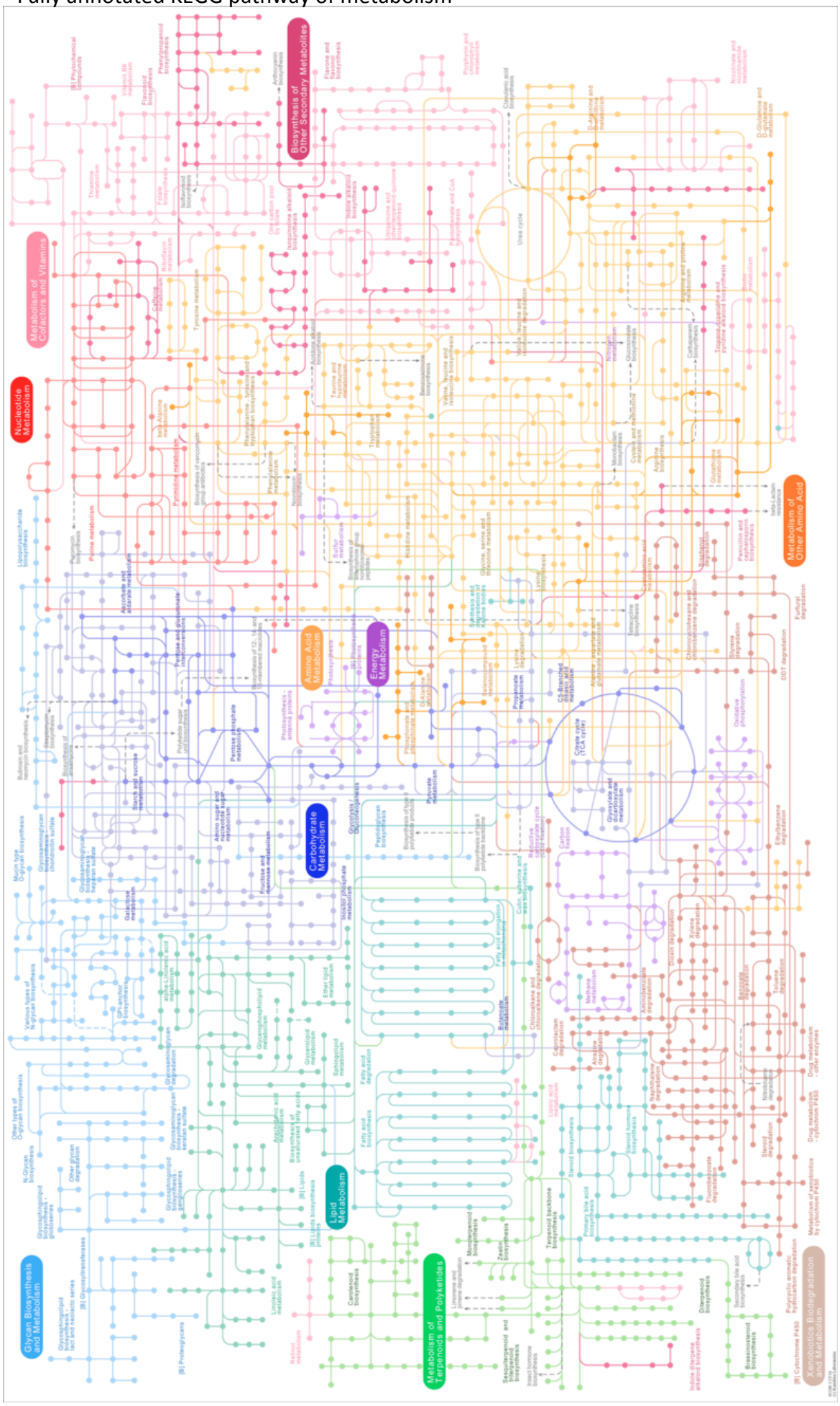

Amino acid flux through culture

Tukey's multiple comparisons test	Mean Diff.	Significant?	Summary	Adjusted P Value
Hydroxyproline				
Evolved at early vs. Evolved at mid	7.676	No	ns	0.9572
Evolved at early vs. Evolved at late	5.515	No	ns	0.9901
Evolved at early vs. Parental at early	-23.8	No	ns	0.0913
Evolved at early vs. Parental at mid	-5.097	No	ns	0.9931
Evolved at early vs. Parental at late	-4.83	No	ns	0.9946
Evolved at mid vs. Evolved at late	-2.161	No	ns	0.9999
Evolved at mid vs. Parental at early	-31.47	Yes	**	0.0074
Evolved at mid vs. Parental at mid	-12.77	No	ns	0.7163
Evolved at mid vs. Parental at late	-12.51	No	ns	0.7342
Evolved at late vs. Parental at early	-29.31	Yes	*	0.0162
Evolved at late vs. Parental at mid	-10.61	No	ns	0.8471
Evolved at late vs. Parental at late	-10.34	No	ns	0.8606
Parental at early vs. Parental at mid	18.7	No	ns	0.3035
Parental at early vs. Parental at late	18.97	No	ns	0.2879
Parental at mid vs. Parental at late	0.267	No	ns	> 0.9999
Histidine				
Evolved at early vs. Evolved at mid	3.215	No	ns	0.9992
Evolved at early vs. Evolved at late	-2.332	No	ns	0.9998
Evolved at early vs. Parental at early	-12.42	No	ns	0.7399
Evolved at early vs. Parental at mid	-0.1109	No	ns	> 0.9999
Evolved at early vs. Parental at late	-7.199	No	ns	0.9675
Evolved at mid vs. Evolved at late	-5.546	No	ns	0.9898
Evolved at mid vs. Parental at early	-15.64	No	ns	0.5097
Evolved at mid vs. Parental at mid	-3.326	No	ns	0.9991
Evolved at mid vs. Parental at late	-10.41	No	ns	0.8572
Evolved at late vs. Parental at early	-10.09	No	ns	0.8728
Evolved at late vs. Parental at mid	2.221	No	ns	0.9999
Evolved at late vs. Parental at late	-4.867	No	ns	0.9944
Parental at early vs. Parental at mid	12.31	No	ns	0.7471
Parental at early vs. Parental at late	5.222	No	ns	0.9923
Parental at mid vs. Parental at late	-7.088	No	ns	0.9696
Tryptophan				
Evolved at early vs. Evolved at mid	4.831	No	ns	0.9946
Evolved at early vs. Evolved at late	0.1576	No	ns	> 0.9999
Evolved at early vs. Parental at early	-14.09	No	ns	0.6229
Evolved at early vs. Parental at mid	0.7423	No	ns	> 0.9999
Evolved at early vs. Parental at late	0.5673	No	ns	> 0.9999
Evolved at mid vs. Evolved at late	-4.673	No	ns	0.9954
Evolved at mid vs. Parental at early	-18.92	No	ns	0.2904

Evolved at mid vs. Parental at mid	-4.088	No	ns	0.9976
Evolved at mid vs. Parental at late	-4.263	No	ns	0.997
Evolved at late vs. Parental at early	-14.25	No	ns	0.6114
Evolved at late vs. Parental at mid	0.5847	No	ns	> 0.9999
Evolved at late vs. Parental at late	0.4096	No	ns	> 0.9999
Parental at early vs. Parental at mid	14.84	No	ns	0.5685
Parental at early vs. Parental at late	14.66	No	ns	0.5814
Parental at mid vs. Parental at late	-0.1751	No	ns	> 0.9999
Methionine				
Evolved at early vs. Evolved at mid	-3.087	No	ns	0.9994
Evolved at early vs. Evolved at late	-12.13	No	ns	0.7588
Evolved at early vs. Parental at early	-13.17	No	ns	0.6891
Evolved at early vs. Parental at mid	-4.889	No	ns	0.9943
Evolved at early vs. Parental at late	-13.64	No	ns	0.6559
Evolved at mid vs. Evolved at late	-9.043	No	ns	0.9164
Evolved at mid vs. Parental at early	-10.08	No	ns	0.8733
Evolved at mid vs. Parental at mid	-1.801	No	ns	> 0.9999
Evolved at mid vs. Parental at late	-10.55	No	ns	0.8503
Evolved at late vs. Parental at early	-1.038	No	ns	> 0.9999
Evolved at late vs. Parental at mid	7.241	No	ns	0.9667
Evolved at late vs. Parental at late	-1.507	No	ns	> 0.9999
Parental at early vs. Parental at mid	8.279	No	ns	0.9414
Parental at early vs. Parental at late	-0.4686	No	ns	> 0.9999
Parental at mid vs. Parental at late	-8.748	No	ns	0.9267
Tyrosine				
Evolved at early vs. Evolved at mid	-5.334	No	ns	0.9915
Evolved at early vs. Evolved at late	-15.41	No	ns	0.5263
Evolved at early vs. Parental at early	-13.08	No	ns	0.6951
Evolved at early vs. Parental at mid	-3.522	No	ns	0.9988
Evolved at early vs. Parental at late	-15.3	No	ns	0.5342
Evolved at mid vs. Evolved at late	-10.07	No	ns	0.8736
Evolved at mid vs. Parental at early	-7.747	No	ns	0.9556
Evolved at mid vs. Parental at mid	1.812	No	ns	> 0.9999
Evolved at mid vs. Parental at late	-9.968	No	ns	0.8785
Evolved at late vs. Parental at early	2.327	No	ns	0.9998
Evolved at late vs. Parental at mid	11.89	No	ns	0.7742
Evolved at late vs. Parental at late	0.1065	No	ns	> 0.9999
Parental at early vs. Parental at mid	9.559	No	ns	0.8963
Parental at early vs. Parental at late	-2.221	No	ns	0.9999
Parental at mid vs. Parental at late	-11.78	No	ns	0.7808
Cystine				
Evolved at early vs. Evolved at mid	-23.38	No	ns	0.1021
Evolved at early vs. Evolved at late	-28.73	Yes	*	0.0198
Evolved at early vs. Parental at early	-4.223	No	ns	0.9972

Evolved at early vs. Parental at mid	-22.55	No	ns	0.1272
Evolved at early vs. Parental at late	-28.18	Yes	*	0.0239
Evolved at mid vs. Evolved at late	-5.349	No	ns	0.9914
Evolved at mid vs. Parental at early	19.16	No	ns	0.2769
Evolved at mid vs. Parental at mid	0.8348	No	ns	> 0.9999
Evolved at mid vs. Parental at late	-4.799	No	ns	0.9948
Evolved at late vs. Parental at early	24.51	No	ns	0.0748
Evolved at late vs. Parental at mid	6.184	No	ns	0.9833
Evolved at late vs. Parental at late	0.5509	No	ns	> 0.9999
Parental at early vs. Parental at mid	-18.33	No	ns	0.326
Parental at early vs. Parental at late	-23.96	No	ns	0.0873
Parental at mid vs. Parental at late	-5.633	No	ns	0.9891
Phenylalanine				
Evolved at early vs. Evolved at mid	-9.223	No	ns	0.9097
Evolved at early vs. Evolved at late	-19.54	No	ns	0.2564
Evolved at early vs. Parental at early	-26.69	Yes	*	0.0388
Evolved at early vs. Parental at mid	-7.698	No	ns	0.9567
Evolved at early vs. Parental at late	-20.78	No	ns	0.1953
Evolved at mid vs. Evolved at late	-10.31	No	ns	0.8622
Evolved at mid vs. Parental at early	-17.46	No	ns	0.3813
Evolved at mid vs. Parental at mid	1.525	No	ns	> 0.9999
Evolved at mid vs. Parental at late	-11.56	No	ns	0.7943
Evolved at late vs. Parental at early	-7.151	No	ns	0.9684
Evolved at late vs. Parental at mid	11.84	No	ns	0.7772
Evolved at late vs. Parental at late	-1.244	No	ns	> 0.9999
Parental at early vs. Parental at mid	18.99	No	ns	0.2867
Parental at early vs. Parental at late	5.907	No	ns	0.9865
Parental at mid vs. Parental at late	-13.08	No	ns	0.6951
Threonine				
Evolved at early vs. Evolved at mid	15.29	No	ns	0.5353
Evolved at early vs. Evolved at late	-2.278	No	ns	0.9999
Evolved at early vs. Parental at early	-34.41	Yes	**	0.0023
Evolved at early vs. Parental at mid	8.47	No	ns	0.9357
Evolved at early vs. Parental at late	-14.71	No	ns	0.5779
Evolved at mid vs. Evolved at late	-17.56	No	ns	0.3746
Evolved at mid vs. Parental at early	-49.7	Yes	****	< 0.0001
Evolved at mid vs. Parental at mid	-6.817	No	ns	0.9743
Evolved at mid vs. Parental at late	-29.99	Yes	*	0.0127
Evolved at late vs. Parental at early	-32.14	Yes	**	0.0057
Evolved at late vs. Parental at mid	10.75	No	ns	0.84
Evolved at late vs. Parental at late	-12.43	No	ns	0.7393
Parental at early vs. Parental at mid	42.88	Yes	****	< 0.0001
Parental at early vs. Parental at late	19.71	No	ns	0.2474
Parental at mid vs. Parental at late	-23.18	No	ns	0.108

Arginine				
Evolved at early vs. Evolved at mid	-2.056	No	ns	> 0.9999
Evolved at early vs. Evolved at late	-17.65	No	ns	0.3689
Evolved at early vs. Parental at early	-27.68	Yes	*	0.0282
Evolved at early vs. Parental at mid	-4.153	No	ns	0.9974
Evolved at early vs. Parental at late	-23.51	No	ns	0.0986
Evolved at mid vs. Evolved at late	-15.6	No	ns	0.5126
Evolved at mid vs. Parental at early	-25.62	No	ns	0.054
Evolved at mid vs. Parental at mid	-2.097	No	ns	> 0.9999
Evolved at mid vs. Parental at late	-21.46	No	ns	0.1667
Evolved at late vs. Parental at early	-10.03	No	ns	0.8758
Evolved at late vs. Parental at mid	13.5	No	ns	0.6657
Evolved at late vs. Parental at late	-5.862	No	ns	0.9869
Parental at early vs. Parental at mid	23.52	No	ns	0.0983
Parental at early vs. Parental at late	4.163	No	ns	0.9973
Parental at mid vs. Parental at late	-19.36	No	ns	0.2658
Isoleucine				
Evolved at early vs. Evolved at mid	9.456	No	ns	0.9005
Evolved at early vs. Evolved at late	-3.792	No	ns	0.9983
Evolved at early vs. Parental at early	-34.87	Yes	**	0.0019
Evolved at early vs. Parental at mid	-5.592	No	ns	0.9894
Evolved at early vs. Parental at late	-11.74	No	ns	0.7834
Evolved at mid vs. Evolved at late	-13.25	No	ns	0.6835
Evolved at mid vs. Parental at early	-44.32	Yes	****	< 0.0001
Evolved at mid vs. Parental at mid	-15.05	No	ns	0.5528
Evolved at mid vs. Parental at late	-21.19	No	ns	0.1775
Evolved at late vs. Parental at early	-31.08	Yes	**	0.0086
Evolved at late vs. Parental at mid	-1.801	No	ns	> 0.9999
Evolved at late vs. Parental at late	-7.945	No	ns	0.9506
Parental at early vs. Parental at mid	29.28	Yes	*	0.0164
Parental at early vs. Parental at late	23.13	No	ns	0.1093
Parental at mid vs. Parental at late	-6.145	No	ns	0.9838
Valine				
Evolved at early vs. Evolved at mid	16.59	No	ns	0.4414
Evolved at early vs. Evolved at late	-0.07855	No	ns	> 0.9999
Evolved at early vs. Parental at early	-29.35	Yes	*	0.016
Evolved at early vs. Parental at mid	7.571	No	ns	0.9597
Evolved at early vs. Parental at late	-5.971	No	ns	0.9858
Evolved at mid vs. Evolved at late	-16.67	No	ns	0.4359
Evolved at mid vs. Parental at early	-45.94	Yes	****	< 0.0001
Evolved at mid vs. Parental at mid	-9.016	No	ns	0.9174
Evolved at mid vs. Parental at late	-22.56	No	ns	0.1269
Evolved at late vs. Parental at early	-29.27	Yes	*	0.0164
Evolved at late vs. Parental at mid	7.65	No	ns	0.9579
Evolved at late vs. Parental at late	-5.892	No	ns	0.9866

Parental at early vs. Parental at mid	36.92	Yes	***	0.0008
Parental at early vs. Parental at late	23.38	No	ns	0.1023
Parental at mid vs. Parental at late	-13.54	No	ns	0.6627
Lysine				
Evolved at early vs. Evolved at mid	13.08	No	ns	0.6953
Evolved at early vs. Evolved at late	-6.97	No	ns	0.9717
Evolved at early vs. Parental at early	-30.24	Yes	*	0.0116
Evolved at early vs. Parental at mid	9.018	No	ns	0.9173
Evolved at early vs. Parental at late	-17.26	No	ns	0.3951
Evolved at mid vs. Evolved at late	-20.05	No	ns	0.2299
Evolved at mid vs. Parental at early	-43.32	Yes	****	< 0.0001
Evolved at mid vs. Parental at mid	-4.06	No	ns	0.9976
Evolved at mid vs. Parental at late	-30.34	Yes	*	0.0112
Evolved at late vs. Parental at early	-23.27	No	ns	0.1052
Evolved at late vs. Parental at mid	15.99	No	ns	0.4841
Evolved at late vs. Parental at late	-10.29	No	ns	0.8634
Parental at early vs. Parental at mid	39.26	Yes	***	0.0003
Parental at early vs. Parental at late	12.99	No	ns	0.7016
Parental at mid vs. Parental at late	-26.28	Yes	*	0.0442
Leucine				
Evolved at early vs. Evolved at mid	10.9	No	ns	0.8321
Evolved at early vs. Evolved at late	-13.27	No	ns	0.6819
Evolved at early vs. Parental at early	-58.51	Yes	****	< 0.0001
Evolved at early vs. Parental at mid	-9.549	No	ns	0.8967
Evolved at early vs. Parental at late	-17.91	No	ns	0.3521
Evolved at mid vs. Evolved at late	-24.17	No	ns	0.0824
Evolved at mid vs. Parental at early	-69.4	Yes	****	< 0.0001
Evolved at mid vs. Parental at mid	-20.44	No	ns	0.2107
Evolved at mid vs. Parental at late	-28.81	Yes	*	0.0193
Evolved at late vs. Parental at early	-45.24	Yes	****	< 0.0001
Evolved at late vs. Parental at mid	3.722	No	ns	0.9984
Evolved at late vs. Parental at late	-4.642	No	ns	0.9956
Parental at early vs. Parental at mid	48.96	Yes	****	< 0.0001
Parental at early vs. Parental at late	40.59	Yes	***	0.0001
Parental at mid vs. Parental at late	-8.364	No	ns	0.9389
Proline				
Evolved at early vs. Evolved at mid	-43.57	Yes	****	< 0.0001
Evolved at early vs. Evolved at late	-62.59	Yes	****	< 0.0001
Evolved at early vs. Parental at early	-122.5	Yes	****	< 0.0001
Evolved at early vs. Parental at mid	-62.25	Yes	****	< 0.0001
Evolved at early vs. Parental at late	-85	Yes	****	< 0.0001
Evolved at mid vs. Evolved at late	-19.01	No	ns	0.2853
Evolved at mid vs. Parental at early	-78.91	Yes	****	< 0.0001
Evolved at mid vs. Parental at mid	-18.68	No	ns	0.3047

Evolved at mid vs. Parental at late	-41.43	Yes	****	< 0.0001
Evolved at late vs. Parental at early	-59.9	Yes	****	< 0.0001
Evolved at late vs. Parental at mid	0.3329	No	ns	> 0.9999
Evolved at late vs. Parental at late	-22.41	No	ns	0.1317
Parental at early vs. Parental at mid	60.23	Yes	****	< 0.0001
Parental at early vs. Parental at late	37.48	Yes	***	0.0006
Parental at mid vs. Parental at late	-22.75	No	ns	0.1209
Glutamic acid				
Evolved at early vs. Evolved at mid	64.33	Yes	****	< 0.0001
Evolved at early vs. Evolved at late	47.6	Yes	****	< 0.0001
Evolved at early vs. Parental at early	-25.02	No	ns	0.0645
Evolved at early vs. Parental at mid	97.03	Yes	****	< 0.0001
Evolved at early vs. Parental at late	99.41	Yes	****	< 0.0001
Evolved at mid vs. Evolved at late	-16.73	No	ns	0.4314
Evolved at mid vs. Parental at early	-89.35	Yes	****	< 0.0001
Evolved at mid vs. Parental at mid	32.7	Yes	**	0.0046
Evolved at mid vs. Parental at late	35.08	Yes	**	0.0017
Evolved at late vs. Parental at early	-72.62	Yes	****	< 0.0001
Evolved at late vs. Parental at mid	49.43	Yes	****	< 0.0001
Evolved at late vs. Parental at late	51.81	Yes	****	< 0.0001
Parental at early vs. Parental at mid	122.1	Yes	****	< 0.0001
Parental at early vs. Parental at late	124.4	Yes	****	< 0.0001
Parental at mid vs. Parental at late	2.382	No	ns	0.9998
Aspartic acid				
Evolved at early vs. Evolved at mid	65.58	Yes	****	< 0.0001
Evolved at early vs. Evolved at late	121.4	Yes	****	< 0.0001
Evolved at early vs. Parental at early	-48.06	Yes	****	< 0.0001
Evolved at early vs. Parental at mid	112.8	Yes	****	< 0.0001
Evolved at early vs. Parental at late	152	Yes	****	< 0.0001
Evolved at mid vs. Evolved at late	55.82	Yes	****	< 0.0001
Evolved at mid vs. Parental at early	-113.6	Yes	****	< 0.0001
Evolved at mid vs. Parental at mid	47.25	Yes	****	< 0.0001
Evolved at mid vs. Parental at late	86.39	Yes	****	< 0.0001
Evolved at late vs. Parental at early	-169.5	Yes	****	< 0.0001
Evolved at late vs. Parental at mid	-8.562	No	ns	0.9328
Evolved at late vs. Parental at late	30.57	Yes	*	0.0103
Parental at early vs. Parental at mid	160.9	Yes	****	< 0.0001
Parental at early vs. Parental at late	200	Yes	****	< 0.0001
Parental at mid vs. Parental at late	39.13	Yes	***	0.0003
Glycine				
Evolved at early vs. Evolved at mid	70.55	Yes	****	< 0.0001
Evolved at early vs. Evolved at late	80.61	Yes	****	< 0.0001
Evolved at early vs. Parental at early	-35.86	Yes	**	0.0013
Evolved at early vs. Parental at mid	62.89	Yes	****	< 0.0001

Evolved at early vs. Parental at late	37.88	Yes	***	0.0005
Evolved at mid vs. Evolved at late	10.07	No	ns	0.8739
Evolved at mid vs. Parental at early	-106.4	Yes	****	< 0.0001
Evolved at mid vs. Parental at mid	-7.652	No	ns	0.9578
Evolved at mid vs. Parental at late	-32.66	Yes	**	0.0047
Evolved at late vs. Parental at early	-116.5	Yes	****	< 0.0001
Evolved at late vs. Parental at mid	-17.72	No	ns	0.3645
Evolved at late vs. Parental at late	-42.73	Yes	****	< 0.0001
Parental at early vs. Parental at mid	98.75	Yes	****	< 0.0001
Parental at early vs. Parental at late	73.74	Yes	****	< 0.0001
Parental at mid vs. Parental at late	-25.01	No	ns	0.0647
Alanine				
Evolved at early vs. Evolved at mid	83.63	Yes	****	< 0.0001
Evolved at early vs. Evolved at late	116.5	Yes	****	< 0.0001
Evolved at early vs. Parental at early	12.86	No	ns	0.7105
Evolved at early vs. Parental at mid	26.69	Yes	*	0.0389
Evolved at early vs. Parental at late	161.5	Yes	****	< 0.0001
Evolved at mid vs. Evolved at late	32.83	Yes	**	0.0044
Evolved at mid vs. Parental at early	-70.77	Yes	****	< 0.0001
Evolved at mid vs. Parental at mid	-56.94	Yes	****	< 0.0001
Evolved at mid vs. Parental at late	77.9	Yes	****	< 0.0001
Evolved at late vs. Parental at early	-103.6	Yes	****	< 0.0001
Evolved at late vs. Parental at mid	-89.77	Yes	****	< 0.0001
Evolved at late vs. Parental at late	45.06	Yes	****	< 0.0001
Parental at early vs. Parental at mid	13.83	No	ns	0.642
Parental at early vs. Parental at late	148.7	Yes	****	< 0.0001
Parental at mid vs. Parental at late	134.8	Yes	****	< 0.0001
Serine				
Evolved at early vs. Evolved at mid	-71.18	Yes	****	< 0.0001
Evolved at early vs. Evolved at late	-153	Yes	****	< 0.0001
Evolved at early vs. Parental at early	-54.32	Yes	****	< 0.0001
Evolved at early vs. Parental at mid	-82.15	Yes	****	< 0.0001
Evolved at early vs. Parental at late	-111.9	Yes	****	< 0.0001
Evolved at mid vs. Evolved at late	-81.83	Yes	****	< 0.0001
Evolved at mid vs. Parental at early	16.86	No	ns	0.4222
Evolved at mid vs. Parental at mid	-10.97	No	ns	0.828
Evolved at mid vs. Parental at late	-40.68	Yes	***	0.0001
Evolved at late vs. Parental at early	98.7	Yes	****	< 0.0001
Evolved at late vs. Parental at mid	70.86	Yes	****	< 0.0001
Evolved at late vs. Parental at late	41.15	Yes	***	0.0001
Parental at early vs. Parental at mid	-27.83	Yes	*	0.0268
Parental at early vs. Parental at late	-57.54	Yes	****	< 0.0001
Parental at mid vs. Parental at late	-29.71	Yes	*	0.0141
Asparagine				

Evolved at early vs. Evolved at mid	79.35	Yes	****	< 0.0001
Evolved at early vs. Evolved at late	-31.32	Yes	**	0.0078
Evolved at early vs. Parental at early	78.99	Yes	****	< 0.0001
Evolved at early vs. Parental at mid	113.9	Yes	****	< 0.0001
Evolved at early vs. Parental at late	-86.05	Yes	****	< 0.0001
Evolved at mid vs. Evolved at late	-110.7	Yes	****	< 0.0001
Evolved at mid vs. Parental at early	-0.3638	No	ns	> 0.9999
Evolved at mid vs. Parental at mid	34.54	Yes	**	0.0022
Evolved at mid vs. Parental at late	-165.4	Yes	****	< 0.0001
Evolved at late vs. Parental at early	110.3	Yes	****	< 0.0001
Evolved at late vs. Parental at mid	145.2	Yes	****	< 0.0001
Evolved at late vs. Parental at late	-54.73	Yes	****	< 0.0001
Parental at early vs. Parental at mid	34.91	Yes	**	0.0019
Parental at early vs. Parental at late	-165	Yes	****	< 0.0001
Parental at mid vs. Parental at late	-199.9	Yes	****	< 0.0001
Glutamine				
Evolved at early vs. Evolved at mid	-558.1	Yes	****	< 0.0001
Evolved at early vs. Evolved at late	-672.4	Yes	****	< 0.0001
Evolved at early vs. Parental at early	-45.53	Yes	****	< 0.0001
Evolved at early vs. Parental at mid	-528.9	Yes	****	< 0.0001
Evolved at early vs. Parental at late	-675.9	Yes	****	< 0.0001
Evolved at mid vs. Evolved at late	-114.2	Yes	****	< 0.0001
Evolved at mid vs. Parental at early	512.6	Yes	****	< 0.0001
Evolved at mid vs. Parental at mid	29.29	Yes	*	0.0163
Evolved at mid vs. Parental at late	-117.7	Yes	****	< 0.0001
Evolved at late vs. Parental at early	626.8	Yes	****	< 0.0001
Evolved at late vs. Parental at mid	143.5	Yes	****	< 0.0001
Evolved at late vs. Parental at late	-3.507	No	ns	0.9988
Parental at early vs. Parental at mid	-483.3	Yes	****	< 0.0001
Parental at early vs. Parental at late	-630.4	Yes	****	< 0.0001
Parental at mid vs. Parental at late	-147	Yes	****	< 0.0001